THE UNIVERSITY OF OKLAHOMA

GRADUATE COLLEGE

IGNITION CHARACTERISTICS OF PLASTICS AND RUBBER

A DISSERTATION

SUBMITTED TO THE GRADUATE FACULTY

in partial fulfillment of the requirements for the

degree of

DOCTOR OF PHILOSOPHY

BY

JOHN R. HALLMAN

Norman, Oklahoma

1971

IGNITION CHARACTERISTICS OF PLASTICS AND RUBBER

APPROVED BY

C. M. Sliepcevich

S. S. Babb, Jr.

F. M. Townsend

J. Reed Welker

DISSERTATION COMMITTEE

IGNITION CHARACTERISTICS OF PLASTICS AND RUBBER

ABSTRACT

There is little or no information reported in the literature concerning the correlation of ignition time of polymers exposed to radiant heat. This study was performed in an attempt to discover the controlling parameters and develop a mathematical expression for predicting ignition time.

The ignition experiments were performed in a cabinet especially designed to provide radiant heating of the specimen from either open diffusion flames or high-temperature tungsten filaments. This versatility in the use of different heating sources provided a means of studying polymer ignition using radiation of two different spectral qualities. Uniform irradiances up to 3.5 cal/cm^2-sec were obtained over the surface of 10-cm square samples from both benzene flames and tungsten lamps. A heated wire coil was placed above the sample as a pilot light. The coil was large enough to preclude any effects of the pilot position on the ignition time.

Polymers chosen for testing were representative samples of present commercial types and grades. Whenever possible, unfilled (UF) and unpigmented (UP) materials were

procured, so that the ignition tests would not be affected by non-polymeric substances. Typical samples obtained were Plexiglas (UF, UP, P), poly(vinyl chloride) (UF, UP), gasketing materials (F, P), Buna rubbers (F, P), phenolics (F, P), nylon (UF, UP), Lexan (UF, UP), polyethylene (UF, UP), polypropylene (UF, UP), polyurethane (F), cellulosic materials (UF, UP), neoprene rubbers (F, P), butyl rubber (F, P) and silicone rubber (F, P).

Pilot ignition times of polymers were found to depend upon six principal variables. Thickness was excluded since all samples tested were standardized at a nominal 1.27-cm thickness, whether solid or of a laminated fabrication. The six effective variables were incident irradiance, average absorptance for the incident radiation, ignition temperature, thermal conductivity, specific heat and density. These parameters were correlated into a form suggested from the analysis of the heat conduction equation for an inert, opaque, constant thermal property, infinite slab with appropriate boundary conditions. The final least squares analysis of the data gave the equation for predicting ignition time as

$$t = 160 \frac{(\Delta T_s)^{1.04} (\rho C_p k)^{0.75}}{(\alpha_{av} H_o)^{2.0}}$$

The most significant information obtained from this study is the following:

1. Pilot ignition time of polymers is inversely proportional to the square of the absorbed energy and directly proportional to the 3/4 power of the thermal inertia ($\rho C_p k$). The time is also directly proportional to approximately the first power of the temperature difference between the ignition and ambient temperatures. The difference in dependence from the square of ΔT (as predicted by the model) is probably due to the change in thermal inertia and the neglect of reradiation and convection in the model.
2. Ignition time is strongly dependent upon the spectral distribution of the incident radiation. In general, most polymers have a lower average absorptance for tungsten lamp radiation than for benzene flame radiation. Because of this difference in average absorptance, light-colored polymers exposed to 1000-watt lamp radiation require 3-4 times as long to ignite as when subjected to flames with the same incident irradiance.

Tables and graphs are included which illustrate ignition times for different irradiances for both tungsten lamps and benzene flames.

A discussion is included of various techniques for the measurement of reflectance and absorptance along with a theoretical analysis of the test methods. A listing of the polymer average absorptances is given for benzene flames, 1000-watt tungsten lamps and solar radiation. Graphs and charts

are included which illustrate the spectral absorptances over the wavelength span of 0.3-6.5 microns. Data are included on the spectral transmittance of several clear plastics for 0.3-6.5 microns.

ACKNOWLEDGEMENTS

A great many people have assisted in the development and completion of this research topic. Among those who contributed greatly to this work in patience, time and inspiration, and deserve both special recognition and gratitude are:

Dr. Cedomir M. Sliepcevich, George Lynn Cross Research Professor of Engineering, for his guidance, direction and unselfish support during the time of academic studies and throughout the experimental and final stages of this research. It is to him that I dedicate this research topic, for without his encouragement and assistance I would have been unable to leave the industrial scene and return to graduate school.

Dr. Stanley L. Babb, Jr., Professor of Physics whose assistance and guidance during the preparation of my General Examination helped me to complete several theoretical analyses.

Dr. J. Reed Welker, Co-director of the Flame Dynamics Laboratory, who has given many hours in direction of the physical research and many suggestions and assistance in the mathematical analysis associated with the research topic.

Professor Walter J. Ewbank and Dr. F. Mark Townsend who have given me many hours of consultation and assistance in my academic studies.

Many associates employed by University Engineers and the Flame Dynamics Laboratory: Dr. Hadi Hashemi, Dr. Jerry Lott, Dr. Jerry Havens, Dr. David Johnson, Dr. Robert Rein, Dr. Harold Wesson, Mr. Robert Loeffler, Dr. Dwight Pfenning, Mr. Harold Bradbury, and Mrs. Billy Ann Brown who have all made many helpful suggestions towards this research.

Mr. Vince Homer, Dr. Hossein Nouri and Mr. John Halloran who worked many hours assisting both in the performance of the ignition tests and the many duties associated with the test preparations and cleanup.

My wife, Florence, and sons, Norman and Leslie, whose many sacrifices have enabled me to return to graduate school, and who have been most patient and understanding during the many hours of study, experimentation, and writing.

Mrs. Joyce Gerald, Mrs. Barbara Everidge, Mrs. Nedra Eaton, Mrs. Connie Kirk, Mrs. Ruth Kempton and Miss Ann Haynes who have given much time in typing and preparation of the many drawings and sketches.

Mr. Edward L. Weld, Director of Nashville State Technical Institute, who provided the necessary staff assistance and school facilities that permitted me to complete the writing of the dissertation.

Finally, I am grateful to General Dynamics Convair in San Diego, California, who authorized the academic leave for the return to graduate work and who permitted the writer to return and use the Space Science Laboratory in study of an

associated research topic. Dr. J. Ternay Neu, director of the laboratory and Mr. Dick Gillson, Test Engineer, gave many helpful suggestions and engineering assistance in the operation of the Convair research equipment.

In conclusion, I am grateful to the various organizations who have provided financial assistance over the course of this research and wish to acknowledge their support. Among these are the U. S. Army, Edgewood Arsenal, which provided funds for personal support and also provided funds for the purchase of experimental materials and equipment, and the Department of Transportation which provided partial funding for personal support.

TABLE OF CONTENTS

LIST OF TABLES

LIST OF ILLUSTRATIONS

Page

IGNITION CHARACTERISTICS OF PLASTICS AND RUBBER

CHAPTER I

INTRODUCTION

Investigations in fire research are concerned with all phenomena associated with burning and with the combustibles involved. Certain aspects of this combustion, i.e., (1) the phenomena associated with the ignition of flammables and (2) the effects of the resultant burning upon adjacent materials, whether flammable or not, have been of major concern to the users of the flammable materials. The users' primary concern is to control flammability and burning rate. Control of the flammability and burning rate of a material requires knowledge of ignition criteria and the mechanisms of combustion that are dependent upon the physical and chemical properties of that material. Koohyar (70) has described the complexity of ignition and burning of flammable materials in the following manner:

> The ignition and combustion of natural and synthetic materials involve complex combinations of physical and chemical processes. The overall process of ignition of solids involves a series of solid-phase decomposition or pyrolysis reactions, a series of gas-phase pyrolysis and oxidation reactions and some solid-gas phase oxidation reactions.

None of these processes is fully understood.

The ignition and combustion of cellulosic materials have been studied in great detail (7, 15, 18, 30, 48, 77, and others) in an attempt to obtain a basic understanding of the processes involved. These studies were concerned with the measurement of surface flammability, rate of charring and decomposition, and the rate of heat penetration into the solid material. Other research has been performed to determine the same qualities and quantities for polymeric materials (2, 12, 14, 19, 20, 28, 33, 47, 53, and others).

The armed forces and civilian agencies are vitally interested in the results of fire research and control methods because of their potential to reduce the drastic losses resulting from fire (27, 54, 60, 66, 68, 88, 95, 106, 109, 119, 120, 134). The urgency of their interest is increased in part by increasing hazard. The use of polymeric materials is in general increase throughout the building trades, and polymers are rapidly replacing wood in its decorative function. This substitution of polymers for wood adds to the complexity of any building fire and to the problems faced by the fire fighter (135).

There is a great interest in the rate of fire propagation due to the rate of flame spread. Materials of high flame spread index* promote an increase in the volume and rate

---

*Flame spread index is determined on a scale on which asbestos-cement board is zero and select grade red-oak flooring is 100.

of burning in the involved fire system.

When a polymeric material is heated, many noxious gases are evolved from the heated surface (6, 16, 24, 26, 112, 128). Continued heating of the material causes further decomposition at a rate sufficient for ignition and continued burning, with such ignition being accomplished either by the heating source or some other ignition source adjacent to the heated material.

At high heating rates, great volumes of volatile flammable gases are evolved from heated materials, thereby adding to the fire propagation due to spontaneous ignition. However, this present investigation is not concerned with spontaneous ignition, but is restricted to the study of piloted ignition. Generally, piloted ignition is described as ignition of the volatile material by an external ignition source, such as a flame or hot wire in the volatile gas stream, but where the igniter itself is not the primary heating source.

Studies indirectly related to ignition have been performed by many different investigators using several different techniques, such as determination of ignition temperature, linear pyrolysis, and/or flammability criteria. The methods of specimen heating include a radiant (gas-fired) panel, tungsten lamps, hot wires, hot gas furnace, hot plates and several others. Most testing methods utilized radiative heating that had thermal emission limited to discrete spectral wavelength regions, such as 0.1-2.0 microns for solar heating or 2.0-5.0 microns for gasoline flames.

General mathematical expressions to explain ignition phenomena have been attempted but no exact solution has been obtained. The difficulties involved in any rigorous mathematical treatment include the following:

1. The products of decomposition being formed at or near the surface of a polymer may cause swelling and bubbling at the surface until ignition is obtained (19, 33, 34, 38, 53, 60, 80, 99, 111, 116), changing the thermal and physical properties.
2. Consideration of the "activation energy, E," or Arrhenius factor, "exp (-E/RT), where R is the gas constant and T the absolute temperature." The activation energy is that energy required to cause bond scission of the polymer with the included breakdown of the polymer into gaseous products which eventually are ignited. Thus, ignition is a transient process which begins at a state of no reaction and proceeds to a state of self-sustaining combustion.
3. Convective and/or conductive heating of the material, the endothermic/exothermic surface reactions, the phase and dimensional changes due to charring, melting or vaporization, and the changes in boundary conditions due to variations in surface properties add to the complexity of mathematical treatment of the ignition problem.

Thus the ability to obtain an exact mathematical solution appears unlikely in the near future.

Various methods for the determination of ignition criteria are discussed in Chapter II. Several analytical techniques have been proposed which omit the effects of diathermanous degradation, while others disregard conduction and convection energy transfer; others assume the complete constancy of the various thermal properties.

Chapter II also describes the development of several criteria for ignition or flammability. Each investigator has proposed a measure of flammability by means of one or more tests, and each frequently includes some mathematical model that refers to his individual study, but does not attempt to correlate the information with that of any other investigator.

In the present work, the type and method for the study of ignition processes is a follow-on to the work of Koohyar (70) and Wesson (132). Heating is supplied by two different sources: (1) a single sheet of free-burning, buoyant diffusion flames, and (2) 1000-watt tungsten lamps. The experimental apparatus is described in Chapter III. The measurements of ignition time and irradiance level are described in Appendix A. Measurement of surface absorptances and the test apparatus are described in Appendix D. Appendix B lists the physical and chemical data of the various plastic, rubber and cellulosic materials tested. Appendix C contains the ignition data for some 800 ignition tests which are discussed in Chapter IV.

It was found that a great diversity of terminology and definitions exists in the literature. In Chapter II, the reader must be alert for this diversity since it is due to the theoretical study, research techniques and method of expression used by the particular investigator cited. A standardized terminology used through the present study is discussed in the first section of Chapter II. The nomenclature used in the presentation and discussion of mathematical expressions is consistent throughout this dissertation. A comprehensive list of nomenclature is listed in Appendix E.

CHAPTER II

A REVIEW OF PREVIOUS INVESTIGATIONS

The ignition criteria for a material depend not only on the method of analysis but also on the definitions of the variables involved. Ignition itself has been described by several concepts. Koohyar (70), during the literature search in his investigation of wood ignition, found numerous criteria used to define ignition. The terminology previously used by Koohyar (70), Wesson (132), and Welker (131) will be continued in this study. For this study, ignition is stipulated as the following:

1. Ignition is defined as the first visible evidence that a volatile product-air mixture shows flame after decomposition of a solid material. The flame must be sustained and not flash intermittently while the radiant heat which causes decomposition is still being applied.
2. Piloted ignition is the ignition of the mixture of volatiles and air by a spark, flame, or heating wire.
3. Spontaneous ignition is the ignition of a volatile product-air mixture when no pilot light is used. The energy for igniting the mixture must come from the radiant heat

source which causes decomposition. Spontaneous ignition is not included as a part of this study.

Ignition and Burning Phenomena

The process of ignition and combustion has occupied researchers for considerable time (1, 8, 17, 18, 25, 39, 55, 57, 58, 59, 74, 98, 113, 115, 116, 117, 124, 133).* Each investigator has developed his own mathematical concept of ignition and/or combustion based upon personal scientific philosophy and method of research. Before proceeding to a review of these studies, a brief mathematical statement of ignition will be presented to assist in the understanding of the basic problems associated with a definition of ignition criteria.

The ignition/burning phenomenon has been described as a function of many variables and can be defined as

$$IG = f(T_z, \bar{T}, T_s, T_o, T_g, R, \Delta H_f, \Delta H_z, E_s, C_p, k, t, L, h, \rho, M, A, \varepsilon_\lambda, \gamma_\lambda, \alpha_\lambda, H_i \ldots) \quad \text{(II-1)}$$

where

IG = ignition criteria

T_g = gas film temperature

$\bar{T}$ = source temperature

T_z = pyrolysis temperature

---

*Brown (18) lists references dating back to 1862.

T_s = surface temperature of the material

T_o = ambient temperature; bulk temperature

R = universal gas constant

E_s = activation energy needed to decompose or degrade the material; may be made up of several energy factors

C_p = specific heat

k = thermal conductivity

t = time

L = thickness of material

h = overall convective heat transfer coefficient

M = molecular weight

A = area of material under test

ε_λ = emittance of surface for each wavelength involved

γ_λ = Lambert's law attenuation factor for each wavelength involved

α_λ = surface absorptance for each wavelength involved

λ = wavelength

ρ = density

H_i = incident irradiance

ΔH_f = heat of fusion

ΔH_z = heat of pyrolysis

As is indicated by the number of parameters involved, ignition characteristics can be investigated by several methods. Four major methods of investigation appeared in literature:

1. Measurement of surface temperature at ignition.
2. Linear pyrolysis as the rate of pyrolysis or burning of a material when the surface is subjected to a high conductive type heat source such as a hot wire or a heated rod.
3. Flammability characteristic: the determination whether a material will ignite and burn, or the acquisition of burning rate data for some indicated incident heat flux.
4. Formal heat transfer analysis using the heat conduction equation as a basis for initial study.

Because such a variety of investigations has been performed, the results of the literature survey will be presented by similar categories.

Temperature and Ignition Relationships

The early literature indicated that most numerical analyses of ignition and/or burning phenomena depended on the temperature of the material (18), so that most emphasis in the research on plastics was directed toward the measurement of the ignition temperature. Ignition was defined as the time of first visible combustion.

Schoenborn and Weaver (113) concluded that a theoretical analysis of the unsteady-state heat transfer was "virtually impossible" because of the physical deformation of the test specimen prior to piloted ignition. In addition, there was a lack of information concerning the physical properties

of plastics, i.e., heat capacity, thermal conductivity, emissivity and other parameters. They suggested, based on the premise of ignition as that point at which a flame first envelopes the surface of the sample, that when the surface is at its ignition temperature, volatile substances and pyrolytic decomposition products are being driven off the heated material at a rate sufficient to support flame at the specimen's surface.

Setchkin (116) continued with the same hypothesis but asserted that before ignition occurs sufficient oxygen must be available to participate in an oxidation reaction with the solid or liquid material, with the vapor, or with gases evolved at elevated temperatures from the decomposition of the material. In order to promote this reaction, the products of oxidation must be continuously removed and fresh portions of oxygen supplied.

Lawrence (74) suggested, based on his own literature search, that ignition was a gas-phase reaction based on the visible oxidation of the volatile products of thermal decomposition, the kindling temperature of the volatile combustion products having been attained or exceeded for ignition to occur. He believed that the ignition time was controlled by the time necessary to reach the kindling temperature which in turn was a function of the surface temperature.

Williams (134) noted that previous investigators (8, 18, 21) considered that under a given set of circumstances

there was a characteristic single temperature at which ignition could be initiated. He pointed out that it is relatively easy to predict the conditions for the attainment of a given temperature within a radiatively heated specimen if accurate surface temperatures on the irradiated material can be obtained.

Hicks (49) indicated that thermal ignition is a function of temperature and time. The solution to this two variable system requires mathematical models that contain nonlinear partial differential equations and therefore are difficult to solve.

Thus, in brief review, the temperature of the material surface or of the volatiles ejected is one parameter in the study of the ignition characteristics of materials, whether wood, plastic or other combustible substance.

The Measurement of Temperature

The present literature search yielded many illustrations of the numerous methods of measuring the ignition temperature of a material. In order to indicate the problems associated with the available data and test methods used, a review of experimental techniques will be presented.

Delmonte and Azam (25) obtained the ignition temperatures of plastics by the contact of a sample with fused NaOH in a furnace. Two temperatures were obtained: (1) the instantaneous ignition temperature where the sample ignited in

less than one second and (2) the minimum ignition temperature where the sample required up to 10 seconds of contact before igniting. The unknown effect of molten NaOH on these samples is cause to question the validity of the ignition temperatures reported.

Schoenborn and Weaver (113) in their review of previous research found wide disagreement in the reported values of ignition temperature for the same material; this disagreement was primarily due to the particular test method employed by each investigator. Schoenborn and Weaver proposed a test method by which small, bar-shaped samples of plastics were inserted into an electric furnace that had stabilized at a known high temperature. Each plastic sample had a standard 30 B and S gage thermocouple inserted into a hole drilled on the centerline of the sample major axis. A series of the same samples was prepared with different hole depths. During the test, time and temperature readings were taken for each sample series. A plot of time and temperature for each sample showed a "break point" (slope change) which indicated the local temperature at a given position within the sample when surface ignition began.

Schoenborn and Weaver (113) plotted the "break point" temperatures versus the distance between the outer bottom surface (of the specimen) and the thermocouple junction and then extrapolated the curve to zero distance (the specimen

surface). The temperature read from the plot at this last point was arbitrarily defined as the apparent surface temperature at the moment of ignition.

The analysis of Schoenborn and Weaver is based upon the criteria that (1) the temperature change within the sample was a linear function of distance from the surface and (2) the rate of heating does not affect the temperature of ignition but affects only the time required to reach ignition. Neither of these assumptions is necessarily true. No air flow was provided. Ignition of the sample was delayed until sufficient volatiles were present and could form a combustible mixture with the contained air. Under these heating conditions the ignition temperatures are probably in error by being too high.

Setchkin (116) did not agree with the several previous investigators in the methods of determination of ignition temperatures. He devised a test furnace that was constructed to provide the following major requirements:

1. The temperature of the air passing the specimen was to be uniform and constant.
2. The air flow was to be steady and controllable.
3. The specimen was to be in a stream of air of known temperature; be visible from the outside; and be easily removable.

Two methods of testing were applied:

1. A rising temperature method where the temperature of the system was raised at a rate of 500°C per hour until ignition occurred spontaneously or by an igniter, or until 750°C was attained. If no ignition occurred by 750°C, the material was considered incombustible.
2. Insertion of the sample into the furnace and impaction by an air stream (3-40 ft/sec depending on the material). The furnace was previously stabilized at a known temperature. The test was repeated using progressively higher temperatures until the sample ignited. The temperature of the sample, either on the surface, or within, was measured via a thermocouple inserted into or placed on the sample surface. The air temperature was also obtained.

Method 1, rising temperature, has a problem that some material heated in this manner will decompose slowly without ignition. Under conditions of slow decomposition, it is probable that higher ignition temperatures would be obtained than are actually characteristic of the test material.

Method 2, constant temperature, has several problems. A thermocouple inserted into the specimen below the surface does not indicate the actual surface temperature. A thermocouple placed on the sample surface is subjected to incident radiation and, because of the absorbed heat, will indicate a somewhat higher temperature than actually exists on the surface. The use of an air rate suitable to the specimen, "in accordance with the trend of the exothermic reaction," would

indicate that ignition was dependent on the oxidative degradation rate. Thus if the tests were performed at a constant air rate, the indicated ignition temperatures would be lower or higher depending on whether the air rate was greater or less than that rate reported by Setchkin for any particular material. A comparison of the relative fire hazard of material by use of ignition temperature would not be accurate if different air rates were used.

It should be noted that the Setchkin test furnace and associated systems (116) have been designated as a standard tool by the ASTM Standards Committee and is known as ASTM Test D 1929.

Underwriters Laboratories (UL) have developed a test for ignition temperature (53) which is described here in part; the UL test employs a high temperature glass flask surrounded by a molten-alloy bath heated by an electric furnace. The flask is conical with a flat bottom and is designed to give a specific test volume and surface area to volume ratio. The samples, 1/4 x 1/4 x 1/8-inch rectangular slugs, or dust-sized particles, are dropped into the flask, after the temperature has reached a steady preselected value, and are checked for ignition.

The UL test has several inherent problems: There will be a finite temperature difference between the outer and inner walls of the flask so that the actual inner temperature will not be known accurately. A comparison of a test

slug and powder ignition temperature of the same material would probably be different, and both will depend upon the ability of the vapors to mix with the encompassed air. The ignition temperature indicated from the test will probably be somewhere between piloted and spontaneous, since this test has a part of each type of ignition.

Burge and Tipper (19) were interested in the burning of polymers to obtain information on the combustion chemistry of the process. Their test consisted of igniting the end of a rod-shaped sample that was contained in a wide glass tube. The ignited end of the rod was enclosed in a glass mantle that permitted a depth of molten polymer of 1-2 centimeters below the flame. Temperature profiles were made from 1 centimeter below the liquid surface to 3 centimeters above the surface. In addition, composition profiles through the flame were obtained and analyzed for the components present. It is unfortunate that the authors did not give any comparison of their results with other studies, but they did indicate that this test system gave promise of permitting rapid analysis from an essentially simple arrangement.

It is possible that the Burge and Tipper test apparatus could be of use in the study of polymer combustion but the test method does not yield any pertinent information on the ignition process.

During the study of the thermal stability of elastomeric materials in a simulated spacecraft environment (pure

oxygen at 5 psia pressure with a rising temperature) Kline (67) developed a technique to associate ignition temperature with thermal degradation. He modified a thermogravimetric unit by adding a photoelectric cell that would respond to a sample flaming or flashing while undergoing test.

Using a plot of temperature with photocell output and a plot of temperature with weight lost, Kline was able (on a double plot) to associate the ignition temperature with the weight loss. No attempt was made to associate rate of weight loss with ignition temperature.

This method shows promise in enabling an association of rate of heating, rate of weight loss and rate of sample degradation, and ignition temperature. Unfortunately, the choice of photometer is dependent on the detector and its sensitivity range. Some plastics burn with almost no visible light and others with a bright yellow or smoky flame. Outside lighting and heat radiation at higher temperatures could cause noise upon or baseline drift of the recorder. However, this system does allow speculation of its capabilities in the combining of several ignition parameters.

The measurement of ignition temperature of polymers is still being performed under the ASTM D 1929 test as previously described. A test similar to that used by Setchkin (116) is presently being used by Khoroshaya, et al. (61) in their study of flame-resistance of polymers and other materials. A 0.5 gm sample is placed in a muffle furnace

previously stabilized at some high temperature. If ignition does not occur, the furnace temperature is increased by 50°C, stabilized and a new sample inserted; the test continues in the same fashion until ignition. The temperature obtained from this test is dependent upon how fast the sample degrades and the vapors form a spontaneous combustible mixture with the air.

While the investigation of ignition temperature has occupied a strong position in the study of ignition and burning, there have been parallel methods of research performed to study the same problem. These methods will be described in following sections of this chapter.

Linear Pyrolysis Studies

An approach to polymer thermal stability other than flammability was employed for the purpose of determining the mechanism of polymer surface degradation. Linear pyrolysis is defined as the steady-state linear rate of surface regression under the influence of a contacting heat source. This rate of regression is taken as a measure of the rate of thermal degradation of the specimen and is illustrated by the hot wire pyrolysis method.

Schultz and Dekker (114) studied the decomposition of Plexiglas in a nitrogen atmosphere by the use of hot wire pyrolysis for the measurement and analysis of linear decomposition as a function of temperature. Their method was to cut

through the sample of plastic using a heated wire and to measure the cutting rate. The temperature of the plastic was measured by means of a fine thermocouple welded to the center of the cutting wire. They repeated this test using several wire temperatures and then performed a graphical analysis of the linear rate of pyrolysis (rate of wire cut) as a function of reciprocal temperature. Using as a basis the transfer of heat between the gas and solid phase reactions, a steady state temperature T_s, was established at the heated surface. A linear burning rate, B, was defined by the equation

$$B = B_o \exp \left(\frac{-E_s}{RT_s} \right) \text{ cm/sec} \qquad \text{(II-2)}$$

where B_o is some constant less strongly dependent upon the temperature than the exponential term. Here the authors (114) assumed that the activation energy term, E_s, was calculated from the slope of the plot of ln B versus reciprocal T. The authors fail to account for the latent heat of fusion or of vaporization of the melting and/or vaporizing polymer, but proceed to develop a mathematical formulation for B_o, the constant of the equation. If the rate of burn, B, is not adjusted for the rate of travel of the wire due to sample melting, the activation energy, E_s, does not indicate an accurate measure of the overall rate constant of the degradation reaction.

Several measurement techniques and assumptions made in this study (114) are questionable:

1. The technique of using a fine thermocouple wire welded to the center of the cutting wire would tend to measure the temperature of the cutting wire, not the plastic surface.
2. All thermoplastic polymers melt; this melting is not thermal degradation, because the plastic material regains its original chemical and mechanical properties after resolidifying and cooling.
3. A thermosetting plastic chars upon heating. The resultant char will develop more resistance to the action of the cutting wire than the original material which will indicate a lower rate of linear pyrolysis.
4. The loading force on the cutting wire will influence the rate of passage through the sample; a higher loading force will increase the rate of cutting but probably not as a linear process.

The experimental work of Schultz and Dekker (114) was extended by Barch, et al. (9) and Chaiken, et al. (22), both groups using a flat hot-plate as a sample surface heater. Later investigators, McAlevy, et al. (85) Nachbar and Williams (92) and Anderson (4) reviewed the data and research methods of the Barch (9) and Chaiken (22) groups and found that the gas film existing between the hot-plate surface and the sample melted surface complicated any specimen surface temperature measurement. Also, any vigorous vapor flow across the specimen surface could cause erosion of that surface if a liquid phase was present before vaporizing. Finally it was concluded

that where substances react chemically while undergoing pyrolysis, the linear rate of regression or pyrolysis equations would probably require additional corrections.

In conclusion, it must be stated that the variables encountered in linear pyrolysis have caused a re-evaluation of the technique with a resulting new direction toward other methods of analysis, such as found in the pyrolysis degradation studies or general flammability testing.

Hilado (52) summarized the flammability tests of materials based on the burning rate, heat release rate and pyrolysis rate. Some of the tests he reviewed are:

1. ASTM D 1692, flammability test for plastic sheeting and cellular plastics, evaluated by rate of burn in inches/minute.
2. ASTM vertical bar test for cellular plastics (1967d), evaluated by rate of burn in grams/minute.
3. ASTM E 162 radiant panel test evaluated by distance burned in inches and the time required for burning. This test includes the heat given off during the test or heat required for pyrolysis.

None of the above tests was used in a quantitative manner for analysis ; all were applied merely to designate a degree of flammability by comparison of the various test results. The flammability rating is determined from the rate of burning.

Flammability Characteristics

> In 1907, at the request of the Steamboat-Inspection Service, the Bureau of Standards made a careful study of the literature of celluloid and other pyroxylin plastics and afterward carried out an investigation of their properties with special reference to the hazard connected with their use and transportation.

The statement quoted is the introductory sentence from the studies of Stokes and Weber (124) in reference to one of the earliest investigations of the flammability of a plastic material. The analysis was performed (1) to determine the percentage of nitrocellulose present in each type of sample and (2) to test the samples in a vacuum at various elevated temperatures. Analysis of the weight loss was made for an extended period up to 10 days. Other samples were maintained at elevated temperatures for several days within a constant air flow. Again weight losses were measured. Additional samples were decomposed in air and also decomposed while enclosed within a mercury bath. Analysis of both tests was made for evaluation of the gaseous products. The authors concluded their studies with the following conclusions, presented in part:

2. The decomposition of nitrocellulose commences in the neighborhood of 100°C...

3. Above 170°C, the decomposition of celluloid takes place with explosive violence...

4. The rate of combustion is five to ten times that of poplar, pine or paper...

5. The vapors evolved by decomposition are poisonous and extremely combustible and may be ignited by the heat of decomposition of the celluloid itself.

As has been described, it is evident that study of the flammability of materials has been of concern for some time.

The literature gives no further references to flammability characteristics until the mid-1940's and the research stimulated by the development of new materials for use in civilian production as well as in warfare.

Delmonte and Azam (25) studied ignition temperature as a measure of flammability. This work is described in a previous section.

Gale, et al. (39) developed a test apparatus that consisted of a nichrome heater coil which was placed concentrically around the specimen under test. An exhaust system provided a constant flow of air around the sample and the vapors were passed through an aperture containing energized spark plugs. At energization of the heater coil and spark plugs, a timer was started and the time of ignition was noted. Heating was continued for 30 seconds after ignition; then the heater coil was de-energized and the time for flame extinguishment was noted. Thermocouples were placed flush with the sample surface to acquire time-temperature information.

The placement of the thermocouple on the specimen surface at the mid-point of the heater coil assembly will indicate some temperature but not the surface temperature. The authors did not attempt to correct nor discuss the radiation effects on the thermocouple junction but did propose an ignition time-surface temperature relationship. No heating

rates were calculated. The data acquired indicated that, for the same material, the longer the ignition time, the lower the ignition temperature. It was concluded from these tests that sufficient accuracy of flammability characteristics could be acquired that would permit the establishment of limits of flammability for materials tested.

The literature search yielded no further information for the next 15 years. In 1960, there was an apparent re-emphasis on the study of material flammability for the establishment of definitions and standards for classification of materials involved with fire safety.

Hilado (50, 51, 52, 53) in his analyses of cellular polymers (rigid and flexible polyether-urethane foams) was concerned with the general combustible characteristics of polymers. He summarized the flammability characteristics of cellular polymers as follows: ease of ignition; surface flame spread; fire endurance; fuel contribution; smoke density; and products of pyrolysis and combustion. Hilado analyzed the problems concerning testing of cellular polymers as he indicated by this partial description: cellular polymers are more difficult to define than solid polymers, such as coatings, because of the difference in physical structure. Both pyrolysis and combustion in the direction perpendicular to the exposed surface become major factors because of the material thickness. The large gas content of cellular polymers gives a low thermal conductivity, concentrating heat at the exposed

surface instead of dissipating it to the underlying material or substrate. At a sufficient rate, the heat applied can destroy a cellular plastic before the heat is dissipated, resulting in the collapse of the polymer mechanical structure.

The American Society for Testing and Materials (ASTM) Committee, as well as several others,* has developed certain specific tests which are intended to indicate the relative flammability of a test material through two independent properties, ignition and burning (111):

1. ASTM E 162-61 T Surface Flammability for Plastics Using a Radiant-Heat Energy Source: The material under test is rated according to how fast the flames spread along the surface at a specific surface heating rate. Feuer and Torres (35) considered that this test was the most adequate for determining the flammability of materials. Nametz (93, 94) recommended that this test be considered one of the best for evaluating duct work for fire retardancy. Hilado (50, 51, 52) considered this test to be useful as a medium-scale evaluation of flammability.

   For this test, the rate of burn is the degree of flammability, but the time for ignition is not considered as a measure of flammability.

2. ASTM D 635-44 Flammability of Plastics Over 0.05 Inches in Thickness: A specified test bar is burned horizontally

---

*Underwriter Laboratories (UL), Military Specifications and individual companies.

with a Bunsen burner, and flammability is determined from continued burning or self-extinguishment; by using markings on the sample, the rate of burn is obtained. This test determines the relative flammability in comparison to other formulation variations. Feuer and Torres (35) considered this test a go/no go test that does not lend itself to practical interpretation. Sauber and Patton (111) indicated that this test, although widely used in comparing the flammability of one series of plastic formulation with another, does not tell whether the best formulation is adequately safe for large-scale application. Nametz (93, 94) also indicated that this test is good only for rough screening work and does not distinguish relative flammability characteristics among good flame-retardant specimens.

Ignition time is not considered as a part of the flammability characteristics, only the capability of being ignited and the rate of burn.

3. ASTM D 757-49 Flammability of Plastics--Self Extinguishing Type: The sample is brought into contact with a globar heating element at 950°F and the burning rate is measured. Feuer and Torres (35) considered this test to be more closely controlled as to ignition, but indicated that the measurement of the rate of flame spread is not made under conditions encountered in an actual fire.

Nametz (93, 94) indicated that this test gave no differentiation between compositions that have a high degree of flame resistance.

For this test, the specimen-globar pressure can affect the test results. No ignition time is considered but merely the ability to ignite and rate of burn.

4. Hooker HLT-15, Intermittent Flame Test (56): HLT-15 is performed by suspending the plastic sample vertically and igniting it at the bottom with a Bunsen burner using a specific flame height. The complete test requires five ignition attempts. Beginning with test 1, the igniter is maintained at the sample for a certain time and this time is increased with each test, test 5 being the longest. In addition the time between each subsequent ignition attempt increases. If the flame of the sample goes out between all five ignitions, the material passes the test, as being non-flammable. Nametz (93, 94) considered the HLT-15 test to be a more severe test than others run because of the vertical testing position and the average numerical value obtained from the five runs.

Although this test has merit as indicating the flammability or combustibility of a material, it does not yield any information on ignition. The multiple ignitions removes this test as a reference with respect to the present study.

5. LP 406 S #2023.2 Flame Resistance (Military Specification): This test is almost identical to that reported by Gale, et al. (39), described at the beginning of this section. Feuer and Torres (35) noted that this test was designed specifically to measure the flame resistance of materials used in electrical equipment and has no practical correlation with industrial fires involving duct work containing the same material. Nametz (93, 94) considered that this test was one of the best for use in determining flame resistance of materials used in electrical equipment where there was danger of arcing. This is not an ignition test, but the test does indicate the degree of combustibility of a material.
6. Butler Chimney Test (71): Test 6 is a modified vertical sample test which encloses the sample in a vertical chimney containing a wire-reinforced glass front to increase energy feedback. The sample is ignited with a specific Bunsen burner tip, yielding a designated temperature. The flame height, sample weight loss and flame extinguishment times are considered a measure of flammability. Hilado (50, 51, 52) commented that this test was considered a small-scale illustration of flammability test. This test is based on the rate of burn and does not yield any ignition information.

King (62) found, in his review of the tests for flammability, that there was a basic problem in duplication of

the tests and interpretation of data. He considered the terms used to define "material flammability" as ambiguous, since the terminology consisted of the words fireproof, fire-resistant, fire-retardant, self-extinguishing, all used interchangeably. The reviewed tests did not evaluate the materials under one specific set of test conditions nor compare the test results with the results found from a known material tested at the same conditions.

Sauber and Patten (111), in their review of present tests for determining the flammability of plastics, found two classifications in terms of two independent properties, ignition and burning. They found that early tests did not determine temperature conditions which would cause an ignition hazard.

Carpenter (20) described flammability tests as falling into categories--those which determine whether a material will burn and its rate of burning, and those which measure the quantity of heat produced when a material is burned and thus determine to what extent it will contribute to a fire which has started elsewhere. He found that there were discrepancies between the several flammability tests performed.

A more recent development in the flammability testing of plastics was illustrated as a "candle-type test." Fenimore and Martin (33) required a simple test that would provide a convenient, reproducible, numerical measure of polymer flammability. To accomplish these requirements, a candle-type

test was developed which utilized an oxygen index as a measure of the burnability of a material. The test was performed by burning a sample strip in an enclosed tube and slowly varying the O_2-N_2 ratio toward a higher percentage of N_2. The ratio [actually the percentage of O_2 in the mixture] can be described as

$$\text{Oxygen Index} = n = \frac{[O_2]}{[O_2] + [N_2]} \qquad \text{(II-3)}$$

It was found that the smaller the limiting n, the more flammable the material. Specific limits found were (1) for materials that do not continue to burn after ignition in air, the value of n was greater than 0.21, (2) the value for polytetrafluoroethylene, as a maximum non-flammability value, attained n = 0.95, and (3) polyoxymethylene, as an example of a high flammability material, had an n = 0.15. The authors found that this candle-test gave a method of comparison and measure of effectiveness of various types of additive flame retardants. In addition they state that the decreasing flammability of the material is reflected by a smaller value of n and this is due to the flame surviving the nitrogen cooling. There is a definite lower limit of oxygen concentration in hydrocarbon-oxygen mixtures where the mixture cannot be ignited. The limiting value of n is probably affected more by this mixture ratio than by the nitrogen cooling of the flame.

A comparison of the results of this test with other flammability or ignition tests would be most difficult. Most flammability tests are based upon a rate of burn in air while this test is based on a minimum oxygen concentration. Generally, flammability test specimens are ignited by a standard heat source, i.e., a Bunsen flame or equivalent, with the igniter flame maintained for a certain specified time. In this test the specimen is ignited by a hydrogen flame, which is promptly removed after specimen ignition. Then the oxygen content of the surrounding atmosphere is decreased until the sample will just burn for its entire length. The limiting oxygen index is then calculated from Equation II-3.

Emmons (30), after visiting numerous fire research organizations in Europe and Asia, summarized his findings:

> What we need at the present time is a considerable [fire] research program at the practical, basic and fundamental levels, in order to find out what we do really want to know. After this is done, it will be easy to devise one internationally agreed-upon test or series of tests. To devise such a test before we know what we want is to risk making, with much test effort, a handbook for material's combustibility, which must be thrown away when future studies show the tests to be inadequate or worthless.
>
> It is, of course, clear to all of the test groups producing this data that the different "standard" tests really measure different mixes of different physical properties and phenomena. What is not now clear is just which properties and phenomena are really essential in a building fire.

In a general summary of this section, it must be stated that the varied flammability criteria indicate that there is little or no correlation existing in the area of

flammability testing of polymers. The numerical indices provided by the several flammability tests previously described will give conflicting designations for a single material that is subjected to more than one type of test. A material with a non-flammable rating in one test can be classified as flammable in another. The various authors cited all agreed that a basic standard would be of great benefit to all users and investigators. As a final note, Hilado (53) lists five general categories of flammability tests which include some 50 individual types of tests used as a measure of fire resistance.

Models of Ignition

A previous literature survey (70) has shown that a great amount of research and study has been performed to describe the mechanism of ignition, particularly of wood; plastic and its ignition characteristics have been investigated to much smaller degree (77). The inherent differences between wood and plastics suggest that the heat transfer mechanisms and the various assumptions made for wood ignition may not necessarily apply to plastics.

Koohyar (70) lists a set of assumptions and ground rules concerning the "necessary conditions and criteria for ignition of cellulosic materials." A review of those criteria in relation to plastics is presented in the following discussion:

"1. The solid material is porous and the transfer of heat and volatile products is one-dimensional." During the testing of cellulose and wood samples (70) it was noticed that the cracks in the wood surface were not uniformly distributed which caused the one-dimensional model for wood to be questioned.

In the plastics and rubber study, there were several different reactions of the sample surface to heat. Some sample surfaces melted and others charred; in some, pitting of uneven hole depth and diameter appeared. Other samples cracked unevenly, some formed giant bubbles or small bubbles, as in a froth, and some samples did not appear to change shape until after ignition occurred (131). Thus, one-dimensional heat transfer may not be correct.

"2. The gaseous products escape with negligible pressure drop." Koohyar (70) found that the amount of energy transfer by gaseous products was relatively small and therefore the assumption was considered valid.

For polymers, some samples gave evidence of gas escaping under pressure because of the jet-like appearance of the vapor and/or smoke. Other sample surfaces bubbled and frothed or spalled to the extent that small particles were ejected from the heated surface (131). Thus, criterion Number 2 may be questionable for polymers.

"3. The vapor temperature at any depth can be approximated as the solid temperature at that depth." Koohyar (70) assumed this item as "fair" based on the small rate of energy loss in the vapor stream.

Criterion Number 3 is also assumed valid for plastics.

"4. The process is diffusion controlled, i.e., it is controlled by the diffusion of heat and not by rate of reaction." Koohyar (70) assumed Criterion Number 4 as valid for wood based upon experimental results found in his literature search.

Polymers exhibit different phenomena under the influence of radiant heat, as discussed in Criterion Number 1. The rate of vaporization and/or melting associated with the surface activity arising from polymer degradation remove the ignition process from that of pure diffusion. Therefore Criterion Number 4 may not be applicable. In addition, the rate of [degradation] reaction is influenced by the activation energy of the particular polymer.

"5. An overall first order reaction with a constant heat of reaction for the weight loss is applicable." According to Koohyar (70) and Havens (48), this item is applicable for wood based upon experimental work and development of the reaction kinetics involved.

Experimental results (37) indicate that polymer degradation is generally a first order reaction, but the

rate of weight loss has more parameters involved than just the activation energy and temperature.

"6. The material is isotropic and its properties are independent of temperature." Koohyar (70) noted that properties of wood are different depending on whether samples are taken across or parallel to the grain, but that thermal diffusivity of wood and charcoal are approximately the same. It was noted that analysis of wood ignition required assumption of constant properties so that simplified models could be used for the heat transfer analysis. Havens (48) permitted the thermal conductivity to vary with density changes in his research, however.

Polymers are processed to be homogeneous so that plastics and rubber can be assumed to be isotropic. Certain exceptions are the laminates where each layer is assumed to be homogeneous. The energy balances and heat transfer mechanisms, to be discussed later, are based upon simplified mathematical models using constant parameters in the same fashion as in the wood analysis.

"7. The intensity of the radiation is constant and uniform over the entire surface boundaries." Koohyar (70) assumed the validity of Criterion Number 7 on the basis of experimental conditions.

The same techniques were experimentally maintained for all plastics and rubber testing.

"8. Average constant values can be used for optical properties of the sample." This item can be considered valid, according to Koohyar (70), if suitable values for the optical and physical properties can be found.

Criterion Number 8 is also considered valid for polymers. The surface absorptance must be based on the average found over the spectral emissive power of the heat source. Thermal properties should be used at the average value for the particular temperature spread, if these properties can be found.

"9. Lambert's law for semi-transparent material is applicable." Koohyar (70) assumed Criterion Number 9 valid provided suitable "average" optical properties were known.

Polymers can be found that vary from complete opaqueness to full transparency depending on the wavelength of the radiation. Polymers have surfaces that vary from smooth, dull, non-reflecting to high mirror-like reflectivity. Further, the effects of light transmission and diathermancy in the material will add complexity to any heat balance model. Polymers generally transmit some radiant energy into the material, depending on the surface condition, plasticizers and fillers, and coloring matter. In the case of optically transparent materials, a significant amount of thermal energy is transmitted through the material while some thermal energy is being

absorbed or retained at different thickness levels. The radiation absorption within a material is called diathermancy. It is probable that all plastics are diathermanous to some degree for some radiation wavelengths, but little or no information is available on this subject. For purposes of this study, it will be assumed that Lambert's law is applicable for transparent and translucent materials.

"10. Some modified physical properties can be used to offset the effect of moisture content." (Koohyar used dried wood samples in all of his tests).*

In any polymer study it can be assumed that plastics and rubber have negligible moisture content.

"11. The dimensions of the solid remain constant." Koohyar (70) found that Criterion Number 11 is usually valid prior to ignition but expansion and/or shrinkage are common during pyrolysis and following ignition. In some cases of slow ignition due to a low heating rate, the same surface changes can occur before the actual ignition.

Polymers exhibit somewhat different activity when subjected to heat. There is a marked difference in the amount of surface activity depending upon the rate of heating. Dimensional stability is more pronounced at high rates of heating (131).

---

*The effect of moisture on physical properties and ignition has been investigated by M. Duvvuri at the Flame Dynamics Laboratory, Oklahoma University Research Institute.

Based upon the eleven above assumptions, the energy balance for a one-dimensional, diathermaneous solid undergoing thermal decomposition, melting and/or vaporization can be defined as follows:

$$Q_{in} - Q_{out} = Q_{end} - Q_{beginning} = Q_{accumulation} \quad \text{(II-4)}$$

With one-dimensional flow, it must be assumed that all gases flowing through any developed porosity in the solid are in temperature equilibrium with the remaining solid contacted. Further, assume a reference temperature $T_o = 0°K$ so that $T_s - T_o = \Delta T = T_s - 0 = T_s$. Equation II-4 can best be illustrated, for some time period Δt and thickness Δx, as indicated in the following sketch in which the heat flow is transmitted through a rectangular section of area A.

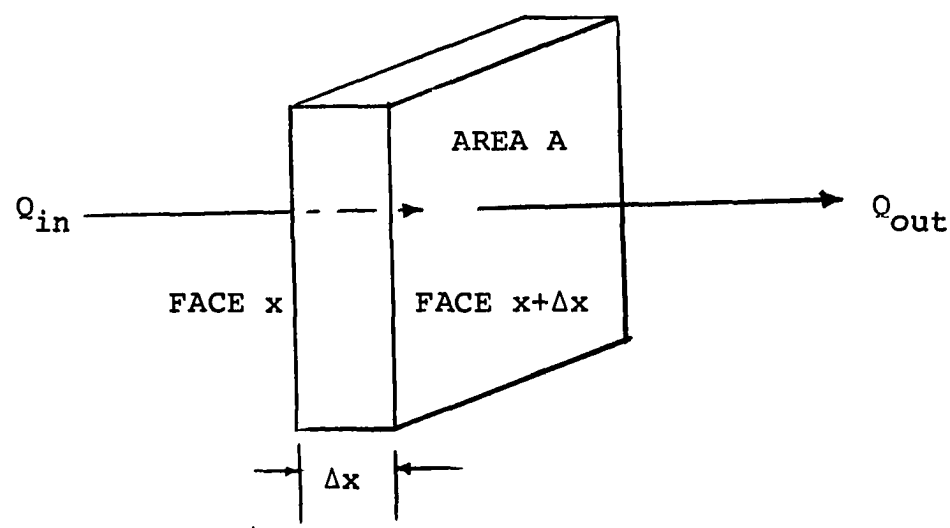

The heat energy flowing into the element of Area A at face x is

$$-k_{in}\left(\frac{\partial T_{in}}{\partial x}\right) A\Delta t = \text{conductive heat input} \qquad \text{(II-5)}$$

$$He^{-\gamma_\lambda x} A\Delta t = \text{radiant heat input} \qquad \text{(II-6)}$$

$$m_{din}\, C_g T_{in}\, A\Delta t = \text{heat input due to flow of pyrolysis gases} \qquad \text{(II-7)}$$

The heat energy flowing out of the element of Area A at face x + Δx is

$$-k_{out}\left(\frac{\partial T_{out}}{\partial x}\right) A\Delta t = \text{conductive heat out} \qquad \text{(II-8)}$$

$$He^{-\gamma_\lambda (x+\Delta x)} A\Delta t = \text{radiant heat leaving thickness } \Delta x \qquad \text{(II-9)}$$

$$m_{dout}\, C_g T_{out}\, A\Delta t = \text{heat out due to flow of pyrolysis gases} \qquad \text{(II-10)}$$

For the heat energy at the end of the accounting period

$$\rho_E C_p T_E A\Delta x = \text{sensible heat content of element} \qquad \text{(II-11)}$$

$$\omega_{VE}\Delta H_v A\Delta x = \text{heat of vaporization} \qquad \text{(II-12)}$$

$$\omega_{fE}\Delta H_f A\Delta x = \text{heat of fusion} \qquad \text{(II-13)}$$

$$\omega_{zE} Q_z A\Delta x = \text{heat of pyrolysis} \qquad \text{(II-14)}$$

For the heat energy at the beginning of the accounting period

$$\rho_B C_p T_B A\Delta x = \text{heat content of element} \qquad \text{(II-15)}$$

$$\omega_{VB} \Delta H_V A\Delta x = \text{heat of vaporization of element} \qquad \text{(II-16)}$$

$$\omega_{fB} \Delta H_f A\Delta x = \text{heat of fusion of element} \qquad \text{(II-17)}$$

$$\omega_{zB} Q_z A\Delta x = \text{heat of pyrolysis of element} \qquad \text{(II-18)}$$

By means of the standard mathematical processes for grouping terms and use of the limiting process, we obtain, assuming ΔH_V, ΔH_f and Q_z constant,

$$\frac{\partial}{\partial x}\left(k \frac{\partial T}{\partial x}\right) + H\gamma_\lambda e^{-\gamma_\lambda x} - \frac{\partial (m_d C_g T)}{\partial x} = \frac{\partial (\rho C_p T)}{\partial t} + \Delta H_V \frac{\partial (\omega_V)}{\partial t} + \Delta H_f \frac{\partial (\omega_f)}{\partial t} + Q_z \frac{\partial (\omega_z)}{\partial t} \qquad \text{(II-19)}$$

The rate of weight loss due to decomposition is

$$\frac{\partial (\omega_z)}{\partial t} = f\left[\omega_z \exp\left(-\frac{\Sigma E}{RT}\right)\right] \qquad \text{(II-20)}$$

assuming a first order decomposition.

It must be noted that ρ is assumed to vary because of the weight loss due to vaporization and decomposition, as shown by

$$\frac{\partial \rho}{\partial t} = \frac{\partial (\omega_V)}{\partial t} + \frac{\partial (\omega_z)}{\partial t} \qquad \text{(II-21)}$$

It is assumed that although melting occurs, there is no liquid flow.

Equation (II-19) differs from the associated Equation of Koohyar (70) by the parameters $\frac{\partial(\omega_V)}{\partial t}\Delta H_V$, $\frac{\partial(\omega_f)}{\partial t}\Delta H_f$, $\frac{\partial}{\partial x}(k\frac{\partial T}{\partial x})$ and ΣE, which represent the factors of energy loss due to vaporization, energy loss due to melting, variable thermal conductivity and the total activation energy respectively.

With unidirectional heat flow and heat transmission by conduction, the initial condition for a semi-infinite material assumed to be at a uniform ambient temperature is $\Delta T = 0$, for any time, $t \leq 0$.

For conditions at $t > 0$, with the front face being heated by radiation, the boundary condition at $x = 0$ (the front face) is

$$-k \frac{\partial T_s}{\partial x} = H - Q_c - Q_s \qquad \text{(II-22)}$$

where $H = \alpha_{av} H_o$ is the heat available for both absorption at the element surface and for penetration into the element by Lambert's law. $-Q_c = h_c A \Delta T$ is the convective heat loss due to gases passing over the front face and $-Q_s = \sigma \varepsilon T_s^4$ is the Stephan-Boltzmann reradiation from the heated front face.

The boundary condition at $x = L$ is

$$\frac{\partial T_L}{\partial x} = f(-Q_L - Q_c) \leq 0 \qquad \text{(II-23)}$$

These further conditions create an even greater complexity to the already complicated mathematical expression. Until more information is obtained concerning ignition, Equation II-19 will remain unsolvable.

For Equations II-19 through II-23 the parameters represented are denoted as

k = thermal conductivity

γ = Lambert's law attenuation factor

C_g = average heat capacity of volatile products

m_d = rate of mass flow of decomposition gases per unit area

ΔH_V = latent heat of vaporization

ω_V = mass of vaporizable polymer per unit volume

H = unreflected, or absorbed radiation

T = absolute temperature

t = time

x = distance

Q_c = convective heat transfer

ω_f = mass of meltable polymer per unit volume

ΔH_f = latent heat of fusion

ω_z = mass of decomposible polymer per unit volume

Q_z = heat of pyrolysis (assumed to be of first order) per unit mass

σ = Stephan-Boltzmann constant

ρ = density

C_p = heat capacity of solid

ΣE = total activation energy; $\Sigma E = E_d + E_\ell + \ldots$ where

d = depolymerization, ℓ = random chain scission,...

$\frac{\partial \omega}{\partial t}$ = rate of weight loss

h_c = convective heat transfer coefficient

R = universal gas constant

f = frequency factor

A = area

ω = weight of polymer

ε = emissivity

Subscripts used indicate the following:

g = decomposition gases

V = vaporization

o = initial

f = fusion

z = pyrolysis

d = decomposition; depolymerization

Bamford, et al. (8) were one of the first research groups to study the theoretical combustion of wood by means of the general heat equation

$$k \frac{\partial^2 T}{\partial x^2} = C_p \rho \frac{\partial T}{\partial t} + Q_z \frac{\partial \omega_z}{\partial t} \qquad \text{(II-24A)}$$

which included the unimolecular rate of

$$-\frac{\partial \omega}{\partial t} = f[\omega \exp (-\Delta E/RT)] \qquad \text{(II-24B)}$$

Simms, et al. (119) were interested in the variation of ignition time due to wood sample size where the wood was subjected to radiant heating, while Blackshear (13) studied the rates of ablation from wooden samples that were being pyrolyzed at both low and high heating rates.

Thomas, et al. (125, 126) studied the aspects of self-heating and ignition of solid cellulosic materials based upon the assumption of heat generation within a conducting solid.

In one of the latest studies, Adomeit (3) was concerned with the ignition of gases at hot surfaces under conditions of non steady-state flow.

Analytical Studies of Ignition Characteristics

As this survey demonstrates, many investigators have been interested in the phenomenon of ignition, particularly of wood. During the past several years, interest in pyrotechnic ignition has also developed. The work of Bamford, et al. (8) was especially reviewed by those later investigators who were interested in material other than wood and frequently used the basic Equation II-24 as an initial starting point for their own analysis.

Lawrence (74) was concerned with the analytical study of materials exposed to high intensity thermal radiation. During his own literature search he found that most previous experimental work and analysis had been concerned with exposure of slabs to high intensity thermal radiation, using one-

dimensional heat flow theory, but excluding material decomposition. Lawrence, however, proposed to investigate the heat transfer problem based upon the following assumptions.

1. Heat transfer to the surface of the slab was totally by radiation.
2. All heat losses must be accounted for. The irradiated surface has heat losses from convection and reradiation; the rear surface of the slab has convection and radiation losses.
3. The slab was initially at a uniform temperature, T_a, the air temperature.
4. The surface convective heat transfer coefficient remained at some constant, average value.
5. The surrounding ambient temperature remained constant.
6. The material was dry and isotropic.
7. Thermal conductivity was independent of temperature.
8. The extinction coefficient was constant, independent of position within the solid or of the spectral quality of the incident radiation.
9. The intensity of the unreflected radiation at the face of the slab was uniform with respect to position. However, because of reradiation, the intensity would vary with time.
10. The slab dimensions remained constant for the whole heating period.
11. Heat of decomposition remained constant.

12. The net effect of the reactions including thermal decomposition could be illustrated by a first order reaction.
13. The rate at which the gaseous decomposition products escaped to the surface was controlled by the rate of decomposition.
14. The thermal constants of the solid and its non-volatile decomposition products were equal.

Lawrence (74) found that as the intensity of radiation was increased, the rate of temperature rise at the irradiated surface approached a maximum limiting value. In addition, the assumption of constant dimensions was not true for plastics since thermal decomposition and phase change did cause changes in the dimensions. Lastly, Lawrence was unable to substantiate the assumption of first order reaction for the thermal decompostion. The pyrolysis involved a combination of both non-flammable and combustible gases, indicating the complexity of the combustion process and thermal degradation reaction.

Lawrence's assumptions include several items that are incorrect or do not define all of the pertinent parameters. Item 4, constant surface convective heat transfer coefficient, may change due to the expulsion of pyrolysis gases from the face of the sample. For Item 7, the thermal conductivity is not necessarily independent of temperature. Polymers soften and decompose and thus change the conductivity. Item 8, constant extinction coefficient, is not always true. The extinction coefficient is dependent on wavelength. In addition many

polymers and other materials have a surface change during heating which can change the coefficient. Item 9, the intensity of the unreflected radiation with respect to position, can be maintained by means of the experimental technique but the source intensity will vary with temperature. The heat of decomposition, Item 11, does not necessarily remain constant. Item 14, thermal constant equality, is not true. Carbon, as a decomposition product, does not have the same thermal properties as a polymer.

Williams (134) continued with and extended the work of Lawrence (74) towards the development of quantitative prediction of the temperature-space-time relationships in the period prior to the inception of thermal damage. While using the same assumptions as Lawrence (74), Williams (134) was more concerned with sample diathermancy/transparency, and the magnitude of heat losses from the back and heated faces of a finite slab. To this extent, he listed the independent variables most concerned with the temperature-space-time relationship as the following

$$T = f(x_\ell, t, H, \rho, C_p, k, L, h_c, \gamma_1, \gamma_2, \cdots \gamma_n, F_1, F_2, \cdots F_n) \qquad \text{(II-25)}$$

where

T = temperature

x_ℓ = the distance below the irradiated surface

t = time

H = intensity of unreflected radiation

ρ, C_p, k = density, specific heat and thermal conductivity, repectively

L = slab thickness

h_c = convective heat transfer coefficient

γ_1, γ_2,... = extinction coefficients for wavelength λ_1, λ_2, ...

F_1, F_2,... = fraction of incident energy associated with extinction coefficient, γ_1, γ_2, ...

λ = wavelength

Considering all of the factors of Equation II-25 Williams (134) initiated his studies with the basic Equation

$$k \frac{\partial^2 T}{\partial x^2} + H\gamma e^{-\gamma x} = \rho C_p \frac{\partial T}{\partial t} \qquad \text{(II-26)}$$

Inherent in the relationship proposed by Equation II-26 are the assumptions that (1) any effects due to moisture migration and chemical reaction prior to damage initiation are negligible and (2) penetration of radiant energy into the sample may be characterized by a Lambert's law decay expression of the form

$$H_x = He^{-\gamma x} \qquad \text{(II-27)}$$

Williams (134) found upon subjecting a sample of polyester plastic to high intensity solar radiation and radiation from a graphite-resistance furnace that the resultant predicted temperature patterns indicated close correlation to

those found by experiment. From tests made on the polyester plastic, he concluded that (1) diathermancy of the material to infrared radiation in the source temperature range of 1650°-2000°K can be characterized by a single extinction coefficient in the range of 2-4 cm^{-1}, (2) the different response of the plastic to the lamp, solar and carbon furnace radiation can be attributed to spectral variations in the sample diathermancy and that a region of maximum diathermancy exists in the 1.0 to 1.7-micron wavelength region.

The analysis performed by Williams indicated that absorbed radiation, H, is dependent upon the intensity of the heat source, but he overlooked the fact that H also depends upon the monochromatic absorptance of the material itself (a discussion of average absorptance can be found in Appendix D). The effect of chemical action prior to damage initiation cannot be neglected. The thermal properties of materials are not necessarily constant and the dimensions of a test specimen do not remain fixed.

Analytical studies and investigations have continued towards obtaining mathematical models of ignition. Several examples of this continued study are presented in the following discussion. It must be noted that no attempt will be made to critique the various investigations, since the method of heating or the testing environment is different from those of the previous authors cited and, in addition, is different from the test method of the present study.

Gray and Harper (44) proposed another approach for the mathematical solution of the ignition problem based upon heat transfer by conduction only. First they approximated the non-linear term of chemical decomposition. They then attempted to solve the problem analytically. Two forms of approximation were chosen:

1. Exponential approximation where the argument of the exponential term was expanded in Taylor's series in $(T - T_o)$ and higher order terms were neglected, resulting in

$$\Delta E/RT \simeq \Delta E/RT_o - (T-T_o)\ \Delta E/RT_o^2$$

Thus $$\exp(-\Delta E/RT) \simeq \exp(-\Delta E/RT_o)\exp(y) \qquad \text{(II-28)}$$

where $$y = (T-T_o)\ \Delta E/RT_o^2$$

2. Quadratic approximation where exp (y) was replaced by a quadratic expression

$$\exp(-\Delta E/RT) \simeq \exp(-\Delta E/RT_o)[a + by + cy^2] \qquad \text{(II-29)}$$

where a, b and c were constants. These authors also proposed further approximations by neglecting the spatial temperature variation, this approximation being valid for thin materials.

Weatherford and Sheppard (130) proposed the concept of a "thermal feedback wave" when a plane slab is exposed to symmetrical convective heating. Upon exposure, the slab surface instantly experienced a heat flux, which, as the initial thermal heating continued, was visualized as moving back

through the slab to the heated surface (counter-current to the net heat flux) by a random self-diffusion process. The authors found that the criterion of a fixed surface temperature did not adequately define ignition.

Smith (120) was concerned that all of the reported evaluations of ignition with incident heat flux disregarded the aspect of specimen reflectance. As he stated, "The reflectance of a species was apparently regarded as a fixed characteristic which might well be taken into account directly in the ignition time." To overcome this apparent deficiency, Smith proposed a numerical relationship in which the retained heat flux or that portion of the incident heat flux which is used to raise the temperature of the irradiated specimen was the desired quantity.

Smith found from both radiant lamp and flame testing that:

1. There was a significant difference in the ignition tests based upon reflectance losses.
2. Lamp filament temperature and distance between a test specimen and lamps for a given lamp heat flux have an important effect on heating rate.
3. There was insufficient data for comparison of various investigators' reported ignition times.
4. Manufacturer's calibrations of heat flux gages were in poor agreement.

In summary of this formal analysis concerning ignition characteristics it has been found that certain parameters are most influential on the heat transfer phenomena and combustion properties of a plastic. These parameters are the absorptance and absorptance change of the material surface, the degradation energy of the polymer, the rate and type of degradation with respect to the heat input, ignition temperature, and thickness of material and the change in value of density, thermal conductivity and specific heat with temperature. Such parameters must be investigated and data obtained before any formal analysis of ignition can be completed.

A Summary of Ignition Testing

The literature review yielded, in particular, evidence that much study and analysis is lacking in the area of plastic ignition characteristics. It was found that definition of ignition and/or flammability was dependent on the particular test performed, and there was still much disagreement as to what test should be made to determine the flammability of a plastic. Theoretical analyses have been conducted, based on a unit absorptance, upon a material that was being subjected to radiant heating. In general, it can be said that little or no correlation has been found among the several and varied methods used in determining ignition characteristics of a plastic material.

CHAPTER III

EXPERIMENTAL METHOD

The work performed previously by Koohyar (70), Welker (131), and Wesson (132) utilized an ignition cabinet in which both flame radiation and tungsten lamps were used as a source of radiant heat. In order to maintain a correlation among the various materials tested, the same cabinet was used for the present research program.

Test Apparatus

Figure III-1 shows the front and left side of the ignition cabinet, while Figure III-2 shows the rear and right side of the cabinet. The cabinet was fabricated of galvanized sheet steel with glass wool insulation on the inside walls; the overall dimensions were 5 ft wide, 3 ft deep and 7 ft high with an open top and bottom. The windows in the cabinet, Figures III-1 and III-2, were Herculite tempered plate glass, to be used both for visual observation and photography. Herculite was used because of its thermal endurance capability of 210°C differential temperature and ability to be used safely to a maximum working temperature of 290°C. In the present study, only one side of a sample was irradiated. Figure III-3

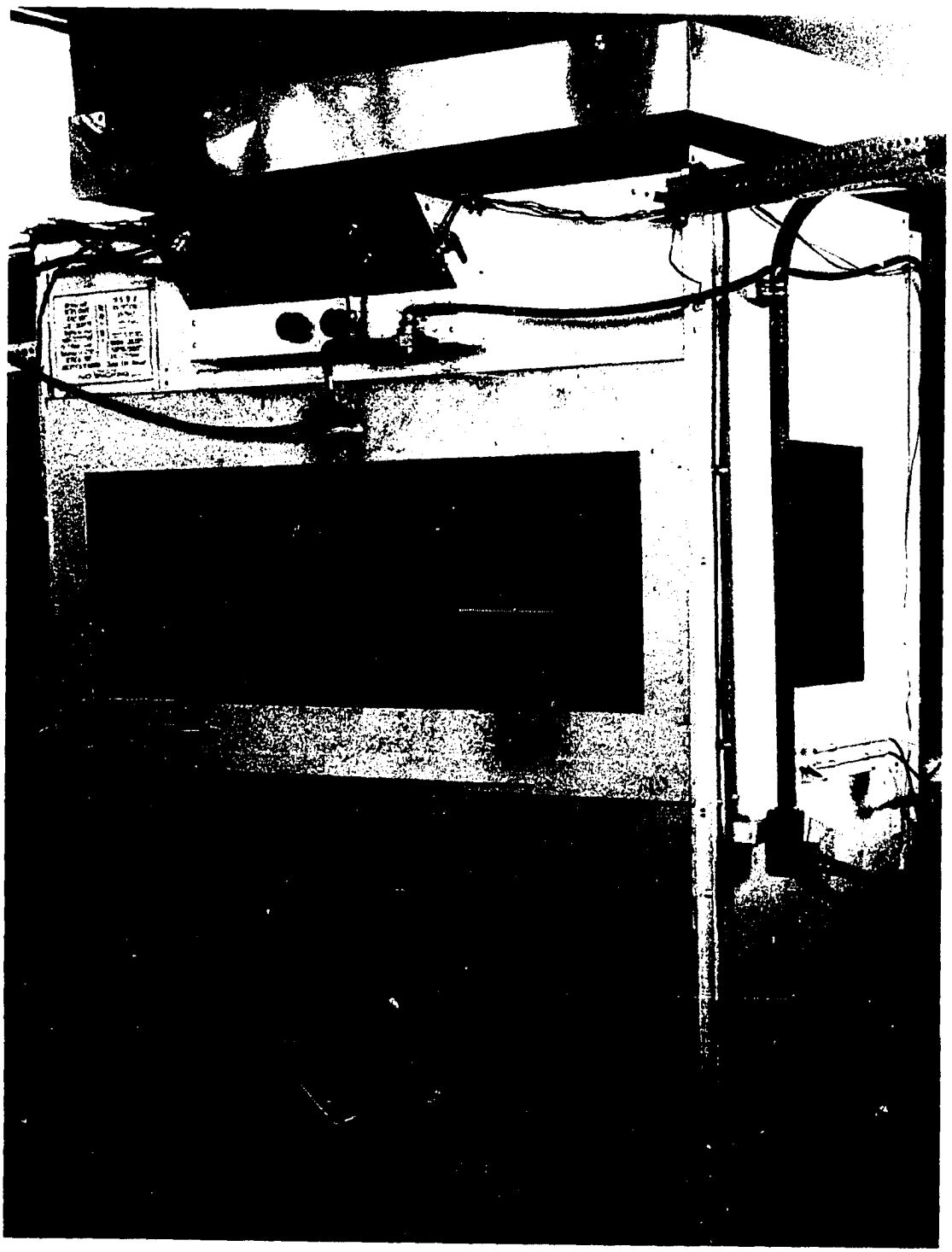

Figure III-1. Front View of the Ignition Cabinet.

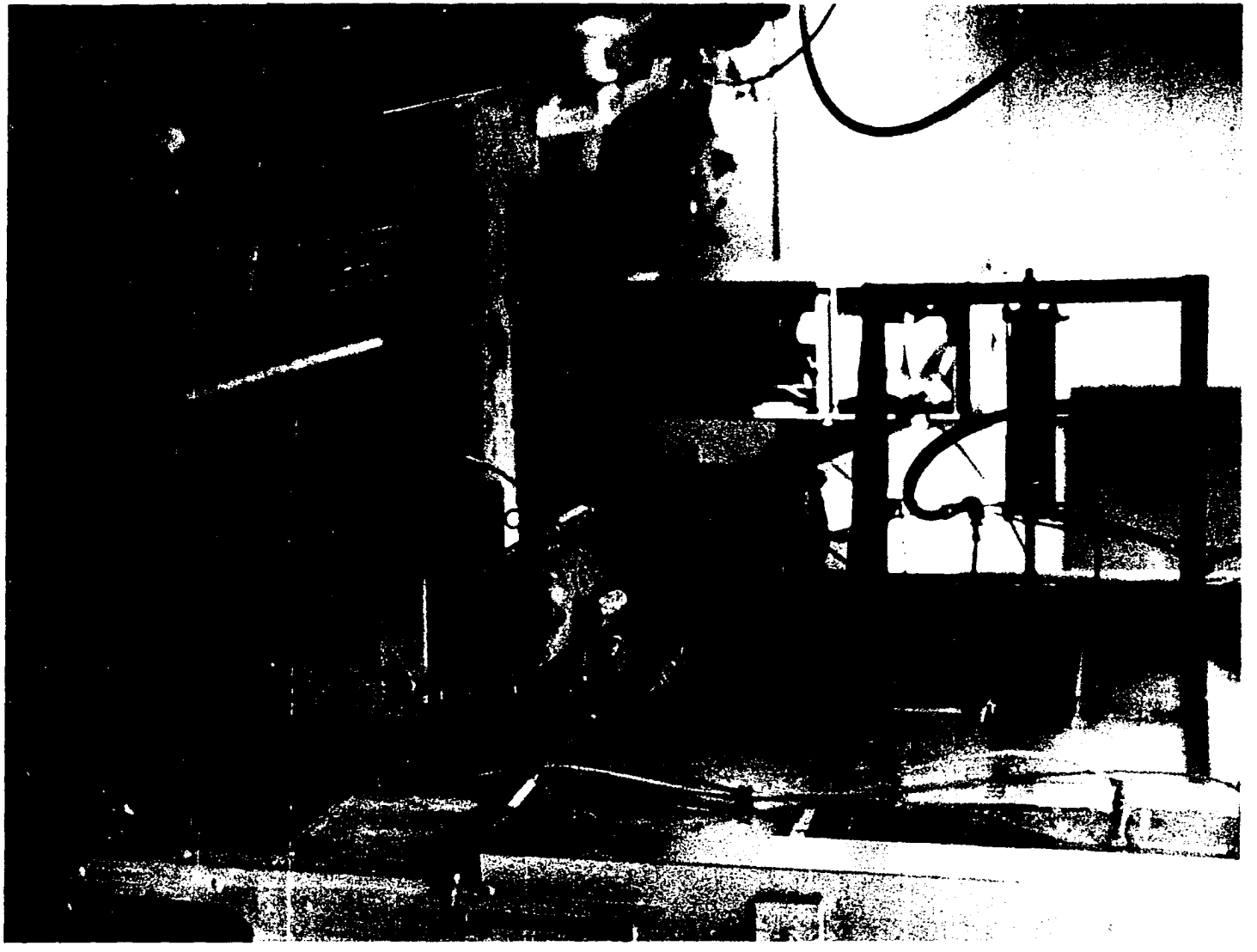

Figure III-2. Rear View of the Ignition Cabinet.

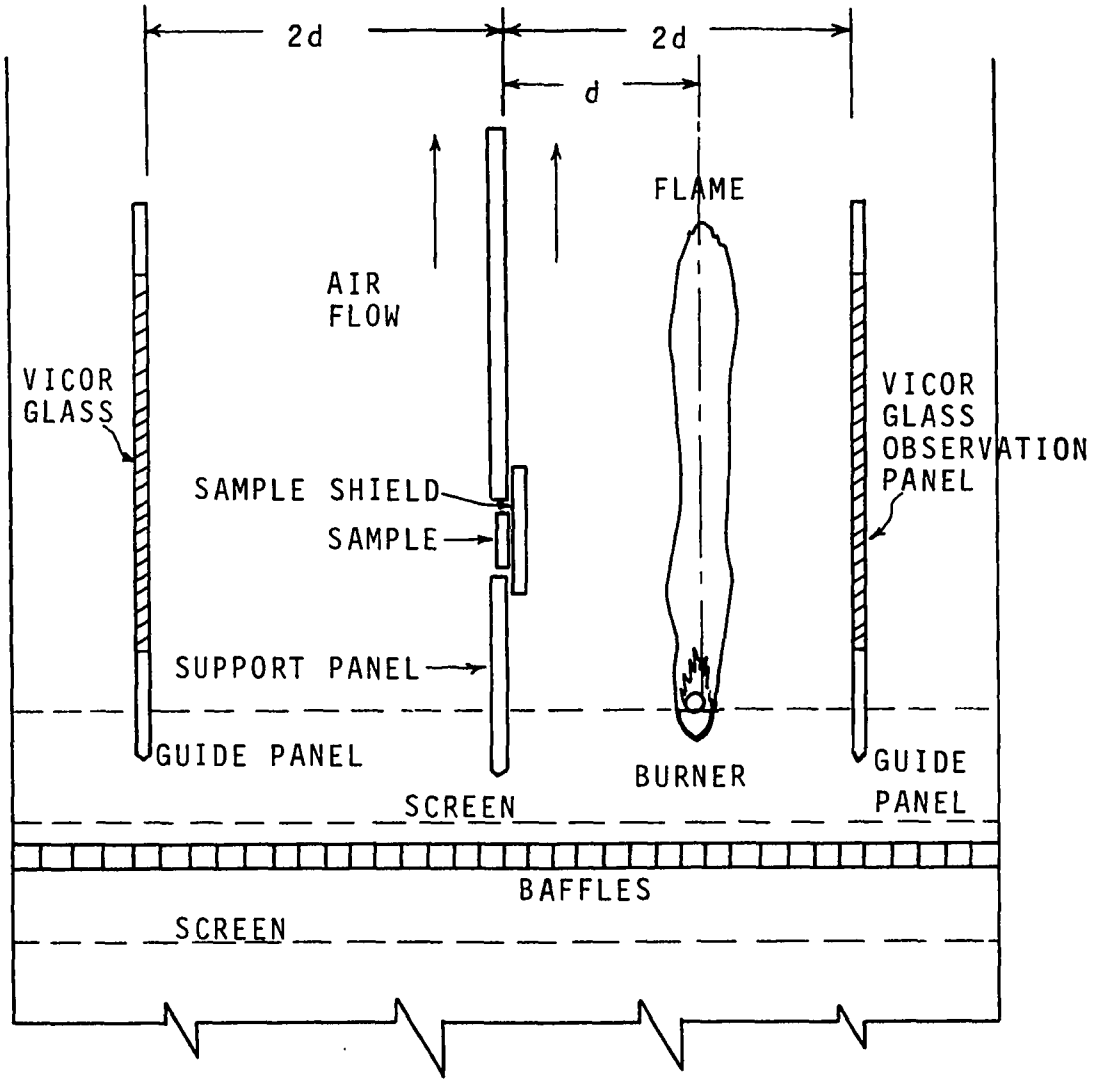

Figure III-3. Schematic Diagram of Single Burner Ignition Cabinet Tests.

diagrams the single surface type radiation tests. The sample material (target) was supported within a stationary vertical panel of "Fiberfrax" laminated ceramic board, designated as the support panel. A channel burner was mounted on a worm gear attached to the front and back sides of the cabinet (see Figure III-3). The burner, fabricated of galvanized steel, was approximately two inches wide and 20 inches long, with an oxygen feed tube placed at the top of the burner channel, along the axis of the burner as shown in Figure III-4.

It was found from previous tests (131, 132) that, in order to develop higher heat fluxes, the previous flame system (70) required oxygen stimulated burning. For this design the oxygen-fuel fire is capable of providing an incident irradiance level of 3.4 cal/cm^2-sec. Figure III-5 diagrams the O_2 supply system.

Koohyar (70) found that when a flame was brought near a wall, the flame tended to lean toward the wall. To counteract this flame bending, another panel of "Fiberfrax" laminated ceramic board, designated as a guide panel (Figure III-3) was mounted on one side of the sample support panel, outboard from the burner. To facilitate sample observation from the end of the cabinet, the guide panel had a "Vicor" glass panel inserted along the panel centerline. The "Fiberfrax" sample panel, 2 1/2 ft high, 2 ft wide and 1/2 inch thick, and the guide panel, 2 ft high, 2 ft wide and 1/2 inch thick, both consisted of laminations of "Fiberfrax" paper with an inorganic

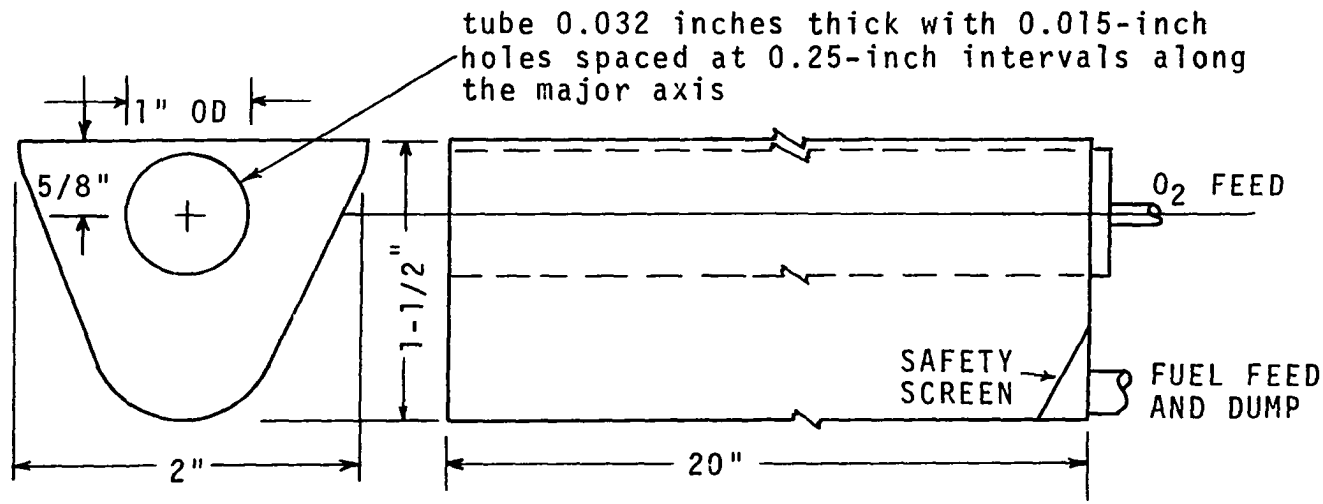

Figure III-4. Diagram of Burner Channel with O_2 Feed Tube.

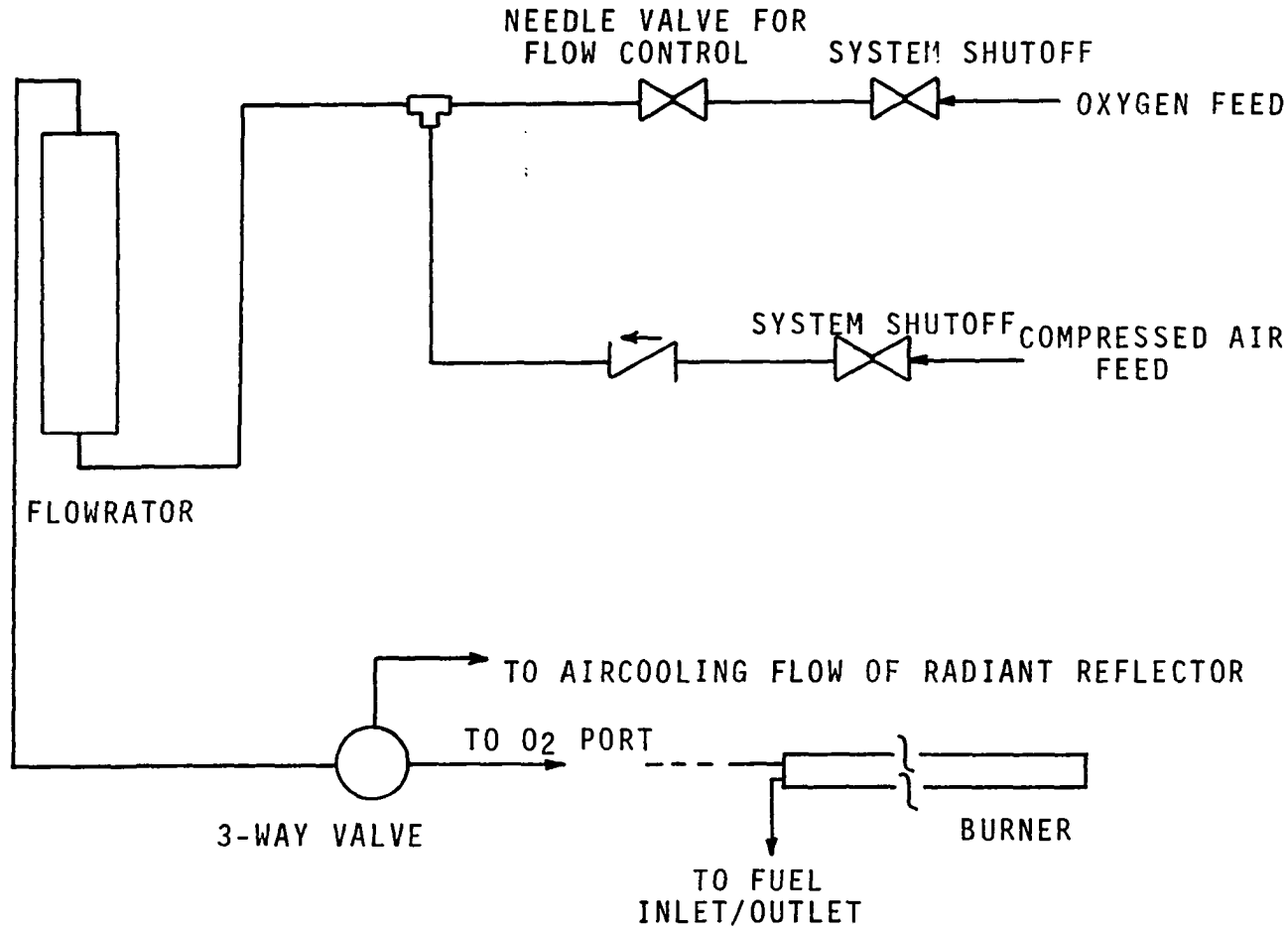

Figure III-5. Schematic Showing the O_2 Supply System Used to Increase the Burner Output.

binder which provided a rigid structure. A subsequent treatment of organic binder provided increased strength and resistance to surface erosion. As received, the panels could be used continuously up to 1260°C and at higher temperatures with intermittent use. The "Fiberfrax" panel has shown good resistance to thermal shock and has provided excellent thermal insulation, since its thermal conductivity has been given as 1.4×10^{-4} cal/cm-sec-°C/cm with a density of 50 lb/cu ft. The "Vicor" glass, being capable of withstanding a maximum working temperature of 1200°C, was chosen for the observation windows.

In order to increase or decrease the irradiance level during the tests, a worm gear drive was provided which would move the channel burner toward or away from the sample. The guide panel was also connected to a parallel worm gear in such a manner that the distance from the guide panel to the sample was always twice the distance from the sample to the burner (Figure III-3). Motive power for the burner and panel was furnished by a 115 V AC reversing-type motor, with suitable reduction gearing. The motor controls were mounted on the face of the cabinet so that visual placement of the burner could be performed (Figure III-1).

Early tests of the cabinet air flow showed that the flame tended to flicker (70). To decrease the flame flicker, provide smooth air flow across the sample, and remove gases and smoke from the cabinet during tests, an exhaust fan was

mounted in the hood above the cabinet, as shown in Figure III-1. In addition, the fan drew air into the cabinet for fuel combustion. A steady sheet of flame was obtained by (1) adjusting the position of a damper in the exhaust line and (2) passing the air flow through a specially designed honeycomb section fastened below the burner and the two panels. The bottoms of the burner and panels were curved to provide a streamline effect of the air flow around them, while screens were placed above and below the honeycomb to decrease the air turbulence.

The fuel used in the present test program was benzene and was supplied by the system as diagrammed in Figure III-6. The supply tank was a 6-inch diameter aluminum pipe of 5 gallons capacity mounted on the left side of the cabinet (see Figure III-1). The supply tank and burner system used the principle of a constant head siphon to provide a constant fuel level in the burner; the fuel in the supply line acted as a seal between the burner and the supply tank. The end of the breather tube was positioned in the supply tank to give the desired fuel level in the burner. As the fuel level in the burner decreased during burning, the fuel flowing out of the supply tank caused a slight vacuum which, in turn, caused an air flow through the breather tube and eventually provided a balanced pressure. The five-gallon supply of benzene sustained approximately one hour of burning.

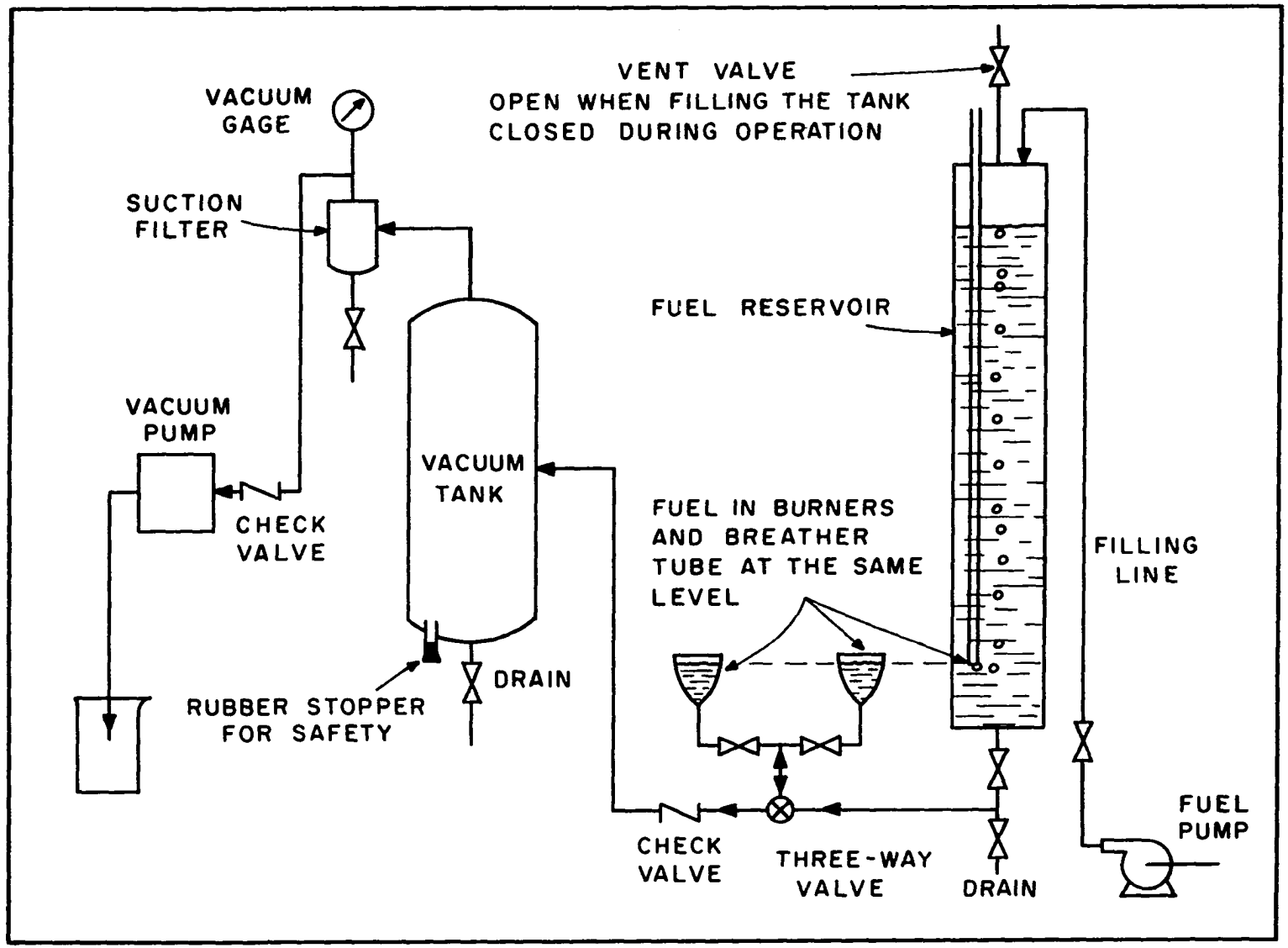

Figure III-6. Schematic Showing the Fuel Supply System to the Burner.

The design of the fuel system used all brass valves with Teflon seals except for the inlet to the burner. Fuel supply lines, fill lines, and dump lines were fabricated from copper tubing and steel pipe. There was a short section of rubber tubing from the fill-dump valve to the burner to permit burner movement.

After sample ignition, unless further heating of the sample was desired, it was necessary to extinguish the flame. This extinguishment was accomplished by switching the three-way control valve to dump position, which then permitted the vacuum system to draw the fuel from the burner and dump it into the holding tank. With proper operation of the vacuum system, the flames were normally extinguished within 10-15 seconds. When flames persisted, a metal cap was placed over the burner which gave immediate extinguishment.

Certain safety precautions were followed during all flame radiation tests, which were similar to those given by Koohyar (70), and are as follows:

1. Flame flash-back to the vacuum holding tank was prevented by the use of a screen installed over the fuel inlet port to the burner.
2. During all flame testing, the vacuum pump was in operation to maintain a reduced pressure system; system vacuum pressure was approximately 24 in mercury.
3. Check valves were installed at the downstream position of the three-way valve and upstream of the vacuum pump

to provide a line blockage in case of fire or explosion in the vacuum tank. These check valves were redundant to the screen of Item 1. See Figure III-6.

4. A rubber stopper was inserted into the bottom of the fuel holding tank and held in position by vacuum, where the stopper functioned as a tank vent in case of fire in the holding tank itself. See Figure III-6.
5. Sand bags were placed around the outer perimeter of the ignition cabinet in case of fuel spillage. See Figure III-1.
6. A fire blanket and extinguishers were kept in close proximity to the cabinet.
7. First aid equipment was placed within reach in case of minor burns from hot samples or flame flashback during the extinguishing procedure.

Tungsten Lamp System

The ignition characteristics of a material do not necessarily agree when subjected to different sources of heat. The spectrum of a flame, as shown in Figure III-7, indicated that its spectral distribution of energy is not the same as the energy spectrum from a 1000-watt tungsten lamp heat source. The hexane emissive power data of Ryan, et al. (110), were used because no data could be found for benzene. It was assumed* that the emissive powers of benzene and hexane would have similar characteristics. The tungsten source data are

*Based upon the research data of Koohyar (70) and Wesson (132).

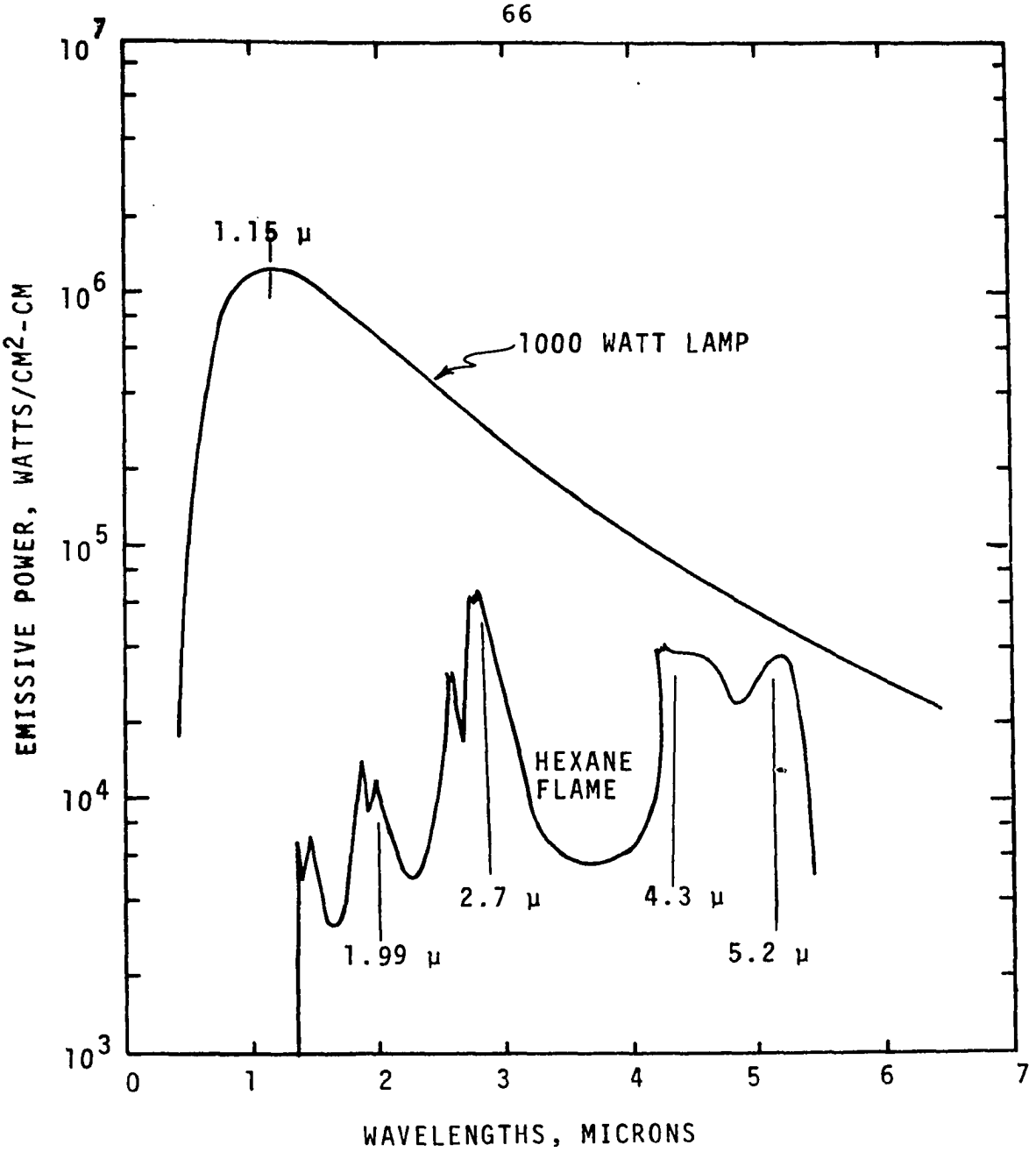

Figure III-7. Comparison of Energy Peaks for a Hexane Flame and a Tungsten Lamp.

calculated from the 2500°K operating temperature as specified by the manufacturer.* As shown in Figure III-7, the two curves are not alike so that additional testing using the tungsten lamps had to be performed to study the effects of the two energy sources on the same material.

A radiant lamp heat source was provided by the use of an 8-lamp radiant reflector as shown in the photograph of Figure III-8. Each tungsten lamp required 1000 watts. The 8-lamp reflector was capable of providing a heat source up to 3.5 cal/cm^2-sec incident irradiance. In order to provide an equivalent testing system the radiant reflector was mounted on the benzene burner channel as illustrated in Figure III-9. Mounting the reflector upon the burner permitted the movement of the reflector forward or backward and thus enabled the variation of radiant flux to any desired level upon the sample.

Power to the heaters was provided by a 230 V AC circuit through a manual switch fused for 60 amps. Cooling of lamp ends and power leads was provided by a low velocity air flow, the velocity being adjusted with a needle valve and monitored by passage through a flowrator. This air cooling system is diagrammed schematically in Figure III-10.

Sample Protection

At the initiation of the burner fire or the application of power to the radiant reflector, there was a finite

---

*General Electric Quartz Infrared Lamps, types 2M/T3/1CL/HT--230-250V and 1000T3/CL/HT--230-250V.

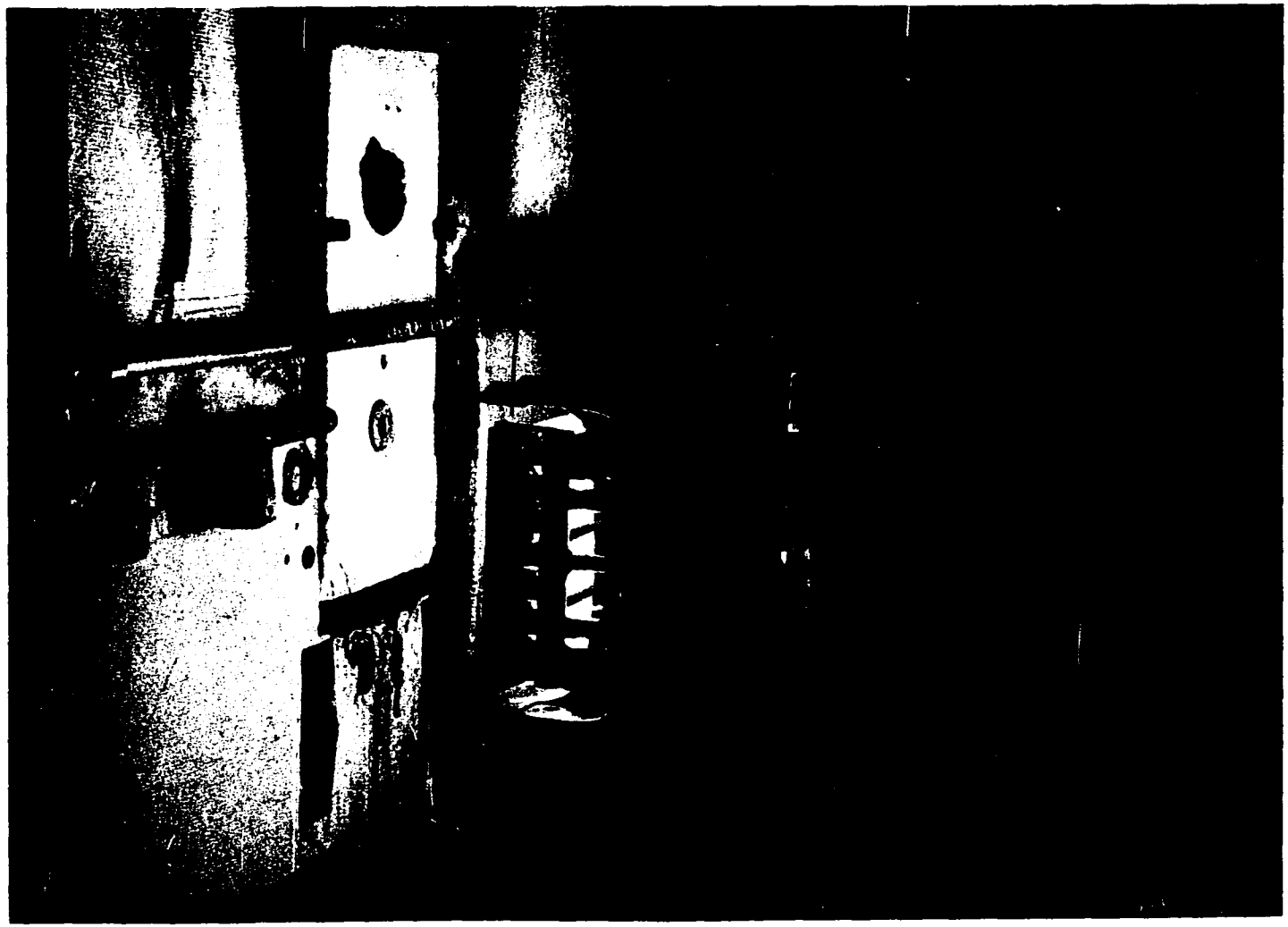

Figure III-8. Radiant Reflector.

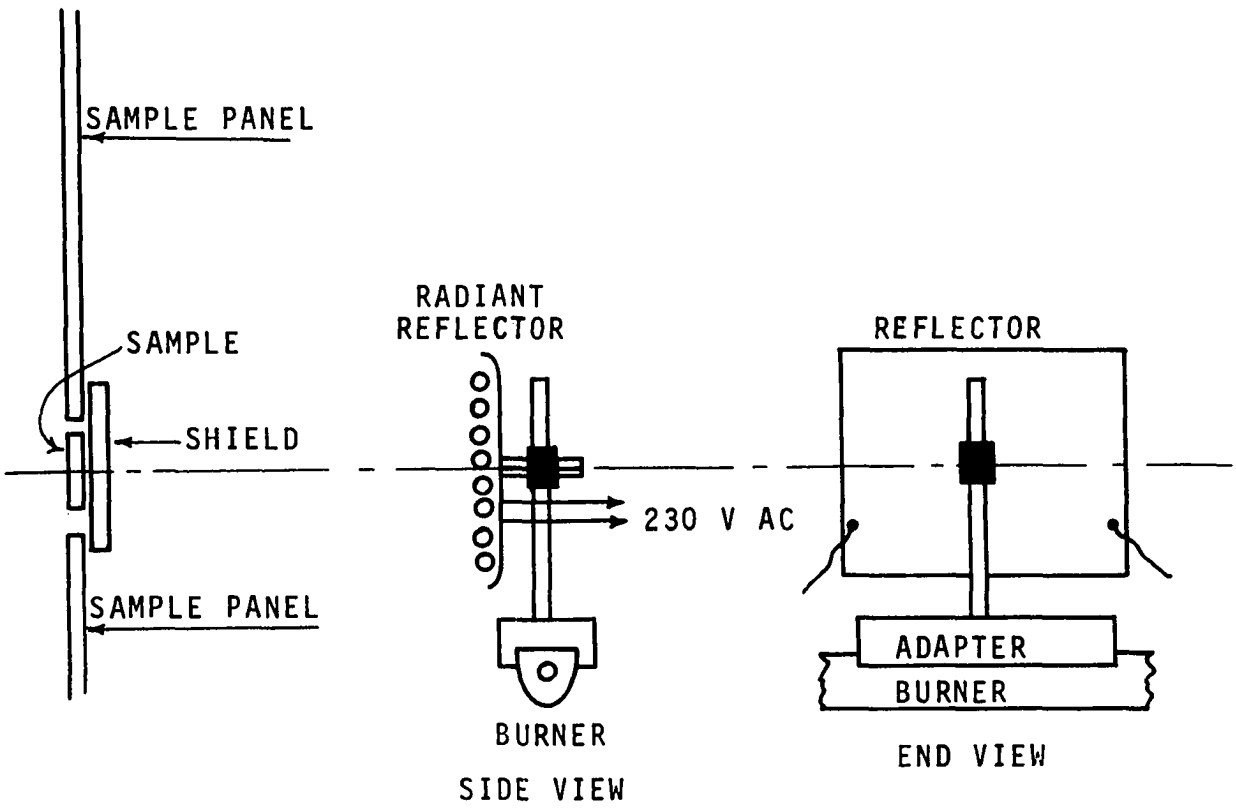

Figure III-9. Installation of 8-Lamp Radiant Reflector.

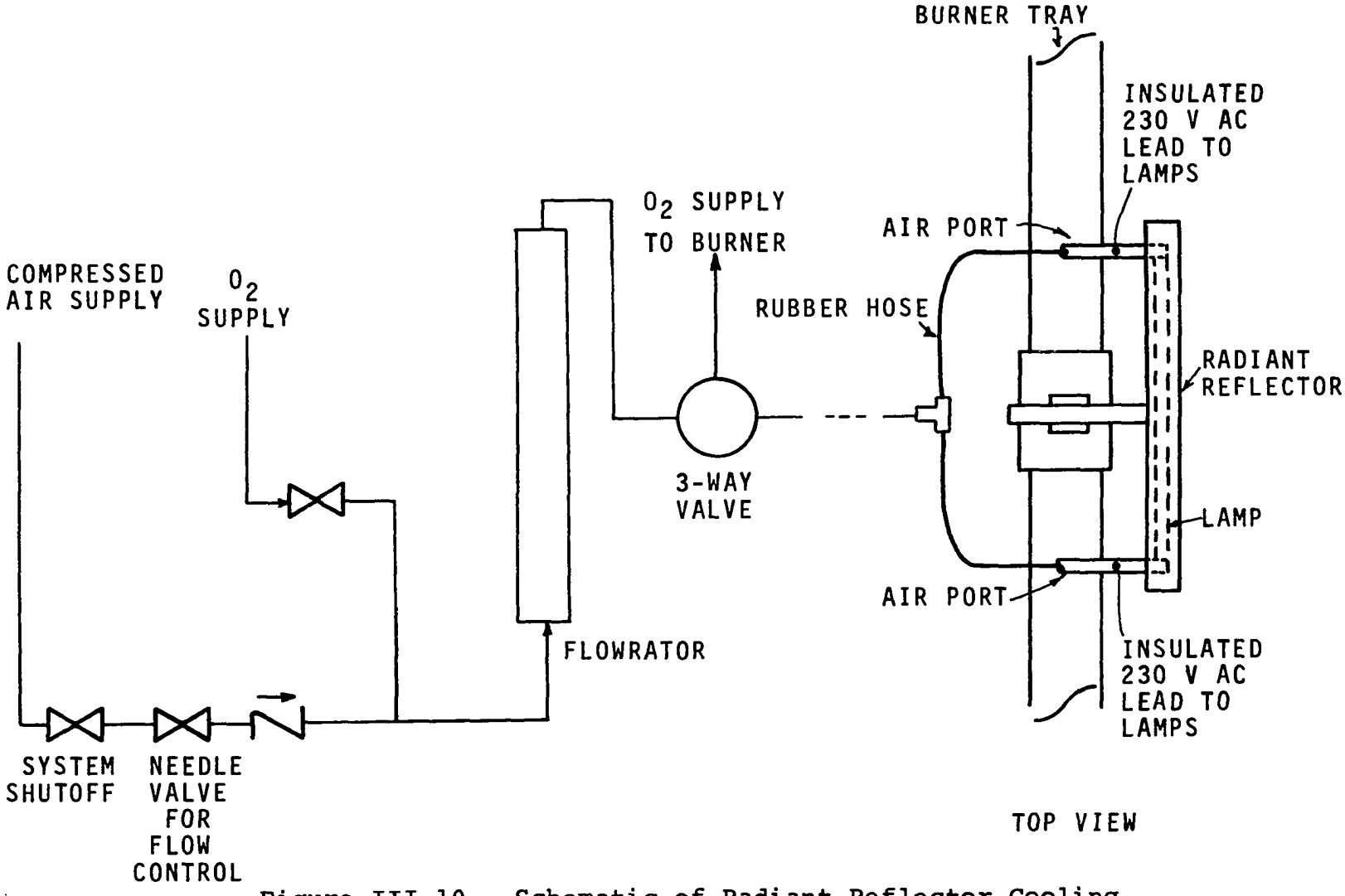

Figure III-10. Schematic of Radiant Reflector Cooling System.

time necessary for both heating systems to reach a steady state flux level. For both systems, the sample had to be protected from the non-steady flux until steady state was attained. This was accomplished by the use of a movable water-cooled shield as illustrated in Figure III-11.

The shield was fabricated with sides of aluminum sheeting with a water cooling passage inside. The shield was positioned by two guide rails and was maintained in either the forward or rearward position by mechanical stops. Motive power for rearward movement was provided by a compressed air cylinder at the rear of the cabinet. The photograph of the rear of the cabinet, Figure III-2, shows the physical attachment of the cylinder to the shield. The shield was manually positioned in front of the sample, and after the radiant heat flux (flame or lamp source) had attained a steady value, operation of a three-way air valve on the cabinet front permitted air flow to the actuating cylinder and the shield moved to the rear of the cabinet. The shield movement to the cabinet rear required approximately 1/10 second so that the exposure to radiation was essentially of a square-wave form. Figures III-12 and III-13 illustrate the positioning of the shield closed, for sample protection, and open, for test, respectively.

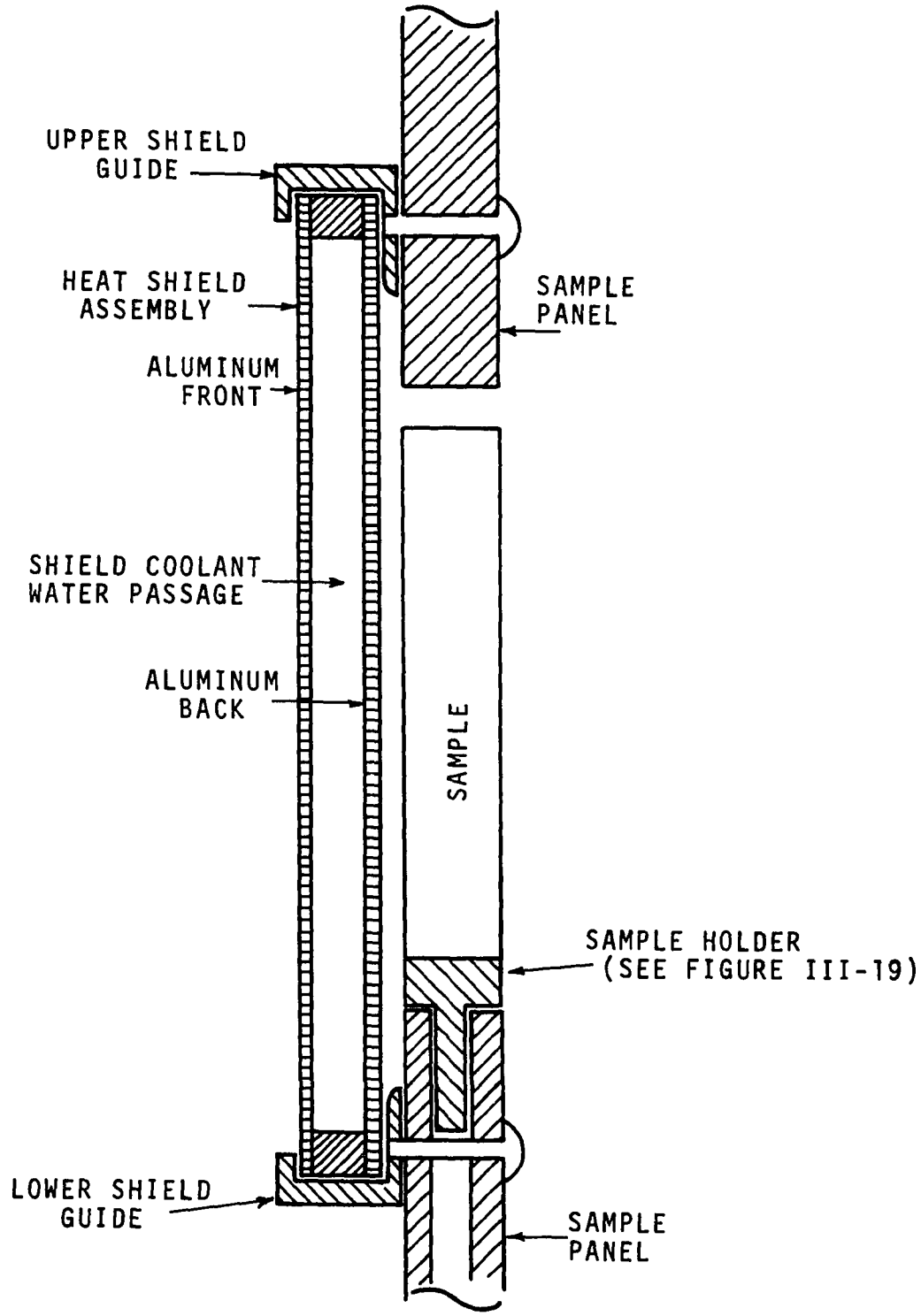

Figure III-11. Diagram of the Heat Shield System used to Protect the Sample Prior to Test.

Figure III-12. Heat Shield in Closed (Sample Protected) Position.

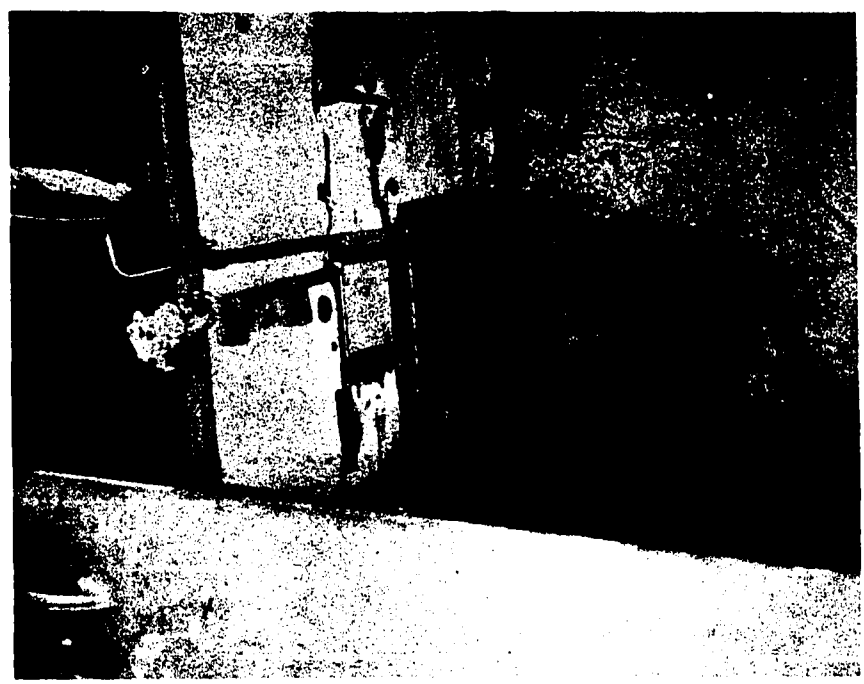

Figure III-13. Heat Shield in Open (Sample in Test) Position.

Pilot Light Ignition System

The method of piloted ignition used in the present study was different from that used previously. In lieu of the single flame jet of Koohyar (70), a coil of nichrome wire was placed above the sample and the input power adjusted to give a red heat. Figure III-14 is a diagram of the pilot light, while Figure III-15 illustrates the positioning of the pilot light with respect to the sample during an actual test. Power to the pilot light coil was obtained through electrical leads inserted in ceramic protectors installed along the top of the heat shield. Adjustment of coil power was provided using a Variac in the 110 V AC circuit. During the radiant reflector tests, the intensity of the light was such that it was impossible to determine visually if the coil was energized, so that a test lamp was installed in the circuit, as diagrammed in the schematic of Figure III-16. During the test program the pyrolysis gases and vapors gradually reacted with the nichrome wire and copper leads, chemically destroying them. Each inactive pilot coil was replaced; it was necessary to readjust the Variac to give a suitable pilot heat setting (as determined by the color of the wire.)

Instrumentation System

Two separate instrumentation systems were installed to permit the acquisition of data; (1) a measure of the time

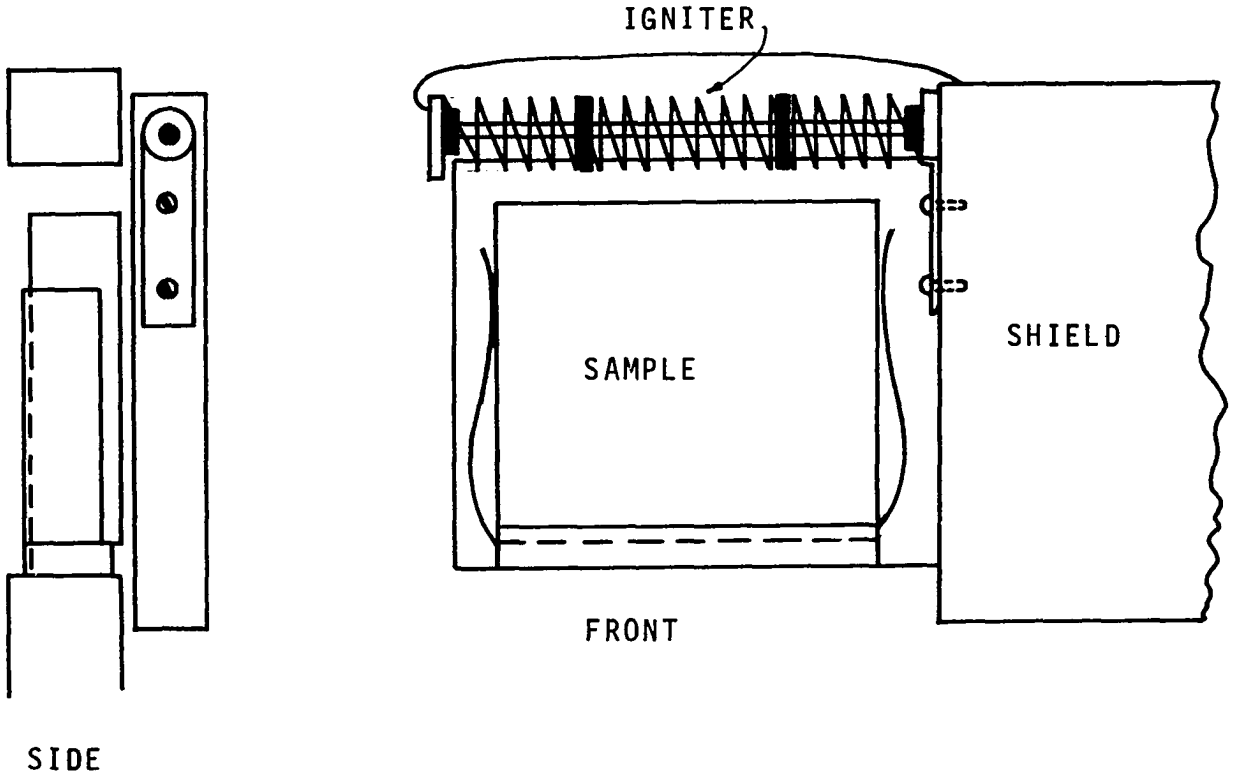

Figure III-14. Diagram of Nichrome Wire Pilot Light.

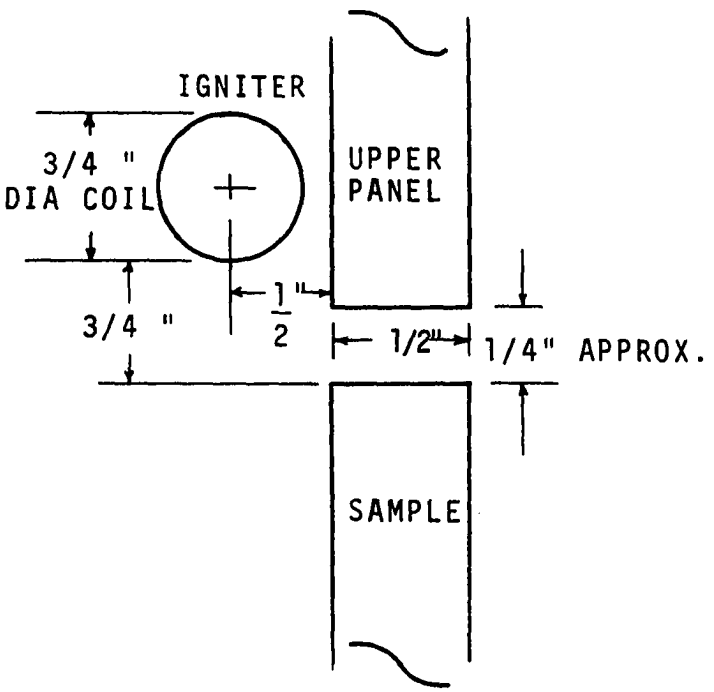

Figure III-15. Diagram of Pilot Light Igniter Position with Respect to Sample.

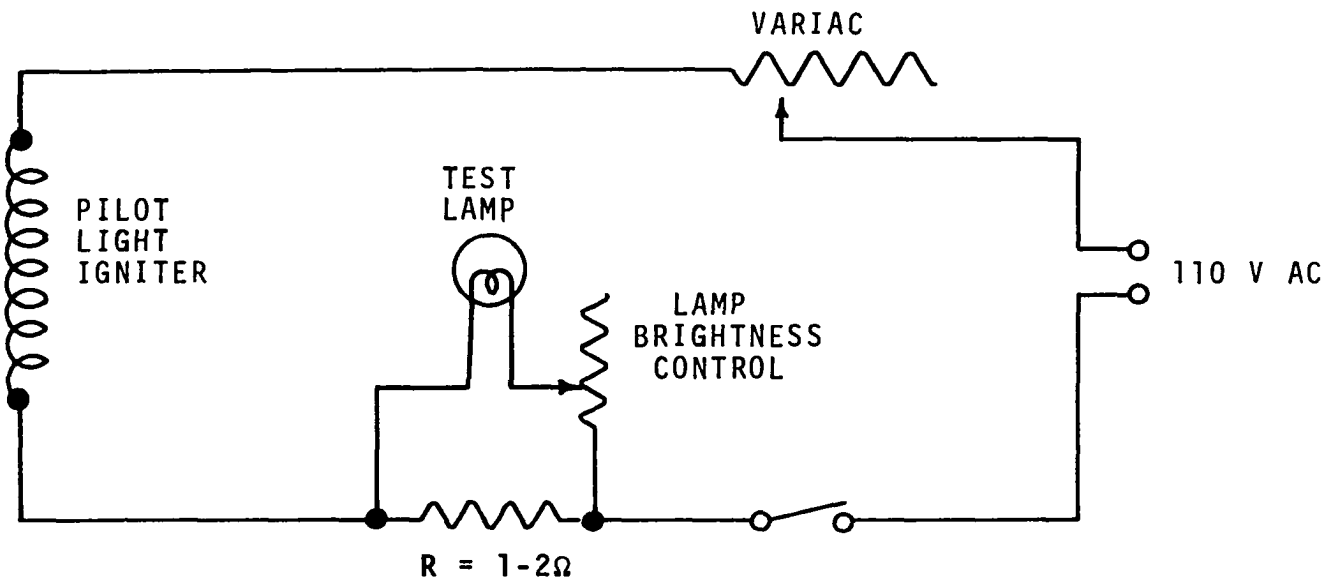

Figure III-16. Pilot Light Control Circuit.

of ignition from first application of heat flux, and (2) a measure of the amount of incident irradiance on the sample.

Time of ignition was provided by a cadmium selenide photo-conductive cell* which exhibited the phenomenon of near infinite resistance under conditions of no-light, but indicated little or no resistance while under the impact of light. The output of the cell was connected to the input of a Minneapolis-Honeywell Model 19 2-channel recorder; circuit voltage was maintained at 6 V DC. Figure III-17 diagrams the placement of the ignition detector system with respect to the sample.

Normal incident heat flux was measured by means of a Heat Technology Laboratory radiometer** whose output was monitored on the same recorder as the ignition detector. Figure III-17 also illustrates the placement of the radiometer with respect to the sample. Calibration of the two instrumentation systems is discussed in Appendix A.

Figure III-18 illustrates a sample of typical traces obtained during a test run using the radiant reflector as a heat source. The difference between the traces obtained from the radiant reflector and benzene flame were in the heat flux trace only. As could be expected, the flame exhibited a steady random fluctuation which caused the output of the

---

*Clairex, Model CL 603 AL; peak response is at 7350 A° wave length.

**Model GTW-10-64-573.

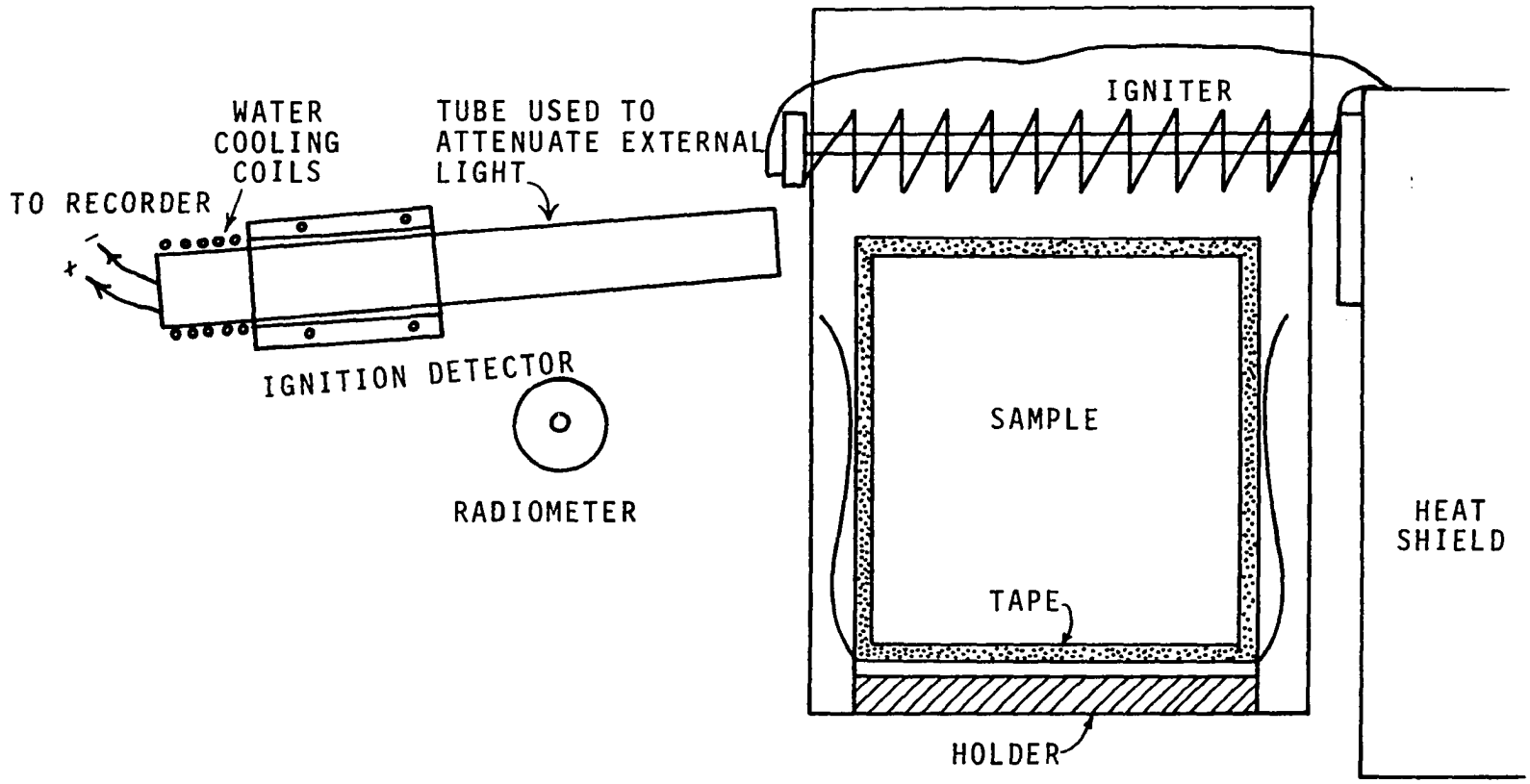

Figure III-17. Diagram of Ignition Detector Unit Placement with Respect to a Sample.

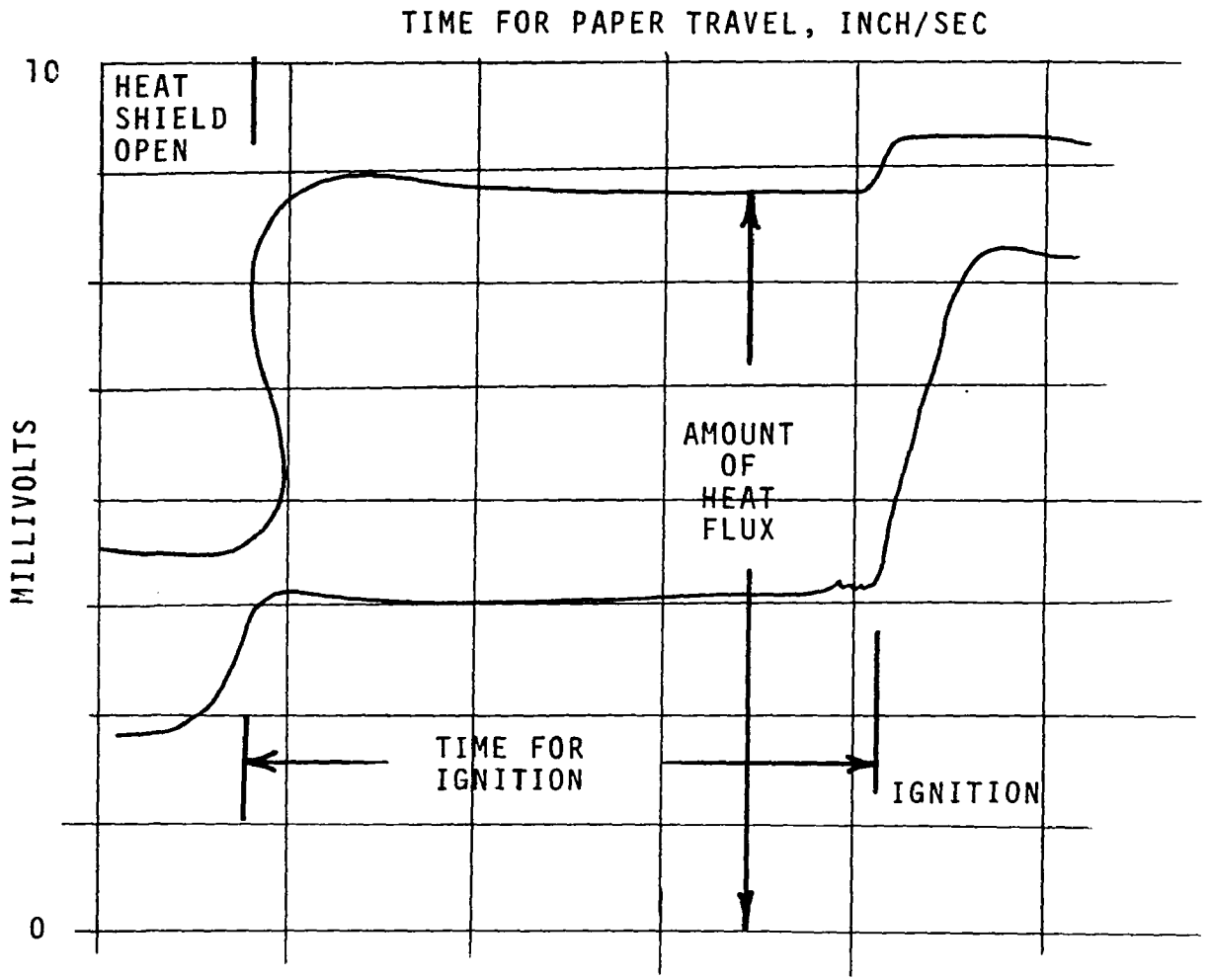

Figure III-18. Typical Test Traces from Recorder System.

radiometer to fluctuate with an average value of ± 0.05 cal/cm^2-sec at a flux level of 3.0 cal/cm^2-sec. The radiant reflector developed a steady trace as illustrated in Figure III-18.

Experimental Procedure

The techniques used in this investigation were essentially those previously used by Koohyar (70), Wesson (132), and Welker (131). In this study samples of plastic and rubber materials were obtained in 1.27 cm thick sheets of various dimensions, depending on the source of supply. However, some samples could not be purchased except in thicknesses of 0.64 cm or 0.32 cm as processed by the individual plastic manufacturer. Samples 1.27 cm thick were laminated from these thinner sheets. Test samples were cut from the various sheets to the nominal dimension of 8.8 cm x 10.9 cm. A diagram of the sample holder is shown in Figure III-19.

Koohyar (70) and the previous investigators (131, 132) had reported that sample edge effects caused variations in the sample dimensions during test conditions. One remedy found was the use of "Permacel" reflecting tape placed over the top edge of the sample extending down 0.32 cm on the face (70). Since the present investigation did not use the tongue and groove type holder of Koohyar (70), but a spring clip device, as shown in Figure III-19, it was decided that the Permacel tape should be applied to the entire sample perimeter

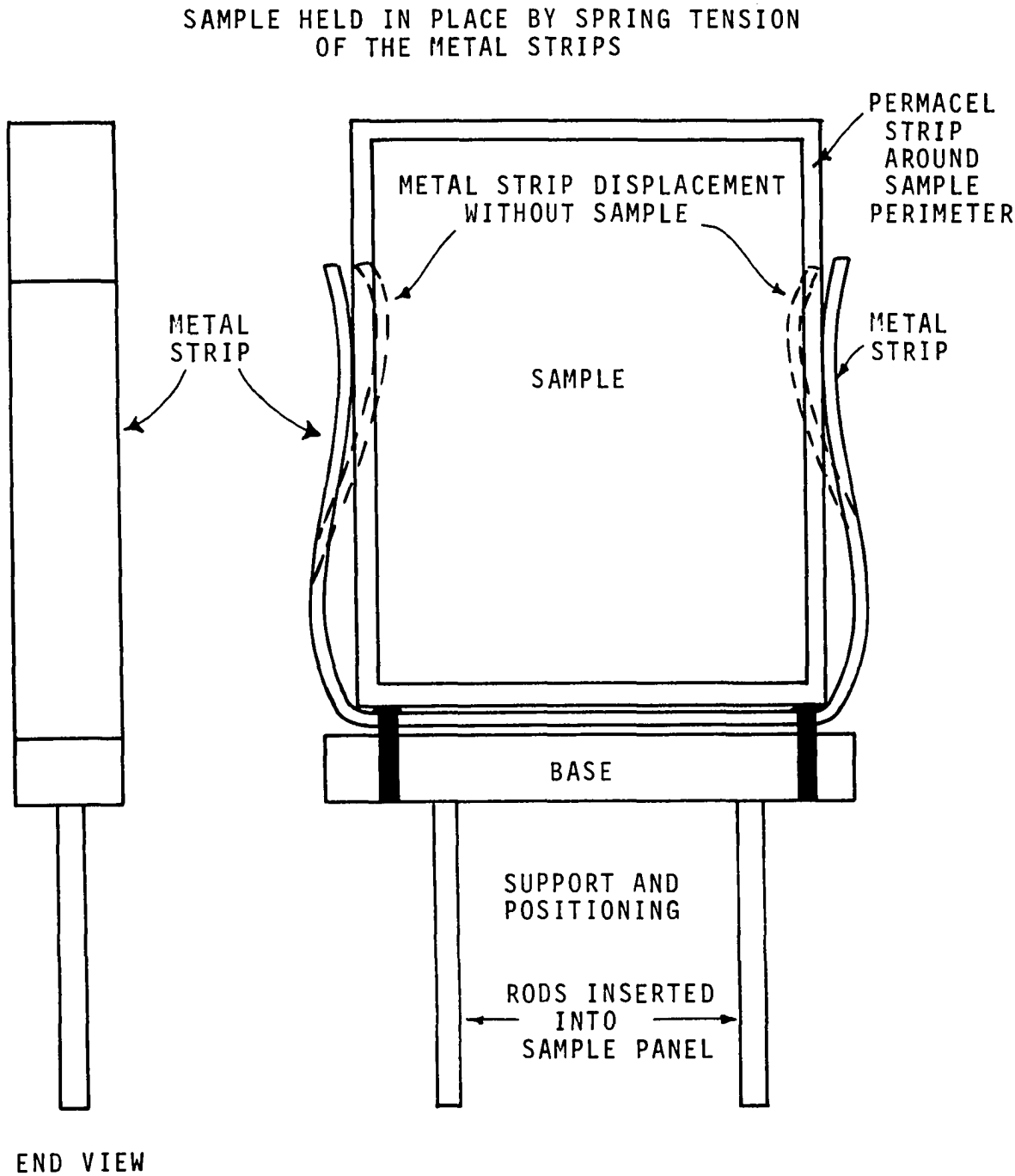

Figure III-19. Diagram of Sample and Sample Holder.

as also illustrated in Figure III-19. It should be noted that the Permacel tape on the top edge of the sample also reduced the radiant energy incident from the pilot light to the top edge (see Figure III-14 and III-15 for diagrams).

Permacel tape, type PE 100, is an aluminum/Fiberglas cloth 6.5 mils thick which was designed to reflect radiant heat. The tape is coated with a silicone type pressure sensitive adhesive which does not disintegrate or burn prior to the sample ignition. The manufacturer reported that the surface temperature rise is lessened by a factor of 1/2 when compared to tests made without the use of the tape.

As previously mentioned, samples of plastic and rubber materials were purchased from the commercial market. The suppliers were Cope Plastic Co., Precision Rubber and Plastic Co. and Industrial Gasket and Packing Company, all of Oklahoma City. Appendix B gives a listing of the various materials tested and a summary of the properties for each material.

During any day of testing certain preparations were made before tests were performed:

1. The exhaust fan was started and the water coolant to the sample heat shield, radiometer and ignition detector turned on.
2. When using the radiant reflector the power leads were connected to the appropriate outlet or, if flame testing was desired, the fuel supply tank was filled with benzene.

3. In the case of the radiant reflector, the coolant air flow was turned on and adjusted to the normal operating flow as indicated by the flowrator.
4. When the flame system was to be used, the O_2 supply was turned on and the pressure adjusted to give the necessary flow rate for the highest heat flux test desired.
5. Simultaneously with the first operations, the power was turned on to the Minneapolis-Honeywell recorder and to the ignition detector for warm-up and calibration.

A normal test was performed in the following manner: a sample was inserted into the holder in the sample panel and the heat shield was moved to the forward (sample protected) position. Generally the shield operation was tested by actual operation to check for stoppage or slow movement. The pilot light was turned on at this time to allow for proper heating; the igniter test light was continuously monitored to insure ignition capabilities. For the flame series, the vacuum pump was turned on at this time and the vacuum pressure monitored for the test condition of 24 in Hg vacuum. Depending upon which type test was in process, either the tungsten lamps were turned on or the benzene flow initiated: for benzene flame, the fuel was ignited after the channel burner held approximately 1 inch depth of fuel. Fuel ignition was accomplished by means of a high voltage sparking system. After radiant reflector heat output stabilized, as ascertained by the radiometer output, the radiant reflector was moved to the required position to

give the desired incident heat flux. When using flames, after the normal burning stabilized, the O_2 flow was started and the resultant irradiance increase monitored via radiometer for stability, then the burner was positioned to give the desired irradiance. When either the radiant reflector or flame system indicated stability at the desired irradiance, the recorder was set at the desired speed in time/inch and the shield was opened. Visual time and recorder trace were measured to determine the ignition time while the radiometer output was used to determine the incident heat flux. Appendix A contains the calibration curves for the radiometer used.

At the completion of the test, if using the radiant reflector, the power to the lamps and the pilot light was switched off, the recorder was set to low speed and the sample was carefully removed and immersed into a water bath. Where noxious gases were suspected, the sample was left in the cabinet until all evidence of smoke or vapor was gone, then the sample was removed and immersed in water.

When using the benzene flame, at test completion, the three-way valve was turned to dump position which drained the fuel. If the flame persisted, the cover was placed over the burner to assist in flame extinguishment. Simultaneously the recorder was placed on a slow speed and the pilot light power turned off. After the flames were out, and the sample gases or vapors reduced, the sample was removed and, as before with the lamps, immersed in water. After each flame test,

the fuel was drained from the holding tank into a safety can for storage.

If no difficulties were encountered in a particular test, another sample was inserted into the test panel and the test series continued; when the test series was completed and testing was to be terminated for that day, the shutdown procedure was essentially the test preparation in opposite sequences; shut off coolant water, turn off power to the recorder and ignition detector, turn off either the oxygen flow or air flow, drain the fuel tank or disconnect the radiant reflector commector, turn off the exhaust fan and close up the cabinet.

Certain techniques and precautions were found during the present test program which are listed here to assist other investigators in eliminating testing errors:

1. The pilot light should be cleaned after each test to insure proper ignition.
2. Maintain a constant air flow to the radiant reflector cooling system.
3. Insure that there is a clean area beneath the sample, so that a constant air flow and pattern is maintained for all tests.
4. In placement of the sample in the holder, insure that the sample surface is vertical and at the edge of the front face of the sample panel, in horizontal alignment with the radiometer; keep the sample face clean and free from scratches.

5. Insure that the air gap between the sample top edge and the sample panel is closed to air flow (see Figure III-19): if the sample pyrolysis vapor or smoke does not pass through the pilot igniter, ignition will be delayed.
6. The Minneapolis-Honeywell recorded used in the present test program required a minimum of one hour warm-up before a stable calibration could be attained; insure proper equipment warm-up as recommended by the manufacturer.
7. Always keep the radiometer face clean; it was found that pyrolysis products sometimes condensed on the face and that soot particles occasionally adhered to the sapphire window.

CHAPTER IV

DISCUSSION OF RESULTS

A review of previous work on the ignition or flammability of plastic and rubber materials, as briefly discussed in Chapter II, revealed the problems concerning ignition criteria as the following:

1. The ASTM radiant panel test was used to determine the flammability of a plastic without regard to the ignition process. All other flammability tests resorted to actual flame impingement upon the material for the determination of a combustibility or non-combustibility rating.
2. Much research has been performed in the area of thermal and oxidative degradation, but no published articles were found which used this information for analysis of the ignition characteristics. Activation energies for many plastic materials have been found that indicated different energy levels within the same material. In addition, the activation energies found for a single material show wide disagreement among investigators; this disagreement is generally caused by the use of different test conditions, such as testing in vacuum, air, or nitrogen.

3. Several articles have proposed a fixed surface temperature as a criterion for the ignition of plastics and other combustible materials. However, the temperatures of ignition of the plastics varied according to the test method used to determine the ignition temperature.
4. Theoretical analyses made, using the general heat transfer equation in conjunction with the total energy balance, have all assumed fixed boundary conditions, constant thermal properties and generally a unit absorptance of the incident radiant energy. No experimental confirmations of these assumptions were found in the literature.
5. The use of unit absorptance of radiant energy, as stated in Item 4, assisted in obtaining a solution to the heat transfer equation, but it did not associate the actual thermal input with the particular heating system. These absorptance, or reflectance, data are necessary to obtain a realistic solution to the actual heating and subsequent ignition of a material.

In consequence to the unknown or little understood factors just presented, most investigators attempted to correlate the ignition data and characteristics with the use of an inert mathematical model.

The purpose of this investigation was twofold: (1) to study the ignition characteristics of plastics and rubber under incident radiation from the buoyant diffusion flame system of Koohyar (70) and the 1000 watt tungsten lamp

radiant reflector system, where use of both systems permitted a comparison of ignition times based upon the spectral distribution of the two types of radiant heating; (2) to develop a mathematical model that would permit a prediction of ignition time of a material when subjected to an incident heat flux. The testing apparatus and experimental procedure have been discussed in Chapter III.

Pyrolysis Conditions

During this ignition study, a large sample or macrosystem type of testing was performed to determine the minimum heat flux for ignition. Koohyar (70) proposed that if the volatile products of [wood] pyrolysis were exhausted before conditions of flaming ignition could be satisfied in the gas phase near the solid, ignition would not occur. Within plastics and rubbers, a low rate of gas evolution, an incomplete mixing of the pyrolysis gases with air, or the combustion retarding effect of non-flammable gases or vapors may be the cause of non-ignition. Also, there is the possibility that the heat losses from the irradiated sample may be great enough to balance the heat input and therefore cause a static pyrolysis condition to be maintained. In previous tests, all of the investigators had assumed a constant heat source with a constant total thermal input to the irradiated sample. In the present study, preliminary tests have indicated that the surface reflectance is some function of the temperature, composition and surface roughness or a combination of these for

any irradiated surface, which directly affects the amount of thermal input to the surface. A discussion of surface reflectance-absorptance is contained in a later section.

Ignition Data

The ignition data are summarized in Appendix C. Measurements were made of ignition time, t, and radiant heat flux, H_o. The radiant heat flux measurements are discussed in Chapter III and Appendix A. Absorptance and reflectance measurements and the associated analyses are discussed in Appendix D. Various physical and chemical properties and typical burning behavior are listed in Appendix B. Ignition burning characteristics of tested polymers are listed in Appendix C (along with the ignition data).

The typical types of recorder outputs are illustrated in Figures IV-1 and IV-2. In Figure IV-1 polyethylene was exposed to a tungsten lamp incident irradiance of 2.0 cal/cm^2-sec which gave an indicated ignition time of 76 seconds. Figure IV-2 shows the results of exposing a second sample of polyethylene to a benzene flame of 2.22 cal/cm^2-sec incident irradiance which ignited in 33 seconds. Calibration curves for the irradiance can be found in Appendix A.

One inherent problem existing with the radiant lamp source is the intensity of the visible light and its effect upon the ignition detector. Figure IV-1 illustrates the problem in the output curve designated as DETECTOR OUTPUT.

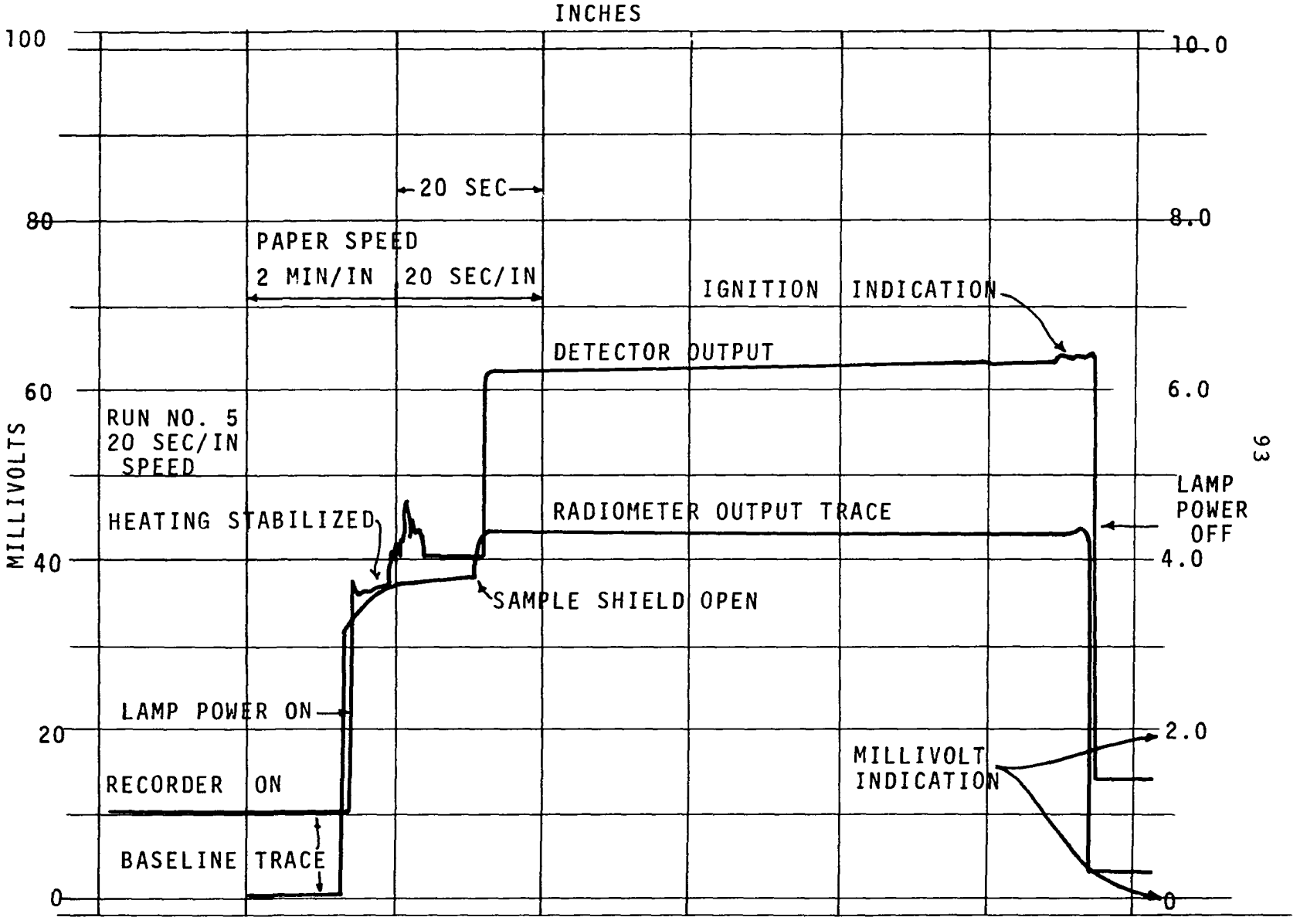

Figure IV-1. Diagram of Ignition of Polyethylene Using Radiant Reflector as a Heating Source. Outline is copy of Actual Recorder Paper.

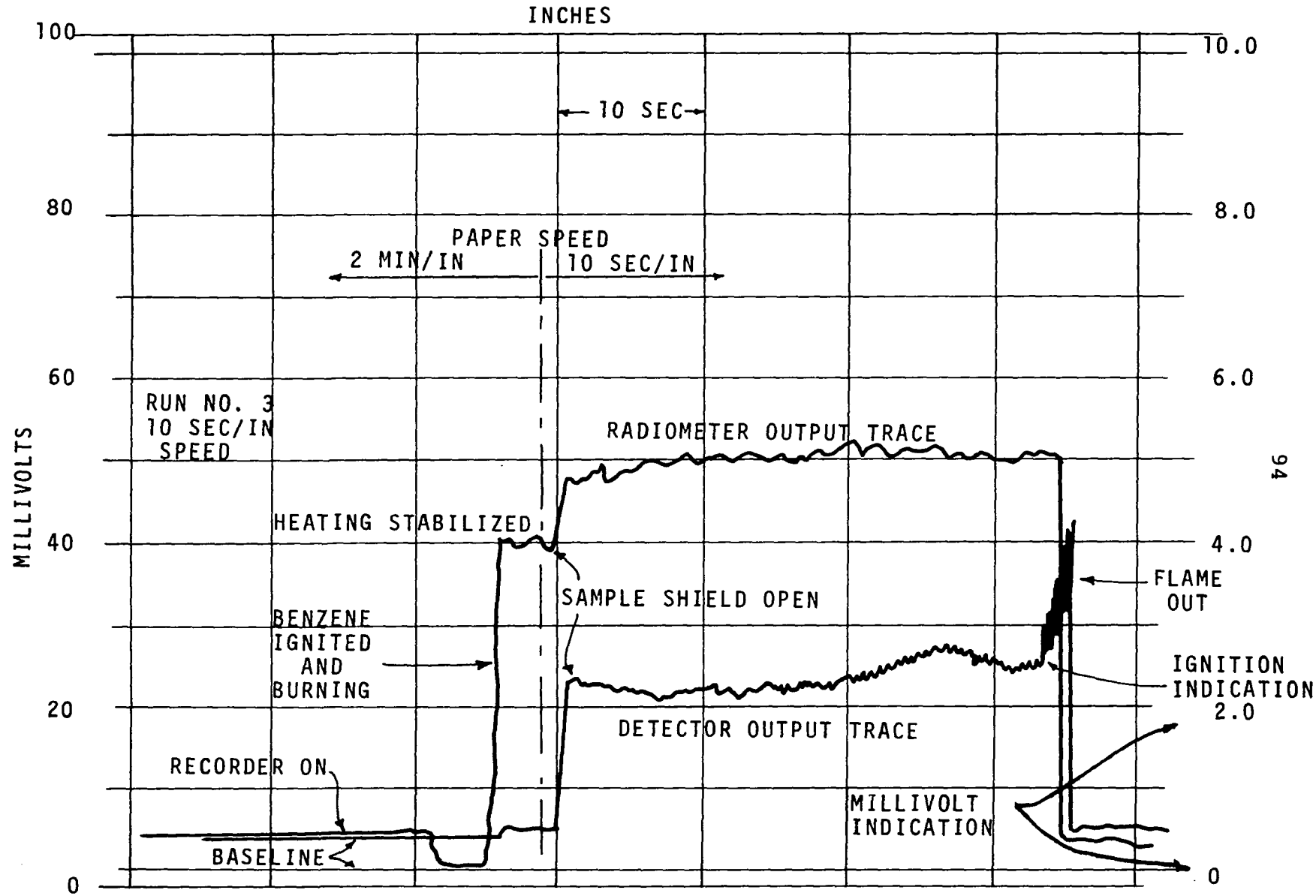

Figure IV-2. Ignition of Polyethylene Using a Benzene Flame as a Heating Source. Outline is Copy of Actual Recorder Paper.

The intensity of the lamp light was so great that the flame following ignition was not easily detected. This very slight movement of the output curve at ignition is typical of all samples tested with the lamps. However, one favorable condition is that one obtains a very steady irradiance as shown by Figure IV-1 for the output curve labeled RADIOMETER OUTPUT. Figure IV-1 indicated rapid stabilization of the incident irradiance as shown by the output curve just prior to the indication SAMPLE SHIELD OPEN (see Figure III-13). Upon activation of the shield, the curve indicated a jump to the total irradiance incident upon the sample and this irradiance indication remained steady until ignition.

In contrast, Figure IV-2 shows the sensitivity of both the ignition detector and radiometer to sudden changes of input from the benzene flame. As equivalent to the radiant lamp flux, the DETECTOR OUTPUT curve indicated a stable output prior to shield open, but after the shield was opened the irradiance curve indicated a deviation of $\pm$ 0.05 cal/cm^2-sec. At higher irradiances the deviation becomes greater. A study of the ignition detector output curve revealed that the gases and vapors being evolved reflect some light which caused the curve to vary. Ignition was easily detected by the sometimes violent and rapid pen fluctuation as indicated by the pen trace. Combustion was always detected by the ignition detector unit while using the benzene flame as a heating source. To insure backup for the electrical detection system an

observer also voiced notice of ignition for both the radiant lamp and benzene flame testing.

As previously stated, the ignition data are listed in Appendix C. In addition to the tables of time for ignition with the associated incident irradiance for each material, the data are presented in a graphic form as illustrated by Figure IV-3, for polyethylene. As can be seen, the data points for the ignition tests of Figures IV-1 and -2 are designated on the graph, and are typical for the testing. The data points were not taken in order, i.e., the tests did not proceed from low-to-high nor high-to-low irradiance, but were obtained from tests proceeding from middle-to-high and middle-to-low irradiance. As Figure IV-3 shows, the time for ignition increased as the incident irradiance decreased and also the reverse. With the upper range of the ignition cabinet capabilities, approximately 3.5 cal/cm^2-sec maximum irradiance, no testing could be made to determine whether there existed any generalized minimum time of ignition for high irradiance levels. In tests at sufficiently low heating rates, most samples smoked, decomposed, melted and ran or developed pits and bubbles on the surface without ignition actually occurring. If the samples did not ignite after 10 minutes of heating, or if the sample disintegrated, the tests were discontinued.

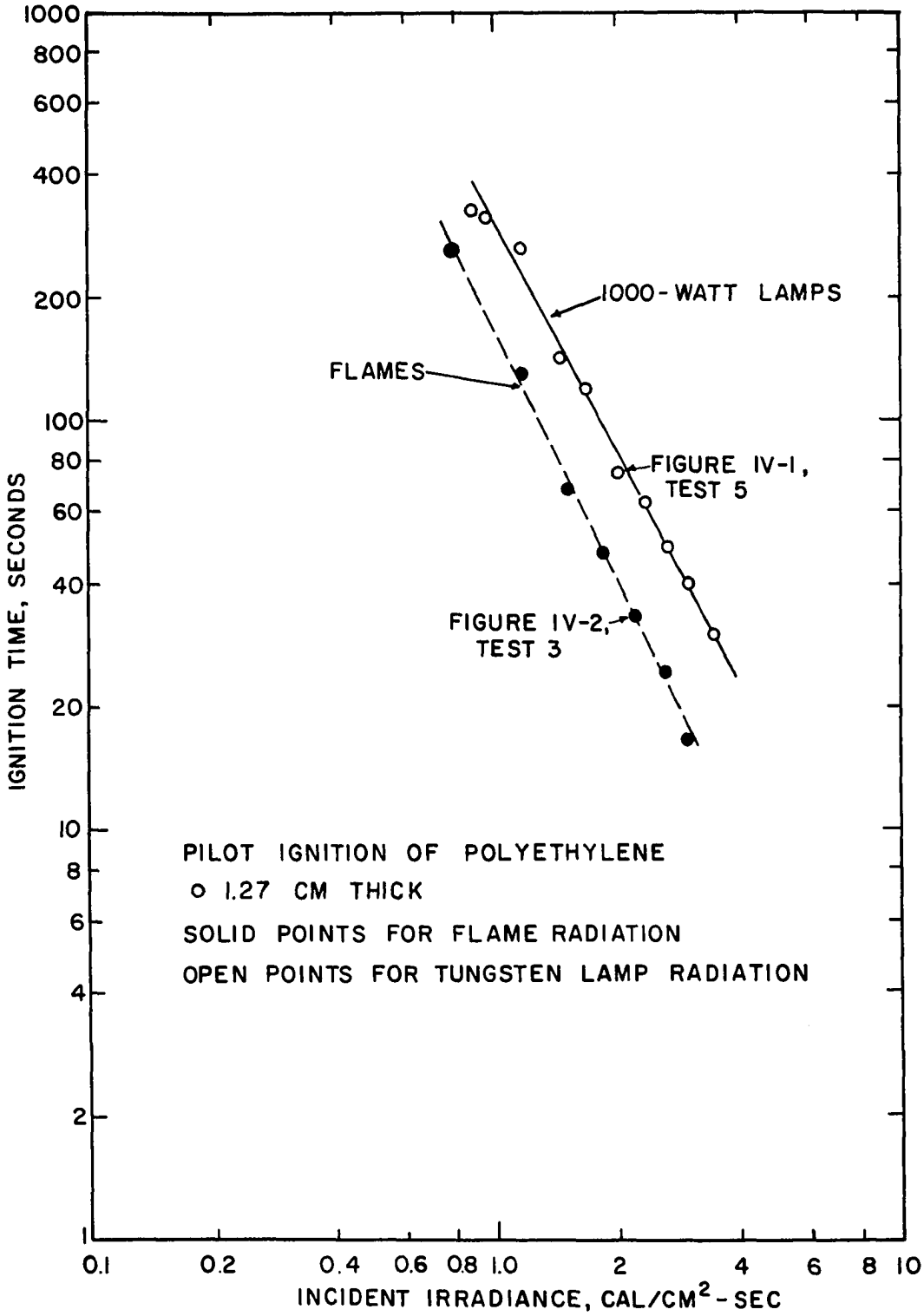

Figure IV-3. Ignition Curves for Polyethylene.

Surface Reflectance-Absorptance Phenomena

During the early phases of the ignition testing, all observers noted that the reflected visible light changed in intensity as the samples were heated. The reflected visible light appeared to reduce in intensity as the surface darkened and charred. In addition, there was a distinct difference in ignition time for some materials depending on whether a tungsten lamp or a benzene flame was used as a radiative heat source. The differences in ignition time tests indicated the surface radiative heat absorptance was a primary parameter in the ignition behavior of some combustible materials. Thus it became necessary to investigate the surface absorptance. No attempt will be made in this section to develop the theoretical aspects of heat absorptance. However, it is intended to present some of the information found during the auxiliary investigation of surface reflectances. The tabular information presented (in Appendix D) is based upon an average absorptance for 18° angular displacement from normal for a particular heat source. A discussion of heat sources and emissive power, and an analytical development for surface reflectance-absorptance relationships can also be found in Appendix D, as well as a presentation of the research methods with graphic illustrations of the spectral absorptances of the individual polymers.

In the measurements of the spectral absorptance of polymers it was found that most variation in absorptance was in the region of 0.3-2.5 μ while the region of 2.5-7.0 μ had relatively constant absorptance. Figure IV-4, spectral absorptance of white polystyrene, illustrates the typical behavior of light-colored polymers. As can be seen, the spectral absorptance is 0.2 to 0.35 for the region of 0.4-1.6 μ while the spectral absorptance jumps to 0.7 at 1.6 μ and then increases to 0.9 at 2.5 μ, beyond which it remains constant. If one compares the peaks of the heat sources (spectral emissive power curves, Figure III-7), 1000 watt tungsten lamps peak at 1.15 μ while the benzene flame peaks at 2.7 and 4.3 μ. This comparison shows that while polystyrene will have a low average absorptance for the lamp radiation it will have a high average absorptance for the benzene flame radiation. Figure IV-5, an ignition time-irradiance level plot shows both incident irradiance and absorbed irradiance as independent variables. The ignition behavior of the corrected relationship (for average absorptance per heat source) is typical of the polymers tested. Several of the corrected plots showed some deviation at the higher irradiance levels. This deviation can be attributed to the change in polymer surface characteristics as the polymer is being heated. Wesson (132) made a partial study of the change in average absorptance values for wood samples that were subjected to several different rates of heating with varied times of heating at each rate. It was

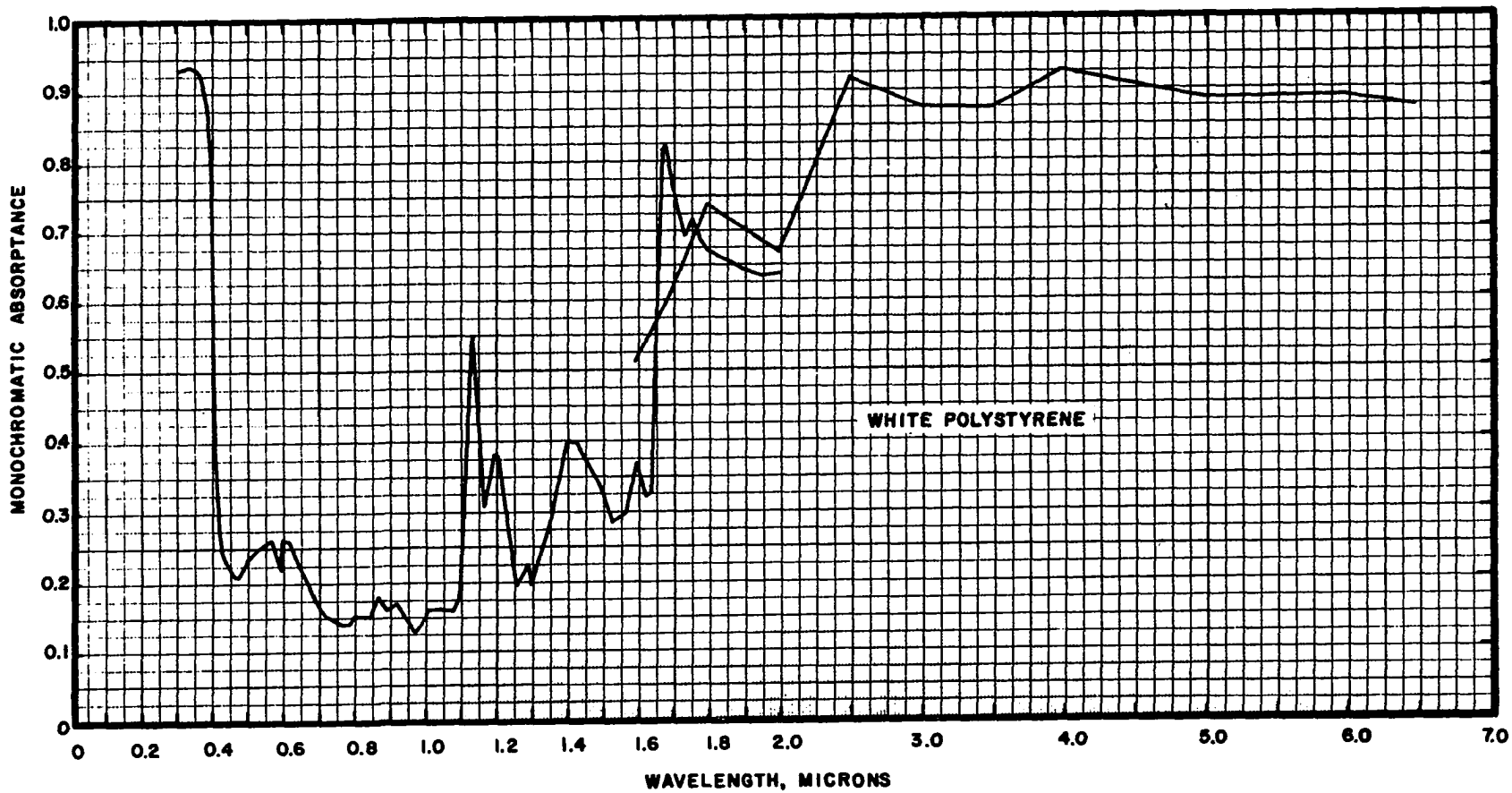

Figure IV-4. Spectral Absorptance of White Polystyrene.

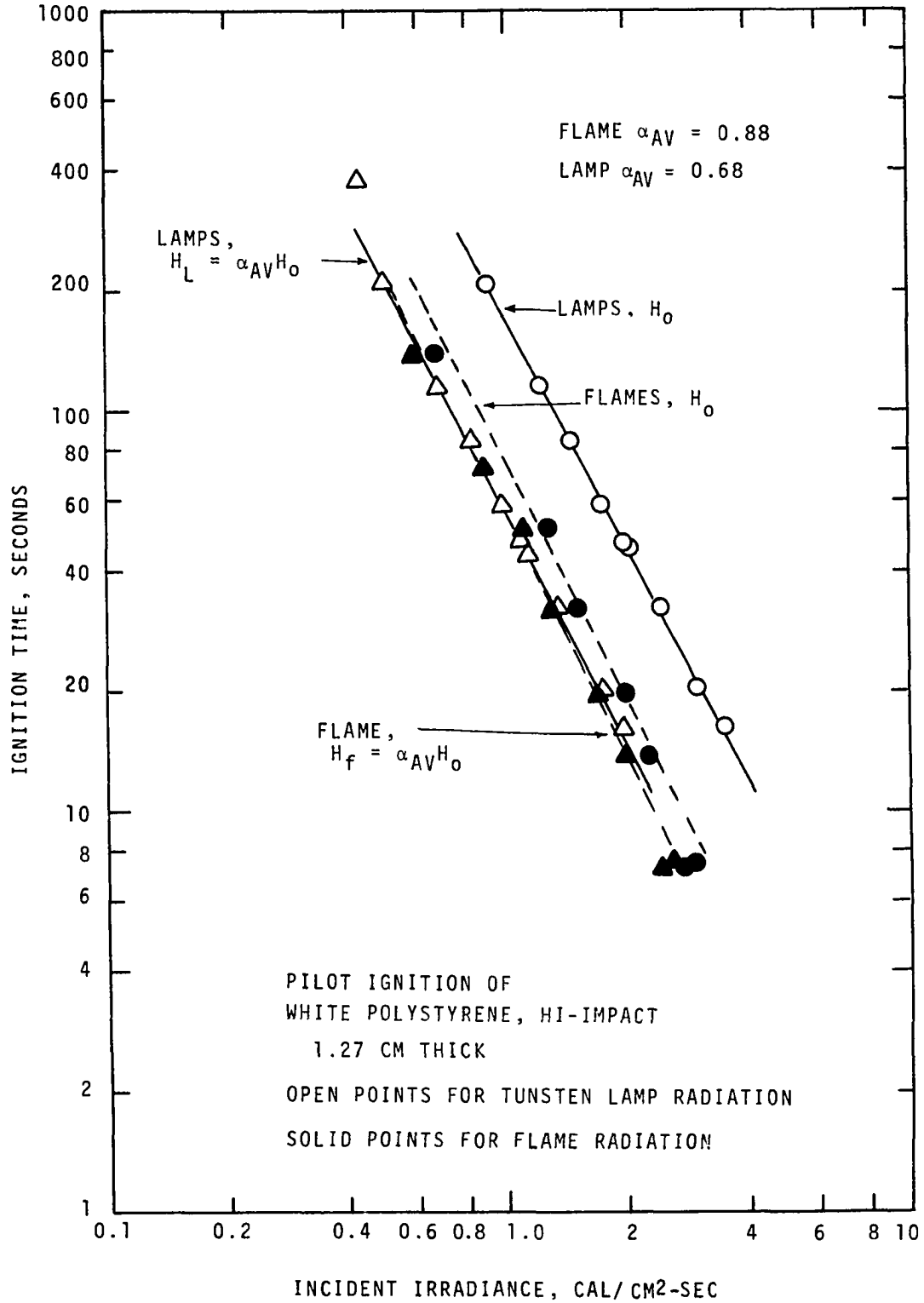

Figure IV-5. Ignition Time for White Polystyrene with Varying Irradiance.

found that rate of average absorptance change was a function of the irradiance level. However, it was also found that the total change of average absorptance* of any wood from the unheated state to that of ignited sample was equal for all irradiance levels, i.e.,

$$(\Delta\alpha_{av})_{0\rightarrow t_{i,I_1}} = (\Delta\alpha_{av})_{0\rightarrow t_{i,I_2}} = (\Delta\alpha_{av})_{0\rightarrow t_{i,I_k}} \qquad \text{(IV-1)}$$

where I_k is the incident irradiance and t_{i,I_k} is the time to ignition at each irradiance level. In the present study, the polymer absorptance data were taken for samples at ambient temperatures. However, to obtain corrected ignition time-irradiance plots, such as Figure IV-5 for white polystyrene, it may be necessary to perform such testing as that done by Wesson (132) on all polymers. The visual observations of the polymers prior to and during ignition are described in Appendix C, Section I. From these observations, it is apparent that the average absorptances do change. A very short test program was performed on several materials that showed some evidence of surface change while being heated. The results of this study are contained in the following paragraph.

One of the more variable surface reflectances (or absorptances) can be found in the study of silicone rubber. The original material is red-orange. As the surface is heated

---

*A discussion of and the calculation of average absorptances can be found in Appendix D.

an outer shell of gray appears which gradually changes to brilliant white. This white (and gray) surface cracks, spalls, and powders during the heating. The intensity of reflected tungsten light (and heat) increases as the surface coloration changes, such that, when the white material is present, the surface appears intensely bright, so bright that visual observation is very difficult. Figure IV-6 is a graphic presentation of the spectral absorptance variation of a silicone rubber surface after heating. No irradiance levels were measured. However, silicone rubber can be used up to 317°-372°C intermittently (5, 45, 118), so that the short-term degradation temperature exceeds 372°C. As can be seen, there is a marked change in the spectral absorptance as the surface whitens. The pink surface is composed of partially degraded silicone and is the layer to be found immediately under the white surface. Using the methods of Equation D-5 (Appendix D), the average absorptances were calculated for silicone and are given in Table 1.

The α_{av} of the natural is nearly equal to the α_{av} of the highly heated sample probably due in part to the physical surface conditions: unheated--red/orange and smooth; heated--white and porous and flaky. Thus it can be seen that surface coloration and condition has a strong effect on the radiative heat absorptance of some materials.

In contrast to silicone rubber, black opaque Plexiglas had an average absorptance of 0.95 for tungsten lamps, 0.94

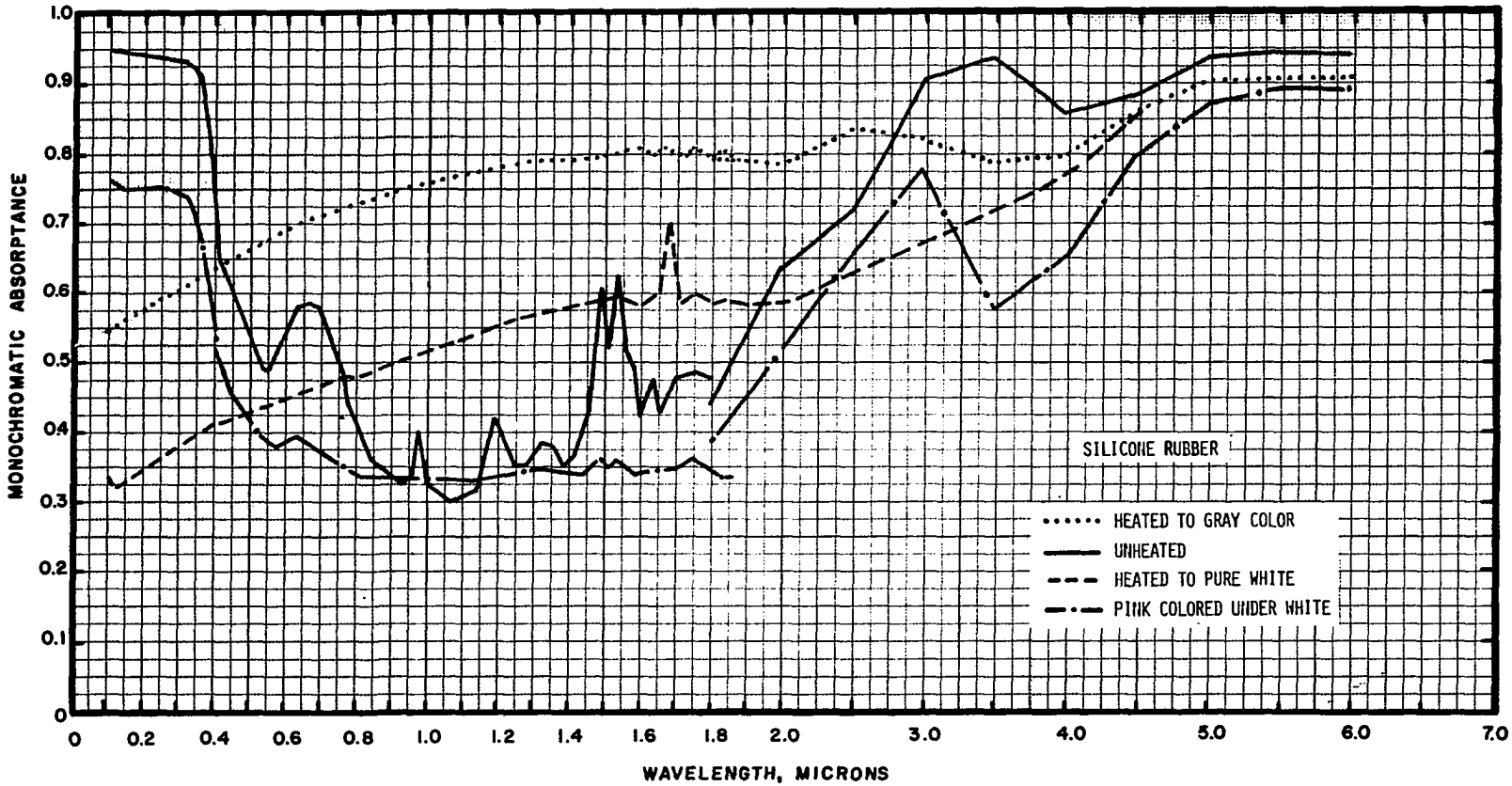

Figure IV-6. Spectral Absorptances for Silicone Rubber.

TABLE 1

AVERAGE ABSORPTANCE VALUES FOR SILICONE RUBBER
AVERAGE ABSORPTANCE, α_{av}

Material	Tungsten Lamp Source	Benzene Flame
Natural, unheated	0.54	0.79
Pink Colored	0.44	0.65
Gray Surface, after heat	0.77	0.81
White Surface, after heat	0.57	0.71

for a benzene flame, and 0.96 for solar radiation. This slight difference is neglible as found in the ignition studies (of black Plexiglas) and illustrated in Figure IV-7, where ignition time has been plotted in relation to the incident irradiance. The plotting of the flame and lamps falls within the capability of experimental reproducibility for either the 0.64 or 1.27 cm thick samples. The difference between the curves is due to both the density and thickness differences in the samples.

The other black samples tested, i.e., Neoprene solid and sponge rubbers, Buna-N rubber, Butyl IIR rubber and Accopac AS-428 gasket material (Buna-N rubber and asbestos mixture) all indicated a slightly higher average absorptance for lamps than for flames whether natural or surface heat treated. Figure IV-8 of Neoprene rubber is a typical example of the spectral absorptance for the black material, both natural and

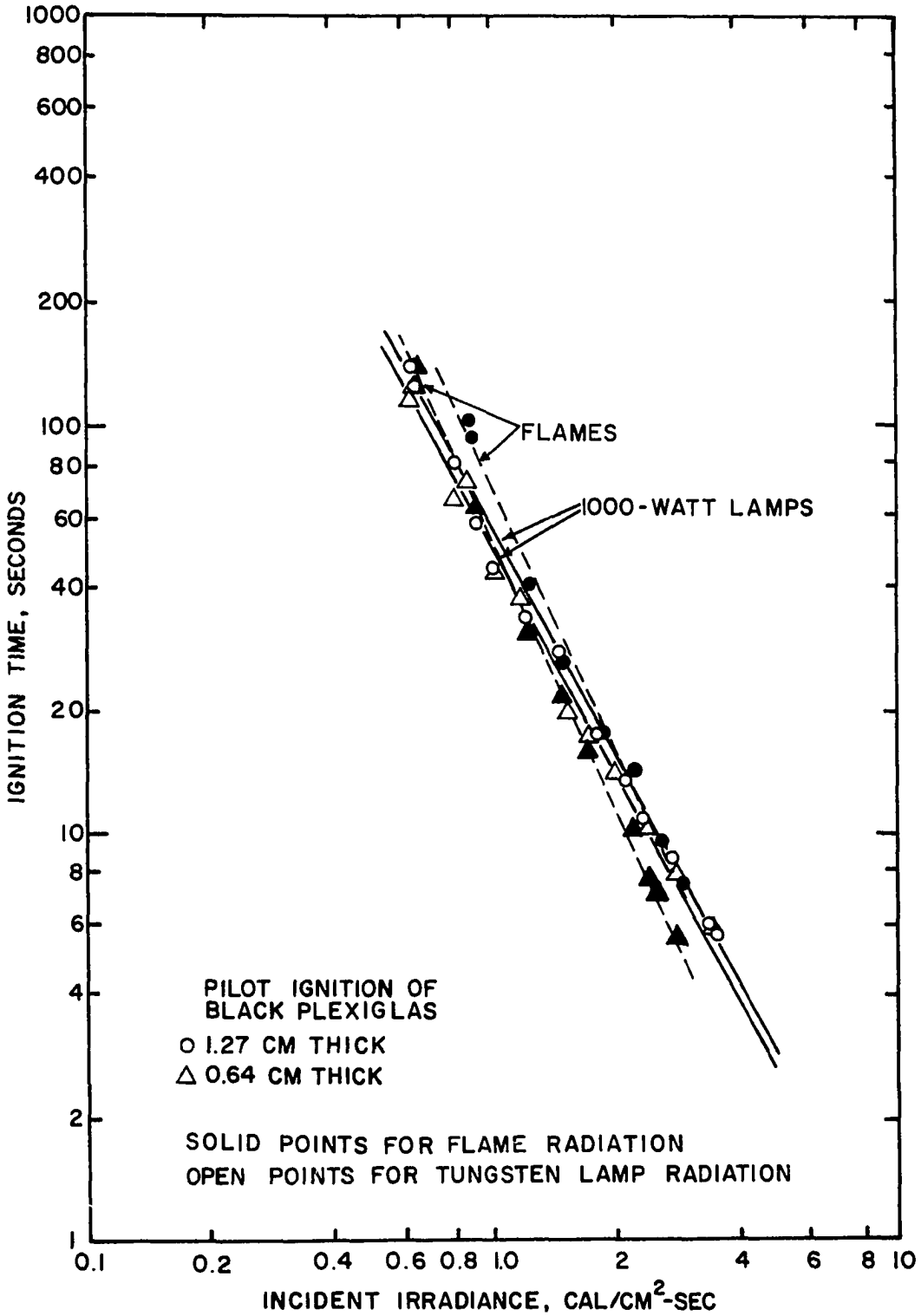

Figure IV-7. Pilot Ignition of Black Plexiglas.

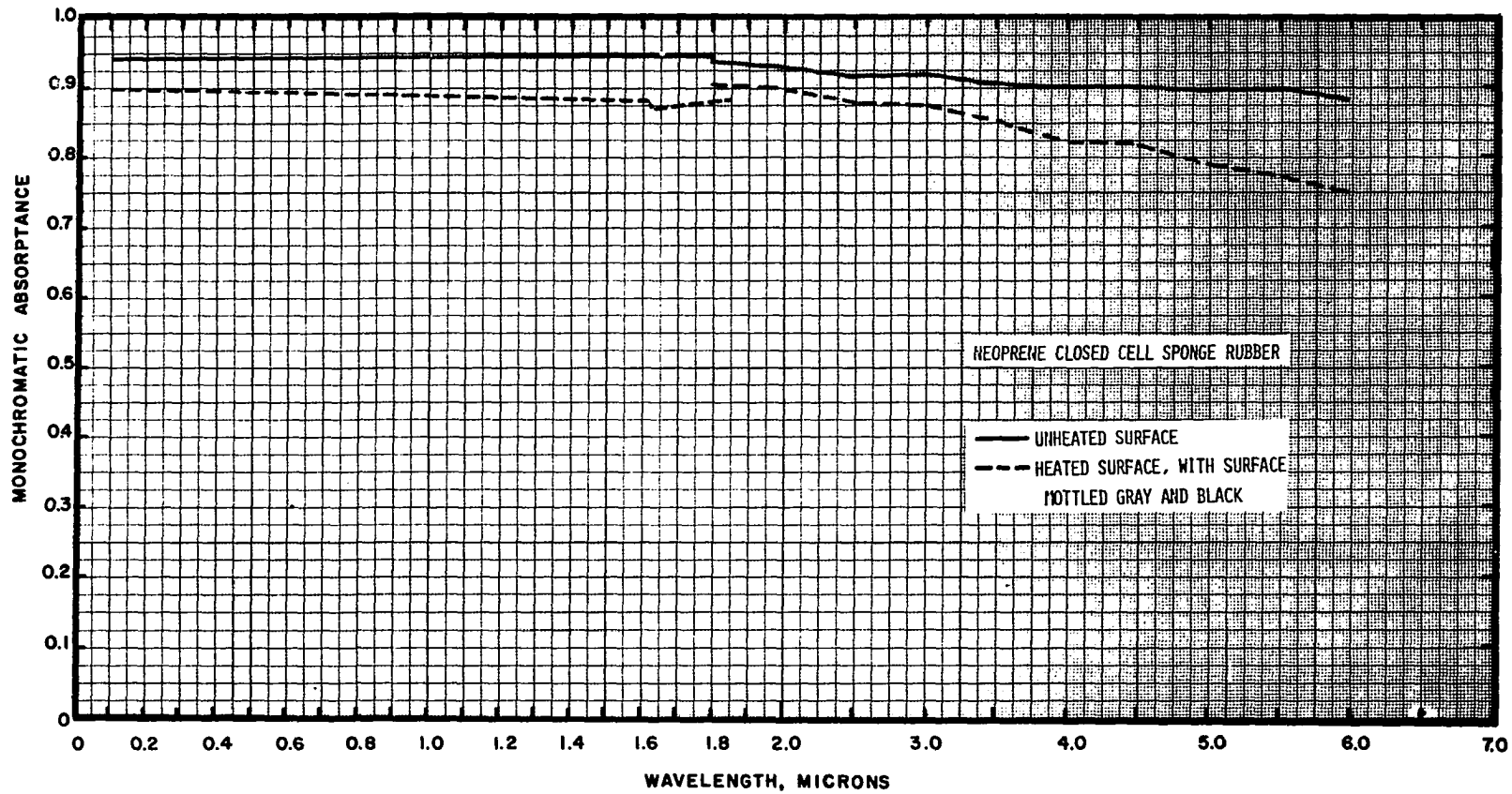

Figure IV-8. Spectral Absorptance of Neoprene Closed Cell Sponge Rubber, Heated and Unheated.

heated. The measurement of the 2.0-7.0 micron wavelength at specific points and the assumption of a constant value between the points may be in error. Further, the sample surface may have been affected by the elevated temperature of the Hohlraum cavity.* It was apparent that some samples decomposed with an accompanying surface reaction since the Hohlraum cavity became contaminated with adsorbed gases from one or more of the test materials. The adsorption was a slow process, requiring several hours to take place, which eliminated the opportunity to find which one or more of the samples had some reaction at the cavity temperature of 370°C. The Hohlraum samples were a maximum of 0.127 cm thick and were epoxy cemented to a metal disk which was inserted into a water-cooled holder. In preparing the rubber samples, it was most difficult to obtain a specimen of uniform thickness. Also, when a rubber specimen was heated it generally turned gray and crumbled, so that the heated cemented samples often fell apart prior to reflectance testing. Figure IV-8 indicates the spectral absorptance variation with wavelength for Neoprene closed cell sponge rubber. As is illustrated, the heated material (gray and black mottled coloration) has a slightly lower absorptance than the natural unheated rubber. Values of average absorptance found were the following:

---

*The Hohlraum cavity was maintained at 365-375°C for all testing while the Cary Spectrophotometer tested samples at room temperature. A discussion of the test equipment and testing techniques can be found in Appendix D.

	Lamps α_{av}	Flame α_{av}
Unheated Neoprene	0.92	0.89
Heated Neoprene	0.89	0.86

One material that indicated a great discrepancy in measured absorptance at 2.0 microns for the Cary instrument and the Hohlraum instrument was Kel-F. Although Kel-F did not ignite during the ignition tests, the absorptance values were investigated to study the transmission variation in a translucent material. Figure IV-9 is the graphic presentation of the monochromatic absorptance with wavelength of Kel-F. As is illustrated, there is a large variation of absorptance values over the range of 1.6-2.0 microns wavelength. The only explanation of the large variation in spectral absorptance between 1.6-2.0 microns is that the heated sample in the Hohlraum must have changed physical characteristics. The average absorptance values of Kel-F for both lamps and benzene flame with respect to the three possible absorptance conditions are indicated in Table 2.

In general, all the remaining polymers tested yielded a higher average absorptance for a flame heating source than the tungsten lamp heat source. Transparent materials, such as Plexiglas, polystyrene and others, were first investigated for spectral transmittance*; then the reflectance measurements were performed.

---

*See Reference 42 for details of transmittance analysis and computation of spectral absorptances.

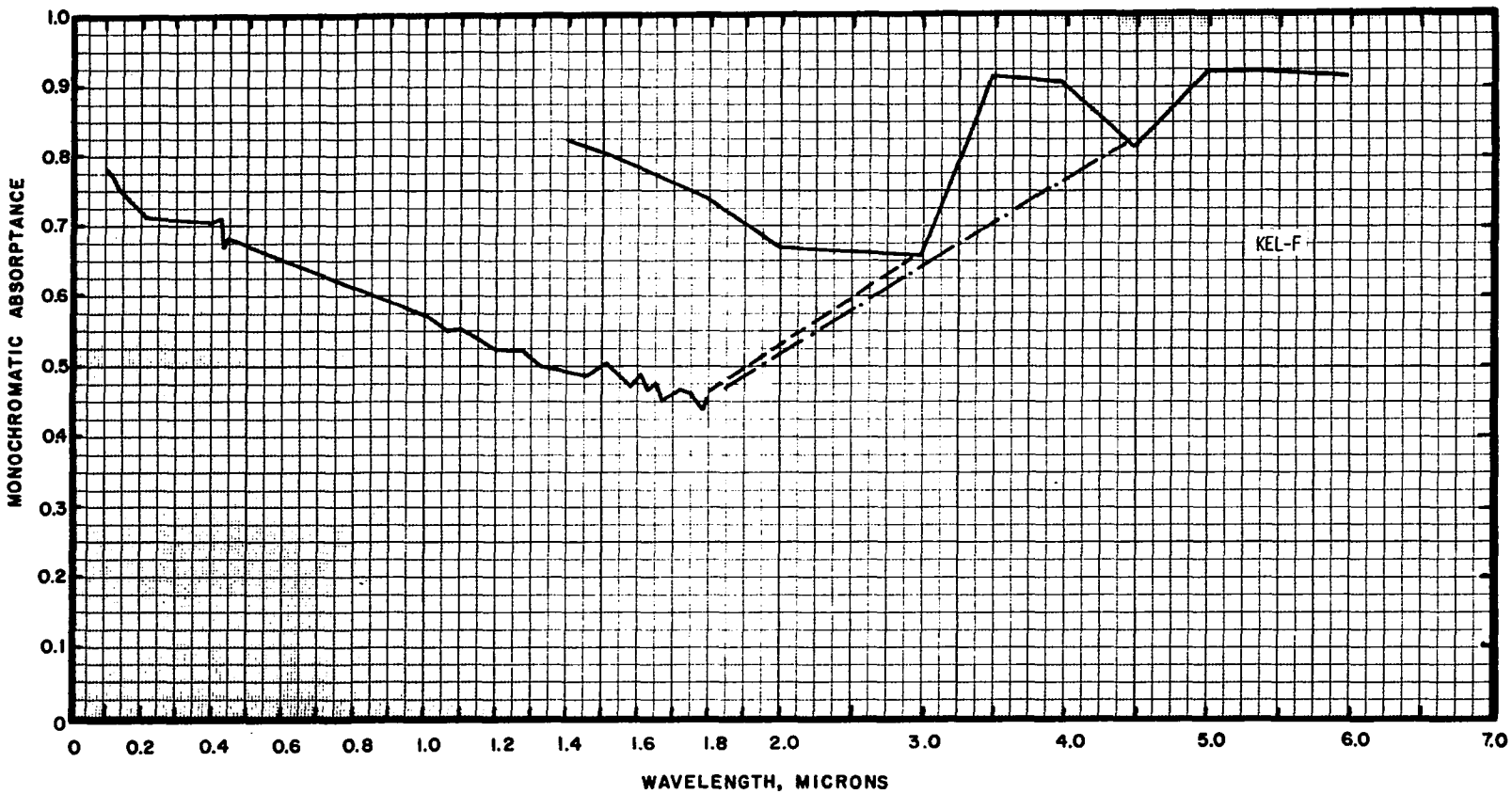

Figure IV-9. Spectral Absorptance of Kel-F.

TABLE 2

VARIATION OF AVERAGE ABSORPTANCES FOR KEL-F
AS DIAGRAMMED IN FIGURE IV-9

Material Variation	α_{av} Lamps	Flame
Normal	0.61	0.77
Partial Correction (dashed line)	0.58	0.74
Full Correction (broken line)	0.57	0.68

In any test program involving the measurement of reflectance, the variation of that reflectance with angular displacement is often questioned. It was previously stated that the reflectance data reported in Appendix D were measured at 18° angular displacement from normal. Additional measurements were made at 30° angular displacement from normal and it was found that the spectral reflectance over 0.3-7.0 μ varied only slightly from the 18° data (less than 2%). In the ignition cabinet described in Chapter III, the sample placement with respect to the ignition source was such that any angular variations in reflectance/absorptance would be at a minimum. Figures III-3 and III-9 indicate that the samples were parallel to both the flame and tungsten lamps during all ignition testing.

Ignition Capability Variations

Some evidence was obtained that at least one plastic material had two levels of ignition capability. Figure IV-10 is the ignition time versus incident irradiance for gray pigmented poly(vinyl chloride) plastic (PVC) and Figure IV-11, the same plotting for clear, unpigmented PVC. As is indicated, there is an apparent displacement in ignition time toward a more rapid ignition at 2.0 cal/cm^2-sec irradiance using the benzene flame. This displacement occurs for both types of PVC in the 1.27-cm and 0.32-cm thick samples. Only the 0.32-cm and 0.64-cm thick clear PVC samples showed any ignition time displacement at 2.0 and 3.0 cal/cm^2-sec irradiance respectively.

Further, it is indicated that the 0.32-cm thick gray PVC has a more rapid ignition time at all input irradiance levels than the 1.27-cm thick material. The slopes are not the same, with the probability of some effect due to different added pigmentation (the samples were obtained from two different manufacturers), but most effect due to the different sample thicknesses.

Stepek, et al. (123) studied the thermal degradation of PVC at low temperatures (170°-190°C) in a nitrogen atmosphere and found a [degradation] activation energy of 34.4 K-cal/mol. Madorsky (79) reported activation energies of 26-32 k cal/mol based on three different polymerization agents at temperatures of 300°-400°C, in a low O_2 pressure atmosphere.

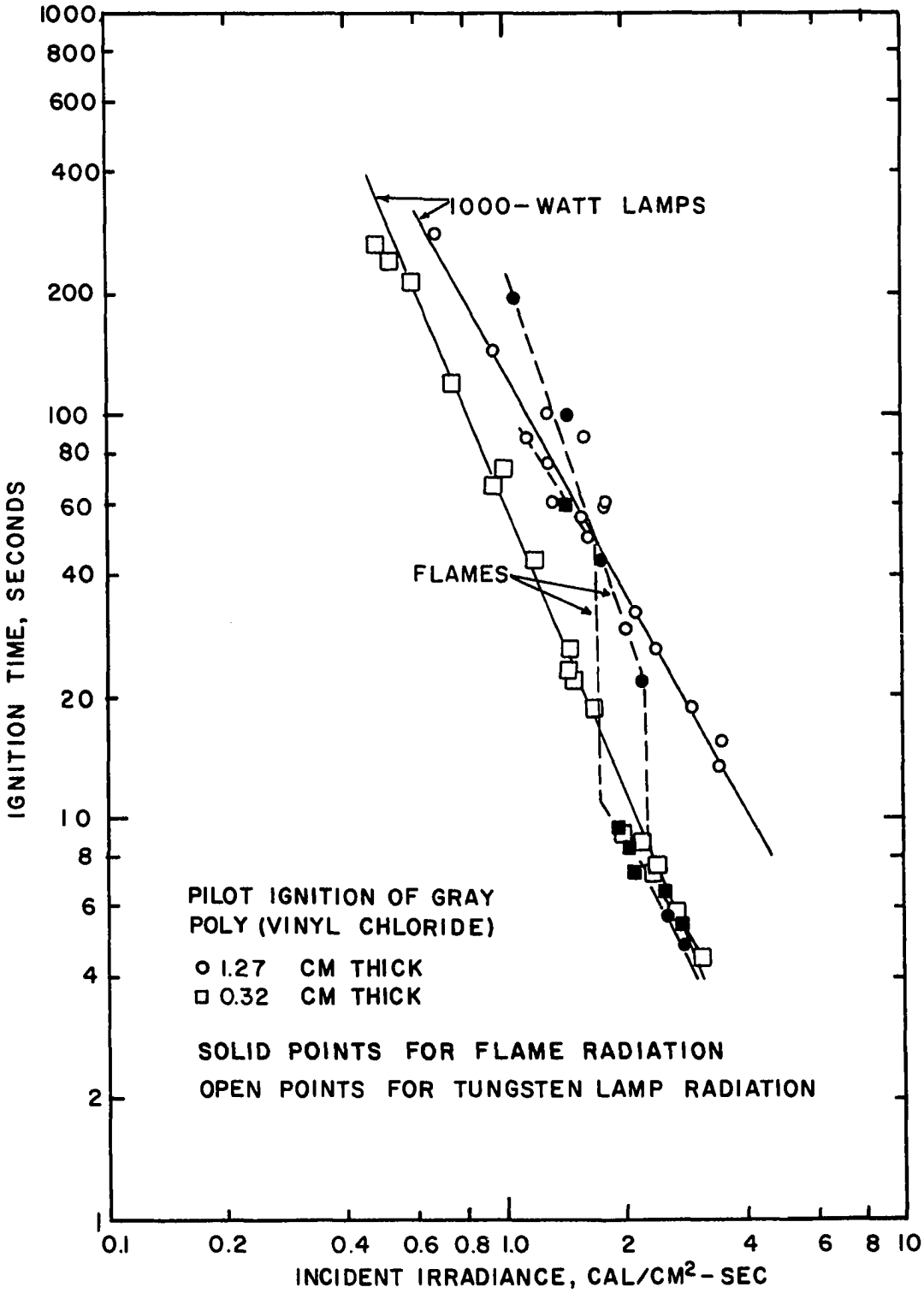

Figure IV-10. Pilot Ignition of Gray Poly(vinyl chloride).

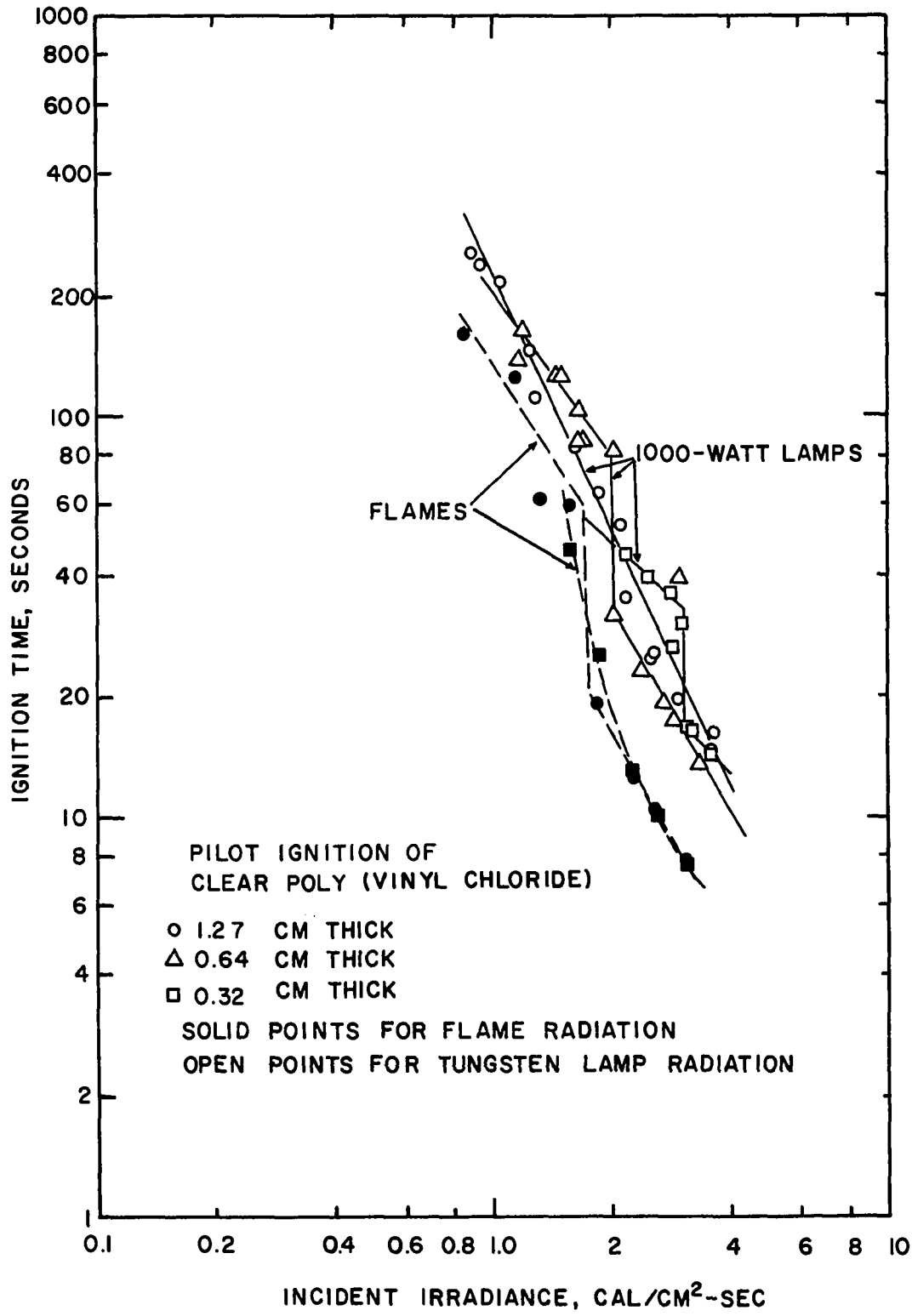

Figure IV-11. Pilot Ignition of Clear Poly(vinyl chloride).

Reich (104) found, by means of a Differential Thermal Analysis (DTA) trace, that at 270°C a reaction starts, with an exothermic reaction peak at 300°C and a second exothermic peak between 375°-425°C. These and other studies (10, 40, 41, 48, 83, 127) gave an indication of the complexity of the reaction kinetics that were developed when PVC was pyrolytically degraded. From these data, it is suggested that, at low heating rates (low irradiance value) the surface temperatures remain low, i.e., less than 350°C, and have a different oxidation reaction with the decomposition products and therefore ignite at a lower temperature than those samples heated at a high rate which attain the reported ignition temperatures of 390°C (99) or 391°C (53). No experimental studies were attempted to provide any confirmation of the lower surface temperature at lower heating rates and vice versa.

Stepek, et al. (123) reported that HCl is given off PVC starting about 170°-190°C. This HCl evolution was confirmed by all the other investigators cited. At higher heating rates in air, the surface temperature reaches and exceeds 300°C yielding first much HCl, followed by a reforming of the polymer fragments to give a small percentage of benzene vapor and much CO gas (127). Application of a high heat flux, where the surface temperature exceeds 600°C, develops a higher concentration of CO and CO_2 with less HCl (127), which would tend to give a more flammable mixture when in contact with an ignition source. Examination of Figures IV-10 and IV-11

indicate that at an irradiance level of 2 cal/cm^2-sec, there is a change in the decomposition kinetics such that, at lower irradiance levels, the evolved vapors are richer in HCl and CO_2 for a longer time period before sufficient quantities of CO and other combustibles are present for ignition. Above 2 cal/cm^2-sec, it appears that the amount of CO and other combustibles is in a greater percentage in the decomposition vapors which causes faster ignition.

It is most unfortunate that the testing performed to date has not incorporated surface temperature, time to ignition, actual heat input rate into the surface, rate of weight loss, and analysis of the pyrolysis vapors and gases, in a simultaneous test procedure. Such a procedure would permit more rigorous analysis of the various parameters involved in a characteristic ignition of a material while under a radiant heat load.

Mathematical Analysis

Thus far in this study, it has been found in the literature search, that there is a great mass of unrelated data concerned with ignition. The parameters that appear to have the most influence upon ignition, based upon previous studies and present tests, are material density, thermal conductivity, specific heat, activation energy, surface absorptance and the spectral distribution of radiant heating. In an attempt to correlate the data available, an equation was

proposed in Chapter II in which the [apparent] most critical parameters were grouped in a single mathematical model, Equation II-19. The complexity of the equation is illustrated by the following:*

$$\frac{\partial}{\partial x}\left(k\,\frac{\partial T}{\partial x}\right) + H\gamma_\lambda e^{-\gamma_\lambda x} - \frac{\partial (m_d C_g T)}{\partial x} = \frac{\partial (\rho C_p T)}{\partial t}$$

$$+ \frac{\partial (\omega_V)}{\partial t}\,\Delta H_V + \frac{\partial (\omega_f)}{\partial t}\,\Delta H_f + Q_z\,\frac{\partial (\omega_z)}{\partial t} \qquad \text{(II-19)}$$

The rate of weight loss due to decomposition is given as

$$\frac{\partial \omega_z}{\partial t} = f[\omega_z \exp - (\frac{\Sigma E}{RT})] \qquad \text{(II-20)}$$

As previously described in Chapter II, Equation II-19 with the included initial and boundary conditions is too complex to solve. Therefore, to facilitate a type of solution, it becomes necessary to reduce the number of parameters and the equation complexity to that of a simpler model.

Assume the polymeric specimen is an infinite slab of inert, opaque material exposed to a constant heat flux on one face with no heat loss on the opposite face. In this assumed model, there is heat transmission through the inert solid by

---

*The nomenclature is listed in Appendix E.

conduction only and the following form of the heat conduction equation for unidirectional heat transfer applies (131, 132, and others):

$$\delta \frac{\partial^2 \Delta T}{\partial x^2} = \frac{\partial \Delta T}{\partial t} \qquad \text{(IV-2)}$$

where δ is the thermal diffusivity. If the solid is assumed to be at ambient temperature prior to testing, then $\Delta T = 0$ for any time, $t \leq 0$. For the present test condition, the front face is assumed to have a constant radiant input, so that the boundary condition for $x = L$ (the front face) at $t > 0$ is

$$-k \frac{\partial \Delta T}{\partial x} = \alpha_{av} H_o \qquad \text{(IV-3)}$$

with H_o = incident irradiance and α_{av} is average absorptance for the particular heat source. Where the back face loses no heat to the surroundings,

$$\frac{\partial \Delta T}{\partial x} = 0 \qquad \text{(IV-4)}$$

at $x = 0$ (the back face).

Using the initial and boundary conditions as specified, a solution to Equation IV-2 has been formulated (page 112, Reference 21) for $\Delta T_s = (T_s - T_o)$, T_s = surface temperature, as

$$\Delta T_s = \frac{\alpha_{av} H_o t^{1/2}}{(k\, C_p \rho)^{1/2}} \sum_{n=0}^{\infty} \left[\text{ierfc} \frac{2nL}{2(\delta t)^{1/2}} + \text{ierfc} \frac{(2n+2)L}{2(\delta t)^{1/2}} \right] \quad \text{(IV-5)}$$

where ierfc denotes the first integral of the complementary error function. Equation IV-5 is the primary relationship for correlating the data of polymer ignition time as a function of ignition temperature, thermal properties and absorbed heat.

The literature search yielded data on some ignition temperatures, thermal conductivities and specific heats of polymers, so that calculation of thermal inertia ($\rho\, C_p k$), and thermal diffusivity, δ, could be made. The present research has yielded ignition time, density and absorbed irradiance. For this study it will be assumed that the thermal diffusivity remains constant over the temperature range up to and including ignition.* In addition, all the present ignition tests were made using a nominal 1.27 cm thick specimen so that both δ and L can be assumed to apply no longer as correlating parameters. As inspection of Equation IV-5 indicates that all of the terms included within the summation (the ierfc function) can be reduced to a single parameter, erf $(\frac{L}{2(\delta t)^{1/2}})$. To determine the magnitude of the error function a single

---

*$\delta = k/\rho C_p$. As a material is heated, the material expands which lowers the density, ρ; i.e., mass/volume, the specific heat, C_p, and the thermal conductivity, k, increase. The action of all three parameters is to maintain a nearly constant thermal diffusivity.

value for density, thermal conductivity, and specific heat was obtained from the respective averages of the 12 plastics tested. In addition, two ignition times were chosen to give values at specific points at 100 and 1000 seconds. Substitution of the above parameters into the summation function of Equation IV-5, using n = 0 to n = 2, yields a value of erf = 1.01 for t = 1000 sec and 0.99^{+} for t = 100 sec. Further investigation of the error function at other times indicates that the magnitude will oscillate about the value 1.0. Since the apparent ignition average for all test samples is approximately 80 seconds, it can be assumed that the error function is unity and Equation IV-5 can be rewritten as

$$t = \Phi \frac{(\Delta T_s)^2 (\rho C_p k)}{(\alpha_{av} H_o)^2} \qquad \text{(IV-6)}$$

Equation IV-6 shows t to be directly related to $(\Delta T_s)^2$ and $(\rho C_p k)$, and inversely related to $(\alpha_{av} H_o)^2$. Using the data acquired during the literature search and the test information from the present study, the ignition time was plotted as a function of the parameter groups of Equation IV-6 and is illustrated in Figure IV-12. The thermal properties data of the various polymers used are listed in Table 3. Figure IV-12 shows a wide scatter of data points but also indicates a possible relationship among the slopes of the various polymers.

Examination of each of the individual polymer data points shows some diversion and/or scatter from a mean slope

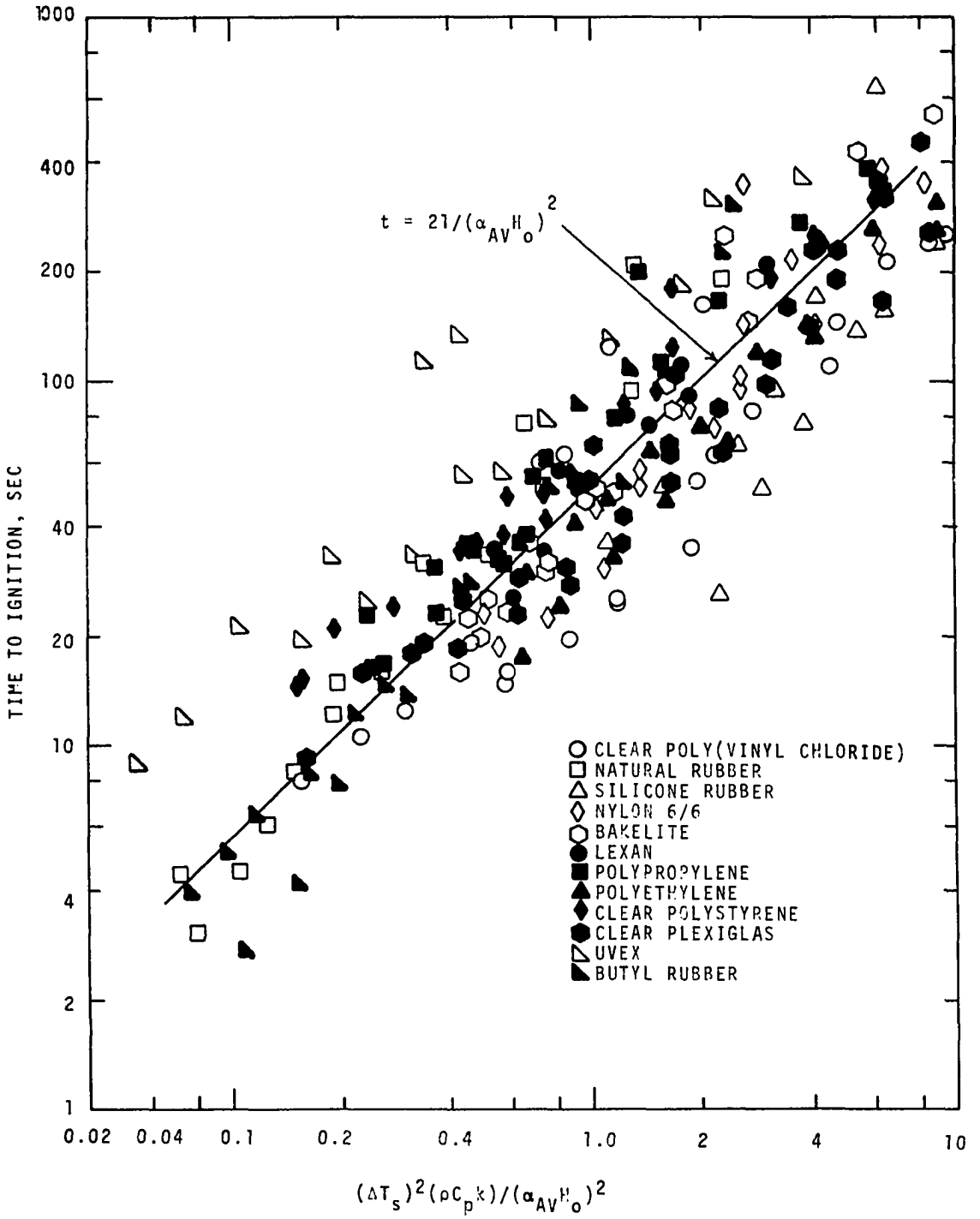

Figure IV-12. A Relationship of Time with Dimensionless Heat Transfer Model

TABLE 3

VARIOUS PARAMETERS AND THEIR VALUES USED IN THE LEAST SQUARES ANALYSIS

Material	Density ρ, gm/cm	Thermal Conductivity, cal/cm^2-sec -°C/cm	Temp Ignition, °K	Specific Heat, cal/gm -°C
Clear PVC	1.31	3×10^{-4}	663 (99)* 573 (104)**	0.20
Natural Rubber	0.99	2.9×10^{-4}	513 (86)	0.45
Silicone Rubber	1.75	5×10^{-4}	763 (53)	0.35
Nylon 66	1.15	5.85×10^{-4}	693 (28)	0.40
Phenolic (Bakelite)	1.37	4.5×10^{-4}	593 (116)	0.36
Polypropylene	0.91	3.7×10^{-4}	598 (47)	0.50
Polycarbonate (LEXAN)	1.19	4.6×10^{-4}	756 (47)	0.30
Polyethylene	0.93	10×10^{-4}	603 (36,53)	0.55
Clear Polystyrene	1.05	2.5×10^{-4}	623 (116)	0.30
Clear Plexiglas	1.19	4×10^{-4}	563 (116)* 493 (81)**	0.35
Cellulose Acetate Butyrate	1.21	4×10^{-4}	432 (113)	0.36
Butyl Rubber	1.09	2.34×10^{-4}	563 (86)	0.46

*High heat rate.

**Low heat rate.

using the same data points as a reference. This divergence is primarily due to the use of room temperature average absorptances for each heating system instead of an average time dependent absorptance. Appendix D discusses the various surface changes occurring for a material as it is heated and ignites. Such surface changes need be tested, as described early in this chapter, and the results analyzed for the average time-dependent absorptance $[\alpha_{av}]_t$. The acquisition of such data will assist in performing more accurate energy balances.

As stated previously, there is a relationship portrayed among the individual plots of the polymers showing a near equality of slopes, but displaced in the time direction. Such a displacement can sometimes be correlated by other mathematical analyses.

A study of the information presented by Figure IV-12 suggested that a least squares analysis could be utilized to group the data into the same parameter groups but with some exponents other than those found from the solution of Equation IV-5. A computer programmed least squares curve fit (105) using the parameters of Table 3, with respect to time, t, yielded

$$t = 160 \frac{(\Delta T_s)^{1.04} (\rho C_p k)^{0.75}}{(\alpha_{av} H_o)^{2.00}} \qquad \text{(IV-7)}$$

Using the data of Table 3, a second plot was made and is illustrated by Figure IV-13. As can be seen, the scatter of

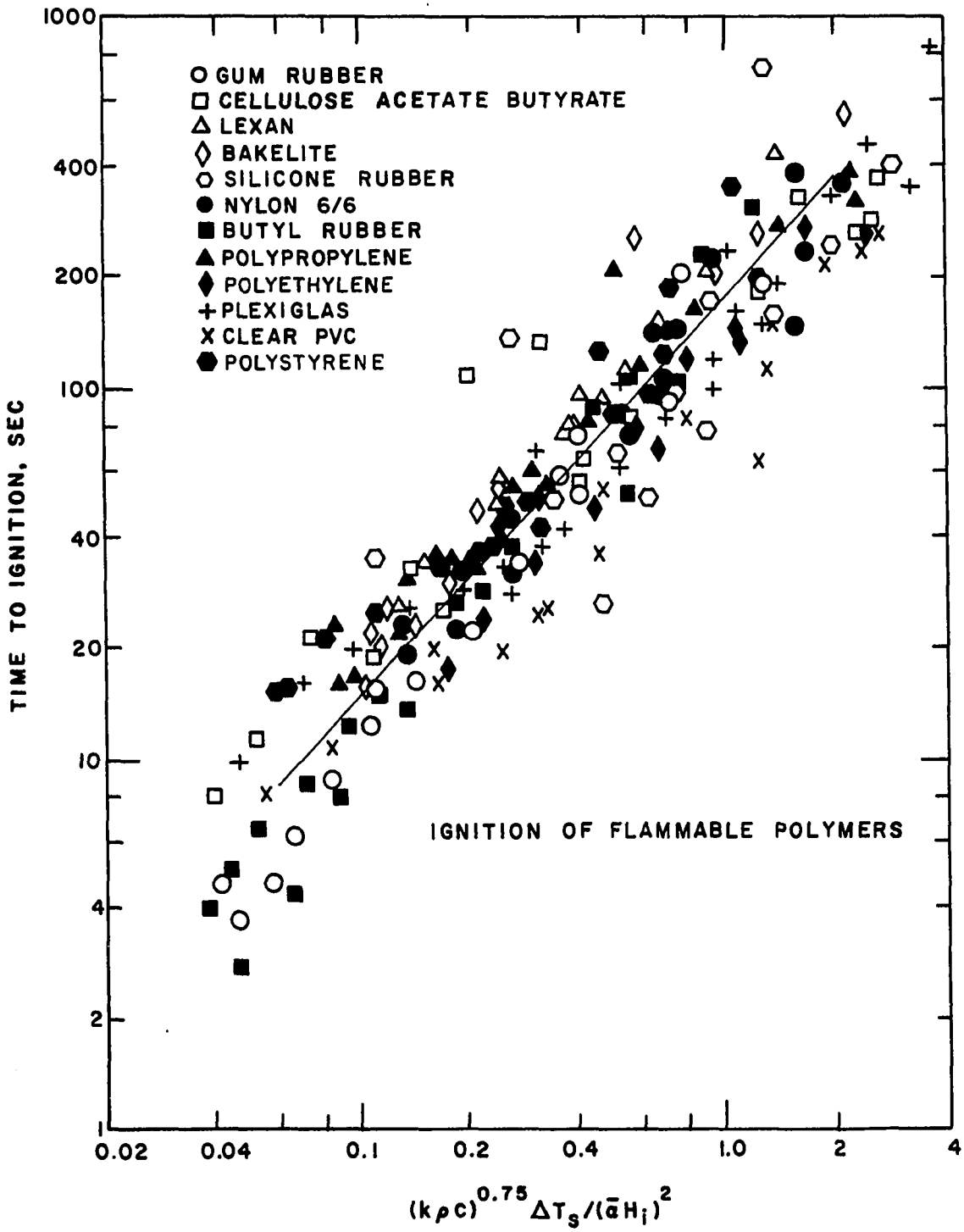

Figure IV-13. Least Squares Curve Fit for Equation IV-9 (Time Relationship with Thermal Inertia, ΔT and Absorbed Heat Energy).

the data points has been greatly reduced and there are fewer displaced data points.

A study of the resultant plot, Figure IV-13, shows several data points that lie below the general grouping of data. These data are a part of the test results obtained from silicone rubber and clear poly(vinyl chloride). The scatter of the silicone rubber is probably due to the changes in surface reflectance as discussed earlier in Chapter IV. Clear PVC was obtained in 0.32 cm thick sheets which required lamination to make up the test specimen thickness of 1.27 cm. During heating, some PVC specimens bowed outward towards the heat source, which caused an increase in incident irradiance of the surface and consequently yielded a more rapid ignition time. Although great care was exercised in preparing all the laminated samples, PVC was the one material that necessitated particular caution to insure complete bonding between layers.

A median slope, drawn through the data points, shows a deviation of ± 100 percent. Part of the deviation is due to the non-time-dependent average absorptance of each material but the remainder is due to the use of average room temperature values of thermal conductivity and specific heat, and the reported ignition temperatures.

The scatter of some data points above the general grouping is due to the suggested following causes:

1. In the case of silicone rubber and clear PVC, the same reasons exist as for the data points below the curve,

except that, in this case, the PVC specimen bowed away from the heat source.

2. The data points for polypropylene (t = 207 sec), polystyrene (t = 350 sec) and phenolic (t = 255 sec and t = 431 sec) are probably due to experimental error or error in technique during the particular test.

In summary, it has been shown that Figure IV-13 illustrates which important parameters must be used for this type of thermal analysis; these are T_i, the ignition temperature, k, the thermal conductivity, C_p, the specific heat, α_{av}, the average surface absorptance of the material, based upon the particular heat source, and ρ, the density. With thermal property information of actual samples available, the relationship of Figure IV-13 will permit prediction of ignition times for those same materials when exposed to a known heat source.

CHAPTER V

CONCLUSIONS AND COMMENTS

This investigation and study is directed towards acquiring information on the ignition characteristics of polymers using the buoyant flame of Koohyar (70) and 1000 watt tungsten lamps as radiant heat sources. Samples tested were of 36 industrial polymeric substances comprising some 25 different chemical formulations, such as polyethylene, polypropylene, polystyrene, poly(vinyl chloride), gasket materials and other compoundings. It was assumed that all samples and materials were dry, i.e., that no moisture was present except that included from the polymerization and/or condensation reaction. The range of sample incident radiation available measured from 0.70 cal/cm^2-sec to 3.54 cal/cm^2-sec for both lamps and flames. Polymer specimen average absorptances ranged from 0.354 to 0.950 for tungsten lamp and from 0.602 to 0.938 for benzene flame. Ignition times varied from 1.1 seconds (cork) to 837 seconds (Plexiglas). No measurement was attempted for surface temperature or weight loss.

The literature search indicated that ignition studies have been confined to (1) investigation of ignition temperature, (2) linear pyrolysis or linear rate of burn, and (3)

formal heat transfer analysis. None of the previous investigators attempted to develop any mathematical models that would relate the parameters of ignition time and irradiance.

Correlation of literature data, i.e., thermal conductivity, specific heat and ignition temperature and test data, ignition time, absorbed heat energy and sample density was attempted through the use of a model based on an inert, opaque solid with constant and uniform properties. The solution to the proposed model and the subsequent computer programmed least squares analysis of the data yielded the equation

$$t = 160 \frac{(\Delta T_s)^{1.04} (\rho C_p k)^{0.75}}{(\alpha_{av} H_o)^{2.00}} \qquad \text{(V-1)}$$

A plot of data using Equation V-1 gave a spread of points of $\pm$ 100 percent of the average over the range of absorbed heat energy.

The most significant information obtained from this study is the following:

1. The pilot ignition time of polymers is inversely proportional to the square of the absorbed energy and directly proportional to the (approximate) first power of the difference between ignition and ambient temperature. The difference in dependence from the direct square is probably due to the changes in thermal inertia of the various polymers and the neglect of reradiation and convection in the model.

2. The ignition time is strongly dependent upon the spectral distribution of the incident radiation. Generally, most polymers have a lower average absorptance for 1000 watt tungsten lamps than for flames. The difference in average absorptance causes the ignition time for light colored polymers, under 1000 watt lamp radiation, to take three to four times as long to ignite as for flames when subjected to the same incident irradiance.
3. A mathematical correlation has been found that will predict the ignition time of several types of plastics when subjected to different sources of radiant heat. To accomplish this correlation certain parameters must be known including the sample density, average surface absorptance, thermal conductivity, specific heat, ignition temperature, and the specific irradiance source and magnitude.

APPENDICES

APPENDIX A

INSTRUMENTATION SYSTEMS AND CALIBRATION TECHNIQUES

The measurement of a desired parameter in any research or investigative project is dependent upon three major items; (1) the technique of measurement itself by means of an instrument capable of attaining the desired range and frequency of sampling, (2) the accuracy of the measuring instrument, and (3) the capability of checking and maintaining the accuracy of the measuring instruments.

In the present ignition study, the measurement of time of ignition and the incident irradiance were the two most important parameters. The techniques and accuracy of the measurements, Items 1 and 2, have been previously described in Chapter III. Item 3, the checking and maintaining of the measuring instruments, is described in the following paragraphs.

Ignition Detector

Pre-operational testing of the cadmium selenide photoconductive cell was performed by flashing a light source into the cell holder opening while the recorder pen circuit was

energized. (See Figure III-17.) The movement of the pen toward full voltage output indicated proper cell response to a momentary impulse of light. An additional test was made using a burning match, again placed in front of the cell holder opening, while observing the fluctuations of the recorder pen to the flickering of the match flame. The recorder pen response was considered as a suitable check that the ignition detector was operational.

Incident Radiation Detector

The permanent radiometer (see Figure III-17) was calibrated for incident heat flux by the use of a second test radiometer as illustrated in Figure A-1. The test radiometer was fixed in a mobile panel that could be inserted in the test panel in place of the sample holder (Figure III-13 and III-17). The lamps (or flame) were turned on at various levels of heat input while the output voltages were recorded simultaneously. By using the calibration curves for the respective radiometers, a graphic relationship between incident heat input to the sample area and the voltage output from the permanent radiometer could be obtained. Figure A-2 is an illustration of a typical calibration curve used to obtain the actual heat flux incident upon any particular sample while under test for ignition capabilities.

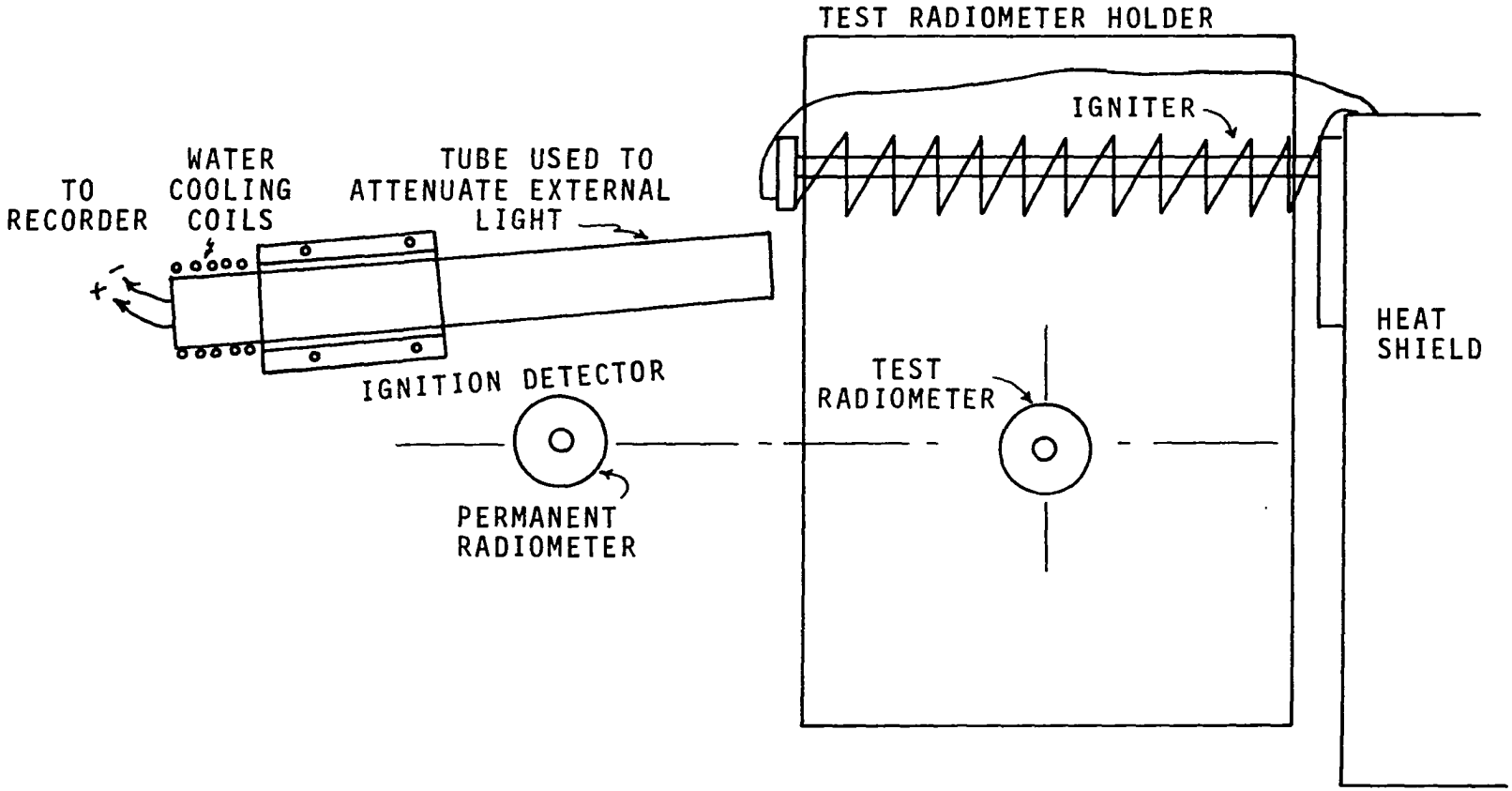

Figure A-1. Diagram of Test Radiometer Placement with Respect to Permanent Radiometer.

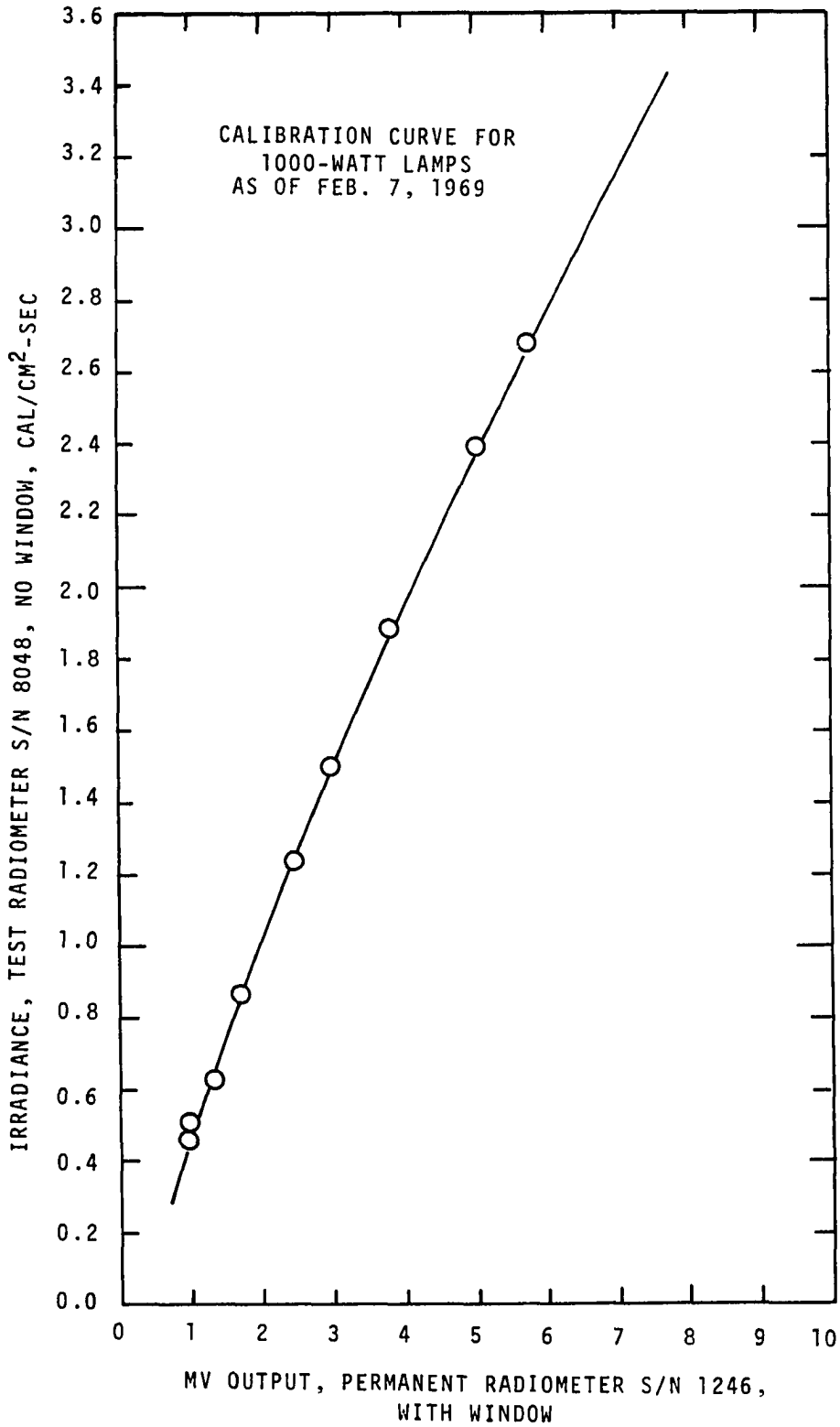

Figure A-2. Calibration Curve for 1000-Watt Lamps.

Recorder System

The Minneapolis-Honeywell (M-H) 2 channel recorder, Model "Electronik 19," was serviced monthly by the M-H representative. Between service periods, a stop watch was used to check the chart speed. Checks were made weekly by operating the chart drive for a 10 second interval, at 1 inch per second, and measuring the output length. Variation in the 10 inches of paper was less than 1/16 inch for the 10 seconds of output.

APPENDIX B

PHYSICAL AND CHEMICAL DATA FOR PLASTICS AND RUBBER

The information concerning each of the tested materials is presented as a compilation of material thermal, chemical and physical properties available in various literature sources.

The designation (L) is used to signify a literature source for the information supplied. For all plastic materials, excluding cork and the elastomers, the following references were used to obtain the desired information: 5, 29, 43, 45, 53, 55, 72, 73, 76, 82, 84, 102, 103, 107, 108, 118, 129.

The designation (S) is used to signify that the indicated information was measured from the test sample.

MATERIALS TESTED

1. Accopac AS-428 Gasket Material
2. Accopac CN-705 Gasket Material
3. Accopac CS-301 Gasket Material
4. Alphalux 400 (Polyphenylene Oxide, PPO)
5. Buna-N Rubber
6. Butyl Rubber IIR
7. Chloroprene DC-100 Gasket Material
8. Cork Gasket Material
9. Cycolac (ABS Type resin)
10. Delrin (Acetyl)
11. Formica (Melamine-Formaldehyde Laminate)
12. Gum Rubber (Natural)
13. Kel-F
14. Kydex (PVC - Acrylate Alloy)
15. Lexan (Polycarbonate)
16. Masonite (Pressed wood)
17. Neoprene Rubber, Closed Cell Sponge
18. Neoprene Rubber, Open Cell Sponge
19. Neoprene Rubber, Solid
20. Nylon 6/6
21. Phenolic (Bakelite)
22. Plexiglas, Black, Opaque
23. Plexiglas, Transparent*

---

*All transparent materials were unpigmented, water-white color.

24. Plexiglas, White, Translucent
25. Polyethylene, Low Density
26. Polypropylene
27. Polystyrene, White, Hi-Impact
28. Poly(vinyl chloride), Transparent (slight Purple cast)
29. Poly(vinyl chloride) + gray filler
30. Silicone Rubber
31. Styrolux (Polystyrene, Transparent)
32. Texin (Polyurethane-Polyester combination)
33. Uvex (Cellulose Acetate Butyrate), Transparent

Material Type: Buna-N Rubber + Asbestos

Trade Name: Accopac AS-428 (Armstrong)

Supplier: Industrial Gasket

Density: 1.243 (S)* g/cm^3

Ignition Behavior: Low resistance to flame

References: (122)

---

*Asbestos, ρ = 0.98 gm/cm^3

Buna-N, ρ = 0.94 - 1.10 gm/cm^3

Material Type: Buna-N Rubber + Cork

Trade Name: Accopac CN-705 (Armstrong)

Supplier: Industrial Gasket

Density: 0.735 (S)* g/cm^3

Ignition Behavior: Low resistance to flame

---

*Cork, ρ = 0.23 gm/cm^3

Buna-N, ρ = 0.94 - 1.10 gm/cm^3

Material Type: Buna-S Rubber + Cork

Trade Name: Accopac CS-301 (Armstrong)

Supplier: Industrial Gasket

Density: 0.722 (S)* g/cm^3

Ignition Behavior: Low resistance to flame

---

*Cork, $\rho = 0.23$ gm/cm^3

Buna-S, $\rho = 0.94 - 1.00$ gm/cm^3

Material Type: Buna-S Rubber

Trade Name: Butadiene + Styrene Copolymer

Specific Heat: 0.44 - 0.48 cal/cm°C

Thermal Conductivity: 6×10^{-5} cal/cm^2-sec°C/cm

Density: 0.92 - 1.00 g/cm^3

Thermal Diffusivity: 0.000136 cm^2/sec

Ignition Behavior: Low resistance to flame

References: (84, 87, 96, 100, 101, 118)

Material Type: Polyphenylene Oxide (PPO)

Trade Name: Alphalux 400 (Westlake Plastics)

Supplier: Cope Plastics

Specific Heat: 0.32 cal/gm°C

Thermal Conductivity: 4.5×10^{-4} cal/cm^2-sec°C/cm

Density: 1.06 (L), 1.0952 (S) g/cm^3

Thermal Diffusivity: .0001286 cm^2/sec

Ignition Behavior: Self-extinguishing

Material Type: Butadiene-Acrylonitrile Copolymer

Trade Name: Buna-N Rubber (Dupont)

Supplier: Industrial Gasket

Specific Heat: 0.47 cal/gm°C

Thermal Conductivity: 60×10^{-5} cal/cm^2-sec°C/cm

Density: 0.94 - 1.10 (L), 1.596 (S) g/cm^3

Thermal Diffusivity: 0.0000801 cm^2/sec

Ignition Behavior: Low-medium resistance to flame.

References: (45, 51, 84, 87, 96, 100, 101, 118)

Material Type: Isobutylene-Isoprene Copolymer

Trade Name: Butyl Rubber, IIR (Phillips Chemical Co.)

Supplier: Tire Retread Co.

Specific Heat: 0.44 - 0.46 cal/gm°C

Thermal Conductivity: 2.34×10^{-4} cal/cm^2-sec°C/cm

Density: 0.92 - 0.98 (L), 1.093 (S) g/cm^3

Thermal Diffusivity: 0.0000465 cm^2/sec

Ignition Behavior: High flammability

References: (45, 72, 84, 87, 96, 100, 101, 118)

Material Type: Neoprene Rubber + Cork

Trade Name: Chloroprene DC-100 (Armstrong)

Supplier: Industrial Gasket

Density: 0.804 (S) g/cm^3

Material Type: Cork Gasket

Trade Name: Cork sheeting #9520 (Dodge Cork)

Supplier: Industrial Gasket

Thermal Conductivity: 13.2×10^{-4} cal/cm^2-sec°C/cm

Density: 0.23 (L), 0.253 (S1)*, 0.244 (S2) g/cm^3

Ignition Behavior: At 250°F, slow distillation effect; ignites on contact with flames only; not sustained.

References: (31, 46, 89, 91)

---

*(S1) As received

(S2) Dried 80°C, 24 hours

Material Type: ABS Resin (Marbon Chemical)

Trade Name: Cycolac (Westlake Plastics)

Supplier: Cope Plastics

Specific Heat: 0.3 - 0.4 cal/gm°C

Thermal Conductivity: $4.6 - 8 \times 10^{-4}$ cal/cm^2-sec°C/cm

Density: 0.99 - 1.15 (L), 1.029 (S) g/cm^3

Thermal Diffusivity: 0.0001535 cm^2/sec

Ignition Behavior: Slow burning rate

Material Type: Acetyl Resin (Dupont Homopolymer)

Trade Name: Delrin (Polymer Corp)

Supplier: Cope Plastics

Specific Heat: 0.35 cal/gm°C

Thermal Conductivity: 5.5×10^{-4} cal/cm^2-sec°C/cm

Density: 1.425 (L), 1.4372 (S) g/cm^3

Thermal Diffusivity: 0.0001094 cm^2/sec

Ignition Behavior: Burning rate, 1.1 inch/min

Material Type: Melamine-Formaldehyde Composite, Laminate and Flock Filler

Trade Name: Formica (SN 52 Grade) Formica Corp

Supplier: Cope Plastics

Specific Heat: 0.35 cal/gm°C

Thermal Conductivity: 7.0×10^{-4} cal/cm^2-sec°C/cm

Density: 1.500 (L), 1.392 (S) g/cm^3

Thermal Diffusivity: 0.0001335 cm^2/sec

Ignition Behavior: Very low burning rate in inches/min.

Material Type: Natural isoprene (Hevea latex)

Trade Name: Gum Rubber (Acme - Hamilton)

Supplier: Industrial Gasket

Specific Heat: 0.45 - 0.50 cal/gm°C

Thermal Conductivity: 2.9×10^{-4} cal/cm^2-sec°C/cm

Density: 0.92 - 0.98 (L), 0.99 (S) g/cm^3

Thermal Diffusivity: 0.0000651 cm^2/sec

Ignition Behavior: Low resistance to flame

References: (84, 87, 96, 100, 101, 118)

Material Type: Chlorotrifluoroethylene (CTFE) (3M)

Trade Name: Kel-F (Saunders Corp. of LA, Type 5441 #S310)

Supplier: Cope Plastics

Specific Heat: 0.22 cal/gm°C

Thermal Conductivity: $4.7 - 5.3 \times 10^{-4}$ cal/cm^2-sec°C/cm

Density: 2.1 - 2.2 (L), 2.099 (S) g/cm^3

Thermal Diffusivity: 0.0001018 cm^2/sec

Ignition Behavior: Non-flammable

Material Type: PVC-Acrylic Copolymer

Trade Name: KYDEX 100 (Rohm and Haas)

Supplier: Cope Plastics

Density: 1.322* (S), 1.309** (S) g/cm^3

---

*Gray Pigment, rolled

**Red Pigment, cast

Material Type: Polycarbonate (LEXAN)

Trade Name: ZELUX (Westlake Plastics)

Supplier: Cope Plastics

Specific Heat: 0.3 cal/gm°C

Thermal Conductivity: 4.6×10^{-4} cal/cm^2-sec°C/cm

Density: 1.2 (L), 1.193 (S) g/cm^3

Thermal Diffusivity: 0.0001286 cm^2/sec

Ignition Behavior: Self-extinguishing

Material Type: Pressed Wood Fibers

Trade Name: Masonite, Prestwood (Masonite Corp)

Supplier: Local Lumber Dealer

Density: 1.02 (L), 1.003 (S) g/cm^3

Ignition Behavior: Same as wood

Material Type: G207N Neoprene (Cellular Prod. Corp)

Trade Name: Closed Cell Neoprene Sponge Rubber

Supplier: Industrial Gasket

Specific Heat: 0.095 cal/gm°C

Thermal Conductivity: 0.831×10^{-4} cal/cm^2-sec°C/cm approx.

Density: 0.1285 - 0.1605 (L), 0.275 (S) g/cm^3

Thermal Diffusivity: 0.00319 cm^2/sec

Ignition Behavior: Non-flammable

Material Type: Open Cell Neoprene Sponge Rubber

Trade Name: Neoprene Sponge (Rubbertex Corp)

Supplier: Industrial Gasket

Specific Heat: 0.20 cal/gm°C

Thermal Conductivity: 1.720×10^{-4} cal/cm^2-sec°C/cm approx.

Density: 0.1285 - 0.1605 (L), 0.564 (S) g/cm^3

Thermal Diffusivity: 0.00153 cm^2/sec

Ignition Behavior: Non-flammable

Material Type: Chloroprene (CR) (Acme-Hamilton Co.)

Trade Name: Neoprene Rubber, solid sheet

Supplier: Industrial Gasket

Specific Heat: 0.52 cal/gm°C

Thermal Conductivity: 4.5×10^{-4} cal/cm^2-sec°C/cm

Density: 1.25 - 1.30 (L), 1.478 (S) g/cm^3

Thermal Diffusivity: 0.0000587 cm^2/sec

Ignition Behavior: High resistance to flame

References: (23, 45, 72, 84, 87, 96, 100, 101, 118)

Material Type: Polyhexamethyleneadipamode

Trade Name: Nylon 6/6 (Dupont)

Supplier: Cope Plastics and Cadillac Plastics

Specific Heat: 0.4 cal/gm°C

Thermal Conductivity: 5.85×10^{-4} cal/cm^2-sec°C/cm

Density: 1.13 - 1.15 (L), 1.116 (S1)*, 1.146 (S2)** g/cm^3

Thermal Diffusivity: 0.0001278 (1), 0.0001266 (2) cm^2/sec

Ignition Behavior: Self-extinguishing

---

*S1 - Cope Plastics, Oklahoma City

**S2 - Cadillac Plastics Co.

Material Type: Phenol-formaldehyde resin

Trade Name: CE Phenolic (cord filler)

Supplier: Cadillac Plastics

Specific Heat: 0.35 - 0.40 cal/gm°C

Thermal Conductivity: 4 - 7 x 10^{-4} cal/cm^2-sec°C/cm

Density: 1.36 - 1.43 (L), 1.368 (S) g/cm^3

Thermal Diffusivity: 0.000977 cm^2/sec

Ignition Behavior: Almost no burn rate

Material Type: Methyl Methacrylate Polymer (Rohm and Haas)

Trade Name: Black Plexiglas (G, unshrunk)

Supplier: Precision Plastics

Specific Heat: 0.35 cal/gm°C

Thermal Conductivity: 4 - 7 x 10^{-4} cal/cm^2-sec°C/cm

Density 1.17 - 1.20 (L), 1.264 (S1)*, 1.219 (S2)** g/cm^3

Thermal Diffusivity: 0.0001355 (S1)*, 0.0001408 (S2)** cm^2/sec

Ignition Behavior: Burn rate = 1.0 - 1.3 inch/min

---

*S1 = 0.63 cm solid sample

**S2 = 1.27 cm laminated sample; 2 x 0.63 cm

Material Type: Methyl Methacrylate (Rohm and Haas)

Trade Name: Clear Plexiglas (G, unshrunk)

Supplier: Cope Plastics and others

Specific Heat: 0.35 cal/gm°C

Thermal Conductivity: $4 - 6 \times 10^{-4}$ cal/cm^2-sec°C/cm

Density: 1.17 - 1.20 (L), 1.187 (S1)*, 1.173 (S2)**, 1.249 (S3)*** g/cm^3

Thermal Diffusivity: 0.000961 (S1)*, 0.000975 (S2)**, 0.001375 (S3)*** cm^2/sec

Ignition Behavior: Burning rate = 1.0 - 1.3 inch/min

*S1 = 1.27 cm sample, Cope Plastics, type G
**S2 = 0.63 cm sample, OURI supply, type G
***S3 = 1.27 cm sample, Cadillac Plastics, type GN

Material Type: Methyl Methacrylate (Rohm and Haas)

Trade Name: White Plexiglas (G, unshrunk)

Supplier: Precision Plastics and Cadillac Plastics

Specific Heat: 0.35 cal/gm°C

Thermal Conductivity: $4 - 6 \times 10^{-4}$ cal/cm^2-sec°C/cm

Density: 1.17 - 1.20 (L), 1.194 (S1)*, 1.219 (S2)**, 1.158 (S3)*** g/cm^3

Thermal Diffusivity: 0.0001435 (S1)*, 0.0001410 (S2)**, 0.0000988 (S3)*** cm^2/sec

Ignition Behavior: Burning rate = 1.0 - 1.3 inch/min

*S1 = 0.63 cm sample, Precision Plastics
**S2 = 0.63 cm sample, Cadillac Plastics
***S3 = 1.27 cm sample, Precision Plastics

Material Type: Polyethylene (Siberling Rubber Co.)

Trade Name: Polyethylene, low density

Supplier: Cope Plastics

Specific Heat: 0.55 cal/gm°C

Thermal Conductivity: 10×10^{-4} cal/cm^2-sec°C/cm

Density: 0.926 - 0.940 (L), 0.930 (S) g/cm^3

Thermal Diffusivity: 0.0001955 cm^2/sec

Ignition Behavior: Burning rate = 1.04 inch/min

Material Type: Polypropylene (Siberling Rubber Co.)

Trade Name: Polypropylene, natural, general purpose

Supplier: Cope Plastics

Specific Heat: 0.5 cal/gm°C

Thermal Conductivity: $3 - 4 \times 10^{-4}$ cal/cm^2-sec°C/cm

Density: 0.90 - 0.91 (L), 0.907 (S) g/cm^3

Thermal Diffusivity: 0.000815 cm^2/sec

Ignition Behavior: Burning rate, slow

Material Type: Polystyrene (Dow Chemical Co.)

Trade Name: White, high-impact Polystyrene

Supplier: Cope Plastics

Specific Heat: 0.32 - 0.35 cal/gm°C

Thermal Conductivity 1.9 - 3.0 x 10^{-4} cal/cm^2-sec°C/cm

Density: 0.98 - 1.10 (L), 1.001 (S1)*, 1.046 (S2)**, 1.092 (S3)***, 0.998 (S4)**** g/cm^3

Thermal Diffusivity: 0.000591 (S1)*, 0.000569 (S2)**, 0.000628 (S3)***, 0.000595 (S4)**** cm^2/sec

Ignition Behavior: Burning rate - slow

*S1 = 0.32 cm sample (10-68)
**S2 = 0.63 cm sample, laminated (2 x 0.32 cm)
***S3 = 1.27 cm sample, laminated (4 x 0.32 cm)
****S4 = 0.32 cm sample (4-68)

Material Type: Clear Poly(vinyl chloride) (Union Carbide)

Trade Name: Rigid Polyvinyl, Clear

Supplier: Precision Plastics

Specific Heat: 0.2 - 0.28 cal/gm°C

Thermal Conductivity: 3.0 - 7.0 x 10^{-4} cal/cm^2-sec°C/cm

Density: 1.35 - 1.45 (L), 1.384 (S1)*, 1.326 (S2)**, 1.315 (S3)*** g/cm^3

Thermal Diffusivity: 0.000174 (S1)*, 0.000182 (S2)**, 0.000114 (S3)*** cm^2/sec

Ignition Behavior: Self-extinguishing

*S1 = 0.32 cm sheet
**S2 = 0.63 cm laminated sample (2 x 0.32 cm)
***S3 = 1.27 cm laminated sample (4 x 0.32 cm)

Material Type: Poly(vinyl chloride) (Union Carbide, type 6200)

Trade Name: PVC, gray pigmented, 1.27 cm

Supplier: Precision Plastics

Specific Heat: 0.2 - 0.28 cal/gm°C

Thermal Conductivity: 3.0 - 7.0 x 10^{-4} cal/cm^2-sec°C/cm

Density: 1.35 - 1.45 (L), 1.433 (S) g/cm^3

Thermal Diffusivity: 0.0001680 cm^2/sec

Ignition Behavior: Self-extinguishing

Material Type: Poly(vinyl chloride) + filler

Trade Name: PVC, rolled gray, 0.32 cm

Supplier: Cadillac Plastics

Specific Heat: 0.2 - 0.28 cal/gm°C

Thermal Conductivity: 3.0 - 7.0 x 10^{-4} cal/cm^2-sec°C/cm

Density: 1.35 - 1.45 (L), 1.427 (S1)*, 1.411 (S2)**, 1.385 (S3)*** g/cm^3

Thermal Diffusivity: 0.0001685 (S1)*, 0.0001711 (S2)**, 0.0001695 (S3)*** cm^2/sec

Ignition Behavior: Self-extinguishing

---

*S1 = 0.32 cm sample

**S2 = 0.63 cm laminated sample (2 x 0.32 cm)

***S3 = 1.27 cm laminated sample (4 x 0.32 cm)

Material Type: Polysiloxane (500 - 600 lb type)

Trade Name: Silicone Rubber (Connecticut Hard Rubber Co.)

Supplier: Industrial Gasket

Specific Heat: 0.35 cal/gm°C

Thermal Conductivity: $\sim 5 \times 10^{-4}$ cal/cm^2-sec°C/cm

Density: 1.1 - 1.6 (L), 1.749 (S) g/cm^3

Thermal Diffusivity: 0.0000818 cm^2/sec

Ignition Behavior: High resistance to flame

References: (45, 69, 72, 84, 87, 96, 100, 101, 118)

Material Type: Polystyrene, clear

Trade Name: Styrolux (Westlake Plastics)

Supplier: Cope Plastics

Specific Heat: 0.3 -0.35 cal/gm°C

Thermal Conductivity: $2.4 - 3.3 \times 10^{-4}$ cal/cm^2-sec°C/cm

Density: 1.04 - 1.09 (L), 1.0513 (S) g/cm^3

Thermal Diffusivity: 0.0000825 cm^2/sec

Ignition Behavior: Slow burning rate

Material Type: Polyurethane Elastomer + Polyester Resin

Trade Name: Texin (A. L. Hyde Co. #355 D)

Supplier: Cope Plastics

Specific Heat: 0.42 - 0.44 cal/gm°C

Thermal Conductivity: 5×10^{-4} cal/cm^2-sec°C/cm

Density: 1.24 - 1.26 (L), 1.200 (S) g/cm^3

Thermal Diffusivity: 0.0000992 cm^2/sec

Ignition Behavior: Slow burning rate

Material Type: Cellulose Acetate Butyrate Sheet

Trade Name: Uvex (Eastman Kodak)

Supplier: Precision Plastics

Specific Heat: 0.3 - 0.4 cal/gm°C

Thermal Conductivity: $4.0 - 8.0 \times 10^{-4}$ cal/cm^2-sec°C/cm

Density: 1.15 - 1.22 (L), 1.199 (S1)*, 1.207 (S2)**,
1.195 (S3)*** g/cm^3

Thermal Diffusivity: 0.0001011 (S1)*, 0.0000996 (S2)**,
0.0000930 (S3)*** cm^2/sec

Ignition Behavior: Slow burning rate

---

*S1 = 0.32 cm sheet

**S2 = 0.63 cm laminated sample (2 x 0.32 cm)

***S3 = 1.27 cm laminated sample (4 x 0.32 cm)

APPENDIX C

A SUMMARY OF IGNITION TIME DATA

The information derived from the ignition testing is presented in three general categories for each polymeric test material:

Section I - Visual observation of the pre-ignition and ignition behavior for both lamp and flame heating source. The indicated results are given for a nominal irradiance of 1.5-2.0 cal/cm^2-sec or greater. Table C-1.

Section II - A figure indicating nominal ignition time as a function of incident irradiance for both flames and lamps heat source. Figures C-1 through C-33.

Section III - A table listing the test data of ignition time-irradiance level for both heat sources, flames and lamps. Tables C-2 through C-20.

MATERIALS TESTED

1. Accopac AS-428 Gasket Material
2. Accopac CN-705 Gasket Material
3. Accopac CS-301 Gasket Material
4. Alphalux 400 (Polyphenylene Oxide, PPO)
5. Buna-N Rubber
6. Butyl Rubber IIR
7. Chloroprene DC-100 Gasket Material
8. Cork Gasket Material
9. Cycolac (ABS Type resin)
10. Delrin (Acetyl)
11. Formica (Melamine-Formaldehyde Laminate)
12. Gum Rubber (Natural)
13. Kel-F
14. Kydex (PVC - Acrylate Alloy)
15. Lexan (Polycarbonate)
16. Masonite (Pressed wood)
17. Neoprene Rubber, Closed Cell Sponge
18. Neoprene Rubber, Open Cell Sponge
19. Neoprene Rubber, Solid
20. Nylon 6/6
21. Phenolic (Bakelite)
22. Plexiglas, Black, Opaque
23. Plexiglas, Transparent*

---

*All transparent materials were unpigmented, water-white color.

24. Plexiglas, White, Translucent
25. Polyethylene, Low Density
26. Polypropylene
27. Polystyrene, White, Hi-Impact
28. Poly(vinyl chloride), Transparent (slight purple cast)
29. Poly(vinyl chloride) + gray filler
30. Silicone Rubber
31. Styrolux (Polystyrene, Transparent)
32. Texin (Polyurethane-Polyester combination)
33. Uvex (Cellulose Acetate Butyrate), Transparent

SECTION I

VISUAL OBSERVATIONS OF IGNITION

TABLE C-1

A SUMMARY OF VISUAL OBSERVATIONS
OF THE IGNITION PROCESS

ACCOPAC AS-428

Flame Ignition

Surface turns dark to black; smoke and vapor emitted with ignition but not sustained; very pungent odor, coupled with odor of burnt wood; surface charred and some cracking after burn; at low heating, sample surface cracked and opened up before ignition occurred; sample face glowed at low heat.

Lamp Ignition

At low heat, sample smoked and surface turned white with no ignition. At higher heats, surface broke open, turned white, much smoke and vapors, ignition and burning sustained; surface white and crumbly after burn.

ACCOPAC CN-705

Flame Ignition

At very low heating, surface turns white with large cracks, not much vapor; at low heat, surface chars and glows with vapors given off, surface cracks and opens up; ignition but not sustained; appearance of NO_2 in gases; after burn, surface is cracked, swelled and charred; gases are pungent and noxious.

Lamp Ignition

Surface darkens, smoke and vapors given off, ignition not sustained long. Very noxious odor, sickening; surface has slight bubbling and cracking at low heating, surface cracks and opens up, much smoke and vapor; surface glows and whitens.

TABLE C-1 (Continued)

ACCOPAC CS-301

Flame Ignition

Surface turns dark, smoke and vapor emitted; ignites and sustains; surface has light char after burn, has odor of burnt wood and pungent; at low heating, ignition retarded until surface cracks and spalls; surface glows at low heating before ignition.

Lamp Ignition

At low heat, surface darkens and blackens, much smoke and vapors-surface cracks, bends and glows; turns white; ignition and burning sustained with much black smoke; pungent rubbery odor; surface charred after burn.

ALPHALUX 400 (PPO)

Flame Ignition

Surface darkens and light vapors given off. Large black bubble forms on surface, when bubble breaks, ignition occurs. Pungent odor of phenol present. Surface charred after burn. Ignition sustained at high heat fluxes.

Lamp Ignition

Surface turns dark, then black. Black bubble(s) form on surface, when bubble(s) break, ignition; surface chars; material reacts like nylon; ignition sustained; surface charred and pitted after test.

BUNA-N RUBBER

Flame Ignition

At low heat vapors given off, surface cracked and swelled; material ignites and sustains burning for only a short time; burns with heavy black smoke, surface charred after burn with strong acidic odor; at low heat, appearance of NO_2 vapors during burning.

TABLE C-1 (Continued)

BUNA-N RUBBER (Continued)

Lamp Ignition

Surface starts to crack, much smoke given off. Surface turns to a gray-yellow color, ignition and burning sustained; at medium heat, surface spalls and crumbles; at low heat, appearance of NO_2 gas (red-brown color), surface has little spalling or crumbling.

BUTYL RUBBER IIR

Flame Ignition

Surface dulls to non-reflecting; gases given off; small bubbles appear then ignition and sustained burning. Surface charred after burn; typical rubber smell.

Lamp Ignition

Vapor and brown smoke evolve; surface becomes mottled and cracks, smoke becomes heavier, then ignition; burns with heavy black smoke, ignition sustained; typical rubber smell, surface gummy and some char after burn.

CHLOROPRENE DC-100

Flame Ignition

At low heat, surface char apparently holds in vapors until surface cracks, then immediate ignition; at higher heat surface turns dark, chars and ignites, much vapor and smoke given off; ignition not sustained; has a blue flame, surface cracks and chars; burnt cork smell; at low heat sample bends and buckles.

Lamp Ignition

Surface turns dark, smoke and vapors emitted; surface cracks and red-brown fumes given off, ignition and sustained; surface black, charred and cracked; after run, very noxious smell. At low heat, samples buckled.

TABLE C-1 (Continued)

CORK GASKET

Flame Ignition

Surface turns dark, while vapors and smoke are emitted; ignition, but only sustained for short interval; material has burnt wood/cork smell; surface charred after burn; at low heat, surface has deep cracks and char, no ignition; at high heat, small cracks in surface.

Lamp Ignition

Surface turns black and chars; much smoke at first, then decreases; ignition not sustained at low heat; surface glows; ignition sustained at high heat; surface gets deep cracks at low heat.

CYCOLAC

Flame Ignition

Surface develops very small bubbles, which grow larger and turn brown. Vapor and smoke given off; ignition and sustained burning with blue/yellow flame; has odor of burnt rubber; surface charred after burn; at high heating rates surface has spongy char; at low heating rates, some flashes prior to ignition.

Lamp Ignition

Surface develops bubbles and vapors are emitted, surface turns brown with heavy smoke, then ignition; material does not run; burning accompanied with heavy black smoke; burning sustained after heat source removed; surface charred after burn; odor like burnt rubber.

DELRIN

Flame Ignition

Bubbles appear on surface with some vapors given off; bubbles break and ignition occurs. Burns with a light blue flame with burning sustained. Surface melts and flows. Surface porous after burn; slight brown coloration, no odor.

TABLE C-1 (Continued)

DELRIN (Continued)

Lamp Ignition

Surface starts to bubble, then turns to froth, ignition difficult to detect; burns with blue and/or colorless flame; little smoke or vapors given off during burn; surface runs during burning; material turns dark after heat source removed; has no odor.

FORMICA

Flame Ignition

Surface discolors, bubbles form and break, heavy white smoke just before ignition; ignition sustained; surface charred and shows layered construction; odor similar to phenol; at low heat flux, surface glows before ignition.

Lamp Ignition

Large bubbles form on surface; at high heat fluxes, ignition; at low heat rates, delayed ignition; surface chars; deep burning shows layered construction; material under surface burns with some smoke; ignition sustained only at high heat rates.

GUM RUBBER

Flame Ignition

Surface turns dark with evolution of smoke and vapor; ignites and sustains burning; surface melts and chars, does not run, gets gummy; some surface swelling typical rubber smell; has black smoke on burning.

Lamp Ignition

Surface turns dark, vapor and smoke evolve, very small bubbles appear on the surface, ignition and burning sustained; typical rubber smell; burns with black smoke. Surface dark and charred after burn. Sample loses structural strength upon heating.

TABLE C-1 (Continued)

KEL-F

Flame Ignition

No testing performed with flames.

Lamp Ignition

Material turns transparent near melting point, decomposes with much smoke and vapor; surface runs slightly; does not ignite.

KYDEX 100, GRAY, ROLLED

Lamp Ignition

Small bubbles at first, then char. Surface becomes crinkley and distorted; heavy white smoke and vapors given off; surface action appears to be of decomposition; sample burns with a blue flame, not sustained after heat source removed, sample charred after test.

KYDEX 100, MAROON, CAST

Lamp Ignition

Surface chars and decomposes; heavy vapors and smoke given off, material does not run; after burn, surface is charred and cracked, ignition not sustained after heat source removed; sample has blue flame during burn.

ZELUX (LEXAN, POLYCARBONATE)

Flame Ignition

Surface becomes glossy, small bubbles and vapors appear, with bubbles gradually enlarging and vapors increasing; surface flows, bubbles break and ignition with sustained burning. Burns with black smoke, surface charred after burn, very distinctive odor.

TABLE C-1 (Continued)

ZELUX (Continued)

Lamp Ignition

Small bubbles form on surface, then surface turns brown, smoke and vapors are emitted; surface starts to flow just before ignition, then runs badly; ignition sustained slightly after heat removed; very peculiar odor during burning; surface charred after burning.

MASONITE

Flame Ignition

Vapors emitted, surface turns dark, ignites and burning is sustained; light colored smoke, normal wood smell, surface charred after burn.

Lamp Ignition

Smokes immediately and ignites rapidly; burns like the wood it is composed of, usually pine; holds shape, surface chars and cracks slightly, ignition sustained.

NEOPRENE CLOSED CELL SPONGE RUBBER

Flame Ignition

Sample expands during heating; surface pits and chars; much vapor before ignition; ignition and sustained; sample curls during burn; surface charred after burn; typical rubber smell.

Lamp Ignition

White smoke plus NO_2 vapors emitted almost immediately; material expands and surface cracks and crumbles, ignition and burning sustained; very pungent odor (similar to nitric acid); material turns gummy after heating, surface all charred.

TABLE C-1 (Continued)

NEOPRENE OPEN CELL SPONGE RUBBER

Flame Ignition

At low heat, surface chars and cracks, bulges out; vapors/smoke given off; surface turns white; material ignites and sustains burning; surface has heavy solid char after burn, flakes off in layers; typical rubber odor.

Lamp Ignition

Surface develops small bubbles, gases and smoke given off, NO_2 emitted in large quantities, ignition, surface spalls, chars. White smoke emitted, ignition sustained; surface charred after burn; very strong, nauseating odor.

NEOPRENE RUBBER, SOLID

Flame Ignition

Surface starts to give off white vapors, pits and cracks; ignition, but not sustained; surface cracked and charred after burn; typical rubber smell, not as strong as regular rubber; at low heat, surface cracks and spalls.

Lamp Ignition

Vapors given off, surface starts to bubble, white smoke emitted, surface spalls and crumbles, ignition but not sustained; surface cracked, brittle and charred after burn, very strong odor; material not rubbery.

NYLON 6/6

Flame Ignition

Surface turns glassy, small bubbles appear, surface browns and starts to foam and large black bubbles form, much gas and vapors given off; surface flows and drips; ignition with sustained burning; burnt hair smell; surface charred after burn.

TABLE C-1 (Continued)

NYLON 6/6 (Continued)

Lamp Ignition

Small bubbles appear on surface, turning to froth; material turns dark with vapors being given off; material runs after ignition, ignition sustained after heat source removed; surface darkens and chars during burn; odor like burnt hair given off during burn.

PHENOLIC (BAKELITE)

Flame Ignition

Surface turns black, vapors and some smoke given off. Ignition and sustained in random cases. Surface slightly charred after burn.

Lamp Ignition

Bubbles form on surface; surface turns dark and chars; heavy smoke and vapors given off during burning; ignition not sustained after heat source removed; typical phenolic smell. Surface activity shows layer of fibers after burn.

BLACK PLEXIGLAS

Flame Ignition

At high heat, slight amount of vapor is given off but surface appears unchanged up to ignition; burns with yellow-blue flame with much black smoke; at low heat, very small bubbles appear prior to ignition; pungent odor, surface charred after burn.

Lamp Ignition

Bubbles on surface, then ignites; burning continues after heat source removed; surface charred after burn; little smoke during burning, has pungent smell.

TABLE C-1 (Continued)

TRANSPARENT PLEXIGLAS

Flame Ignition

Surface does not appear to change up to ignition, very little vapors given off; ignition is sustained; surface turns dark and some bubbles appear; pungent odor; burns with a blue flame with some light yellow flame.

Lamp Ignition

Small bubbles first form on surface, then grow larger and break, releasing vapors. Flame burns with heavy black smoke. Surface turns brown during burn, some char after burn. Ignition sustained after heat source removed. Vapors have bitter, pungent smell; sample melts during burning, and runs.

WHITE PLEXIGLAS

Flame Ignition

At low heat, small bubbles appear, then grow larger and break; surface melts and vapors given off; acid smell; ignition, burning sustained. Surface brown after burn; material gives off black smoke during burning.

Lamp Ignition

Small bubbles form on surface, then grow larger and break. Vapors released. Material melts rapidly and flows. Heavy black smoke after ignition, sample turns brown during burn; some char after burn; ignition continues after heat source removed; vapors have pungent odor.

TABLE C-1 (Continued)

POLYETHYLENE, LOW DENSITY

Flame Ignition

Surface turns glassy, then brown with much vapor emitted. Small bubbles appear, then ignition with burning sustained; surface flows; some discoloration and char after burn.

Lamp Ignition

Material turns transparent near melting point; sample softens and runs; vapors are given off as surface softens and turns brown, increasing to high rate near ignition; heavy black smoke during burning; surface mottled after burn; ignition sustained after heat source removed.

POLYPROPYLENE

Flame Ignition

Surface changes to glassy, vapors appear, surface ripples appear and start to flow; ignition and sustained burning; material flows well; burns with black smoke; has distinctive odor; at low heat, surface flows readily and becomes difficult to ignite.

Lamp Ignition

Surface turns glassy and vapors emitted; surface melts and slowly runs; ignition with black smoke, and burning continues after heat source removed; surface turns dark after burning.

POLYSTYRENE, HI-IMPACT

Flame Ignition

Surface becomes glassy, turns brown and flows; sample ignites and burns with dark black smoke; ignition is sustained; material structural strength decays rapidly with heat.

TABLE C-1 (Continued)

POLYSTYRENE (Continued)

Lamp Ignition

Material shows few small bubbles, then surface turns glassy, then brown color; ignites and burns with yellow flame and much black smoke; surface melts and runs; ignition sustained; surface shows some char after burn; pungent smell during burn.

POLY(VINYL CHLORIDE), TRANSPARENT

Flame Ignition

Surface develops ripples, then small bubbles appear giving a white frothy effect, surface turns brown with dark brown smoke given off. Ignition not sustained; surface charred after burn.

Lamp Ignition

Surface dulls, gets mottled effect, white bubbles appear turning brown, then frothy appearance; ignition not sustained, burns with blue flame at times; at low heat, large bubbles appear before ignition; burned surface has a melted and spongy char appearance.

POLY(VINYL CHLORIDE), GRAY, 1.27 CM

Flame Ignition

Very heavy smoke, surface appears to react and darken, surface forms bubbles then smoke, then char; surface has appearance of fluffy, dark colored ash; ignition not sustained, but will ignite.

Lamp Ignition

Surface develops small bubbles then turns brown-black color; white smoke first given off followed by dark brown smoke. Ignition was developed at the pilot igniter, not at the sample. Surface froths and chars. Surface had spongy char after burn. Burning not sustained.

TABLE C-1 (Continued)

POLY(VINYL CHLORIDE), GRAY, 0.32 CM

Flame Ignition

Surface turns glassy, the bubbles appear and turn brown and black. Smoke is emitted, first white and then brown. Surface has deep charring of spongy appearance; sample ignites but not sustained.

Lamp Ignition

Sample decomposes and loses strength rapidly; heavy black smoke and vapors emitted; ignites with much smoke but ignition not sustained after heat source removed; ignites only at high heat flux.

SILICONE RUBBER

Flame Ignition

Color turns from red to gray pink; small bubbles or dislocations appear on surface, vapor is given off, surface turns white with glow burning; white is soft, ash-like material; surface under white material discolored and cracked; ignition not sustained, glow only.

Lamp Ignition

Surface darkens, vapors given off, surface turns spotty white, then ignition, surface burns and turns all white; ignition sustained, surface glows, white smoke. SiO_2 appears to be in the emitted vapors, since the pilot igniter becomes coated with a white powder or film.

STYROLUX (POLYSTYRENE), TRANSPARENT

Flame Ignition

Surface melts and slowly flows, vapors given off then ignition and burning sustained. Burns with yellow flame and much black smoke. Surface charred after burn. Material shows brown coloration under char, pungent smell; at low heats, small bubbles appear on the surface.

TABLE C-1 (Continued)

STYROLUX (Continued)

Lamp Ignition

Surface starts to melt, small bubbles form, some vapor and smoke; ignites and sustains burning with heavy black smoke; very pungent odor during burning.

TEXIN

Flame Ignition

Surface becomes glossy, small ripples appear, the surface flows; surface turns brown and bubbles, flows like water, ignites with much smoke; much soot in smoke; yellow flame; burning is sustained.

Lamp Ignition

Material softens quickly and runs; very messy, burns with heavy black smoke prior to ignition, bubbles form on surface; ignition sustained after heat source removed; very noxious gases and odor during burn; surface charred after burn.

UVEX (CELLULOSE ACETATE BUTYRATE), TRANSPARENT

Flame Ignition

Small white bubbles appear on surface, some vapor and smoke; ignites and burning is sustained. Surface turns brown, melts and flows; surface charred after burn; material loses structural strength rapidly with heating. On thick samples, the bubbles give a frothy appearance.

Lamp Ignition

Small bubbles form on surface, then froth, turning brown; then surface runs, very putrid smell; not much smoke but some vapors emitted; ignition and sustained; material melts and will flow.

SECTION II

IGNITION TIME-IRRADIANCE PLOTS

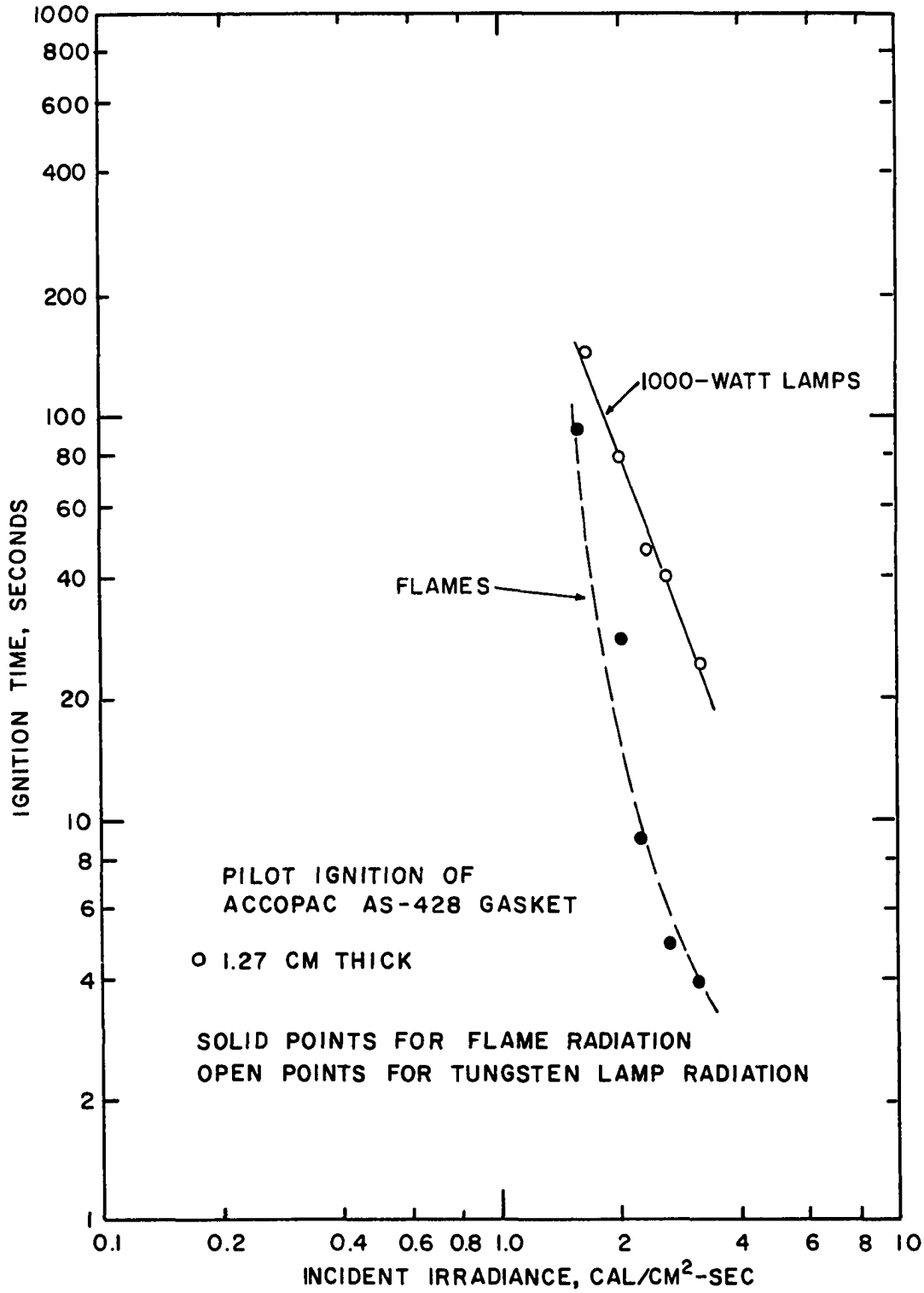

Figure C-1. Pilot Ignition of Accopac AS-428 Gasket.

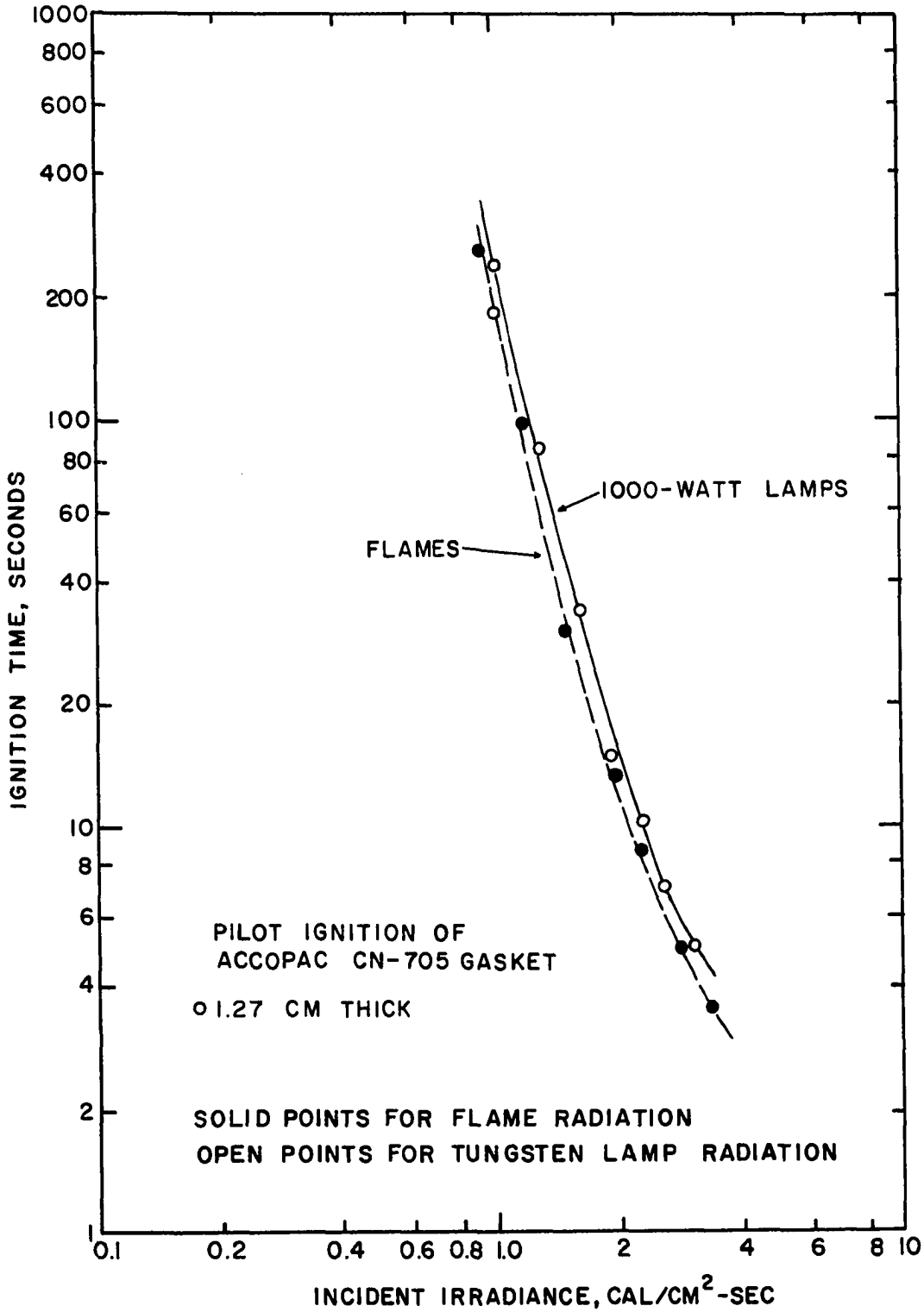

Figure C-2. Pilot Ignition of Accopac CN-705 Gasket.

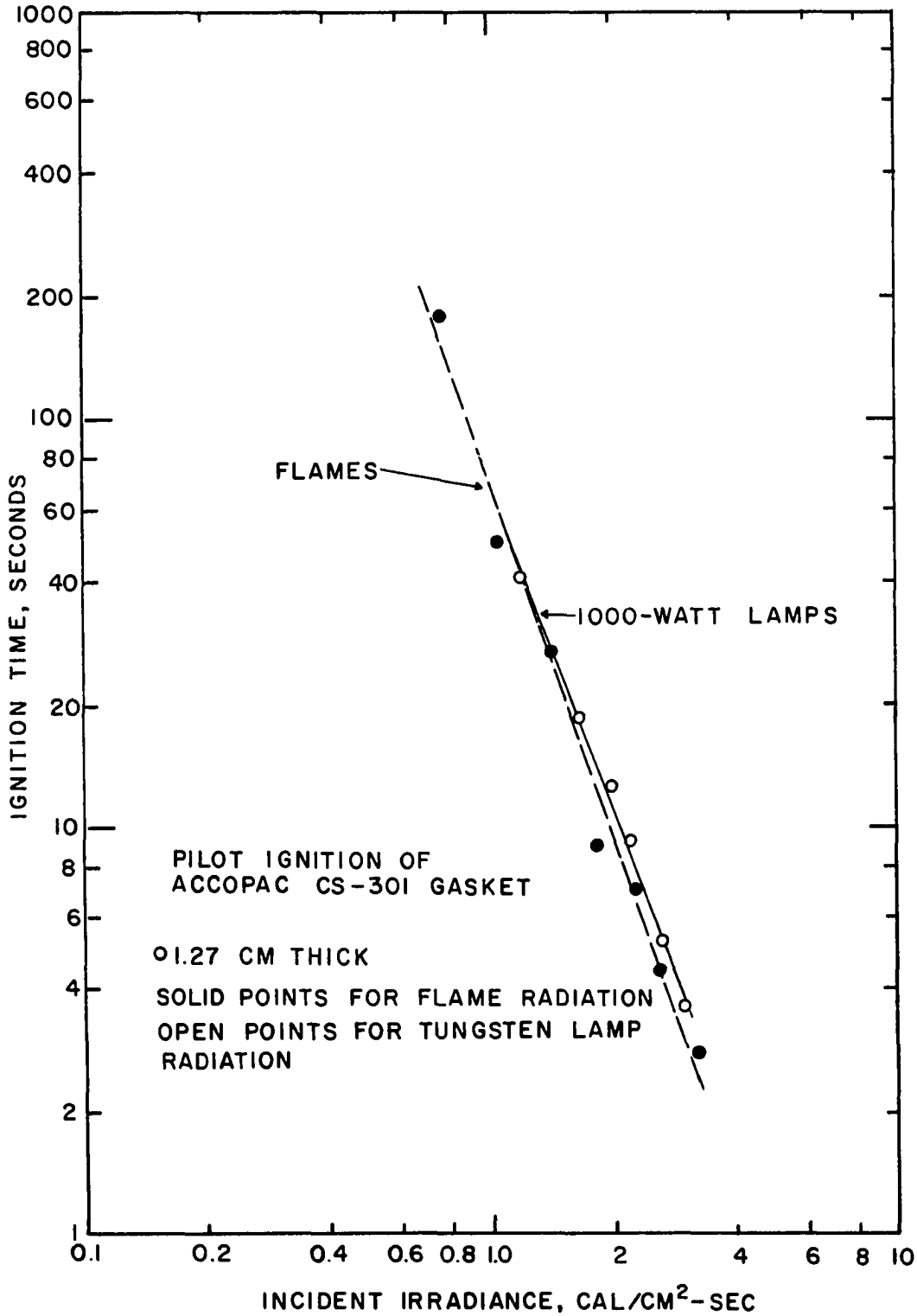

Figure C-3. Pilot Ignition of Accopac CS-301 Gasket.

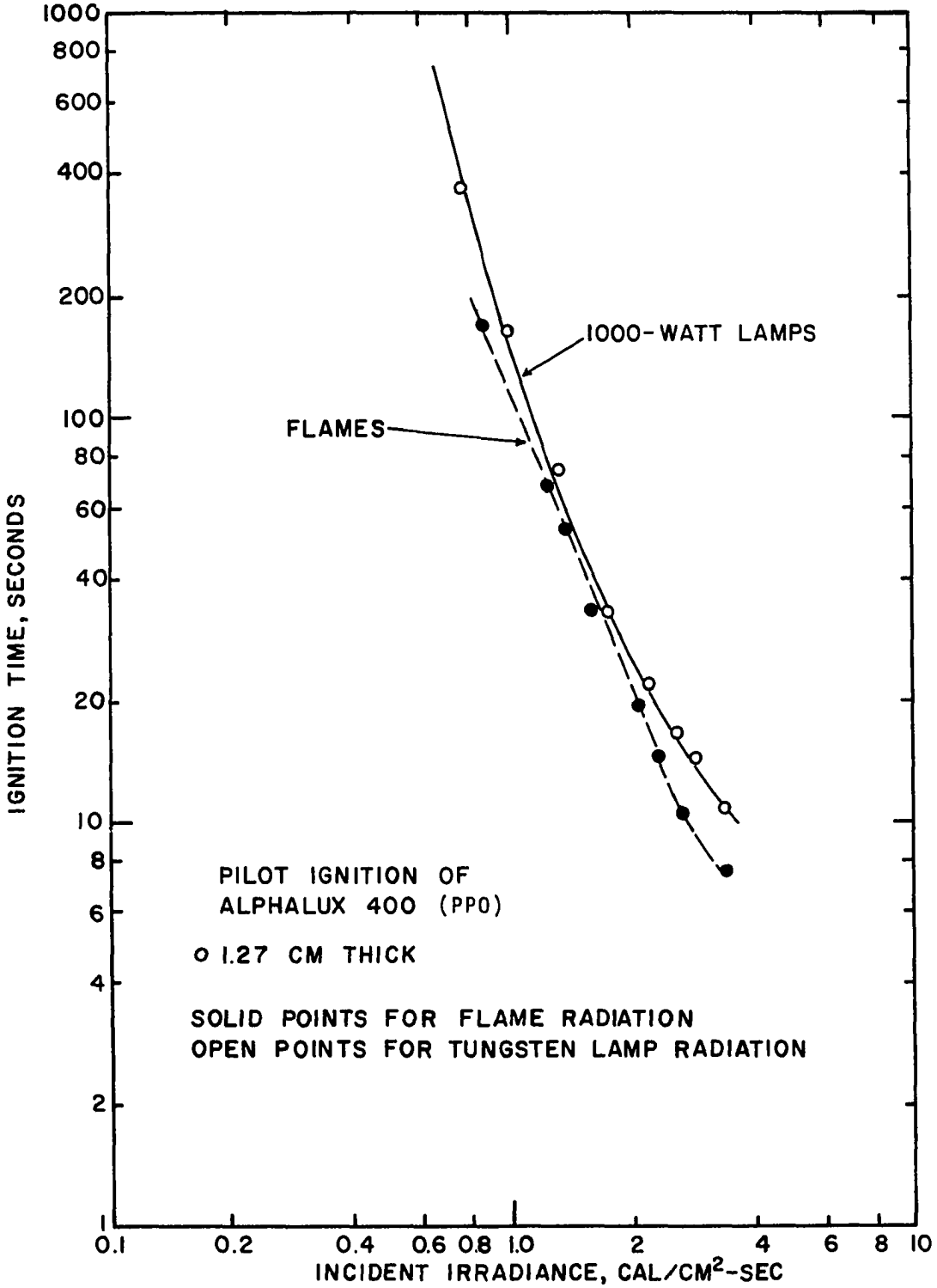

Figure C-4. Pilot Ignition of Alphalux 400 (PPO).

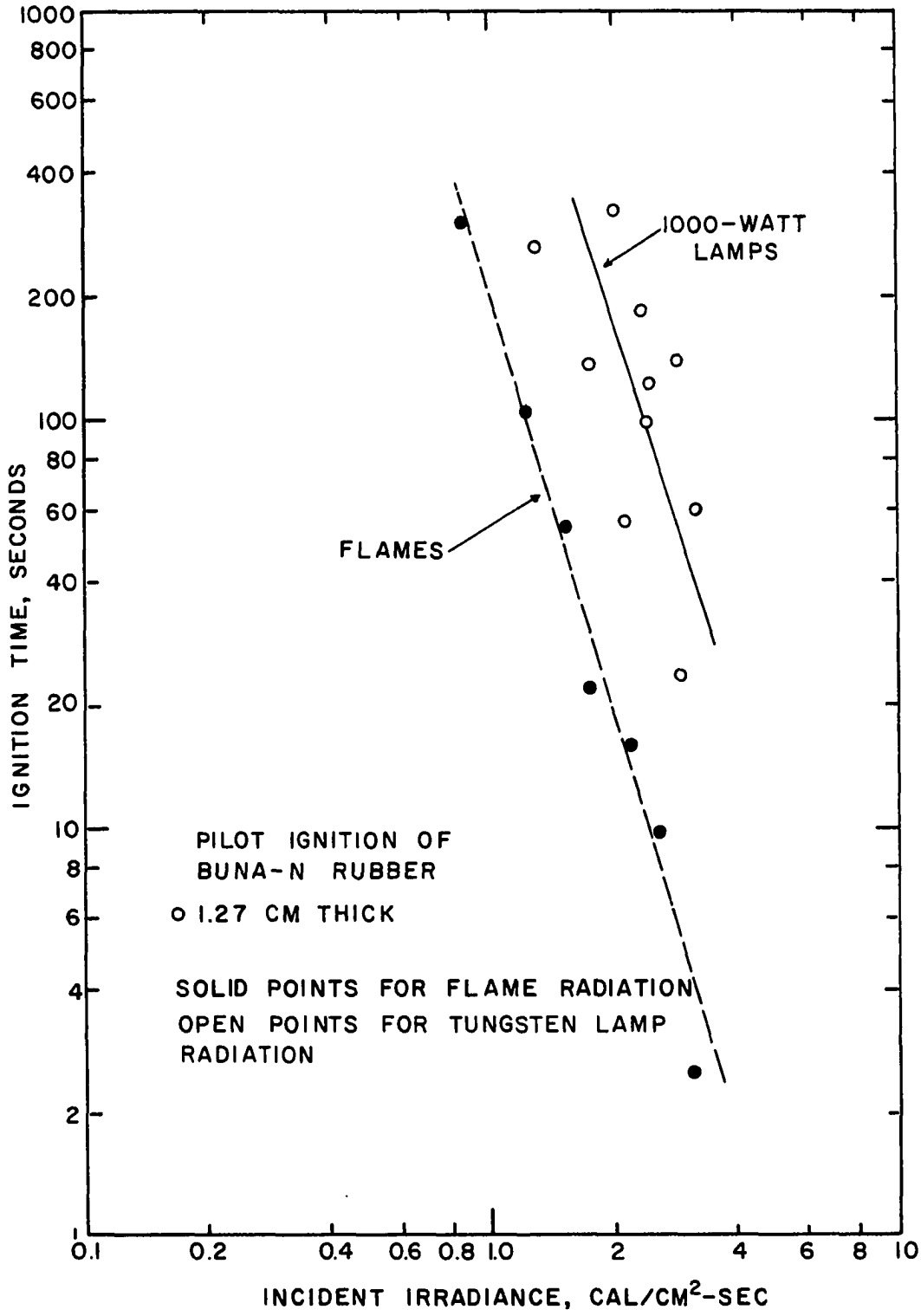

Figure C-5. Pilot Ignition of Buna-N Rubber.

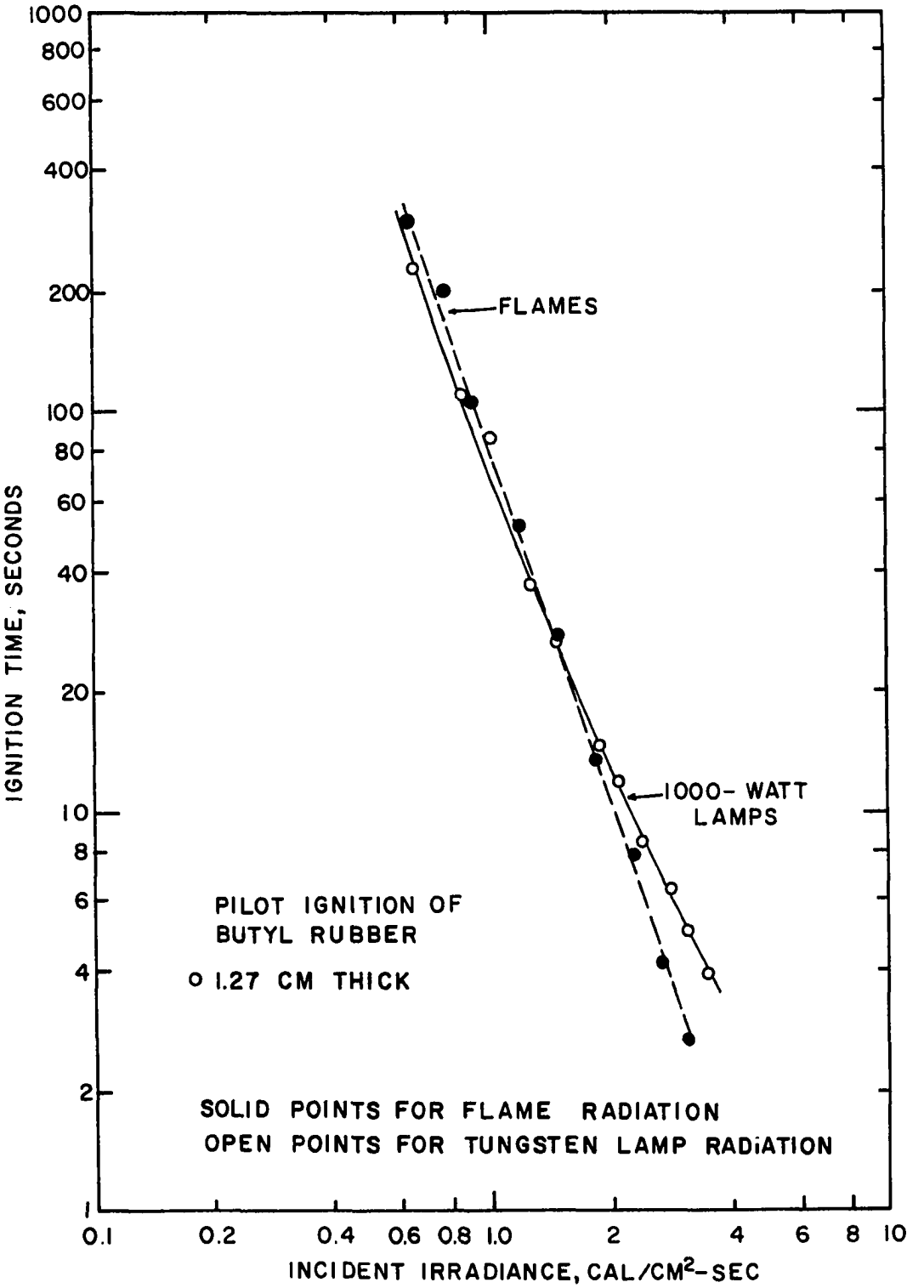

Figure C-6. Pilot Ignition of Butyl Rubber.

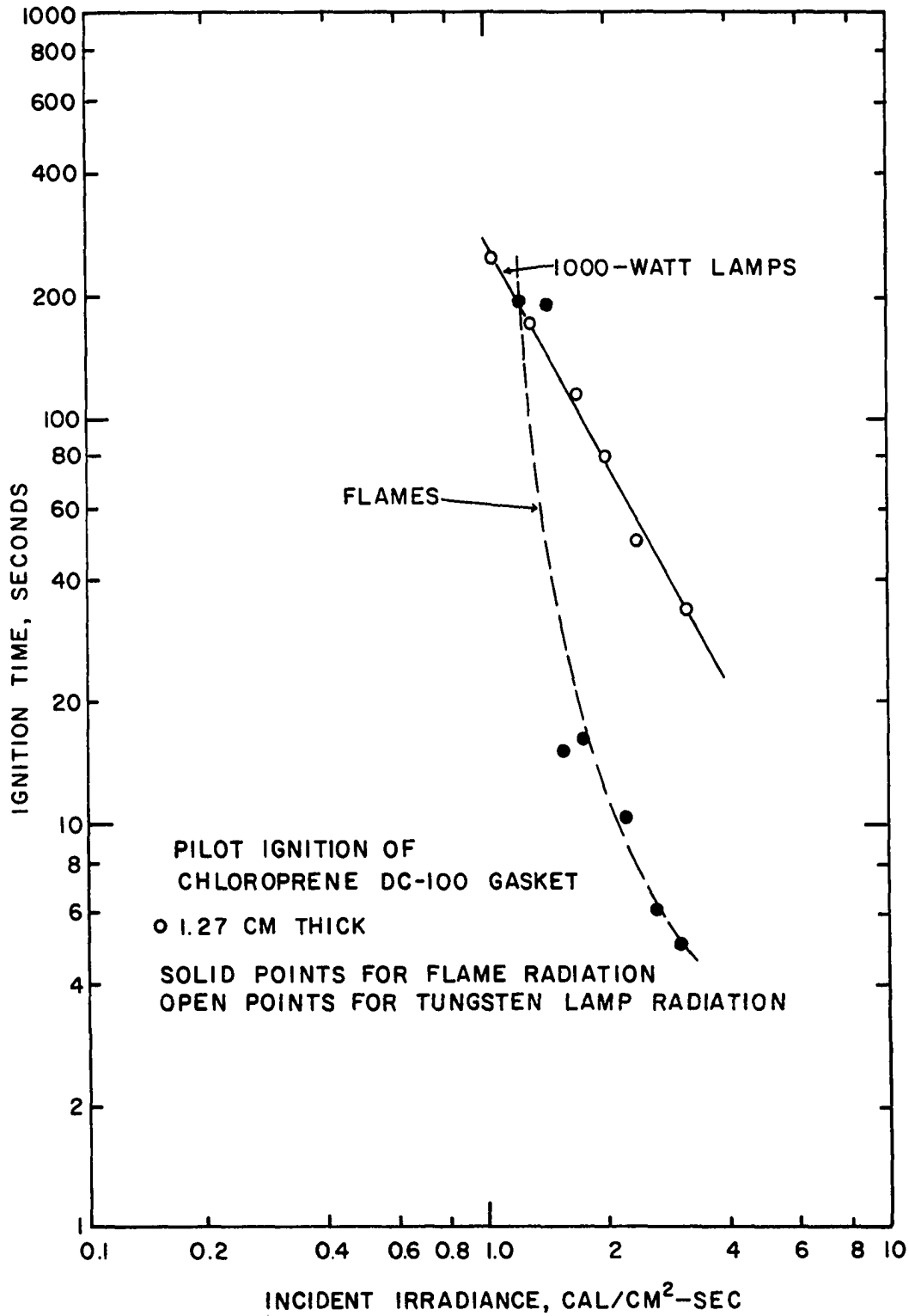

Figure C-7. Pilot Ignition of Chloroprene DC-100 Gasket.

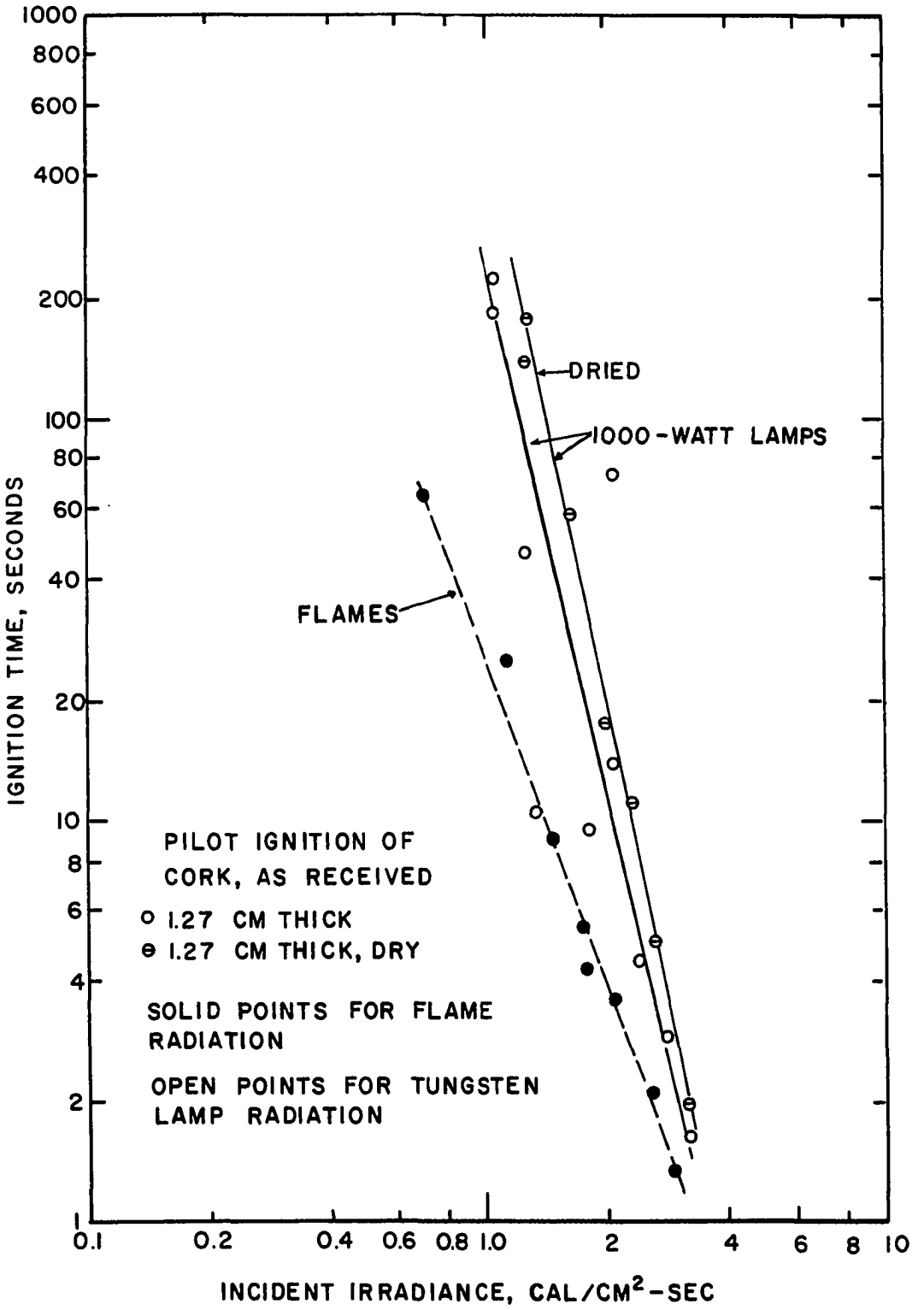

Figure C-8. Pilot Ignition of Cork Gasket Material.

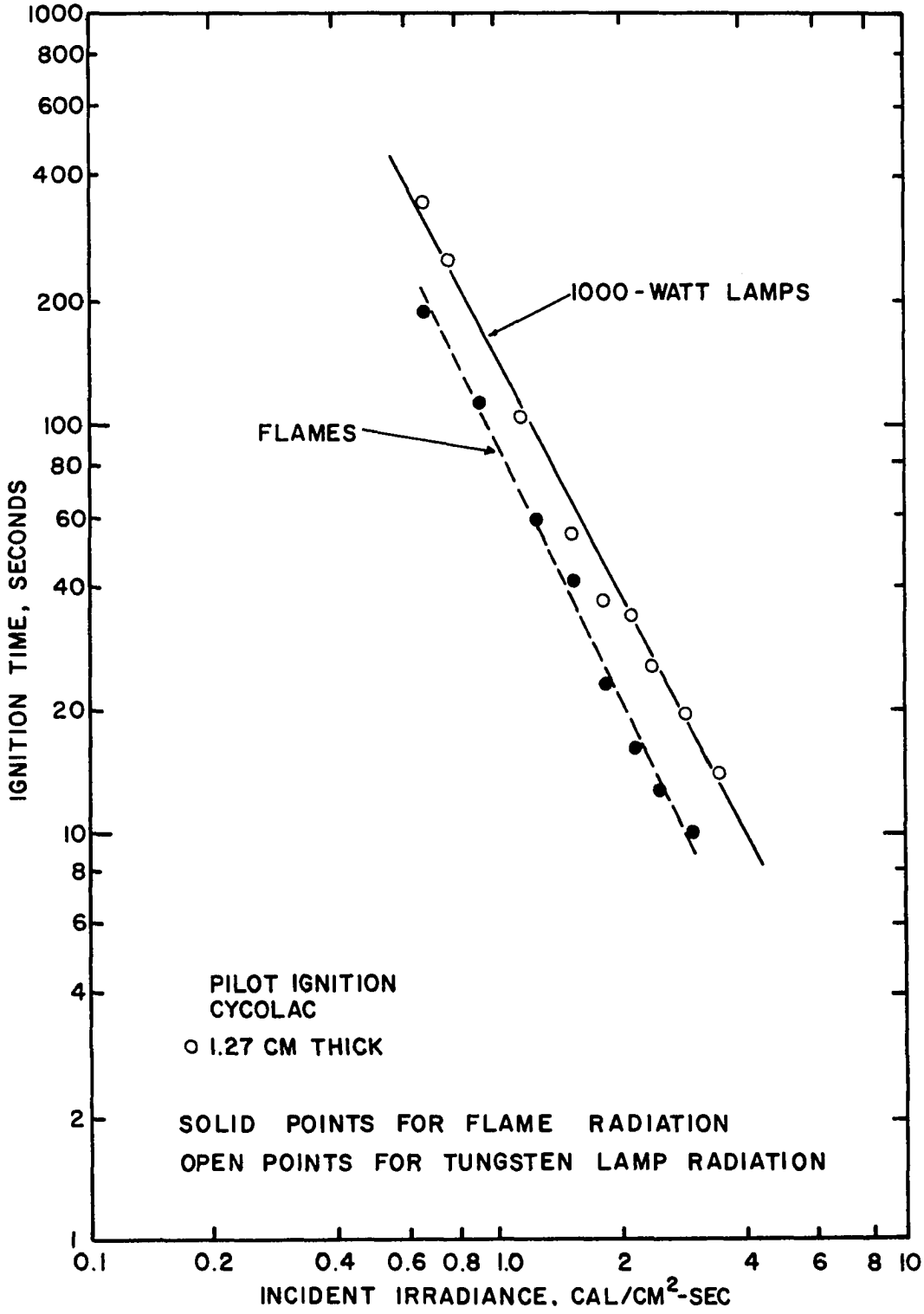

Figure C-9. Pilot Ignition of Cycolac (ABS).

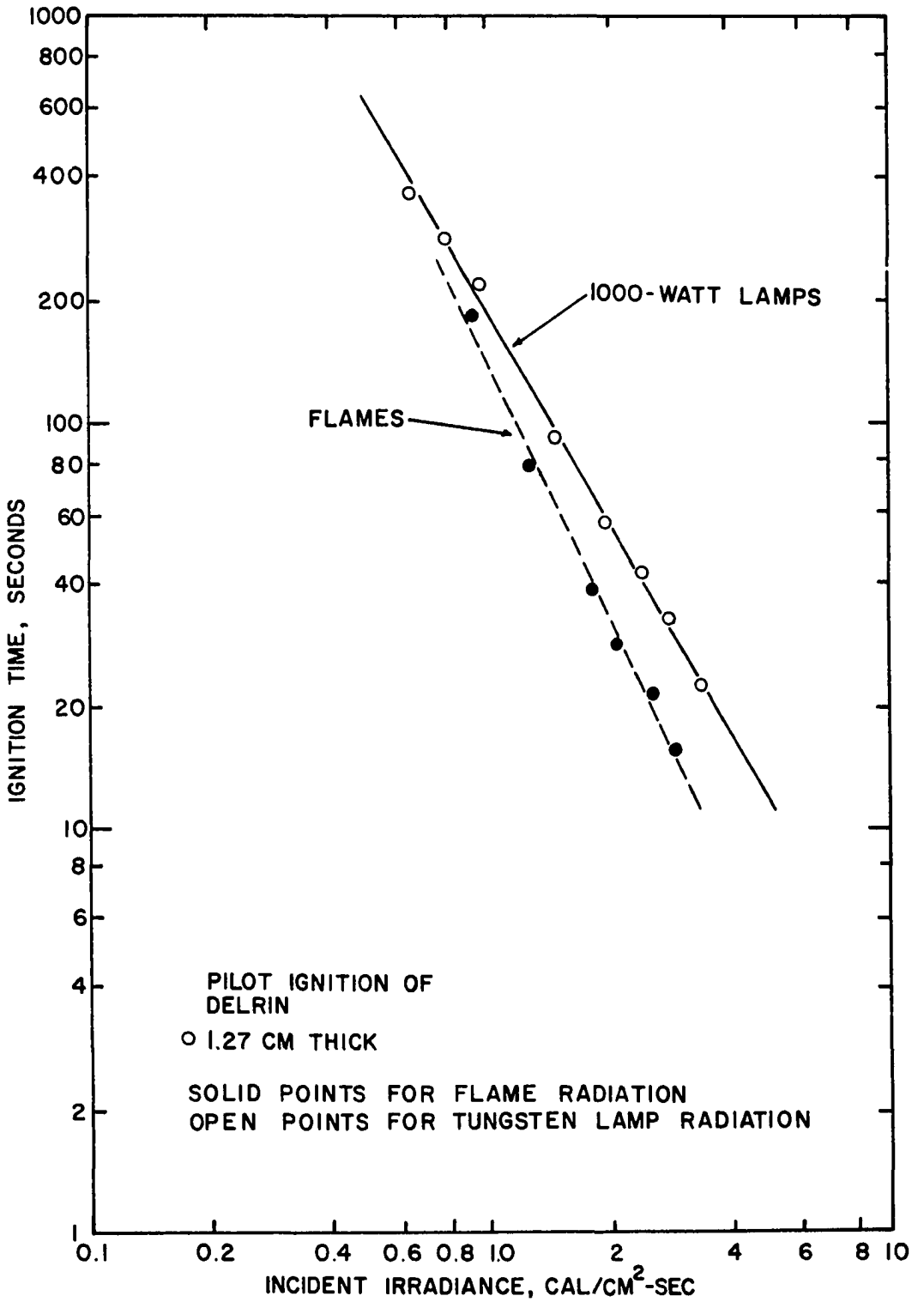

Figure C-10. Pilot Ignition of Delrin.

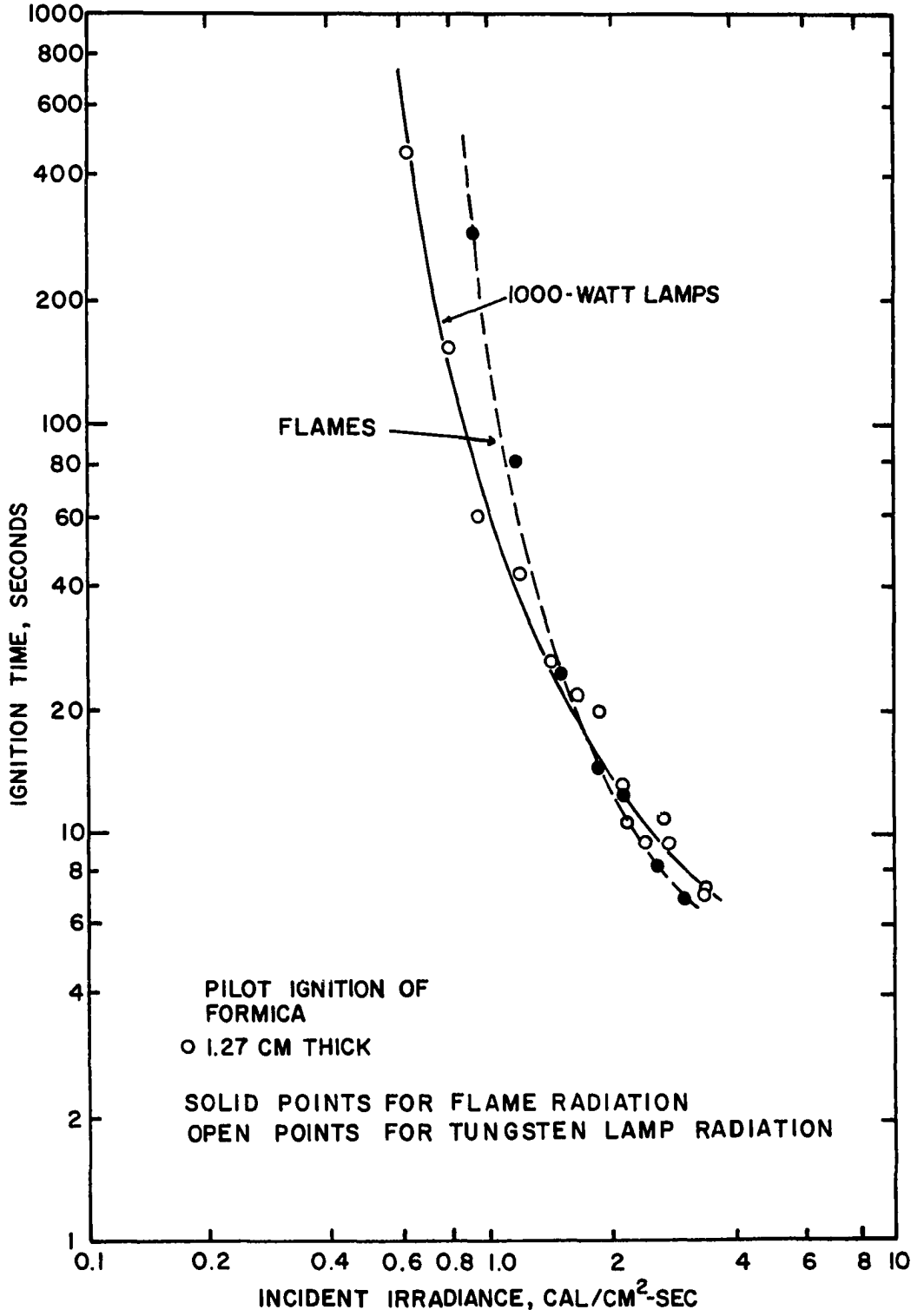

Figure C-11. Pilot Ignition of Formica.

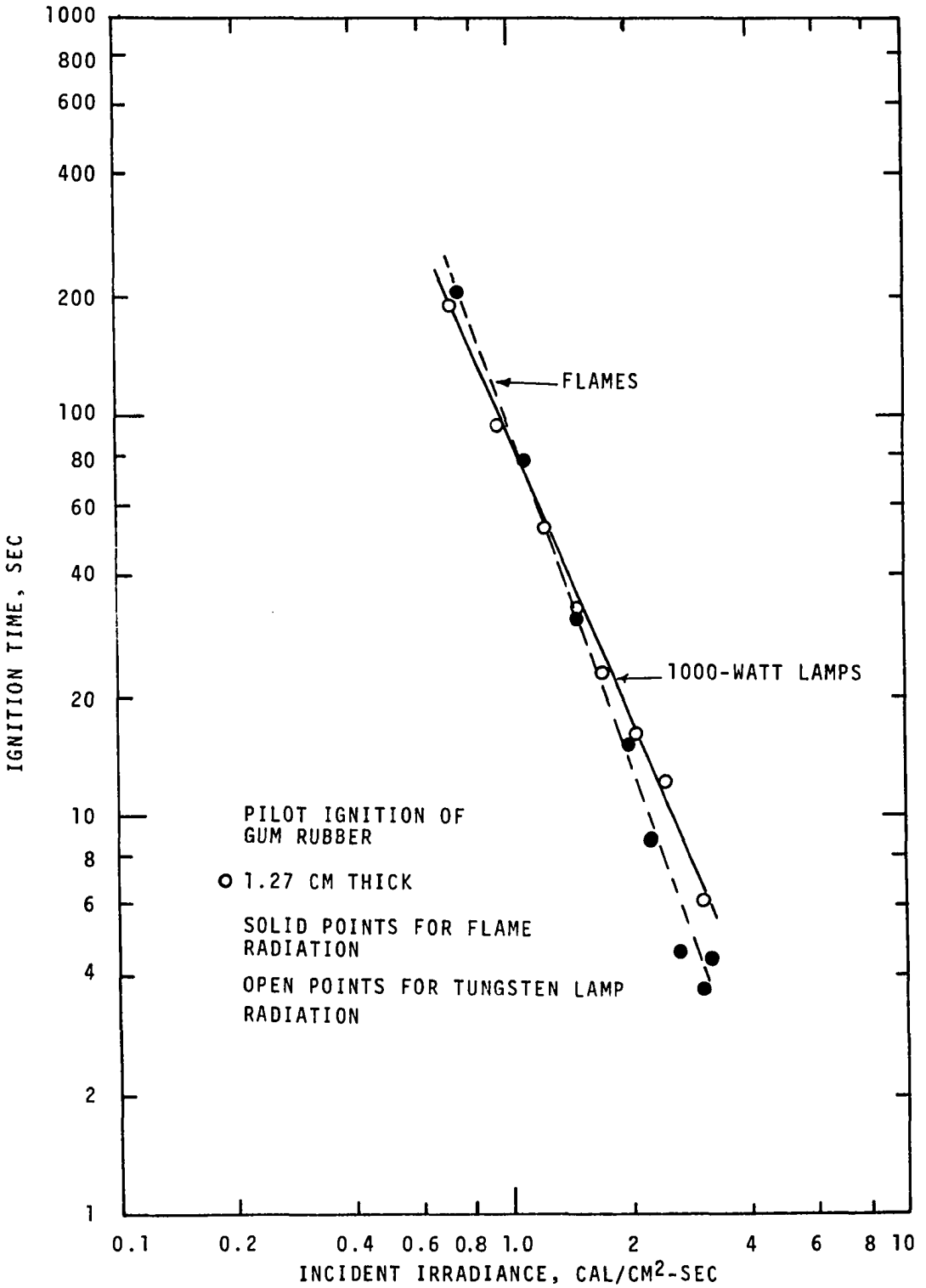

Figure C-12. Pilot Ignition of Gum Rubber.

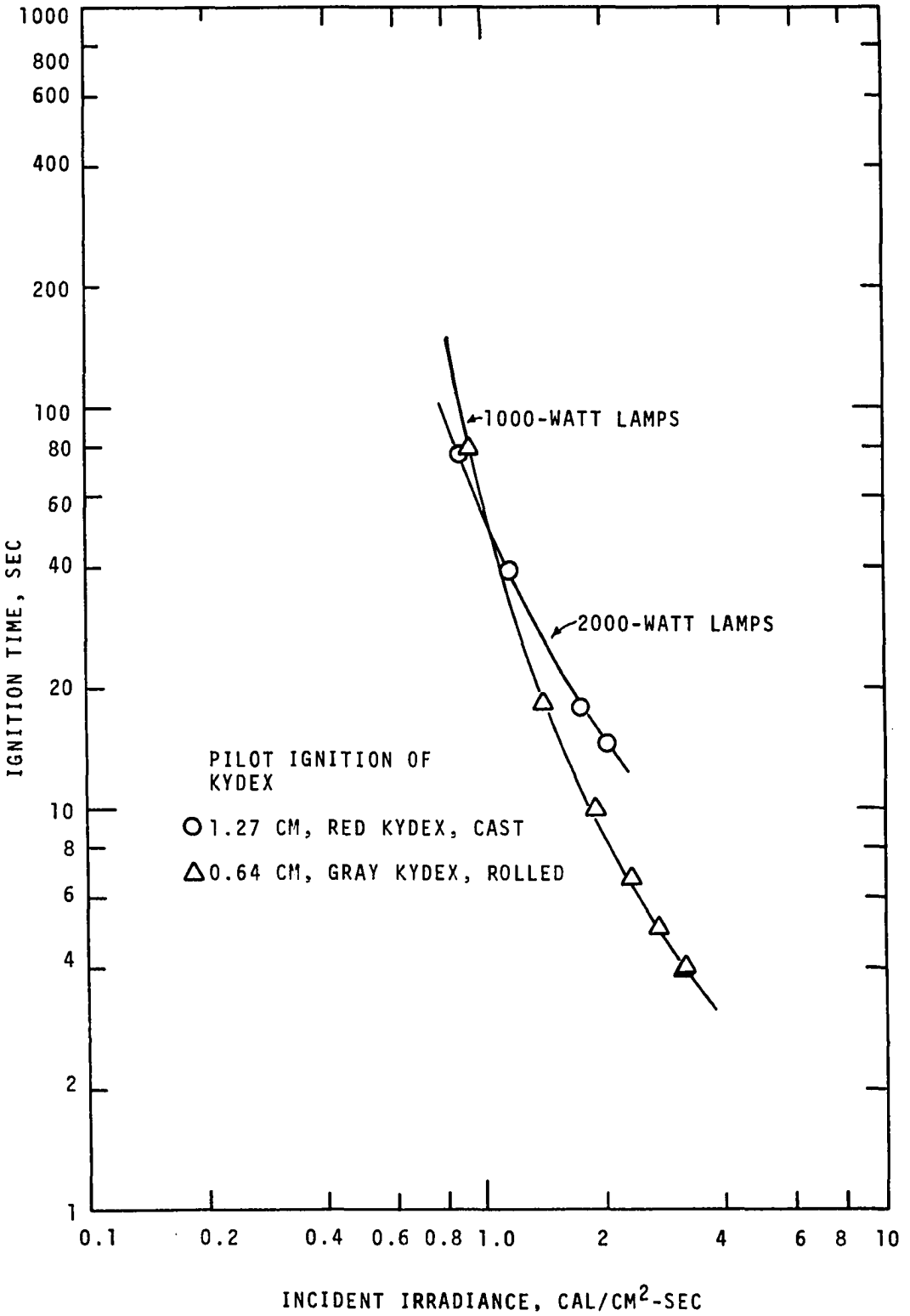

Figure C-13. Pilot Ignition of Kydex.

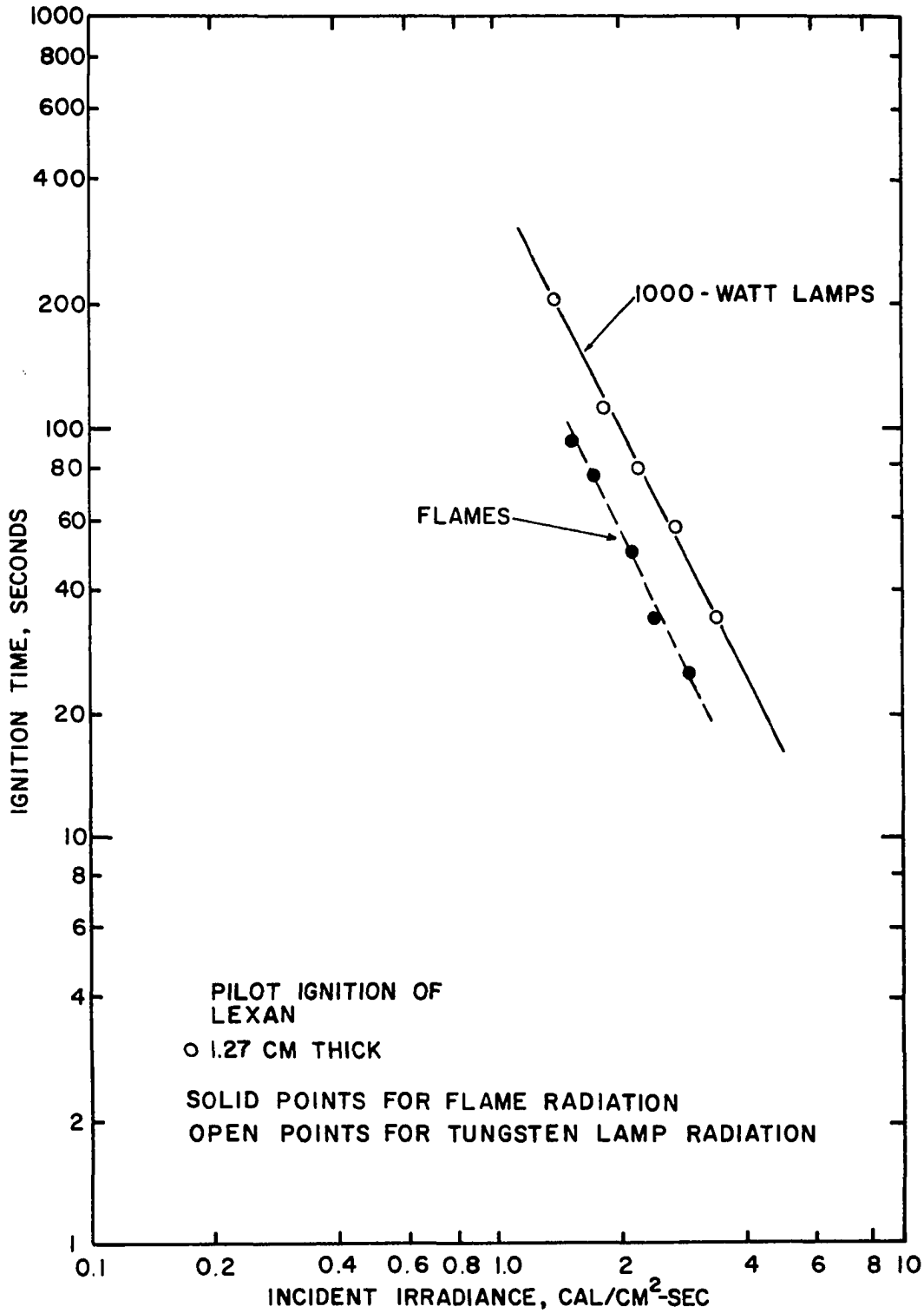

Figure C-14. Pilot Ignition of Lexan.

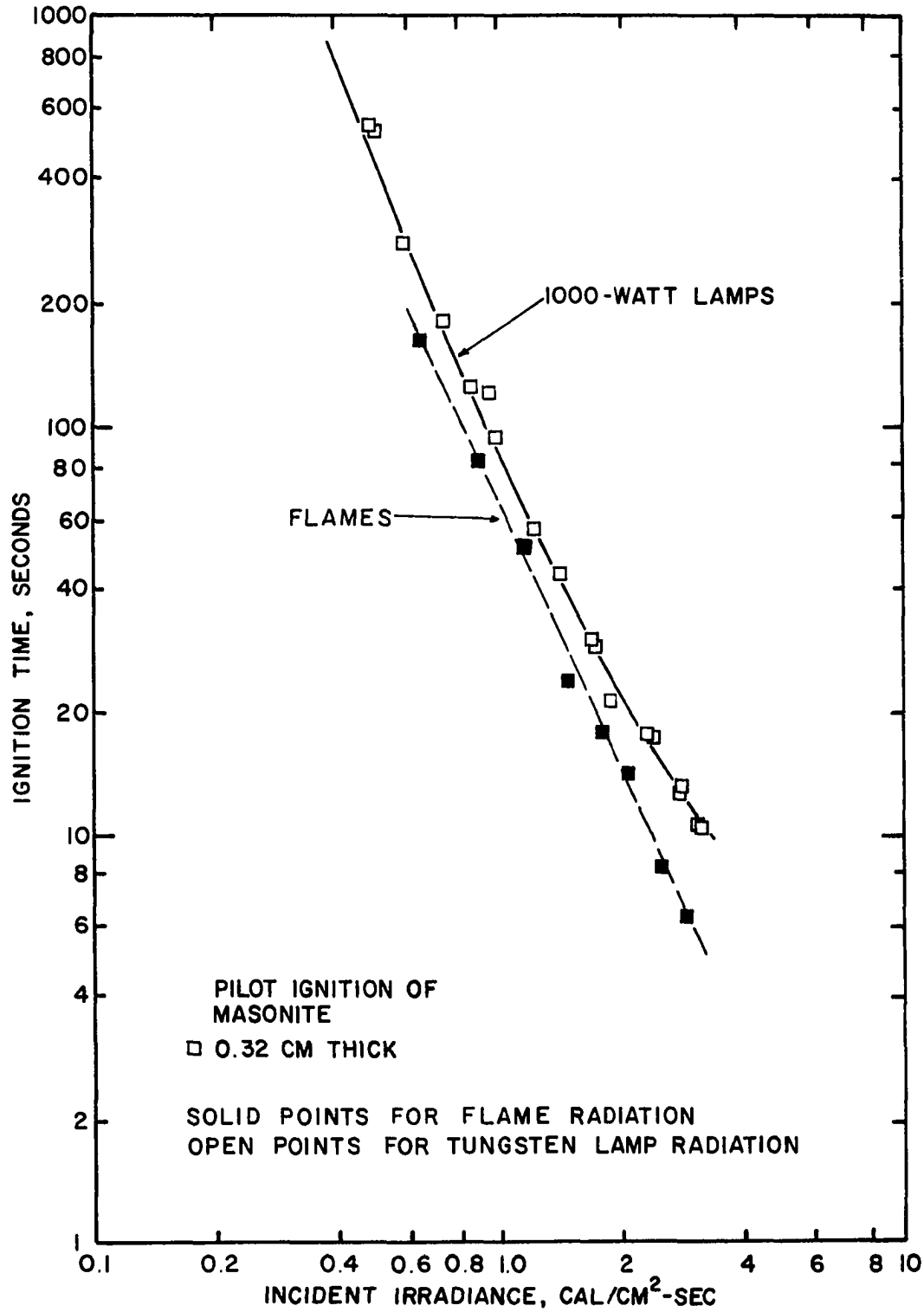

Figure C-15. Pilot Ignition of Masonite.

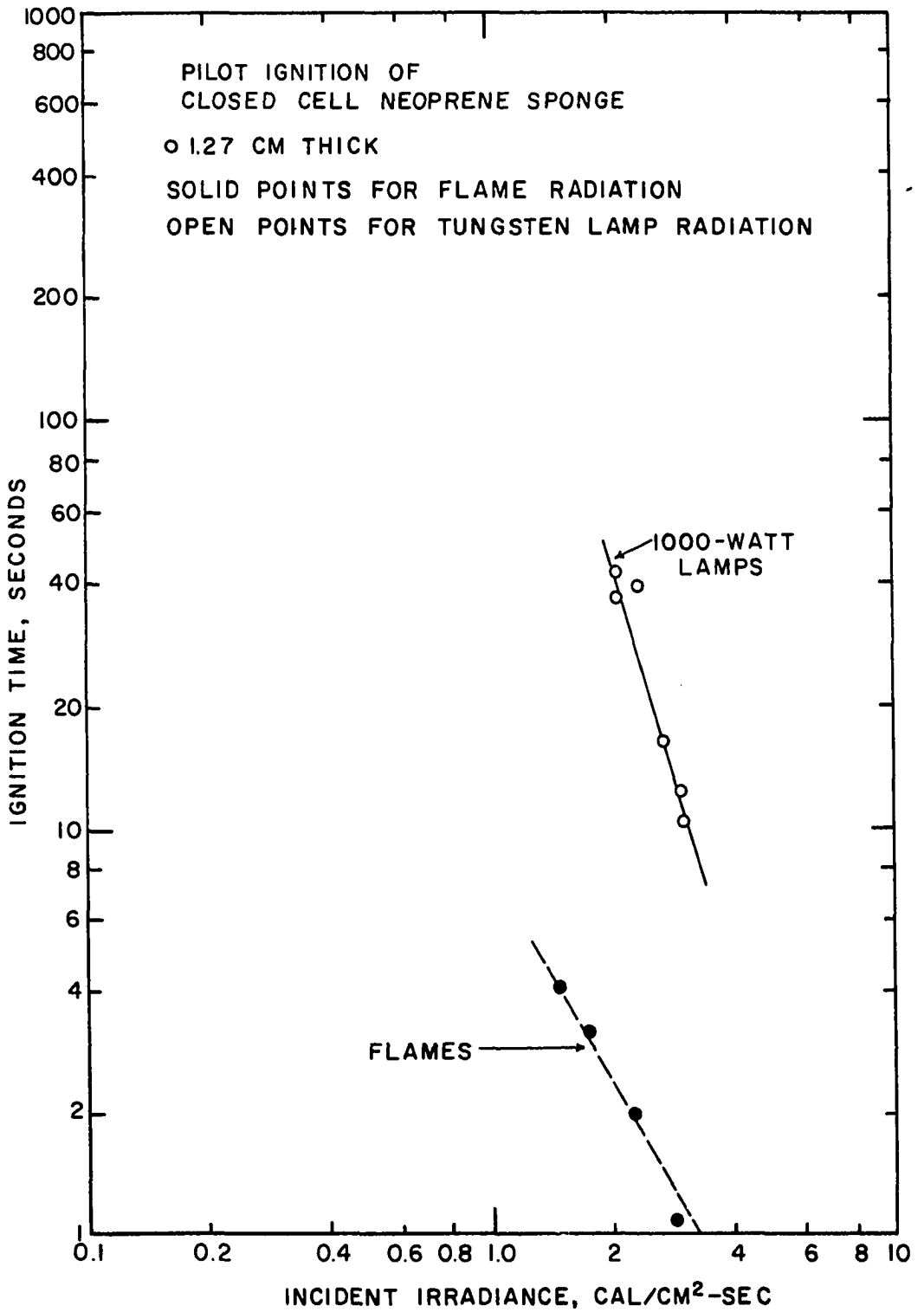

Figure C-16. Pilot Ignition of Neoprene Closed Cell Sponge Rubber.

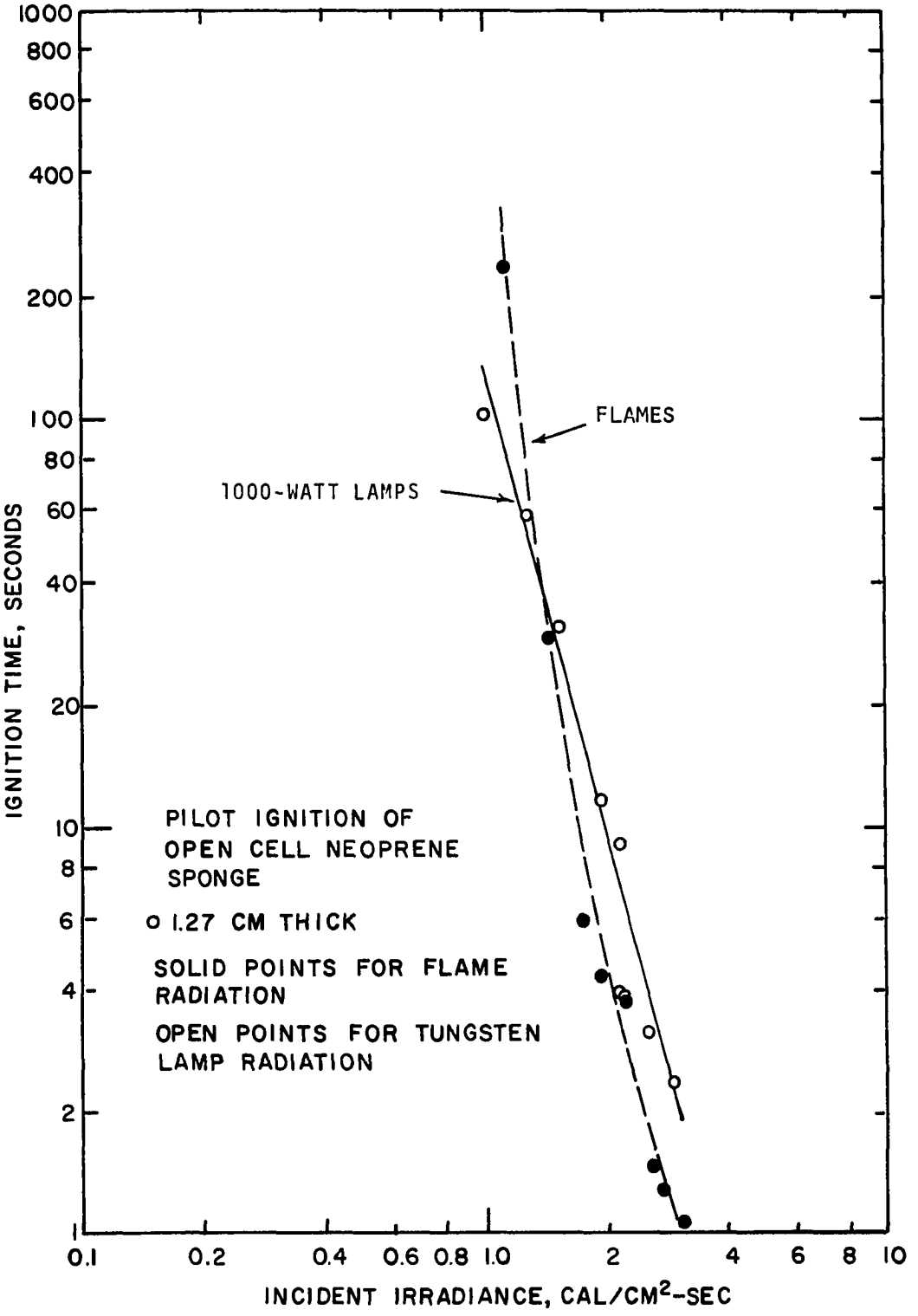

Figure C-17. Pilot Ignition of Neoprene Open Cell Sponge Rubber.

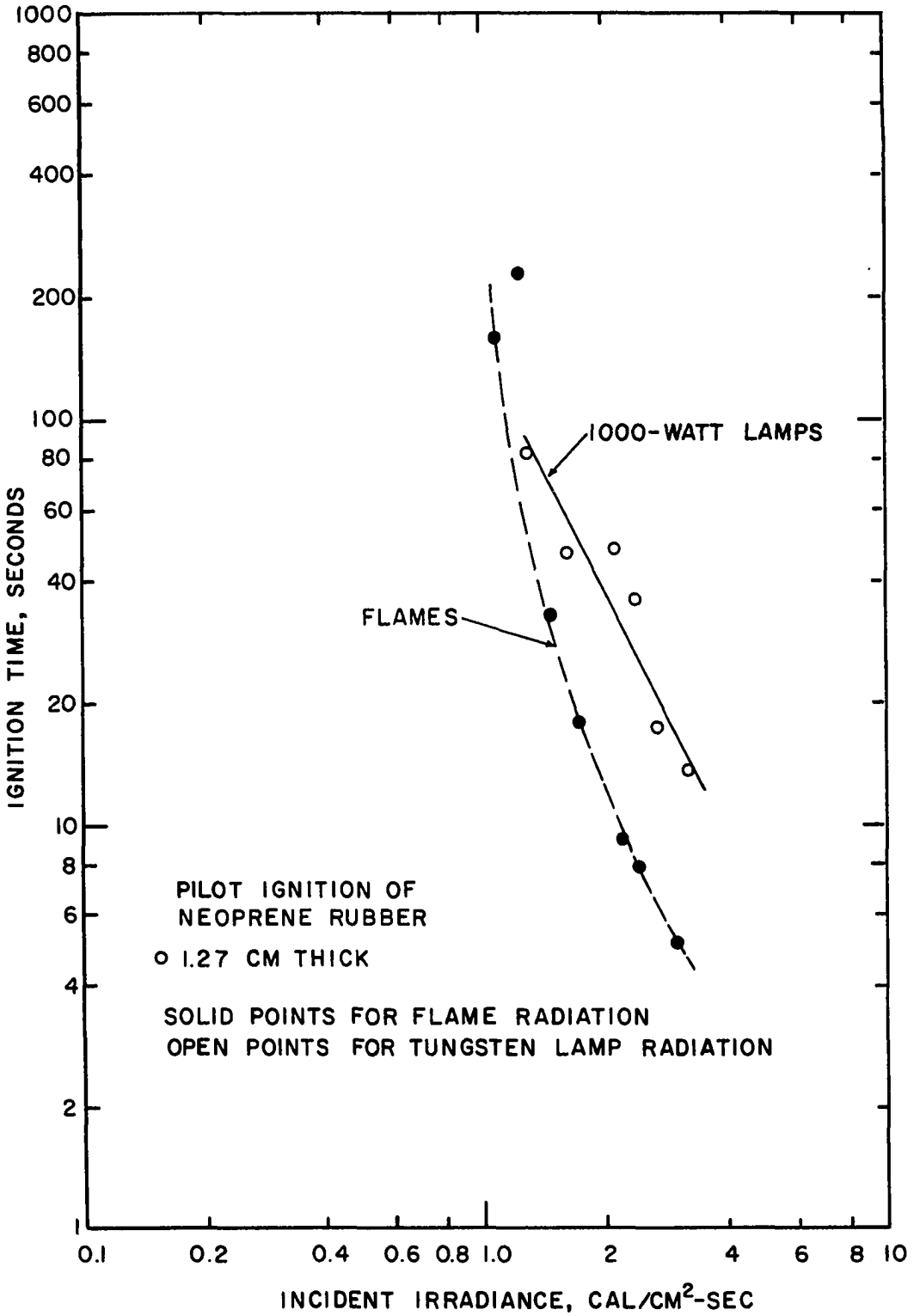

Figure C-18. Pilot Ignition of Solid Neoprene Rubber.

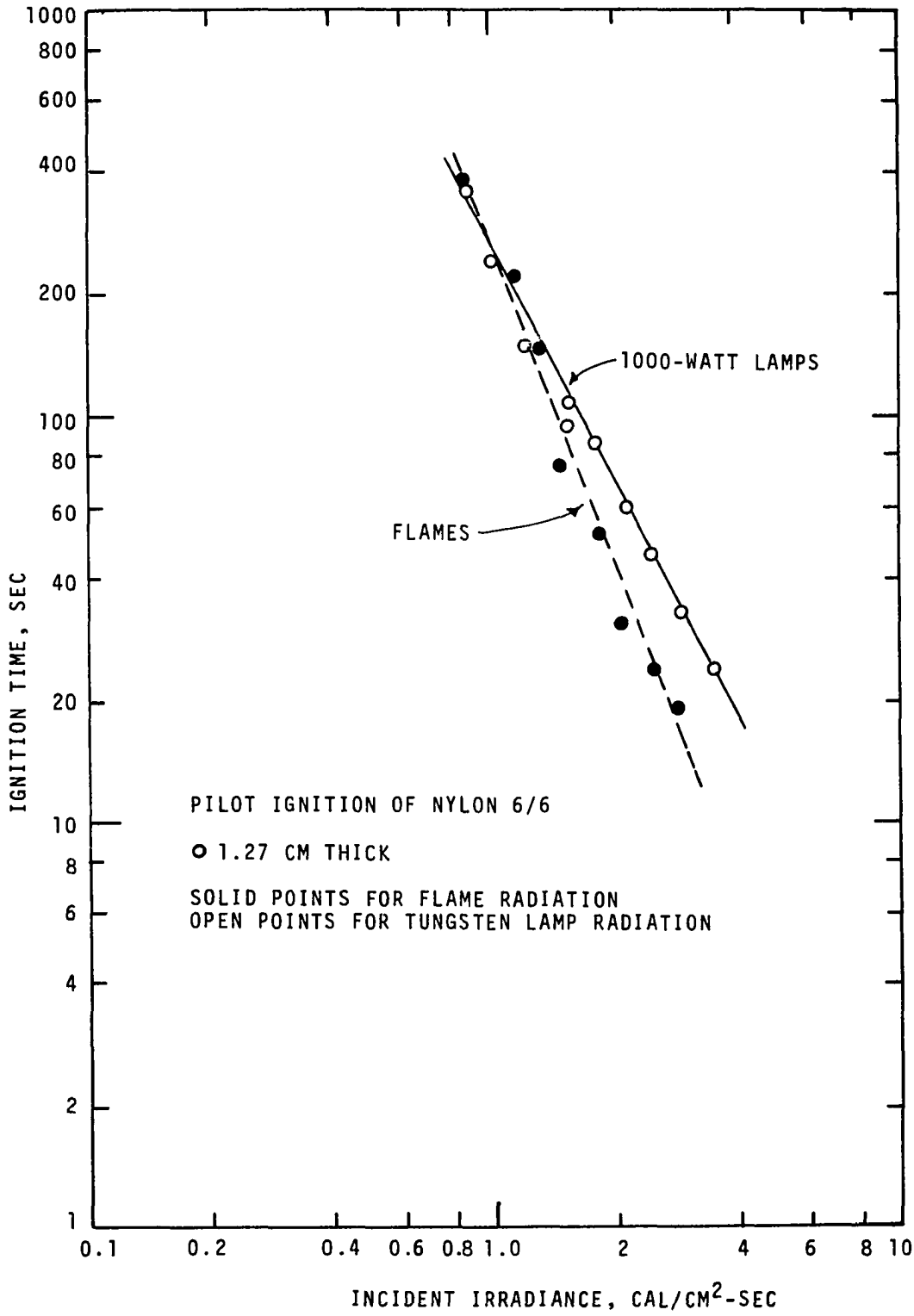

Figure C-19. Pilot Ignition of 6/6 Nylon.

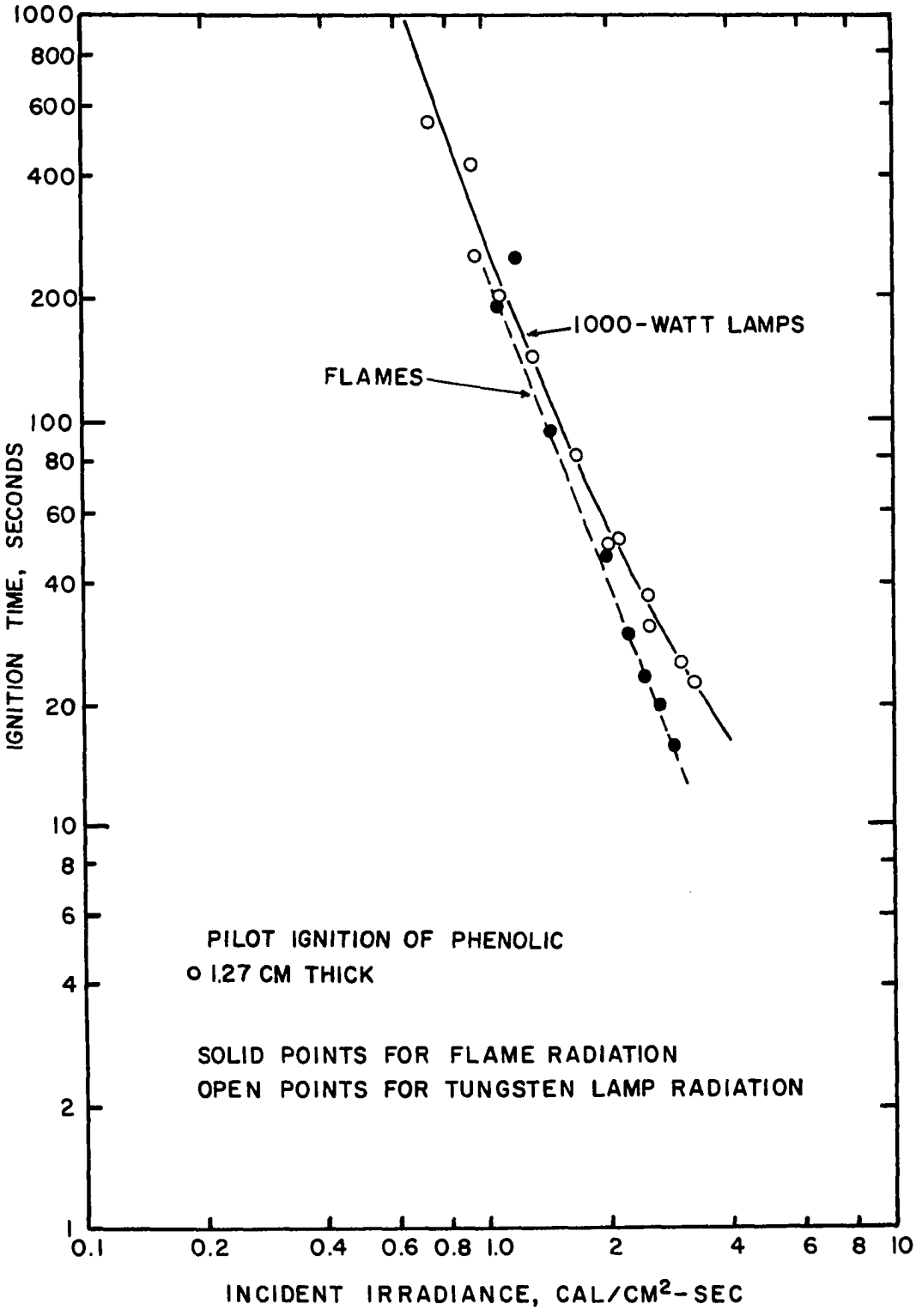

Figure C-20. Pilot Ignition of Phenolic Material, Bakelite.

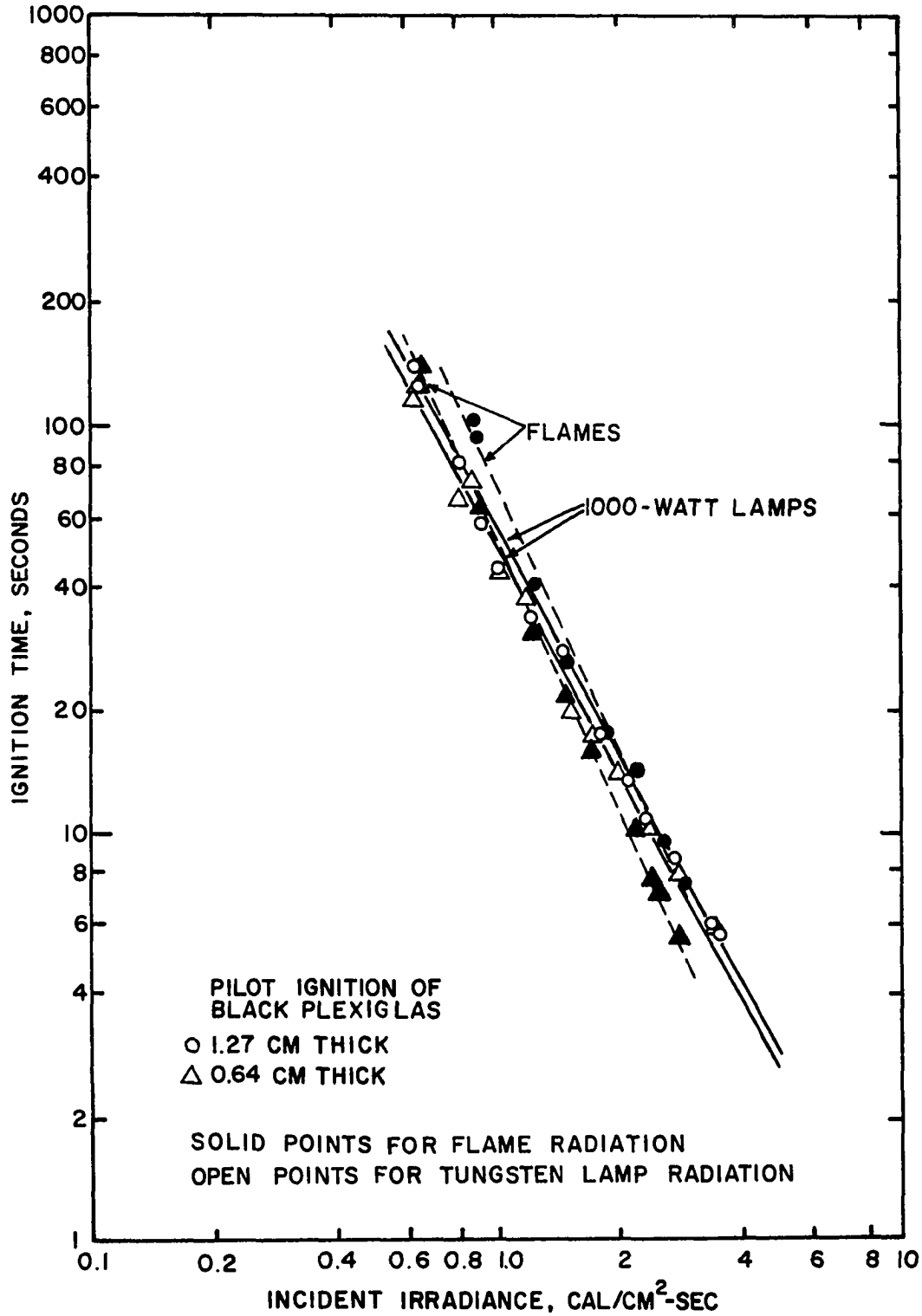

Figure C-21. Pilot Ignition of Black Plexiglas.

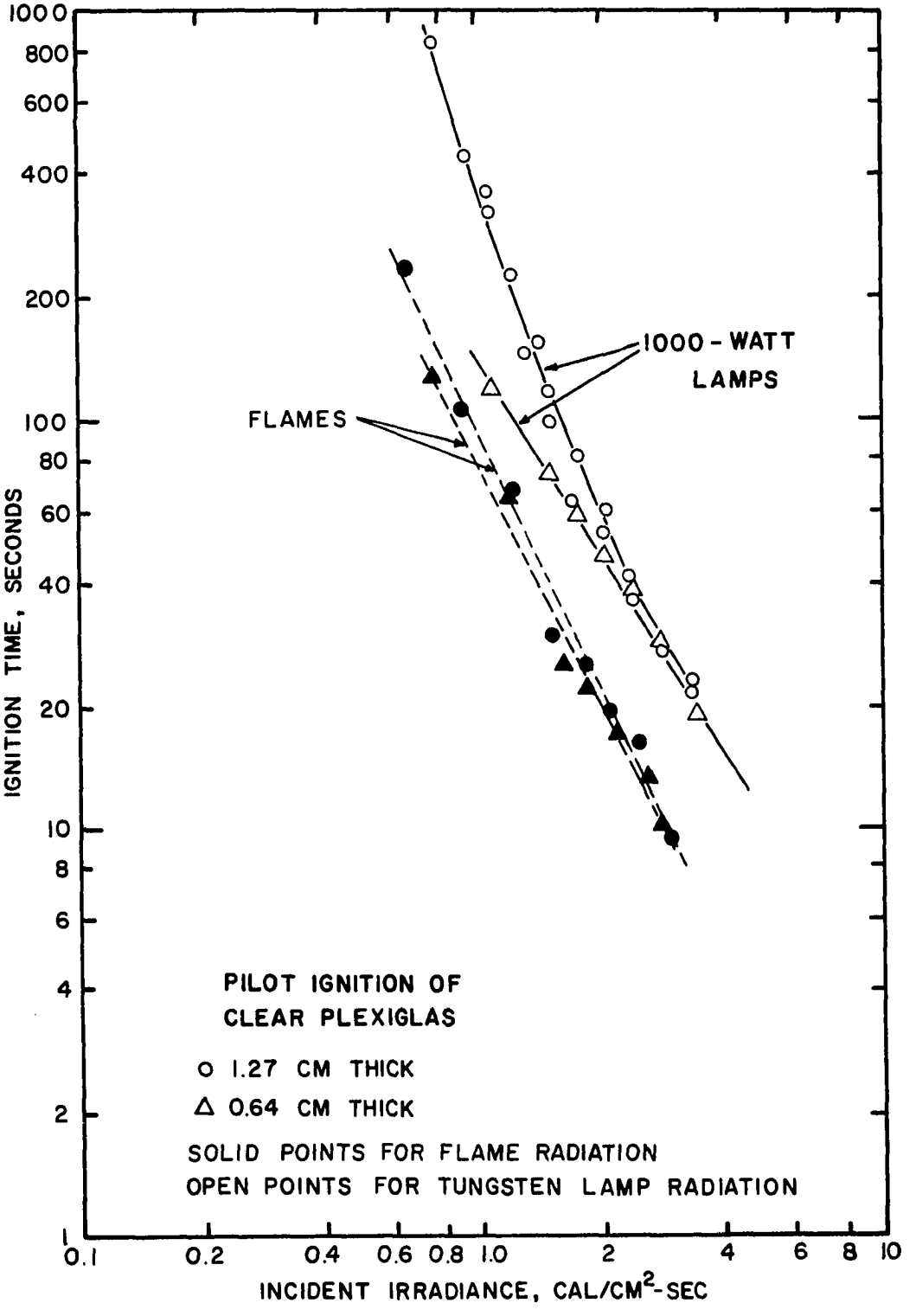

Figure C-22. Pilot Ignition of Clear Plexiglas.

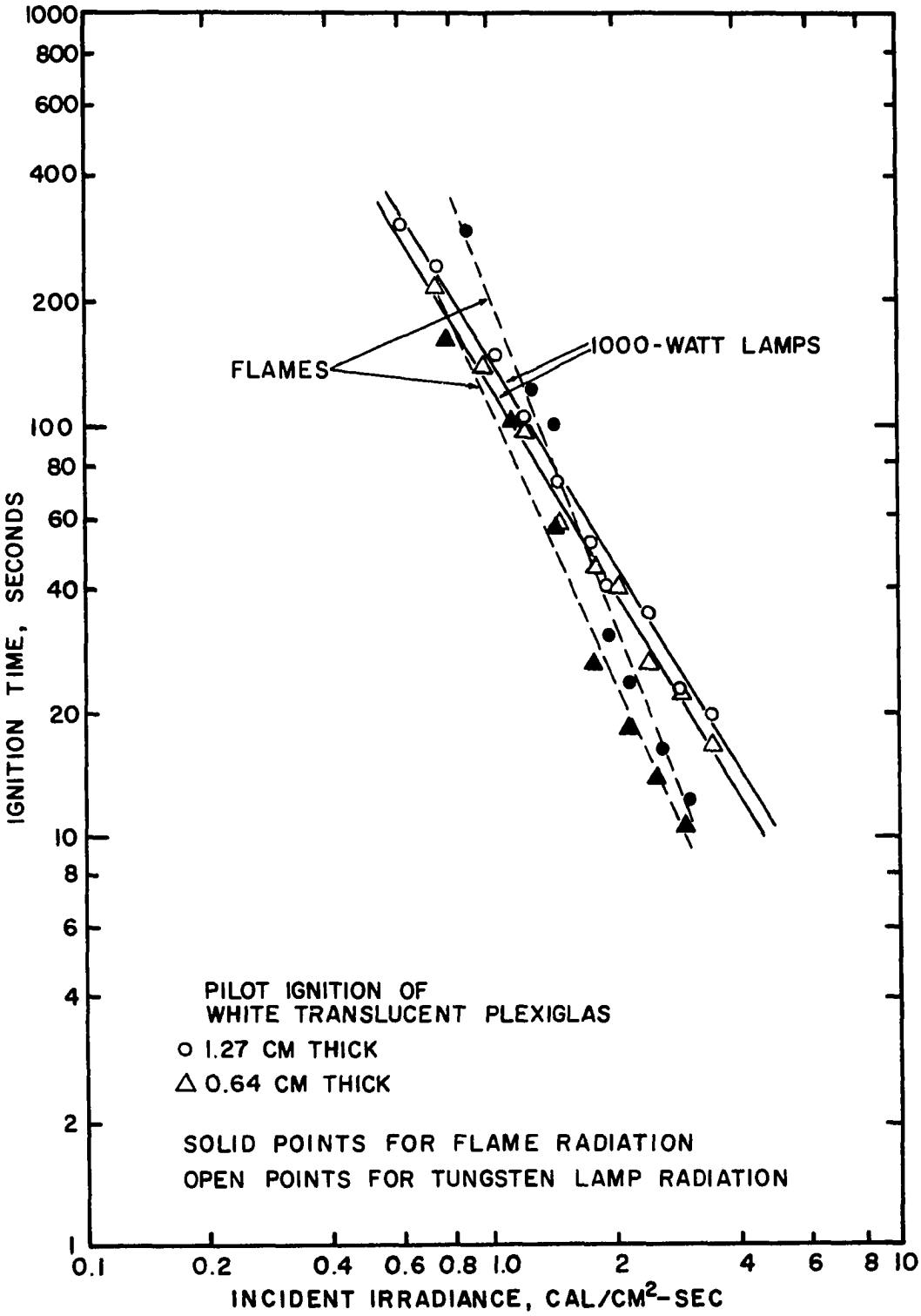

Figure C-23. Pilot Ignition of White Translucent Plexiglas.

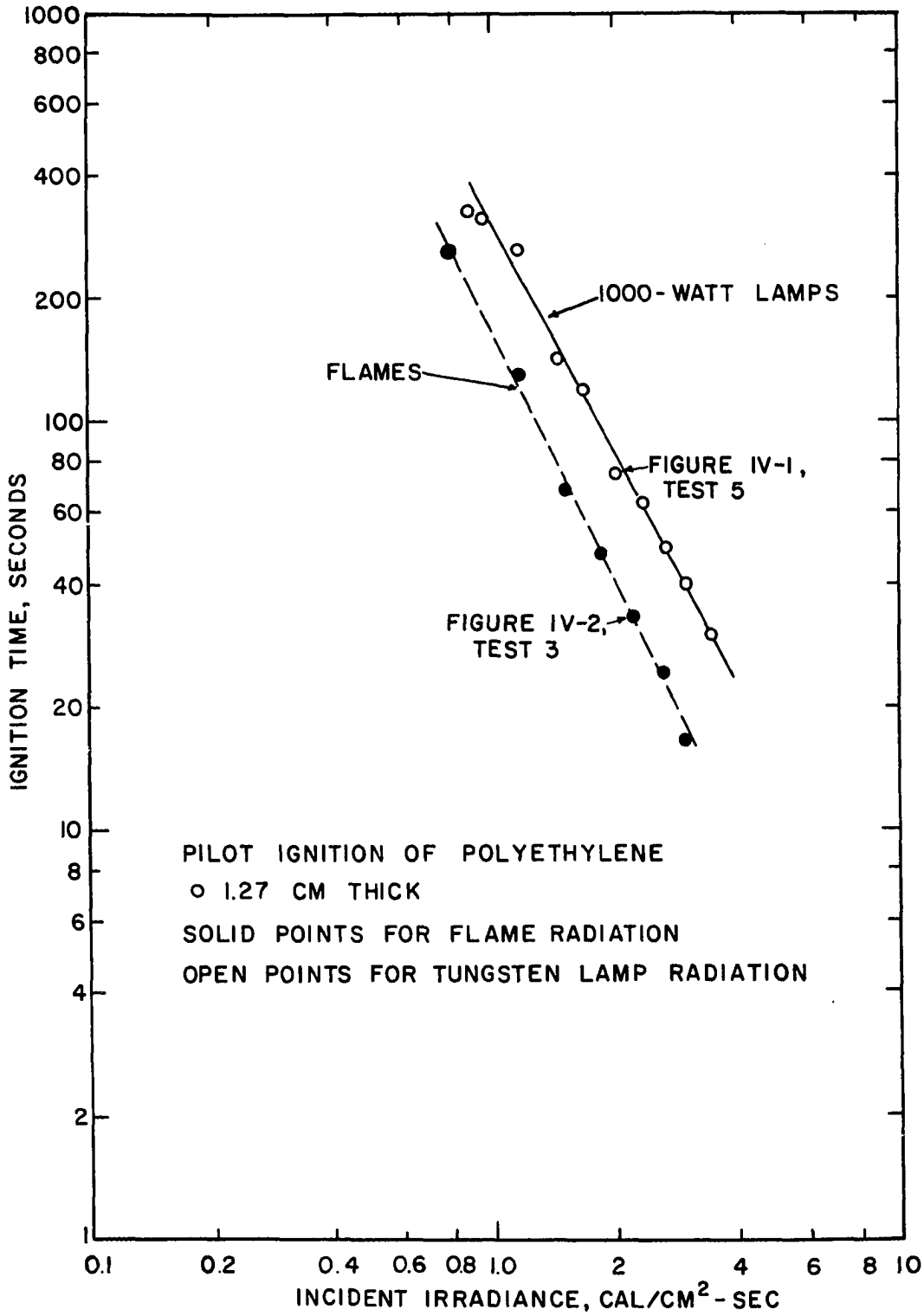

Figure C-24. Pilot Ignition of Polyethylene.

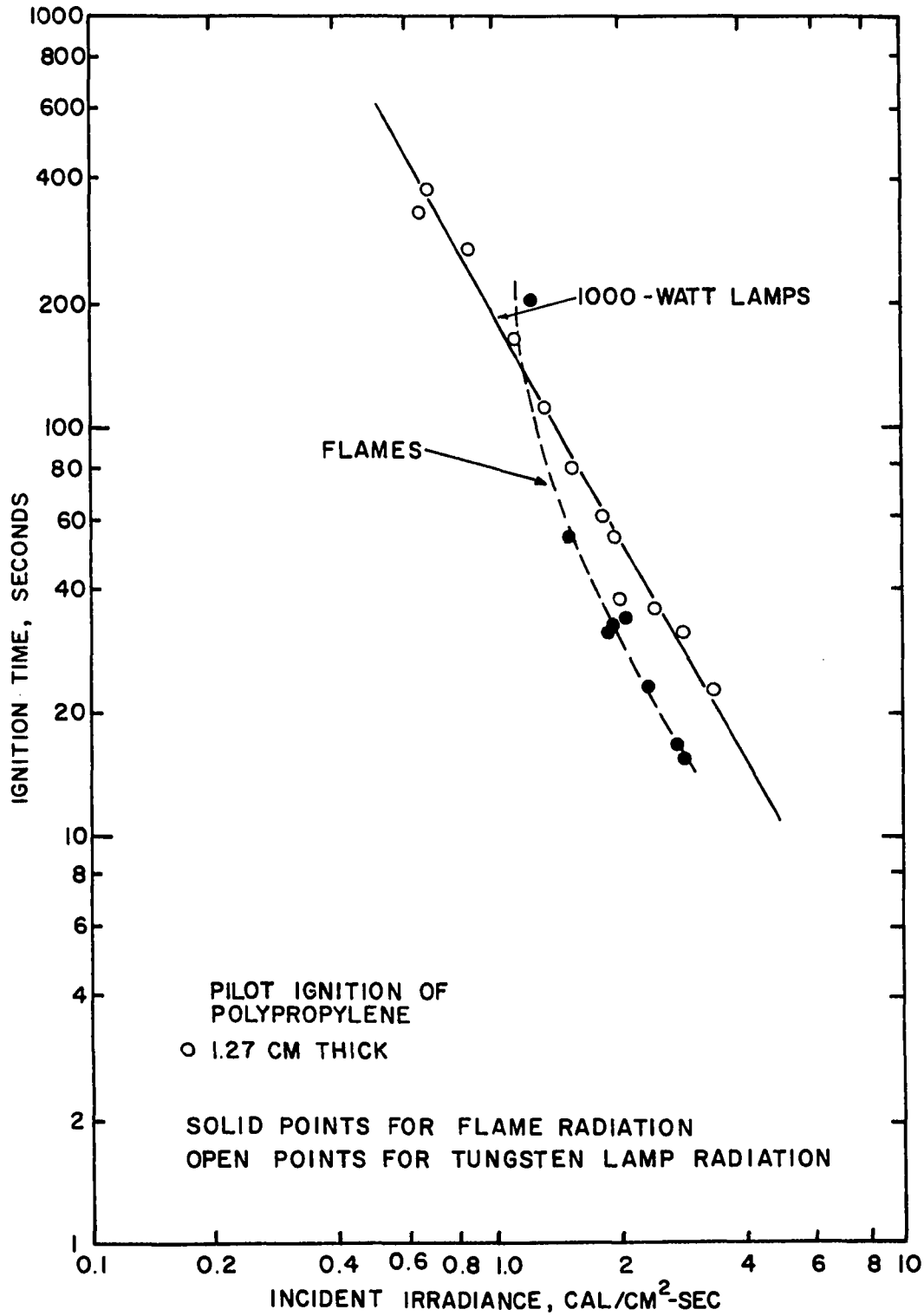

Figure C-25. Pilot Ignition of Polypropylene.

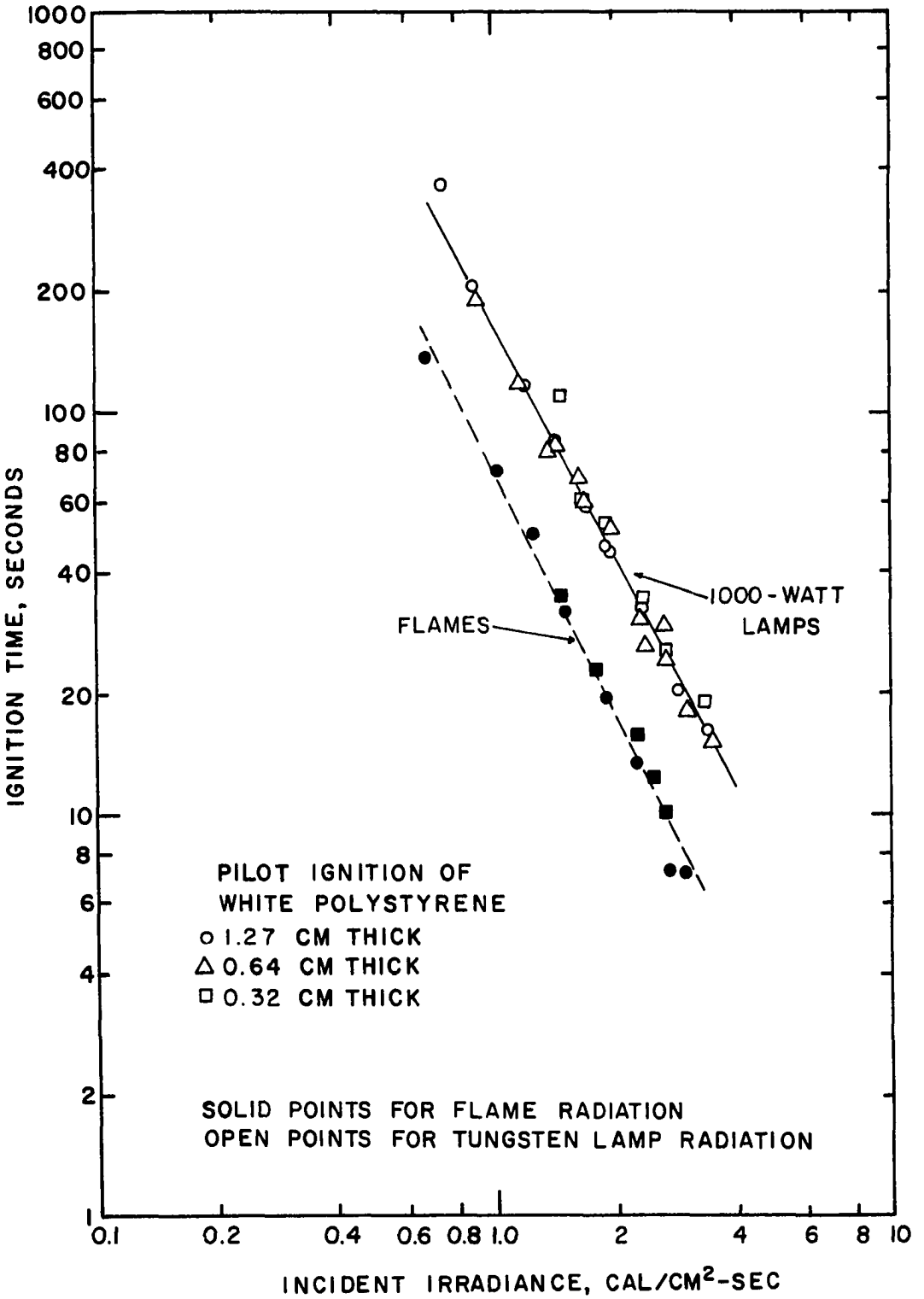

Figure C-26. Pilot Igniton of White Polystyrene.

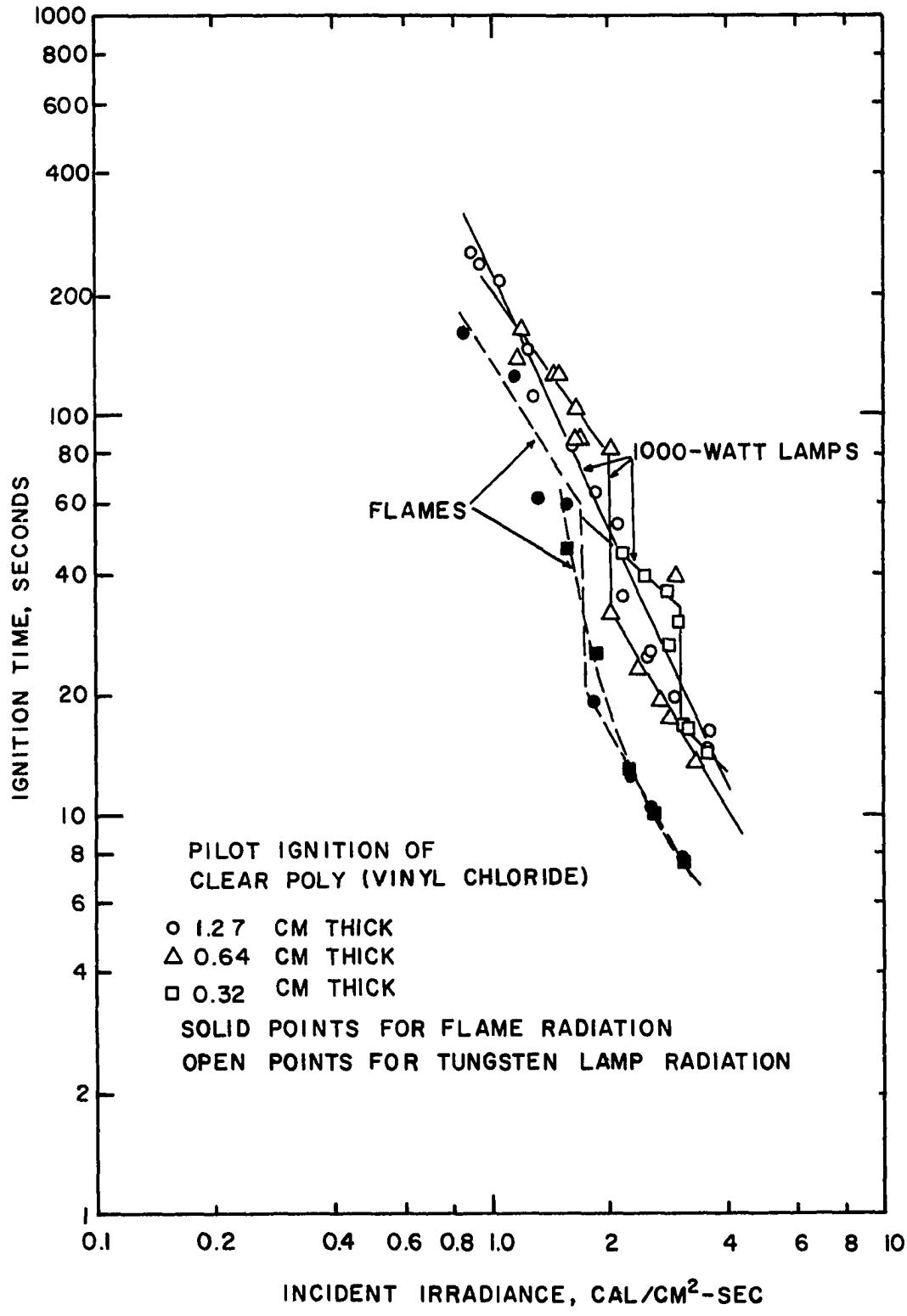

Figure C-27. Pilot Ignition of Clear Poly(vinyl chloride).

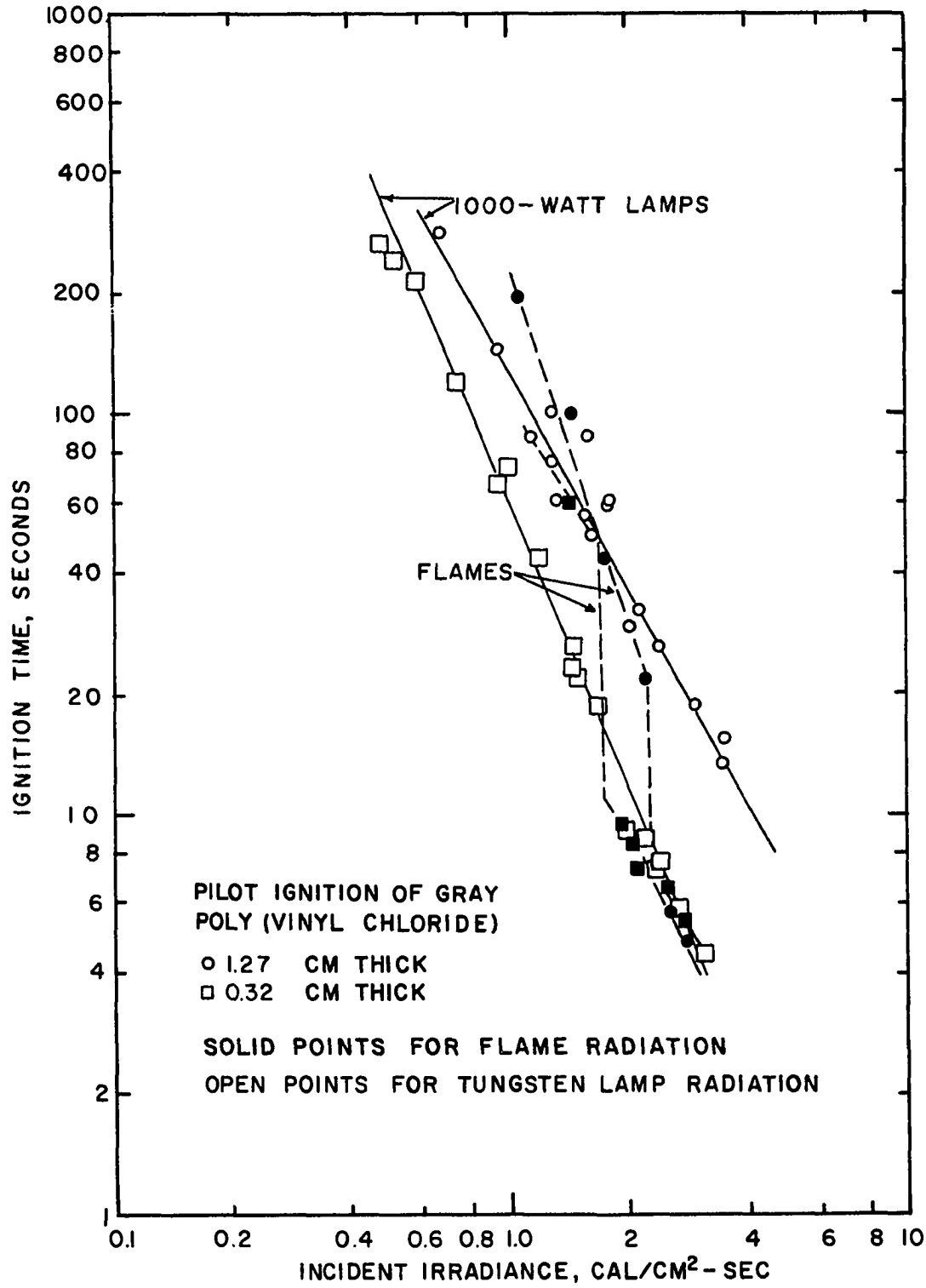

Figure C-28. Pilot Ignition of Poly(vinyl chloride), Gray, Solid.

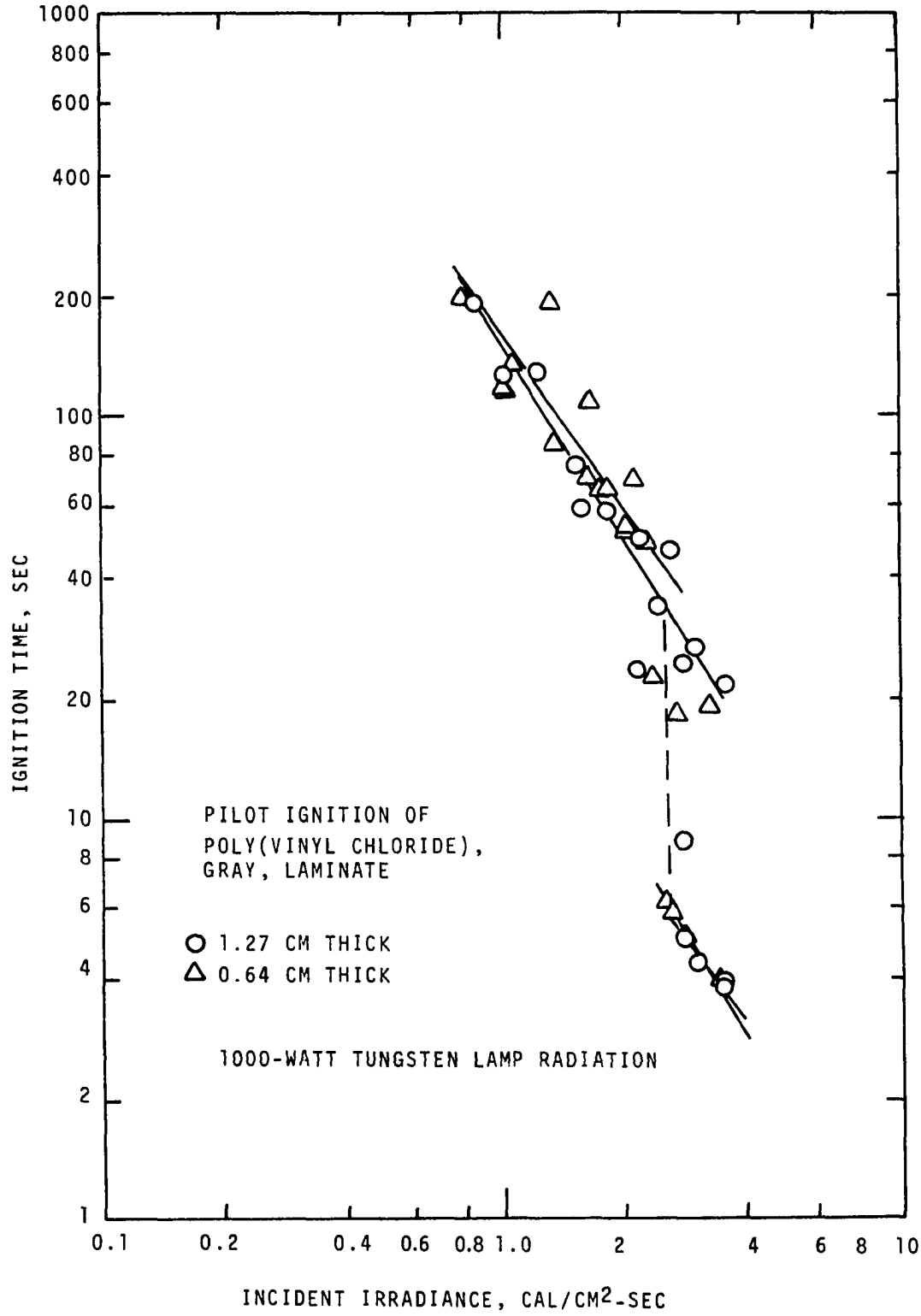

Figure C-29. Pilot Ignition of Poly(vinyl chloride), Gray, Laminate.

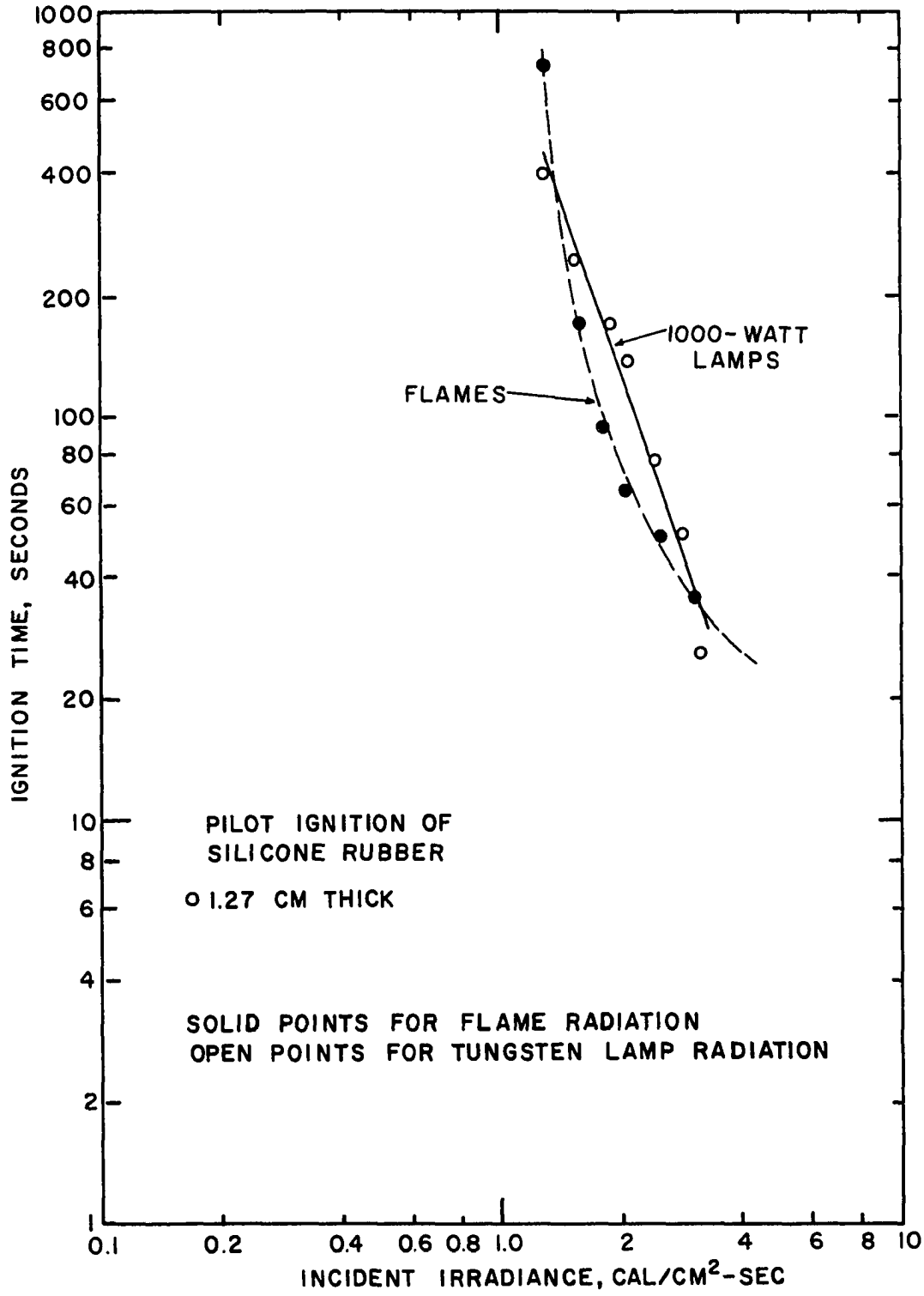

Figure C-30. Pilot Ignition of Silicone Rubber.

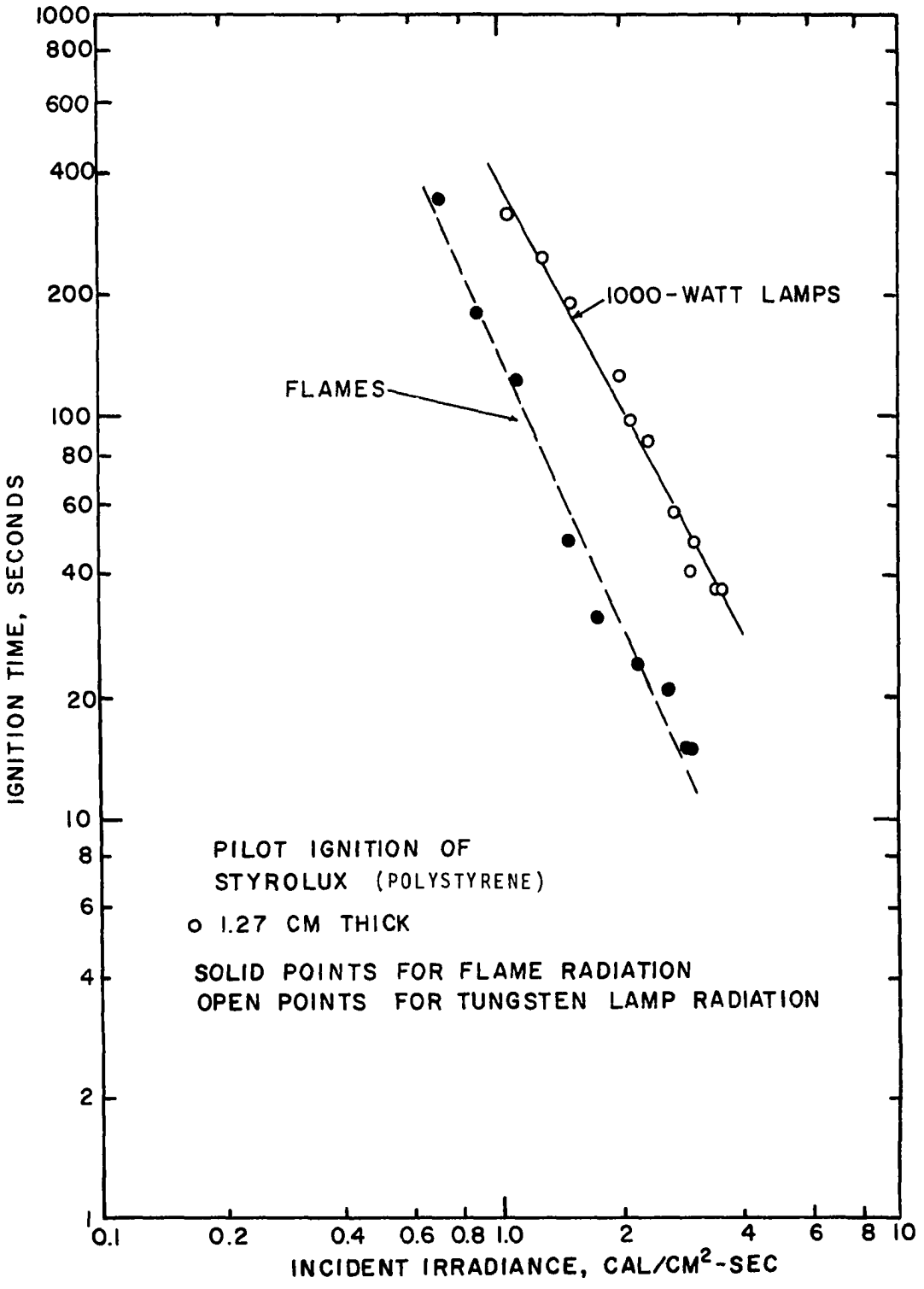

Figure C-31. Pilot Ignition of Styrolux (Polystyrene).

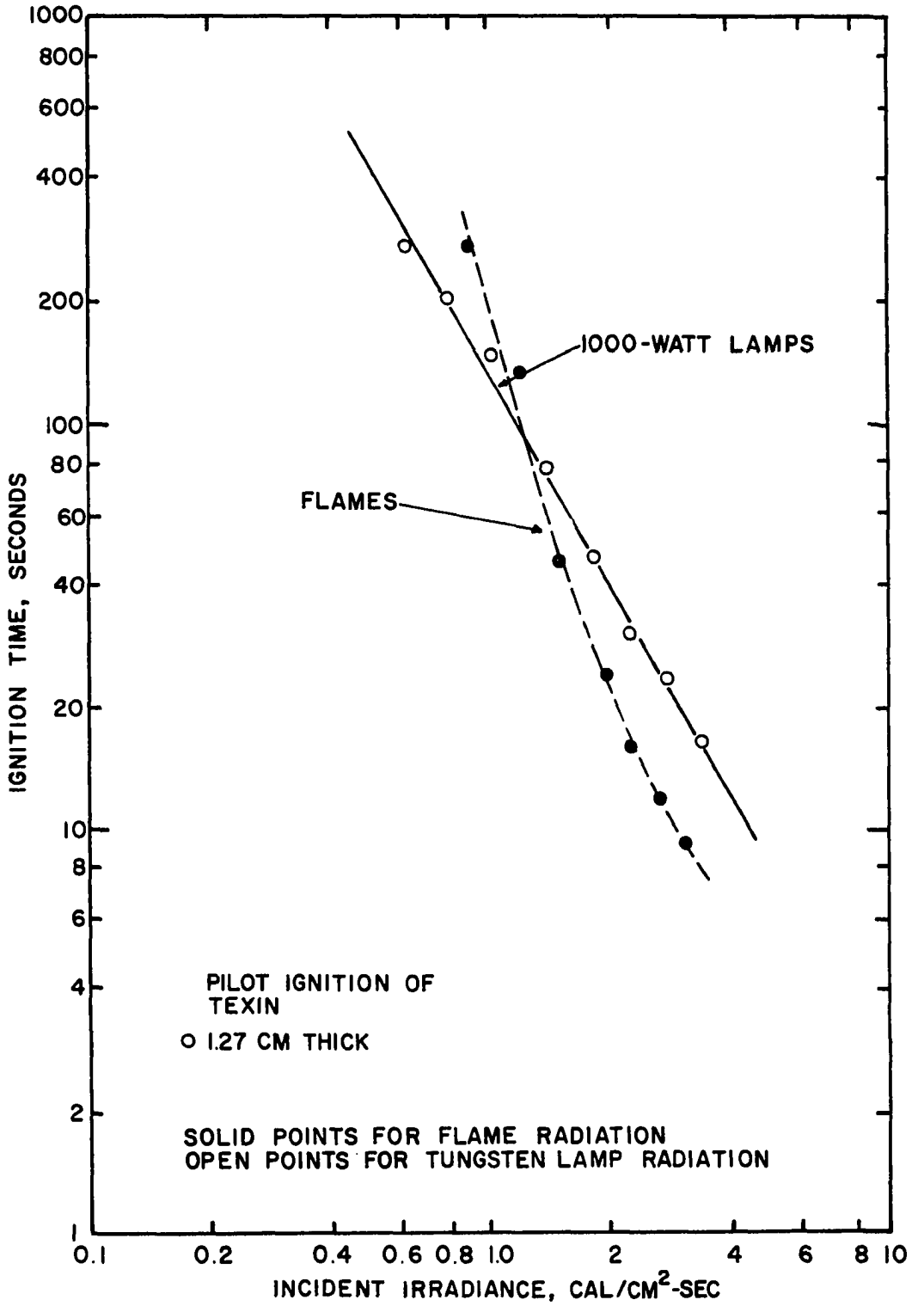

Figure C-32. Pilot Ignition of Texin.

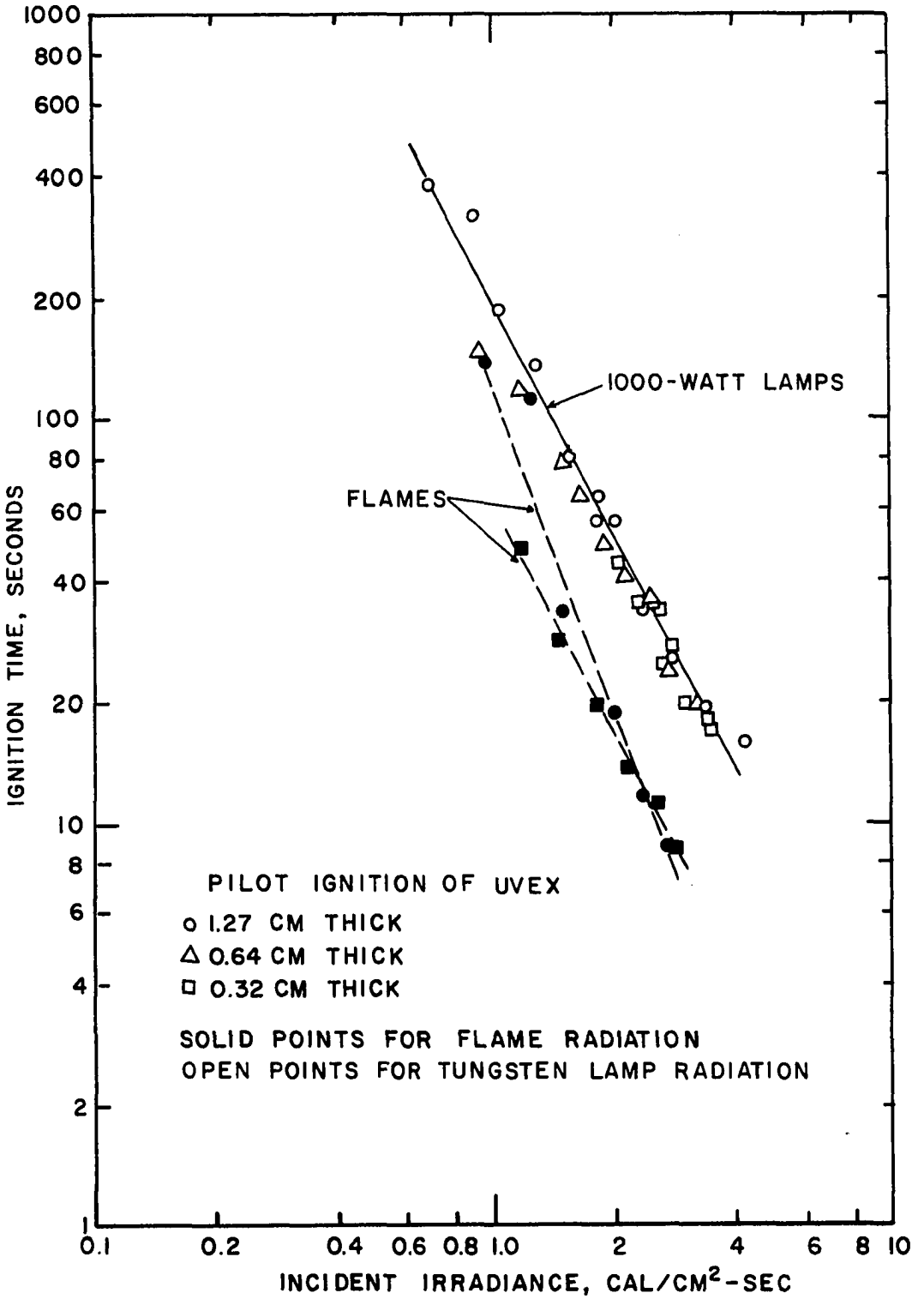

Figure C-33. Pilot Ignition of Uvex.

SECTION III

IGNITION TIME-IRRADIANCE DATA LISTINGS

TABLE C-2

SUMMARY OF IGNITION TIME DATA

Material	Benzene Flame. H_o cal/cm^2-sec	Benzene Flame. t sec	Tungsten Lamps H_o cal/cm^2-sec	Tungsten Lamps t sec
Accopac AS-428	1.25		1.31	
ρ = 1.243 gm/cm^3	1.57	92.	1.65	147.
L = 1.195 cm	2.00	28.	2.00	79.5
	2.22	9.0	2.35	43.5
	2.67	4.9	2.66	40.2
	3.18	3.9	3.21	24.3
Accopac CN-705	0.91	264.	1.00	185.
ρ = .734 gm/cm^3	1.15	99.	1.01	240.
L = 1.295 cm	1.46	30.8	1.30	85.
	1.90	13.5	1.67	34.4
	2.18	8.8	1.98	15.
	2.72	5.0	2.36	10.3
	3.23	3.6	2.67	7.1
			3.13	5.1
Accopac CS-301	0.76	181.	1.23	41.
ρ = 0.722 gm/cm^3	1.07	51.	1.66	18.4
L = 1.22 cm	1.44	27.2	2.01	12.5
	1.85	9.0	2.26	9.2
	2.30	7.0	2.68	5.2
	2.60	4.5	3.04	3.65
	3.21	2.8		
Alphalux 400 (PPO)	0.86	169.	0.76	372.
ρ = 1.095 gm/cm^3	1.22	68.	0.99	165.
L = 1.27 cm	1.38	53.	1.31	74.5
	1.54	33.	1.77	33.
	2.06	19.6	2.19	22.
	2.27	14.3	2.55	16.8
	2.63	10.4	2.83	14.5
	2.88	7.6	3.37	10.9

TABLE C-3

SUMMARY OF IGNITION TIME DATA

Material	Benzene Flame		Tungsten Lamps	
	H_o cal/cm^2-sec	t sec	H_o cal/cm^2-sec	t sec
Buna-N Rubber	0.86	300.	1.30	276.
ρ = 1.596 gm/cm^3	1.26	105.	1.73	139.
L = 1.22 cm	1.53	55.	2.04	330.
	1.76	22.	2.12	57.
	2.27	16.	2.38	187.
	2.59	9.7	2.42	99.
	3.18	2.5	2.44	125.
			2.88	140.
			2.93	24.
			3.19	60.2
Butyl IIR Rubber	0.63	304.	0.65	228.
ρ = 1.093 gm/cm^3	0.78	103.	0.86	110.
L = 1.09 cm	0.91	52.	1.01	86.2
	1.16	53.3	1.27	36.8
	1.44	28.	1.48	26.8
	1.80	13.2	1.88	14.6
	2.22	7.8	2.08	12.
	2.53	4.2	2.40	8.4
	3.00	2.7	2.83	6.4
			3.10	5.0
			3.50	3.9
Chroloprene, DC 100	0.95		1.04	240.
ρ = 0.804 gm/cm^3	1.22	193.	1.28	174.
L = 1.22 cm	1.42	192.	1.68	117.
	1.54	15.2	1.98	81.
	1.76	15.5	2.38	50.
	2.25	10.5	3.20	34.
	2.64	6.1		
	3.01	5.0		

TABLE C-4

SUMMARY OF IGNITION TIME DATA

Material	Benzene Flame		Tungsten Lamps	
	H_o cal/cm^2-sec	t sec	H_o cal/cm^2-sec	t sec
Cork, gasket	0.60		1.05	184.
ρ = 0.253 gm/cm^3	0.70	64.5	1.05	225.
L = 1.27 cm	1.13	25.1	1.05	126.
(As received)	1.46	9.0	1.26	46.5
	1.73	5.5	1.30	10.5
	1.80	4.3	1.79	9.5
	2.10	3.6	2.04	14.
	2.63	2.1	2.09	7.3
	2.86	1.35	2.38	4.5
			2.77	2.9
			3.16	1.65
Cork, gasket,			1.29	174.
Dried 24 hours			1.30	136.
at 80°C			1.65	57.
ρ = 0.244 gm/cm^3			2.01	17.3
			2.35	11.
			2.67	4.95
			3.21	1.95
Cycolac (ABS)	0.66	186.	0.67	349.
ρ = 1.029 gm/cm^3	0.90	110.	0.77	250.
L = 1.32 cm	1.23	57.5	1.16	103.
	1.53	40.3	1.51	54.
	1.81	22.5	1.81	37.
	2.16	16.	2.14	34.
	2.48	12.5	2.41	25.6
	2.97	9.8	2.92	19.6
			3.51	14.

TABLE C-5

SUMMARY OF IGNITION TIME DATA

Material	Benzene Flame		Tungsten Lamps	
	H_o cal/cm^2-sec	t sec	H_o cal/cm^2-sec	t sec
Delrin	0.90	181.	0.65	371.
ρ = 1.437 gm/cm^3	1.25	78.	0.80	289.
L = 1.32 cm	1.80	37.	0.97	220.
	2.08	28.5	1.49	93.
	2.54	21.3	1.99	57.
	2.88	15.3	2.47	42.5
			2.87	33.
			3.42	22.5
Formica	0.90	148.	0.63	467.
ρ = 1.392 gm/cm^3	1.15	81.5	0.80	155.
L = 1.27 cm	1.48	24.5	0.95	60.
	1.83	14.5	1.21	43.5
	2.14	12.4	1.43	26.7
	2.59	8.3	1.66	22.
	3.00	6.9	1.90	20.
			2.15	13.3
			2.33	10.7
			2.49	9.6
			2.77	11.3
			2.81	9.6
			3.42	6.1
			3.42	7.5
Gum Rubber	0.76	206.	0.71	190.
ρ = 0.990 gm/cm^3	1.07	77.	0.95	94.
L = 1.27 cm	1.50	31.3	1.25	52.
	1.97	15.	1.50	33.5
	2.25	8.6	1.73	22.6
	2.68	4.5	2.06	16.
	3.02	3.02	2.43	12.1
	3.22	4.5	3.05	6.1

TABLE C-6

SUMMARY OF IGNITION TIME DATA

Material	Benzene Flame		Tungsten Lamps	
	H_o cal/cm^2-sec	t sec	H_o cal/cm^2-sec	t sec
Kel-F			2.11	
ρ = 2.099 gm/cm^3			2.55	
L = 0.71 cm			2.77	
			2.77	
Kydex, Gray, Rolled			1.42	18.5
L = 0.32 cm			1.90	10.
			2.33	6.7
			2.73	5.0
			3.15	3.95
			3.17	4.0
Kydex, Red, Cast			0.87	75.
L = 0.32 cm			1.16	39.
			1.77	18.
			2.04	14.6
Lexan	1.26		1.42	206.
ρ = 1.193 gm/cm^3	1.56	92.	1.88	111.
L = 1.30 cm	1.75	76.	2.25	80.
	2.20	49.7	2.76	57.5
	2.48	33.6	3.42	34.5
	2.97	25.2		

TABLE C-7

SUMMARY OF IGNITION TIME DATA

Material	Benzene Flame		Tungsten Lamps	
	H_o cal/cm^2-sec	t sec	H_o cal/cm^2-sec	t sec
Masonite	0.65	163.	0.49	538.
ρ = 1.203 gm/cm^3	0.89	82.	0.50	525.
L = 0.32 cm	1.18	51.	0.59	283.
	1.50	24.	0.73	184.
	1.85	17.9	0.85	127.
	2.15	14.4	0.95	122.
	2.60	8.3	0.98	96.
	3.00	6.15	1.22	57.
			1.41	44.
			1.72	30.1
			1.76	29.
			1.90	21.7
			2.33	18.
			2.44	17.4
			2.81	12.8
			2.85	13.4
			3.18	10.6
			3.18	10.7
Neoprene, closed	1.02		1.59	
cell sponge rubber	1.27		1.63	
ρ = 0.275 gm/cm^3	1.46	4.1	2.04	37.
L = 1.27 cm	1.58		2.06	43.
	1.73	3.2	2.31	40.
	2.22	2.0	2.67	16.5
	2.87	1.1	2.96	12.4
			3.00	10.5

TABLE C-8

SUMMARY OF IGNITION TIME DATA

Material	Benzene Flame		Tungsten Lamps	
	H_o cal/cm^2-sec	t sec	H_o cal/cm^2-sec	t sec
Neoprene, open cell sponge rubber ρ = 0.564 gm/cm^3 L = 1.27 cm	1.08		1.01	103.
	1.12	238.	1.29	59.5
	1.42	29.6	1.58	31.7
	1.75	6.0	1.94	11.8
	1.92	4.4	2.19	9.5
	2.22	3.8	2.20	4.0
	2.59	1.5	2.28	3.9
	2.78	1.3	2.55	3.2
	3.15	1.1	2.93	2.4
Neoprene Rubber solid ρ = 1.478 gm/cm^3 L = 1.37 cm	1.09	158.	1.05	
	1.27	224.	1.30	83.
	1.48	33.	1.62	47.
	1.73	17.7	2.09	48.5
	2.22	9.1	2.39	36.
	2.59	7.9	2.67	17.1
	3.05	5.1	3.12	13.5
Nylon 6/6 ρ = 1.116 gm/cm^3 L = 1.30 cm	0.88	383.	0.87	355.
	1.16	220.	1.00	237.
	1.36	146.	1.23	146.
	1.50	75.5	1.55	93.
	1.88	51.	1.55	103.
	2.13	31.	1.82	84.
	2.56	23.8	2.13	58.
	2.97	19.	2.48	45.
			2.92	32.7
			3.52	23.5

TABLE C-9

SUMMARY OF IGNITION TIME DATA

Material	Benzene Flame		Tungsten Lamps	
	H_o cal/cm^2-sec	t sec	H_o cal/cm^2-sec	t sec
Bakelite	1.08	196.	0.73	543.
ρ = 1.368 gm/cm^3	1.20	255.	0.93	431.
L = 1.37 cm	1.45	96.	0.96	257.
	1.95	47.	1.10	202.
	2.13	30.	1.31	146.5
	2.41	23.5	1.69	82.
	2.62	20.	2.01	50.
	2.83	16.	2.16	51.
			2.51	32.
			2.53	37.
			3.06	25.5
			3.24	22.8
Plexiglas, Black	0.66	137.	0.64	118.
ρ = 1.264 gm/cm^3	0.92	61.	0.64	123.
L = 0.635 cm	1.26	30.	0.80	65.5
	1.53	21.2	0.87	74.
	1.76	15.3	1.02	44.
	2.27	10.2	1.18	38.
	2.48	7.6	1.53	20.
	2.58	7.0	1.72	17.4
	2.84	5.5	2.00	14.2
			2.43	10.2
			2.87	8.0
			3.49	5.9

TABLE C-10

SUMMARY OF IGNITION TIME DATA

Material	Benzene Flame		Tungsten Lamps	
	H_o cal/cm^2-sec	t sec	H_o cal/cm^2-sec	t sec
Plexiglas, Black	0.88	101.	0.63	140.
ρ = 1.29 gm/cm^3	0.90	91.5	0.64	125.
L = 1.27 cm	1.24	41.2	0.80	80.
(laminate)	1.50	26.	0.92	57.5
	1.91	17.6	1.01	43.5
	2.22	14.3	1.22	33.5
	2.59	9.5	1.47	28.
	2.99	7.4	1.82	17.7
			2.15	13.5
			2.36	10.9
			2.79	8.7
			3.46	6.0
			3.61	5.7
Plexiglas, Clear	0.79	127.	1.02	
ρ = 1.173 gm/cm^3	1.21	75.	1.02	
L = 0.635 cm	1.65	25.	1.21	107.
	1.89	22.	1.50	75.
	2.22	17.	1.76	58.6
	2.63	13.	2.03	47.1
	2.86	10.	2.40	38.5
			2.82	29.5
			3.42	19.4

TABLE C-11

SUMMARY OF IGNITION TIME DATA

Material	Benzene Flame		Tungsten Lamps	
	H_o cal/cm^2-sec	t sec	H_o cal/cm^2-sec	t sec
Plexiglas, Clear	0.66	232.	0.76	837.
ρ = 1.187 gm/cm^3	0.91	104.	0.79	353.
L = 1.27 cm	1.21	67.	0.90	261.
	1.51	29.	0.93	455.
	1.84	25.2	1.04	168.
	2.10	19.	1.04	324.
	2.50	15.9	1.07	362.
	3.02	9.3	1.21	189.5
			1.21	229.
			1.30	147.
			1.41	157.
			1.49	118.
			1.50	99.5
			1.70	63.
			1.75	82.
			2.04	53.3
			2.04	61.2
			2.04	61.4
			2.38	41.5
			2.40	36.5
			2.82	27.3
			2.85	31.8
			3.38	23.

TABLE C-12

SUMMARY OF IGNITION TIME DATA

Material	Benzene Flame		Tungsten Lamps	
	H_o cal/cm^2-sec	t sec	H_o cal/cm^2-sec	t sec
Plexiglas, White	0.80	161.	0.63	
ρ = 1.194 gm/cm^3	1.17	99.	0.63	
L = 0.635 cm	1.48	56.5	0.74	220.
	1.83	26.5	0.97	140.
	2.24	18.1	1.23	97.5
	2.61	13.8	1.48	58.
	3.08	10.7	1.82	45.5
			2.09	41.1
			2.43	26.4
			2.94	22.7
			3.52	16.7
Plexiglas, White	0.89	302.	0.61	310.
ρ = 1.158 gm/cm^3	1.24	122.	0.75	247.
L = 1.25 cm	1.43	100.	1.05	148.
	1.93	30.5	1.23	105.
	2.18	23.7	1.48	73.
	2.62	15.4	1.79	52.
	3.02	12.2	1.95	40.6
			2.48	34.6
			2.93	22.7
			3.51	19.8

TABLE C-13

SUMMARY OF IGNITION TIME DATA

Material	Benzene Flame		Tungsten Lamps	
	H_o cal/cm^2-sec	t sec	H_o cal/cm^2-sec	t sec
Polyethylene	0.79	264.	0.75	
ρ = 0.930 gm/cm^3	1.17	130.	0.85	325.
L = 1.20 cm	1.51	68.	0.95	315.
	1.86	47.	1.17	267.
	2.22	33.	1.44	144.
	2.63	24.5	1.67	120.
	2.94	17.5	2.00	76.
			2.36	64.
			2.69	49.5
			3.00	40.5
			3.49	30.2
Polypropylene	1.25	207.	0.66	336.
ρ = 0.907 gm/cm^3	1.50	54.	0.69	381.
L = 1.27 cm	1.89	31.8	0.87	275.
	1.92	32.8	1.12	166.
	2.08	34.5	1.33	112.
	2.34	22.7	1.56	80.
	2.78	16.5	1.85	61.
	2.90	16.3	1.99	54.
			2.04	38.
			2.46	36.5
			2.77	31.5
			3.41	23.
Polystyrene,	1.20	97.4	1.47	110.
white, hi-impact	1.45	35.5	1.69	60.
ρ = 1.001 gm/cm^3	1.75	23.0	1.94	53.
L = 0.318 cm	2.23	15.7	2.32	34.5
	2.46	12.5	2.71	25.2
	2.68	10.	3.41	19.

TABLE C-14

SUMMARY OF IGNITION TIME DATA

Material	Benzene Flame		Tungsten Lamps	
	H_o cal/cm^2-sec	t sec	H_o cal/cm^2-sec	t sec
Polystyrene, white, hi-impact ρ = 1.046 gm/cm^3 L = 0.635 cm (laminate)			0.92	195.
			1.18	120.
			1.40	82.
			1.45	84.
			1.65	65.5
			1.99	52.4
			2.32	31.5
			2.42	26.4
			2.58	30.3
			2.72	24.2
			3.10	18.2
			3.54	15.3
Polystyrene, white hi-impact ρ = 1.092 gm/cm^3 L = 1.27 cm (laminate)	0.67	140.	0.76	380.
	1.01	73.5	0.90	209.
	1.26	51.5	1.22	117.
	1.50	32.5	1.48	85.5
	1.89	19.9	1.73	58.
	2.24	13.7	1.94	47.
	2.75	7.3	2.06	44.5
	2.98	7.4	2.41	32.5
			2.93	20.5
			3.49	16.3
Poly(vinyl chloride) clear ρ = 1.384 gm/cm^3 L = 0.305 cm	1.44		2.00	
	1.55	46.	2.13	45.
	1.82	25.3	2.41	38.5
	2.22	12.7	2.80	35.8
	2.58	10.0	2.80	26.8
	3.00	7.6	3.00	30.7
			3.06	16.7
			3.07	16.3
			3.50	14.3

TABLE C-15

SUMMARY OF IGNITION TIME DATA

Material	Benzene Flame		Tungsten Lamps	
	H_o cal/cm^2-sec	t sec	H_o cal/cm^2-sec	t sec
Poly(vinyl chloride)			1.16	140.
clear			1.19	161.
ρ = 1.326 gm/cm^3			1.48	126.
L = 0.66 cm (laminate)			1.50	127.
			1.64	87.
			1.68	105.
			1.70	87.
			2.01	83.
			2.01	31.5
			2.38	23.5
			2.40	23.
			2.71	19.3
			2.86	17.5
			2.93	39.5
			3.33	13.6
Poly(vinyl chloride)	0.84	161.	0.88	253.
clear	1.15	124.	0.92	237.
ρ = 1.478 gm/cm^3	1.32	62.	1.04	216.
L = 1.32 cm	1.55	60.	1.25	148.
(laminate)	1.80	19.	1.27	110.
	2.23	12.5	1.62	83.
	2.53	10.5	1.83	63.
	3.07	7.9	2.10	53.5
			2.13	35.
			2.49	24.5
			2.50	25.
			2.87	19.6
			3.53	16.
			3.54	14.5

TABLE C-16

SUMMARY OF IGNITION TIME DATA

Material	Benzene Flame		Tungsten Lamps	
	H_o cal/cm^2-sec	t sec	H_o cal/cm^2-sec	t sec
Poly(vinyl chloride)	1.07	197.	0.69	285.
gray	1.43	100.	0.95	146.
ρ = 1.433 gm/cm^3	1.76	44.	1.13	88.
L = 1.32 cm	2.20	22.2	1.29	100.
	2.54	5.7	1.33	61.
	2.80	4.9	1.60	88.
			1.61	49.4
			1.80	61.
			1.81	58.
			2.04	29.3
			2.11	32.3
			2.40	26.8
			2.92	19.
			3.47	13.8
			3.49	15.6
Poly(vinly chloride)	1.47	61.	0.49	
gray	1.96	9.4	0.74	121.
ρ = 1.427 gm/cm^3	2.07	8.5	0.95	66.
L = 0.315 cm	2.12	7.3	0.99	71.8
	2.54	6.6	1.17	43.8
	2.82	5.45	1.46	22.5
			1.47	22.1
			1.48	21.3
			1.48	21.3
			1.69	18.3
			1.95	8.8
			2.19	8.6
			2.33	7.0
			2.36	6.7
			2.42	7.5
			2.76	5.3
			2.80	5.4
			3.07	4.5

TABLE C-17

SUMMARY OF IGNITION TIME DATA

Material	Benzene Flame		Tungsten Lamps	
	H_o cal/cm^2-sec	t sec	H_o cal/cm^2-sec	t sec
Poly(vinyl chloride)			0.82	194.
gray			1.00	116.
ρ = 1.411 gm/cm^3			1.01	114.
L = 0.635 cm (laminate)			1.07	135.
			1.36	189.
			1.38	84.
			1.58	58.
			1.62	71.
			1.70	107.
			1.72	65.
			1.85	65.
			2.04	52.
			2.06	54.
			2.14	69.8
			2.16	23.
			2.33	48.
			2.37	22.3
			2.47	33.5
			2.59	6.2
			2.61	5.8
			2.68	18.
			2.81	8.7
			2.87	5.1
			3.27	18.8
			3.42	3.8
			3.51	3.8

TABLE C-18

SUMMARY OF IGNITION TIME DATA

Material	Benzene Flame		Tungsten Lamps	
	H_o cal/cm^2-sec	t sec	H_o cal/cm^2-sec	t sec
Poly(vinyl chloride)			0.87	187.
gray			1.01	125.
ρ = 1.385 gm/cm^3			1.23	127.
L = 1.32 cm			1.56	75.
(laminate)			1.58	58.
			1.88	57.5
			2.16	23.
			2.25	49.
			2.47	33.5
			2.63	46.
			2.81	8.7
			2.81	5.0
			2.88	24.4
			3.00	26.4
			3.03	4.4
			3.51	3.8
			3.55	3.9
			3.61	21.4
Silicone Rubber	1.31	736.	1.29	400.
ρ = 1.749 gm/cm^3	1.59	170.	1.55	242.
L = 1.22 cm	1.80	95.	1.88	157.
	2.06	67.	2.10	137.
	2.60	52.	2.43	77.
	3.09	36.	2.79	51.
			3.20	26.

TABLE C-19

SUMMARY OF IGNITION TIME DATA

Material	Benzene Flame		Tungsten Lamps	
	H_o cal/cm^2-sec	t sec	H_o cal/cm^2-sec	t sec
Styrolux (Polystyrene)	0.72	350.	1.06	315.
clear	0.90	182.	1.27	248.
ρ = 1.051 gm/cm^3	1.12	123.	1.27	247.
L = 1.27 cm	1.52	49.3	1.50	190.
	1.78	34.	2.00	126.
	2.22	24.5	2.10	96.
	2.66	21.	2.34	86.
	2.96	15.	2.76	57.
	3.05	15.	3.01	41.5
			3.06	48.5
			3.48	37.5
			3.54	36.7
Texin	0.90	275.	0.65	285.
ρ = 1.200 gm/cm^3	1.21	137.	0.80	208.
L = 1.42 cm	1.50	46.	1.03	148.
	1.95	24.	1.41	78.
	2.26	16.	1.85	47.
	2.63	11.9	2.28	30.6
	3.06	9.3	2.83	23.8
			3.44	16.7
Uvex (Cellulose			0.97	147.
Acetate Butyrate)			1.20	115.
ρ = 1.207 gm/cm^3			1.56	77.
L = 0.635 cm			1.78	64.
(laminate)			2.00	48.
			2.22	40.5
			2.56	35.5
			2.85	23.8
			3.35	19.6

TABLE C-20

SUMMARY OF IGNITION TIME DATA

Material	Benzene Flame		Tungsten Lamps	
	H_o cal/cm^2-sec	t sec	H_o cal/cm^2-sec	t sec
Uvex (Cellulose Acetate Butyrate) ρ = 1.199 gm/cm^3 L = 0.318 cm	0.90		2.11	42.7
	1.21	48.	2.36	
	1.50	28.	2.40	35.
	1.88	19.4	2.48	
	2.25	13.6	2.57	
	2.66	11.	2.57	36.4
	3.00	8.5	2.63	
			2.65	35.7
			2.65	35.6
			2.72	34.5
			2.76	25.
			2.96	28.
			3.15	20.
			3.57	18.2
			3.60	17.3
Uvex (Cellulose Acetate Butyrate) ρ = 1.211 gm/cm^3 L = 1.27 cm (laminate)	0.76		0.71	370.
	1.02	136.	0.94	314.
	1.30	110.5	1.04	182.
	1.56	33.7	1.31	133.
	2.08	21.	1.59	79.
	2.47	11.8	1.86	56.
	2.87	9.0	2.09	55.
			2.45	33.
			2.86	25.
			3.47	19.4

APPENDIX D

ABSORPTANCE COEFFICIENTS OF POLYMERS

During the preliminary analyses of the polymeric ignition data, it was found that there was a difference in the relative times of ignition for the same incident radiant flux from two different energy sources. Koohyar (70), Wesson (132) and Welker (131) had previously found the same phenomenon during their ignition testing of woods. It was concluded that this difference in ignition times was due primarily to the actual amount of incident irradiance absorbed by the material. Therefore, before any further analyses could be made using the ignition data, it became necessary to investigate and determine the absorptance properties of the polymeric materials under test.

Theoretical Considerations

When radiation impinges upon a perfect surface, the radiation can be either reflected, absorbed, transmitted or a combination of all three. If the material is opaque, the radiation is either reflected or absorbed. The reflection occurs in two forms, diffuse or specular. Figure D-1 diagrams these two types of reflections. I_1 is the intensity of the

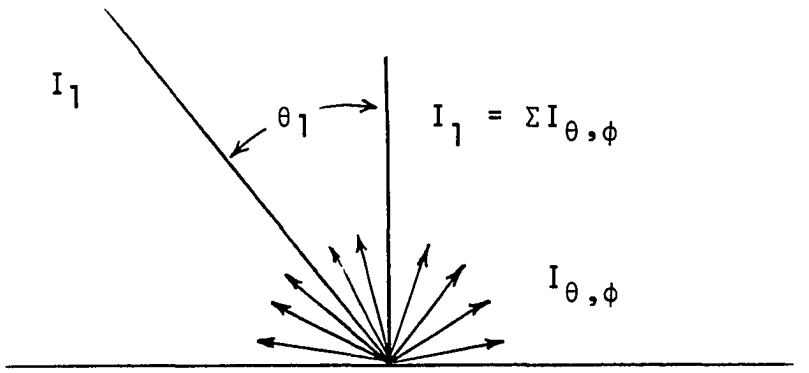

(a) Ideal Diffuse Surface

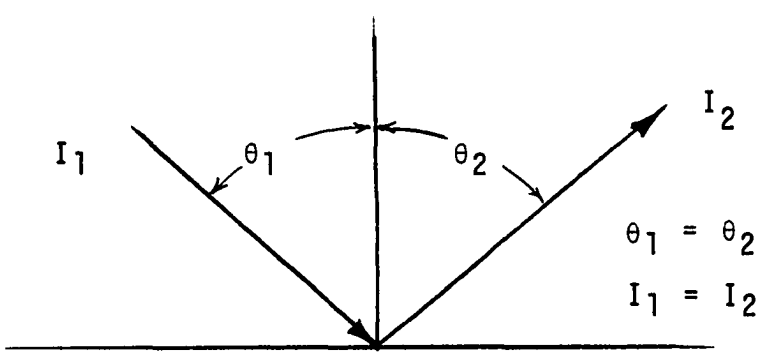

(b) Ideal Specular Surface

Figure D-1. Surface Reflection.

incident beam, I_2 is the intensity of the reflected beam, $I_{\theta,\phi}$ is the intensity of the individual rays of the total hemisphere and θ_1 and θ_2 are the incident and reflected angles, respectively.

As can be seen, the ideal diffuse surface reflects the incident beam into the hemispherical pattern while the ideal specular surface reflects the entire incident beam at the same angle from normal. A real surface contains a combination of both of these ideal surface reflections and surface absorptance as shown in Figure D-2. Here I_α is the absorbed energy.

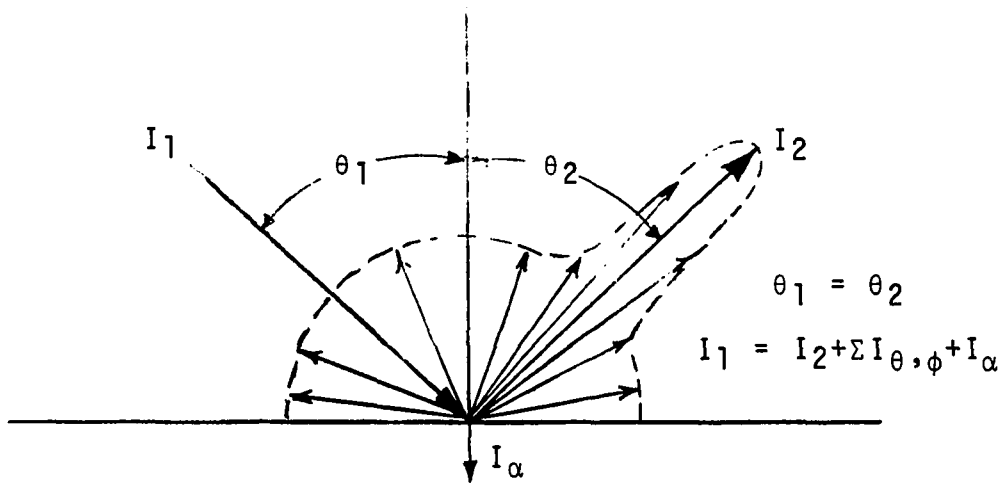

Figure D-2. Real Surface Reflection.

Kirchoff devised a general law describing radiation upon a surface as

$$\varepsilon = 1 - r \tag{D-1}$$

where ε is the emittance and r is the reflectance. However, this equation does not take into account any directional values. If the directional values are considered, Equation D-1 becomes

$$\varepsilon_\lambda\ (\theta,\phi) = 1 - r_\lambda\ (\theta_1,\ \phi_1,\ \theta_2,\ \phi_2) \tag{D-2}$$

where θ and ϕ are the cosines of the polar angle from normal and azimuth angle respectively; the symbol λ indicates monochromatic radiation. If the law of reciprocity applied, i.e.,

$$r_\lambda\ (\theta_1,\ \phi_1,\ \theta_2,\ \phi_2) = r_\lambda\ (\theta_2,\ \phi_2,\ \theta_1,\ \phi_1) \tag{D-3}$$

then $$r_\lambda\ (\theta_1,\ \phi_1) = r_\lambda\ (\theta_2,\ \phi_2) = r_\lambda\ (\theta,\phi)$$

and $$\varepsilon_\lambda\ (\theta,\phi) = 1 - r_\lambda\ (\theta,\phi) \tag{D-4}$$

Under conditions of thermodynamic equilibrium $\varepsilon = \alpha$ and $\varepsilon_\lambda = \alpha_\lambda$ so where only normal incident radiation impinges on a surface,

$$\alpha_\lambda = 1 - r_\lambda \tag{D-5}$$

Where a material is not opaque but partially transparent, i.e., transmits some radiation, Kirchoff's law can be generalized for normal incident radiation (11) to

$$\varepsilon_\lambda (T) + r_\lambda (T) + \tau_\lambda (T) = 1 \qquad \text{(D-6)}$$

where τ_λ is the monochromatic transmittance. In this case the emittance, reflectance and transmittance are in equilibrium at temperature T. Again, for condition of thermodynamic equilibrium, Equation D-6 reduces to

$$\varepsilon_\lambda + r_\lambda + \tau_\lambda = 1 \qquad \text{(D-7)}$$

Heat Sources and Absorptance

Studies have indicated that different heat sources have different intensities at different wavelengths (75, 97, 103, 110). Figure D-3 is a graphic illustration of the emissive powers of solar, tungsten lamp and hexane flame radiation. The tungsten lamp manufacturer (see Chapter III for details and manufacturer) has indicated that the emissive power is essentially that of a blackbody at 2500°K which shows a maximum peak at 1.15-micron wavelength (75, 78). The spectral emissive power of the hexane flame and other hydrocarbons was measured by Ryan, Penzias and Tourin (110). As indicated by Figure D-3 hexane has primary emissive power peaks at 2.7 μ and 4.3 μ which are characteristic of water vapor and carbon dioxide. The smaller peaks near 2 μ represent radiation emitted by hot carbon particles in the flame. The solar radiation data (6000°K solar surface temperature) have been included to enable a comparison of both emissive

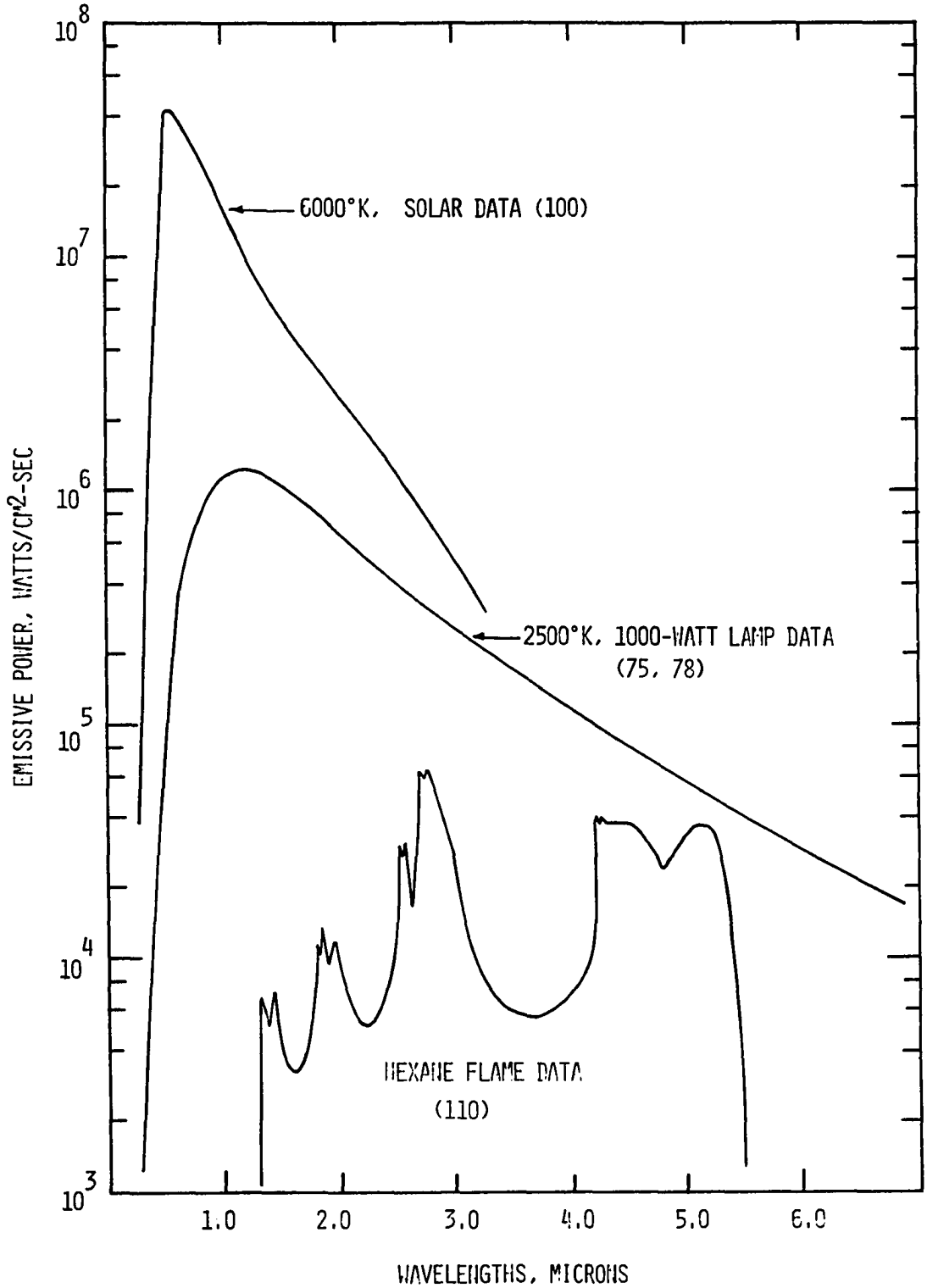

Figure D-3. Monchromatic Emissive Power of Several Heat Sources.

power intensity and wavelength span.* Reflectance data are available for some materials using sunlight as the radiative power source (11).

Tungsten lamp radiation is not true blackbody radiation, but for purposes of this study, it is assumed to behave as a graybody which, by definition, assumes that the emittance is constant at all wavelengths. The studies of hydrocarbon flame spectral emissive power (110) did not include that of benzene. However, because of the chemical similarity to hexane, it has been assumed that the hexane data represent a satisfactory approximation of benzene flame.

Figure D-3 indicates that the lamp emissive power is greatest in the span 0.7-2.5 μ while the benzene flame will have the strongest emissive power in the spans 2.5-3.2 μ and 4.2-5.4 μ. This difference is such that all reflectance/absorptance data must be adjusted both in magnitude and wavelength span.

To account for the variations in absorbed irradiance it is necessary to determine the magnitude of the monochromatic absorptance and the magnitude of radiation intensity at the same wavelength and to integrate over the total wavelength span involved. Equation D-8 illustrates this relationship,

---

*The solar radiation curve was drawn as an approximation from the solar monochromatic emission data and the use of measured solar temperature of 6000°K in the Stephan-Boltzmann radiation equation.

$$\alpha_{av} = \frac{\int_{\lambda_1}^{\lambda_2} \alpha_\lambda I_\lambda d\lambda}{\int_{\lambda_1}^{\lambda_2} I_\lambda d\lambda} \qquad \text{(D-8)}$$

where α_{av} is the average absorptance coefficient for a combination of target material and radiation source, α_λ is the monochromatic absorptance of the target and I_λ is the monochromatic radiant intensity of the heat source.

Equation D-8 was converted into a trapezoidal rule summation for use in a standard computer program as illustrated by Equation D-9,

$$\alpha_{av} = \frac{\Sigma\ \alpha_\lambda I_\lambda \Delta\lambda}{\Sigma\ I_\lambda \Delta\lambda} \qquad \text{(D-9)}$$

Average absorptance values obtained by this computer program can be found in Table D-1. The limits of integration are the wavelengths which include significant amounts of energy.

Measurement Techniques

The experimental methods used to measure the surface absorptance of a material vary in test configuration and application. Love (78) has discussed several methods which are applicable to this study. In all cases, however, the surface reflectance was obtained by a combination of measurement and calculation and the absorptance coefficient determined mathematically. (This absorptance determination will be discussed in a later section.)

TABLE D-1

AVERAGE ABSORPTANCE FOR SEVERAL RADIATION SOURCES

Material	Radiation Source Blackbody Temperature, °K						Heat Sources	
	1000	1500	2000	2500	3000	3500	Flames	Solar
Gum Rubber	0.88	0.82	0.76	0.72	0.69	0.68	0.89	0.69
Cork Gasket Material	0.70	0.59	0.50	0.45	0.43	0.44	0.67	0.35
Neoprene Rubber, Solid	0.91	0.92	0.93	0.93	0.93	0.93	0.91	0.94
Chloroprene DC-100 Gasket	0.72	0.63	0.55	0.52	0.51	0.52	0.71	0.62
Formica	0.91	0.88	0.85	0.82	0.80	0.79	0.91	0.80
Polyphenylene Oxide (PPO)	0.86	0.78	0.70	0.63	0.57	0.53	0.88	0.48
Kydex, Red, Cast	0.91	0.90	0.89	0.88	0.87	0.86	0.92	0.86
Kydex, Gray, Rolled	0.88	0.87	0.86	0.85	0.84	0.83	0.88	0.81
Texin	0.92	0.89	0.83	0.77	0.72	0.68	0.93	0.62
Delrin	0.92	0.86	0.78	0.71	0.64	0.59	0.93	0.48
Hi-Impact White Styrene	0.86	0.75	0.63	0.53	0.45	0.40	0.88	0.29
Plexiglas, White	0.91	0.86	0.78	0.70	0.62	0.56	0.92	0.42
Plexiglas, Black	0.94	0.94	0.95	0.95	0.95	0.95	0.94	0.96
Plexiglas, Clear	0.85	0.69	0.54	0.41	0.31	0.25	0.89	0.097
Lexan, Rough Surface	0.87	0.83	0.78	0.75	0.72	0.71	0.88	0.69
Polypropylene	0.87	0.83	0.78	0.74	0.70	0.68	0.86	0.62
Polyethylene, Low Density	0.92	0.88	0.82	0.77	0.72	0.68	0.93	0.57
Polyvinyl Chloride, Gray	0.90	0.90	0.89	0.89	0.89	0.89	0.91	0.89
Polyvinyl Chloride, Clear 0.33 cm	0.81	0.65	0.49	0.38	0.30	0.24	0.85	0.15
Silicone Rubber	0.79	0.66	0.58	0.54	0.52	0.53	0.79	0.62
Buna-N Rubber	0.92	0.93	0.93	0.93	0.93	0.93	0.92	0.94

TABLE D-1--Continued.

Material	Radiation Source Blackbody Temperature, °K						Heat Sources	
	1000	1500	2000	2500	3000	3500	Flames	Solar
Butyl IIR Rubber	0.92	0.93	0.94	0.94	0.95	0.95	0.92	0.95
Nylon 6/6	0.93	0.90	0.86	0.82	0.75	0.71	0.93	0.62
Polystyrene, Clear (Styrolux)	0.75	0.60	0.46	0.35	0.28	0.22	0.78	0.095
Butyrate (Uvex)-Cellulose Acetate Butyrate	0.84	0.71	0.56	0.43	0.34	0.27	0.88	0.12
Cycolac	0.91	0.86	0.77	0.71	0.65	0.61	0.92	0.55
Phenolic-Bakelite	0.90	0.86	0.81	0.77	0.75	0.75	0.91	0.78
Cork	0.64	0.56	0.49	0.46	0.44	0.44	0.60	0.52
ACCOPAC Gasket CS-301	0.71	0.63	0.60	0.60	0.62	0.65	0.69	0.74
ACCOPAC Gasket CN-705	0.57	0.51	0.47	0.46	0.47	0.50	0.60	0.62
ACCOPAC Gasket AS-428	0.92	0.92	0.92	0.92	0.92	0.92	0.91	0.92

Method I. Hemispherical Reflectometer

This method uses a hemispherical first surface mirror that contains a small aperture allowing an incident beam of radiation to impinge on a sample. The reflected energy from the sample strikes the mirror surface and is reflected back onto a detector. Figure D-4 illustrates this method.

The theoretical aspects of this method are the following (11): Assume the radiant energy, J, arriving at the detector when the test surface, s, is illuminated by radiation, I_o, can be defined as

$$J\ (s1) = I_o r_s r_m C_s + \varepsilon_s r_m C_s + \varepsilon_t C_s^2 r_m^2 r_s' \qquad (D\text{-}10)$$

where $I_o r_s r_m C_s$ = incident energy reflected off the test surface corrected for the reflectivity of the mirror surface and loss through the aperture

$\varepsilon_s r_m C_s$ = energy emitted by the test surface

$\varepsilon_t C_s^2 r_m^2 r_s'$ = energy originating at the detector itself which arrives back on the detector after reflection from the test surface

J = energy at detector

I_o = incident energy

r_s = reflectance of surface

r_m = reflectance of mirror

C_s = coefficient of directional reflection characteristics of test sample

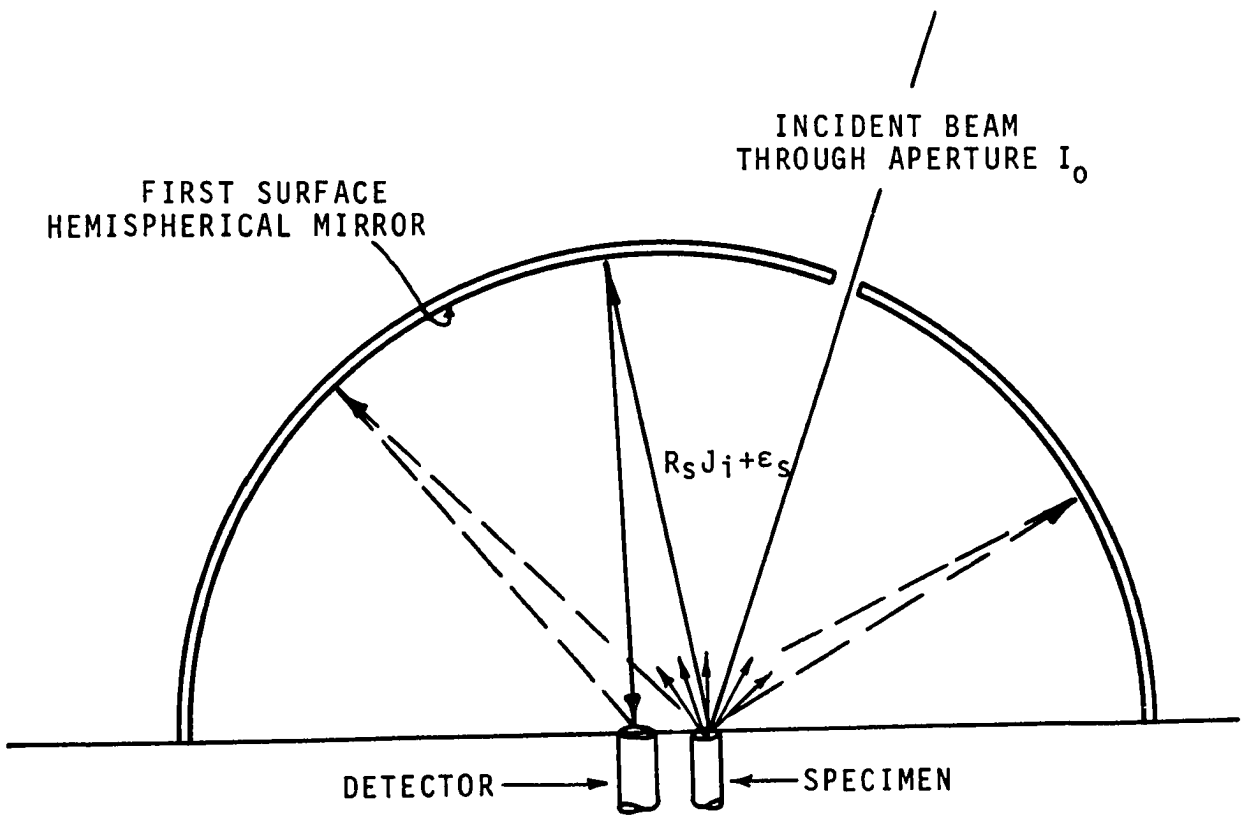

Figure D-4. Hemispherical Reflectometer.

ε_s = surface emittance

ε_t = emittance of detector

r_s' = second reflectance from the test surface

If the aperture is closed to external radiation where $I_o = 0$, then the energy arriving at the detector is

$$J\ (s2) = \varepsilon_s r_m C_s + \varepsilon_t C_s^2 r_m^2 r_s' \qquad \text{(D-11)}$$

Solving both Equations D-10 and D-11 for r_s,

$$r_s = \frac{J\ (s1) - J\ (s2)}{I_o r_m C_s} \qquad \text{(D-12)}$$

The same analysis can be performed for a reference surface, r_r, which gives

$$r_r = \frac{J\ (r1) - J\ (r2)}{I_o r_m C_s} \qquad \text{(D-13)}$$

Combining Equations D-12 and D-13, the reflectance of the test surface becomes

$$r_s = r_r \frac{C_r}{C_s} \left(\frac{J\ (s1) - J\ (s2)}{J\ (r1) - J\ (r2)} \right) \qquad \text{(D-14)}$$

If the reference material is chosen to have directional reflectance characteristics similar to the sample where $C_r \simeq C_s$, then

$$r_s = r_r \left(\frac{J\ (s1) - J\ (s2)}{J\ (r1) - J\ (r2)} \right) \qquad \text{(D-15)}$$

Equation D-15 can be transformed into terms of the spectral reflectance of a material as

$$r_\lambda = \frac{(r_s)_\lambda}{(r_r)_\lambda} \tag{D-16}$$

and finally

$$r_\lambda = \frac{[J\ (s1) - J\ (s2)]_\lambda}{[J\ (r1) - J\ (r2)]_\lambda} \tag{D-17}$$

The data obtained from this system reduces to a relationship in terms of absorptance, i.e.,

$$\alpha_\lambda = 1 - r_\lambda \tag{D-5}$$

where α_λ is the monochromatic absorptance of the specimen at wavelength λ.

Method II. Integrating-Hemisphere Reflectometer

In this technique, the hemisphere of Method I is used, but with a second aperture. Here, the incident beam is projected through one aperture upon a diffuser which in turn reflects the radiation back to the first surface hemispherical mirror. The diffuse radiation from the mirror is projected onto the specimen surface and this latter radiation from the sample surface is monitored by a detector. Figure D-5 is an illustration of Method II.

In this method, the absorptance of the specimen is obtained in a similar manner to that of Method I where again

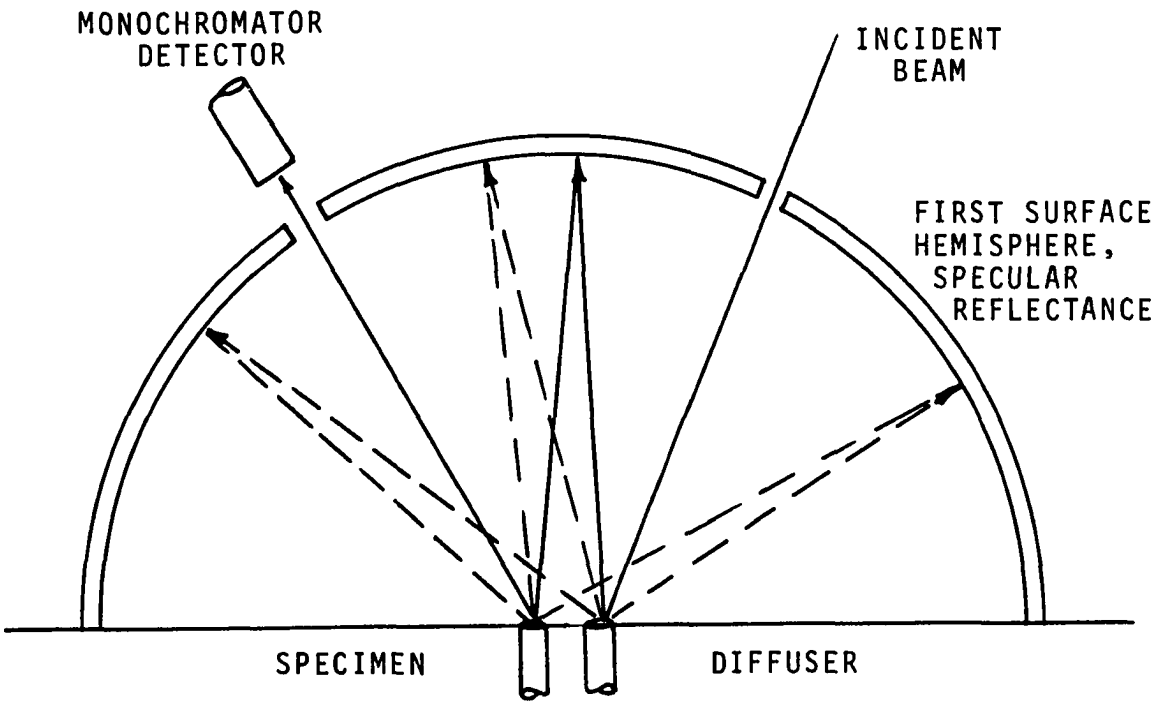

Figure D-5. Integrating Hemisphere Reflectometer Absorptance.

$$\alpha_\lambda = 1 - r_\lambda \qquad \text{(D-5)}$$

Both Methods I and II have errors introduced because the specimen and detector or specimen and diffuser are displaced from the focus of the mirror. Further, both systems require a standard surface which is used both as a calibration and as a reference for actual measurement.

Method III. Integrating-Sphere Reflectometer

One of the most widely used techniques for the acquisition of reflectance data is the integrating sphere. Here a hollow sphere is used that contains three openings, one for the admission of the radiant energy, a second for the monitoring by the radiation detector and the third for the specimen mounting. The interior of the sphere is coated with a thick layer of a highly reflective, diffuse coating, usually magnesium oxide. In use, a beam of energy is projected upon the specimen which in turn reflects the impinging radiation back to the sphere. The detector monitors the amount of radiation received from spherical walls. Figure D-6 illustrates Method III.

Birkebak (11) has shown that the measurement of "absolute" reflectance can be accomplished if any specular reflection from a sample is first intercepted and reradiated back into the spherical cavity as shown in Figure D-6. The detector response, V_s, is, if one assumes uniform irradiance on the spherical wall,

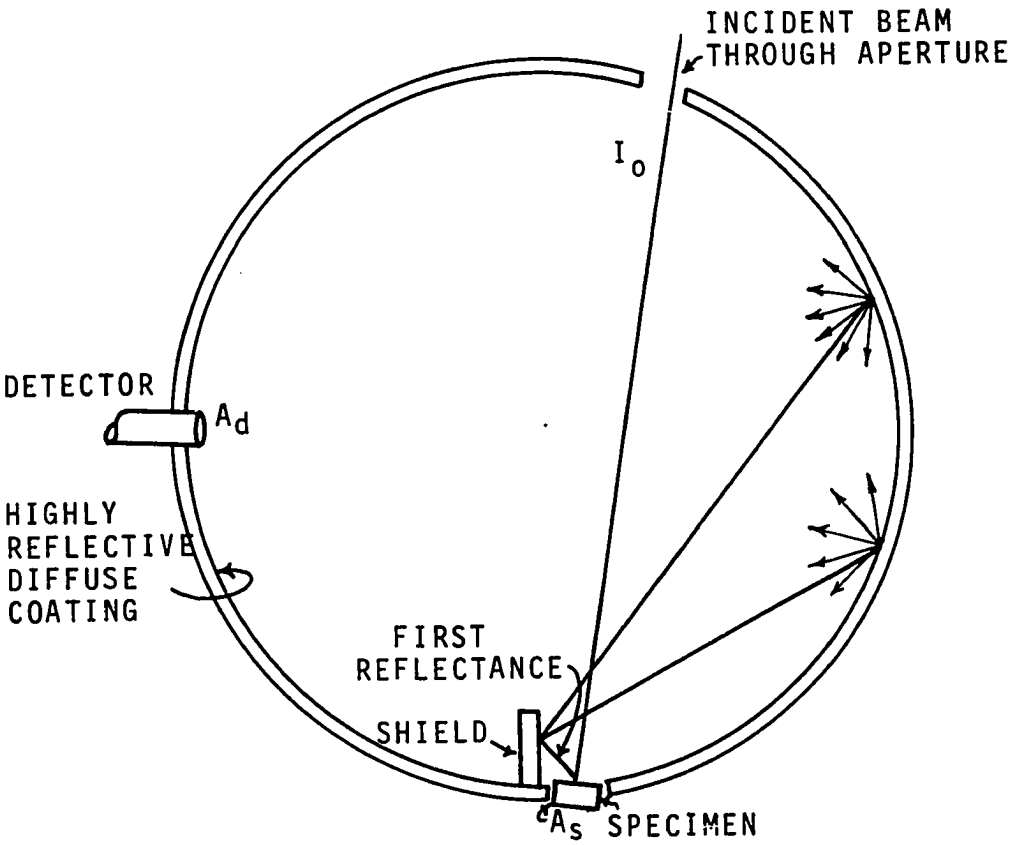

Figure D-6. Integrating-sphere Reflectometer.

$$V_s = \frac{KA_d I_o r_s}{A} \cdot \frac{r_w}{1-r_w} \qquad \text{(D-18)}$$

where V_s = detected irradiance from sample

K = system constant

A_d = area of detector

A = area of sphere

I_o = irradiant energy input

r_s = sample reflectance

r_w = wall reflectance

If the source collimating tube or projector is adjusted so that the spherical wall is illuminated, then the first reflection from the wall can be detected. The detector response from the wall energy, V_w, is

$$V_w = \frac{KA_d I_o r_w}{A} \cdot \frac{1}{1-r_w} \qquad \text{(D-19)}$$

If Equations D-18 and D-19 are solved for r_s, there is obtained

$$r_s = \frac{V_s}{V_w} \qquad \text{(D-20)}$$

where the spectral reflectance is desired

$$r_\lambda = (r_s)_\lambda \qquad \text{(D-21)}$$

Model III yields information which permits calculation of the absorptance, i.e.,

$$\alpha_\lambda = 1 - r_\lambda \qquad \text{(D-5)}$$

As before, this method can also utilize a standard surface for calibration and reference.

There are several inherent inaccuracies to this third method of reflectance measurement: (1) loss of energy from the multiple openings in the sphere, (2) degradation of the internal surface coating of the sphere, and (3) lack of an absolutely diffuse internal coating.

One other problem that is a concern in any reflectivity study regardless of test method, is the measurement of the radiative energy itself. However, the problems inherent in radiation detection are not a part of this study. Information on detection methods and devices can be found in the publications by Kingslake (63, 64, 65).

Reflectance and Transmittance Measurement Apparatus

The writer is indebted to General Dynamics Convair (GDC), San Diego, California, for the use of their reflectance apparatus to obtain the necessary data for computing the plastic and rubber absorptances.

The measurement of directional reflectance in the wavelength region of 0.3 to 2.1 microns was made with a Cary Model 14 spectrophotometer with an integrating sphere

attachment. Figure D-7 is a photograph of the test apparatus. The Cary Model 14 is a double beam instrument with automatic scan and a readout which is linear with wavelength. The monochromator contains a grating in series with a fused silica prism. The detectors are a photo tube in the range from 0.3 to 0.6 microns and a PbS cell from 0.6 to 2.1 microns. The integrating sphere consists of a 7-inch diameter sphere coated on the inside with a thick layer of MgO. The sample, located at the center of the sphere, is uniformly illuminated by a tungsten source. One beam of the Cary spectrophotometer originates from the sample and the other beam originates from the MgO wall. The ratio of these two beams is the reflectance of the sample and is displayed by the recorder as a function of wavelength. The system is capable of making measurements from normal to 85 degrees.

Measurement of transmittance is made using the Cary Model 14 spectrophotometer in the range of 0.3 to 2.6 microns and a Beckman IR-4 spectrophotometer in the range 1.0 to 7.0 microns. Figure D-8 is an illustration of the Cary Model 14 spectrophotometer in the transmittance testing configuration. The Beckman IR-4 unit differs by the use of a globar element to provide the longer wavelength energy necessary for transmittance measurements up to 16.0 microns.

The measurement of reflectance above 2.1 microns requires the use of additional specialized equipment. The reflectance in the range of 2.0 to 7.0 microns is obtained

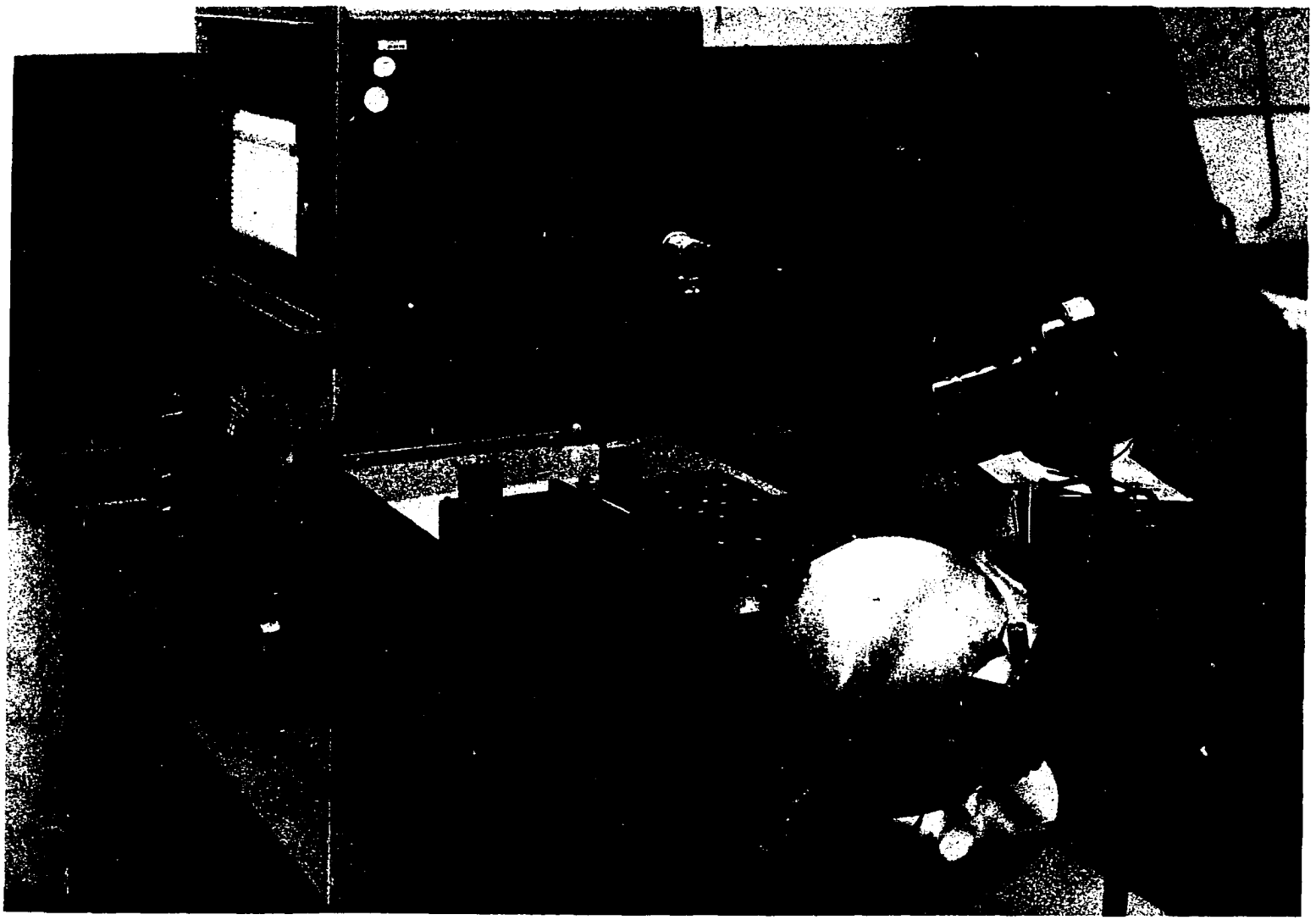

Figure D-7. Cary Model 14 Spectrophotometer and Attached Integrating Sphere.

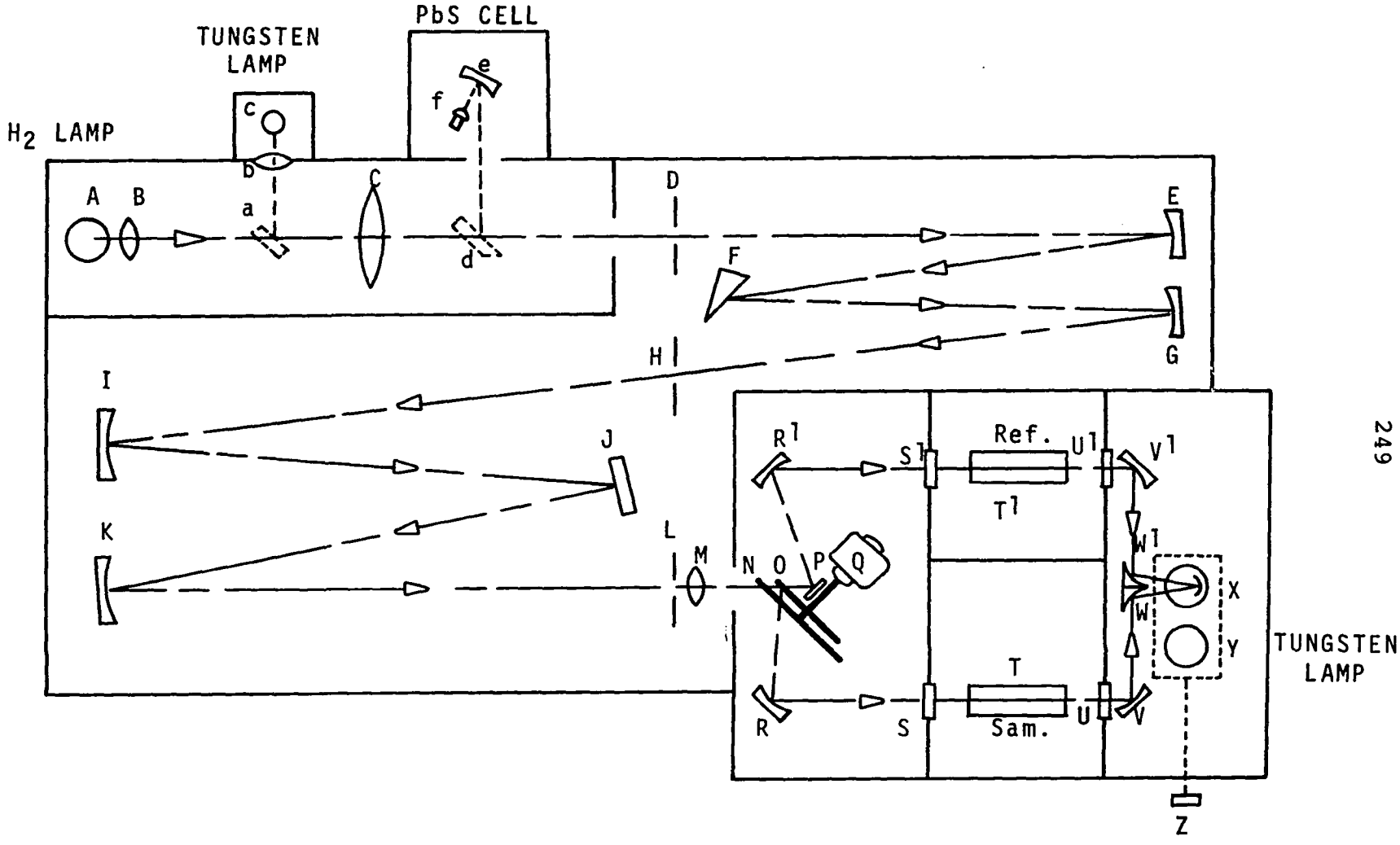

Figure D-8. Optical System Cary Model 14 Spectrophotometer.

through the use of a Gier-Dunkle infrared reflectivity Hohlraum in conjunction with a Perkin-Elmer Model 99 double beam spectrometer and associated optics. Figure D-9 is a photo of the total system while Figure D-10 is an illustration of the optical path. The basic experimental apparatus consists of a source unit, light collection system, a chopper, a monochrometer and a detector. The unit works on the single beam principal, wherein light from the sample surface is collected, chopped, passed through a monochrometer and displayed on the detector. The magnitude of the light intensity from the sample surface is recorded as a function of wavelength. The output can also be displayed on a digital voltmeter. The reflectance of a material is obtained by use of the ratio of the reflectance of the sample to the reflectance of gold at the same wavelength. A thermocouple detector is used throughout the Hohlraum system testing to monitor the Hohlraum cavity temperature, which is maintained at 370°C.

Experimental Procedure

The measurement of spectral reflectance using the Cary instrument and modified spherical cavity was performed in a different manner from that of a regular integrating-sphere reflectometer, previously illustrated by Figure D-3. The Convair integrating sphere is designed so that the incident energy is projected onto a diffuse, highly reflective target which then re-radiates to the cavity walls and onto

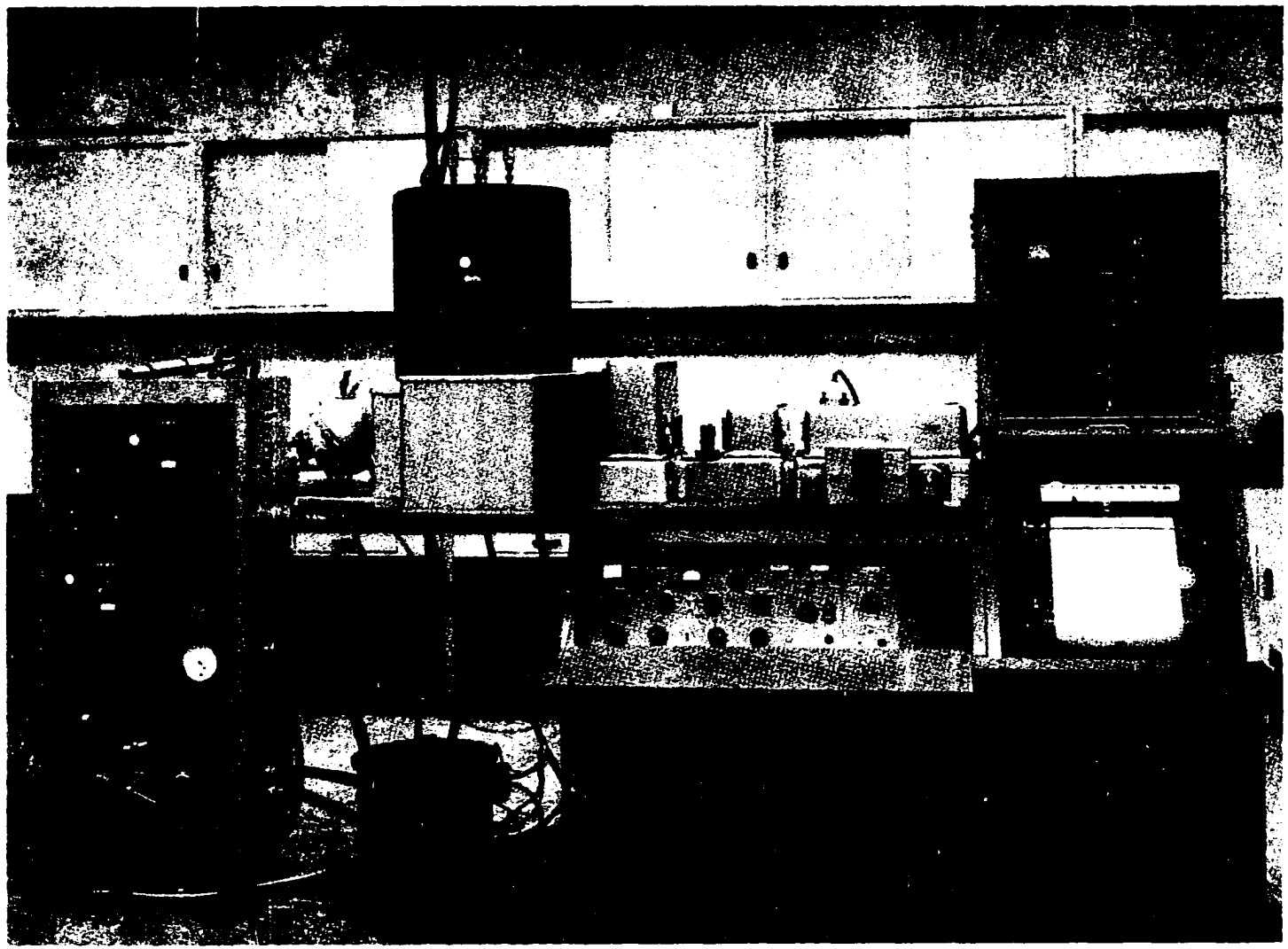

Figure D-9. Reflectivity Apparatus.

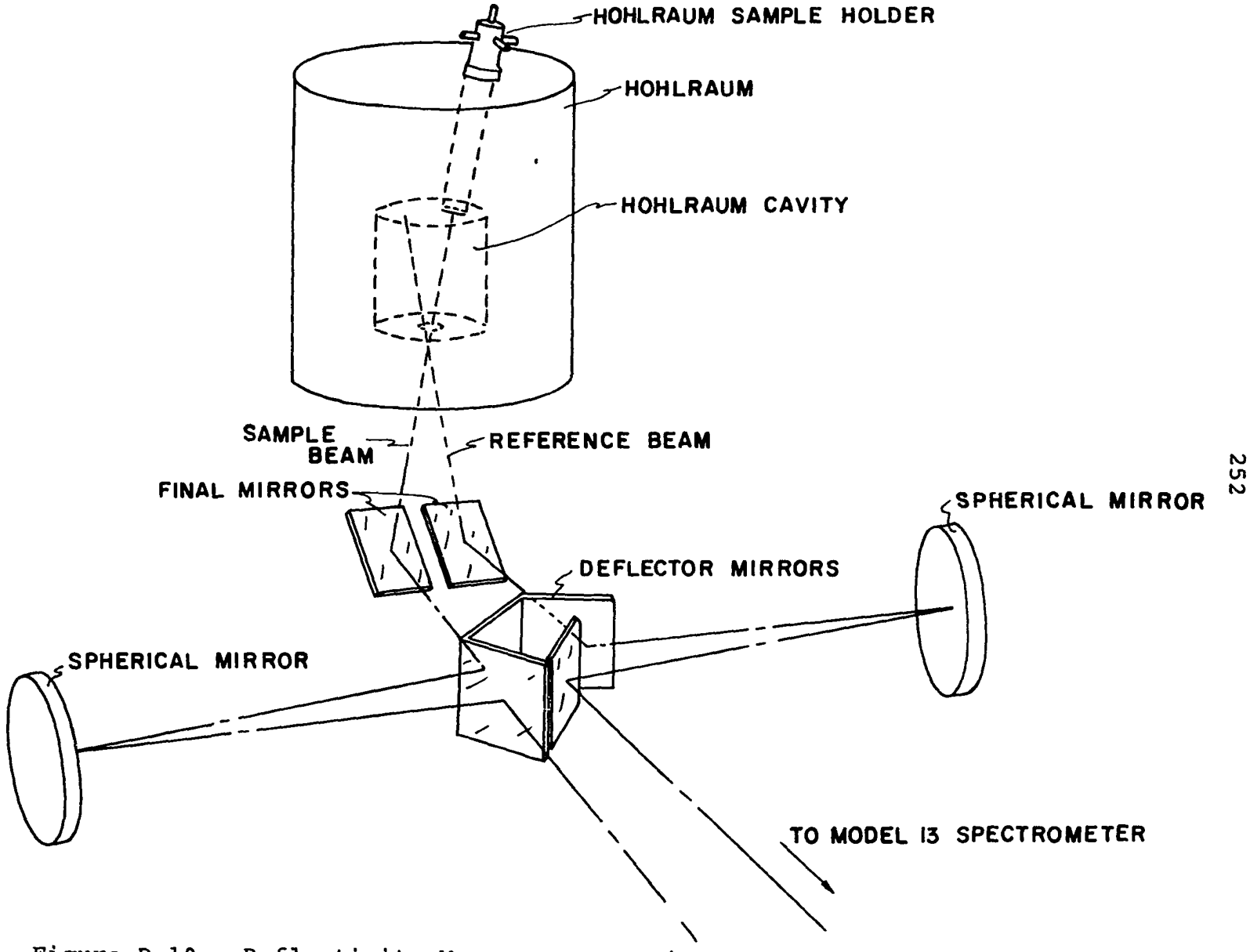

Figure D-10. Reflectivity Measurement Optical Path to Spectrometer.

the sample. Figure D-11 diagrams this test method. The sphere is divided into two halves with a latch closure and swing hinge. The sample, of 1 inch diameter or 1 inch square, 1/8 inch thick, is attached to the holder by means of a magnetic clasp.

To measure the reflectance of a material, the sample is inserted into the sphere and the sphere closed. The sample holder is set at the desired viewing angle and the energy source activated. The Cary spectrophotometer is then initiated to view the specimen automatically over the desired wavelength and the recorder automatically prints the relative spectral reflectance. After a test the sample is removed and a new test started.

The mathematical basis for the GDC type reflectometer system is the following: Using the MgO surface of the sphere as the reference standard, it can be seen that the detector does not see the first reflectance of the incident radiation into the cavity, so that $V_1 = 0$, where V is the detected energy and the 1 designates the first reflection. The radiation striking the detector from the second reflection, i.e., radiation reflected from the target holder to the wall and then to the detector is

$$dV_2 = r^2 w I_o \frac{d\Lambda_w}{A} \frac{A_d}{A} \qquad \text{(D-22)}$$

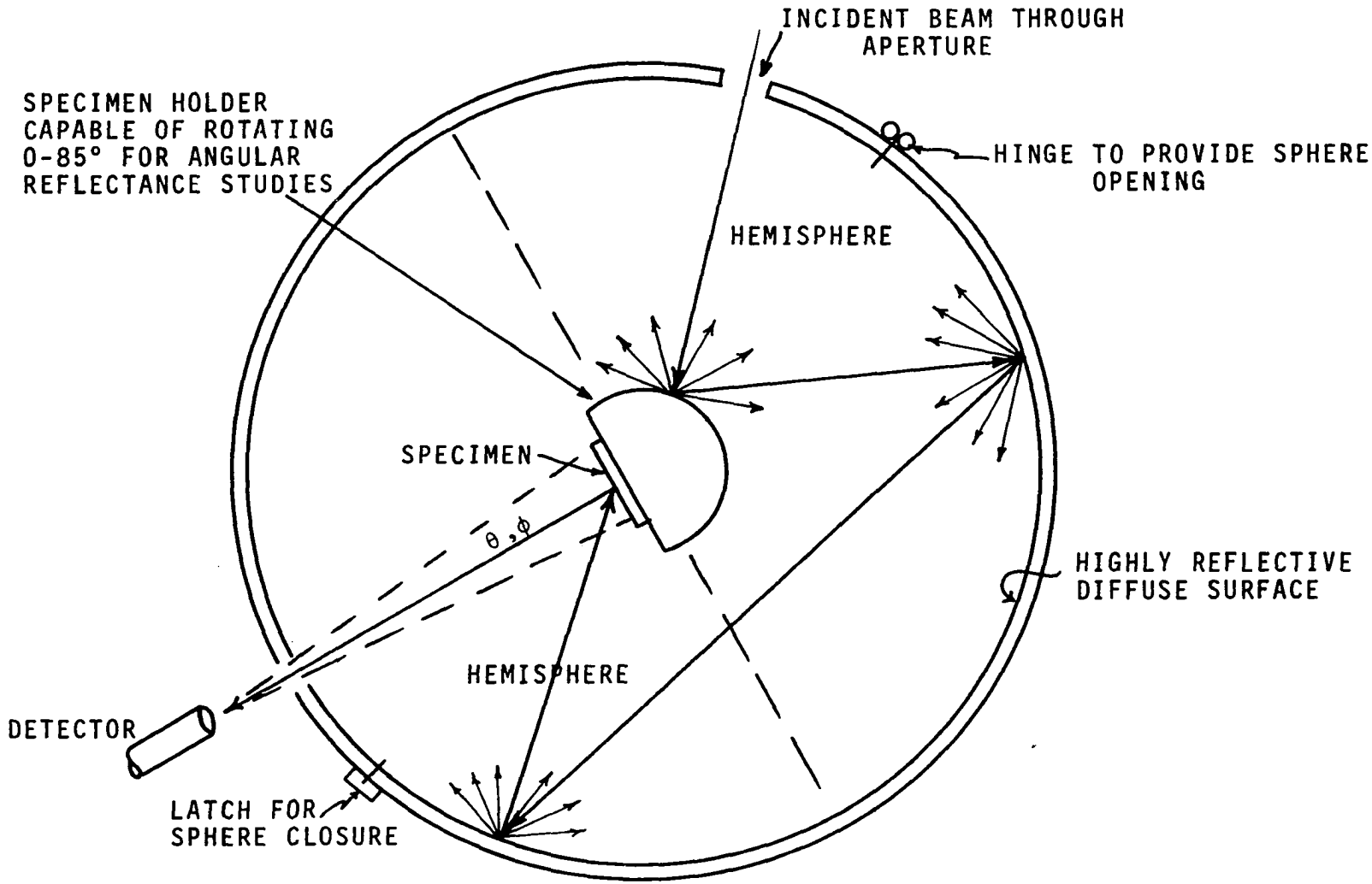

Figure D-11. Modified GDC Integrating-Sphere Reflectometer.

for each unit area dA_w. Summing over all the unit areas the detector response is

$$V_2 = Kr_w^2 I_o\left(\frac{A_d}{A}\right) \tag{D-23}$$

The detector response for the third reflection is

$$V_3 = Kr_w^2 r_w I_o\left(\frac{A_d}{A}\right) \tag{D-24}$$

The total detector response for all reflections for the reference standard is

$$V_{st} = \sum_{i=1}^{\infty} V_i = K \frac{I_o A_d}{A} (0 + r_w^2 + r_w^3 + \ldots + r_w^{n-2}) \tag{D-25}$$

where V_{st} is the total energy detected from the reference surface. The closed form of Equation D-25 is

$$V_{st} = K \frac{I_o A_d}{A} \left(\frac{r_w^2}{1 - r_w}\right) \tag{D-26}$$

When a specimen is placed in the cavity and is illuminated by the input radiated energy, the detector does not see the first or second reflections, with $V_{s1} = V_{s2} = 0$, but sees the third reflection and on. Performing the same analysis as with the standard surface, the radiation striking the detector from the third reflection, i.e., the incident energy is reflected from the target holder to the wall and thence to the sample and then to the detector, gives

$$V_{s3} = r_w^2 r_s I_o \left(\frac{A_d}{A} \right) \qquad \text{(D-27)}$$

For the fourth reflection to the detector

$$V_{s4} = r_w^3 r_s I_o \left(\frac{A_d}{A} \right) \qquad \text{(D-28)}$$

The total detector response in closed form for the test specimen is

$$V_s = \frac{K r_s I_o A_d}{A} \left(\frac{r_w^2}{1 - r_w} \right) \qquad \text{(D-29)}$$

The ratio of sample to standard gives the reflectance of the sample and is

$$r_s = \frac{V_s}{V_{st}} \qquad \text{(D-30)}$$

The measurement of spectral reflectance of polymers above 2.0 μ required the use of the Hohlraum system and the included optics and detector. To insure system stability the cavity heaters should be turned on 24 hours prior to the scheduled test period, and the cavity wall thermocouple monitored for the approach to a stable temperature. Equilibrium conditions between the water-cooled sample holder and cavity is maintained by using a blank specimen in the holder, turning on the cooling water and placing the holder assembly in the receptacle in the cavity. At the beginning of the test day, the cavity temperature is again checked for proper

setting and the detector system activated. It was found that the detector system and readout device required a minimum time of one hour for proper warmup to attain stable operation. After system warmup and stability, the specimen holder is removed from the Hohlraum and the blank disk replaced by a first surface gold mirror, then the assembly is replaced into the Hohlraum. When the readout device indicates a stable condition in the cavity, a calibration is performed for the individual wavelength settings in the same manner as for a test specimen, i.e., viewing the cavity wall, rotating the Hohlraum drum to the specimen viewing position, noting the value of the readout and rotating the drum back to the first position. If the readout device indicates the same reading as before drum movement, the system is stable. If not, the test is performed again until before and after readings are equal.

During actual polymer testing, a sample one inch in diameter and 0.050 inch thickness is placed in the specimen holder assembly, Figure D-12, placed in the Hohlraum cavity and the system is permitted to attain equilibrium. As before, the cavity wall is viewed, the drum rotated to view the sample, then the drum rotated back to the first position.

To obtain the relative reflectance of the specimen, one uses the ratio of the specimen energy detection to the detection of energy from the gold surface at the same temperature and wavelength. (The data from the gold must be

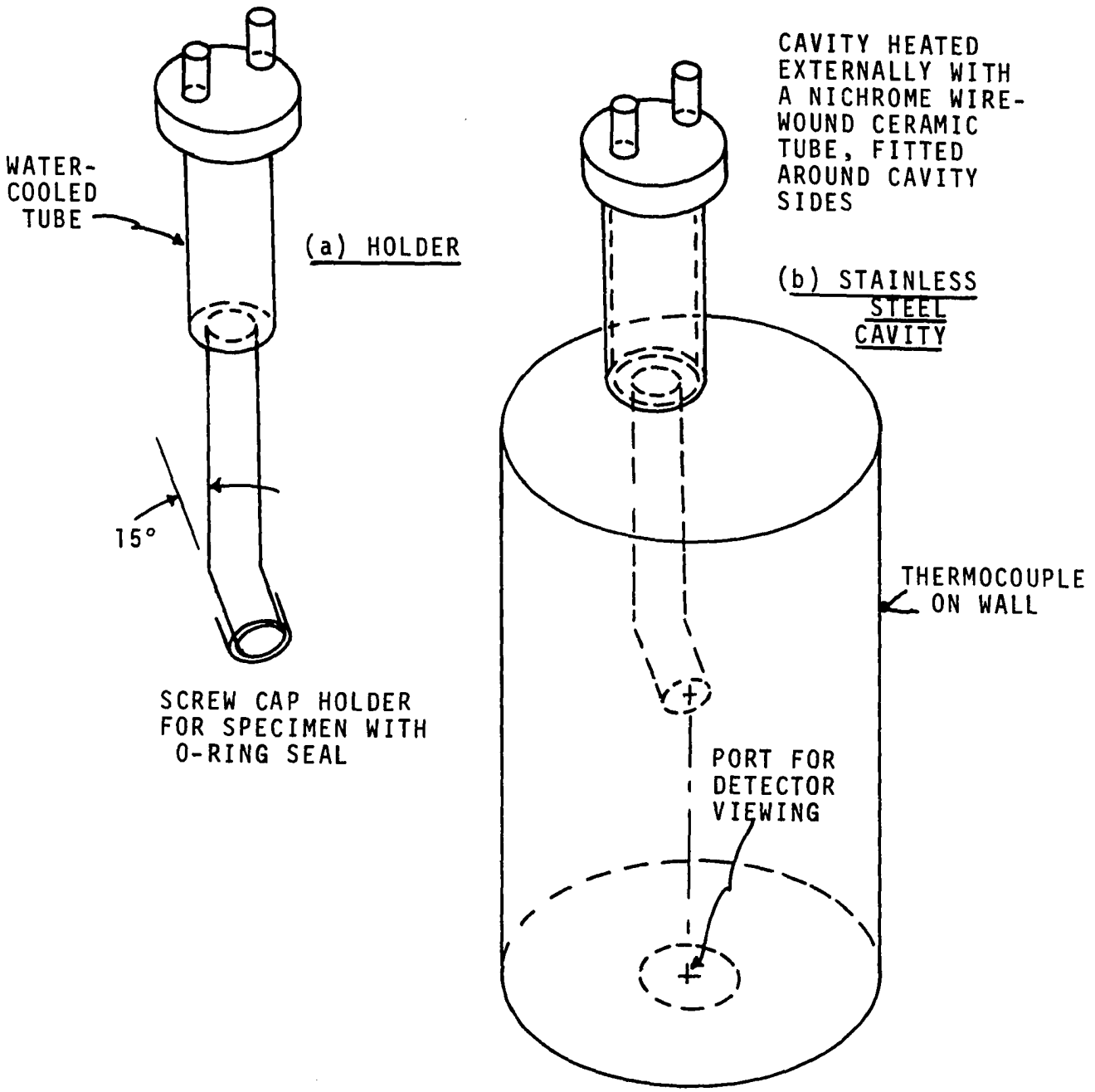

Figure D-12. Sketch of Specimen Holder and Hohlraum Cavity.

corrected to standard spectral values.) This ratio can be expressed mathematically (11) in terms of measured reflectance as

$$r_{sm}(\theta) = \frac{V_s}{V_{st}} \qquad \text{(D-31)}$$

where $r_{sm}(\theta)$ = measured reflectance at some standard angular displacement from normal

V_s = energy detected from the sample

V_{st} = energy detected from the gold surface reference

From the general reflectance relationship, the spectral absorptance can be calculated by means of Equation D-5, i.e.,

$$\alpha_\lambda = 1 - r_\lambda \qquad \text{(D-5)}$$

Discussion of Test Results

In using the Cary reflectance testing system, as illustrated in Figures D-7 and D-11, it must be noted that there are several problems inherent in the measurements and test procedure. There is an assumed constant energy leakage from the sphere due to the two apertures for energy input and monitoring, and another energy leakage from the imperfect closure of the two hemispheres. The MgO coating on the inside of the sphere is very fragile and flakes off around the hemispherical closures and also flakes off the sample holder. Any

touching of the MgO surface causes a pit or crack and this irregularity will degrade the surface reflection at that point. One major concern is the measurement of the sample reflectance. Unlike the integrating-sphere of Figure D-6, the GDC system measures the pre-diffused radiation as reflected from the specimen surface. This difference in energy reflection may affect any reflectance measurements that are made with the sample off the normal angle to the detector. However, since a reflectance measurement system of Figure D-6 was not available for test comparison, the writer could not perform further study in this area.

The investigations of polymer transmittance using both the Cary and Beckman IR-4 equipment were performed in the same manner. The samples were inserted into the specimen holder (see Figure D-8) and the unit activated. Both test systems gave a printout of specular transmittance over the desired wavelength. No problems were encountered in either of the systems.

The measurement of reflectance in the Hohlraum gave some problems, particularly because the 370°C cavity and 18°C water coolant temperatures caused some specimens to bow outward slightly in the holder and not present a flat surface for the reflectance studies. Some of the samples apparently had some surface degradation because the gold first surface mirrors became contaminated during recalibrations. The procedure required lengthy testing time since the Hohlraum must

be rotated back and forth for each specific monochromatic setting. If the reading of the detector-output did not agree before and after each Hohlraum rotation, the system was not in equilibrium and the test had to be repeated. Unlike the Cary, the Perkin-Elmer spectrophotometer was operated at discrete wavelengths, which gave a monochromatic reflectance at specific points. Since no other test equipment was available, there was no capability of determining reflectance at other wavelengths and it was necessary to assume a linear change between the acquired data points. One problem that is connected with the high cavity temperature is the magnitude of the specimen surface temperature. Since there is no way of measuring the specimen surface temperature without disturbing the reflectance measurements, it was assumed that there was little or no effect on the surface reflectance. Examination of the monochromatic absorptance diagrams, Figure D-12 and on, indicates that the closure point, at 2 microns wavelength for all samples, was well within the experimental accuracy of the equipment and that the assumption of no surface reflectance attenuation due to temperature was applicable in this study.

Calculation of Absorptance

As previously described, Equation D-9 was adapted to a digital computer using the trapezoidal rule for integration. Discrete values for the monochromatic emissive power I_λ were supplied to the computer in tabular form.

Where the tested material was transparent, Equation D-7 was first used to obtain the monochromatic absorptances by the adaptation of a special GDC computer program (42) which utilized an iterative procedure to calculate α_λ. The average absorptance of the transparent material was then obtained by the same procedure using Equation D-9.

Values of average absorptance, α_{av}, were obtained for benzene flames, blackbodies at 1000°-3500°K and solar radiation and are listed in Table D-1. Values of the average absorptances based upon the 1000 watt tungsten lamps were determined using the assumption of blackbody radiation at 2500°K.

Graphical Presentation

The test data, both as measured in the case of reflectance-absorptance information, using Equation D-5, and calculated, as illustrated by Equation D-7, are diagrammed in the included graphical presentations. The various relationships between α, τ, and λ are as follows:

A. Opaque Materials

1. Monochromatic absorptance, α_λ, as a function of wavelength, λ, from 0.3-7.0 microns.
2. Monochromatic absorptance, α_λ, as a function of wavelength, λ, for normal, and 18°, 45°, and 70° angular displacement from normal, for the wavelength span of 0.3-2.0 microns.

B. Transparent or Semi-Transparent Materials

1. Monochromatic transmittance, τ_λ, as a function of wavelength, λ, for the span 0.3-2.0 microns (Cary instrument) and the span 1.0-7.0 microns (Beckman Instrument).

2. Items (1) and (2) above.

DIAGRAMS OF SPECTRAL ABSORPTANCES

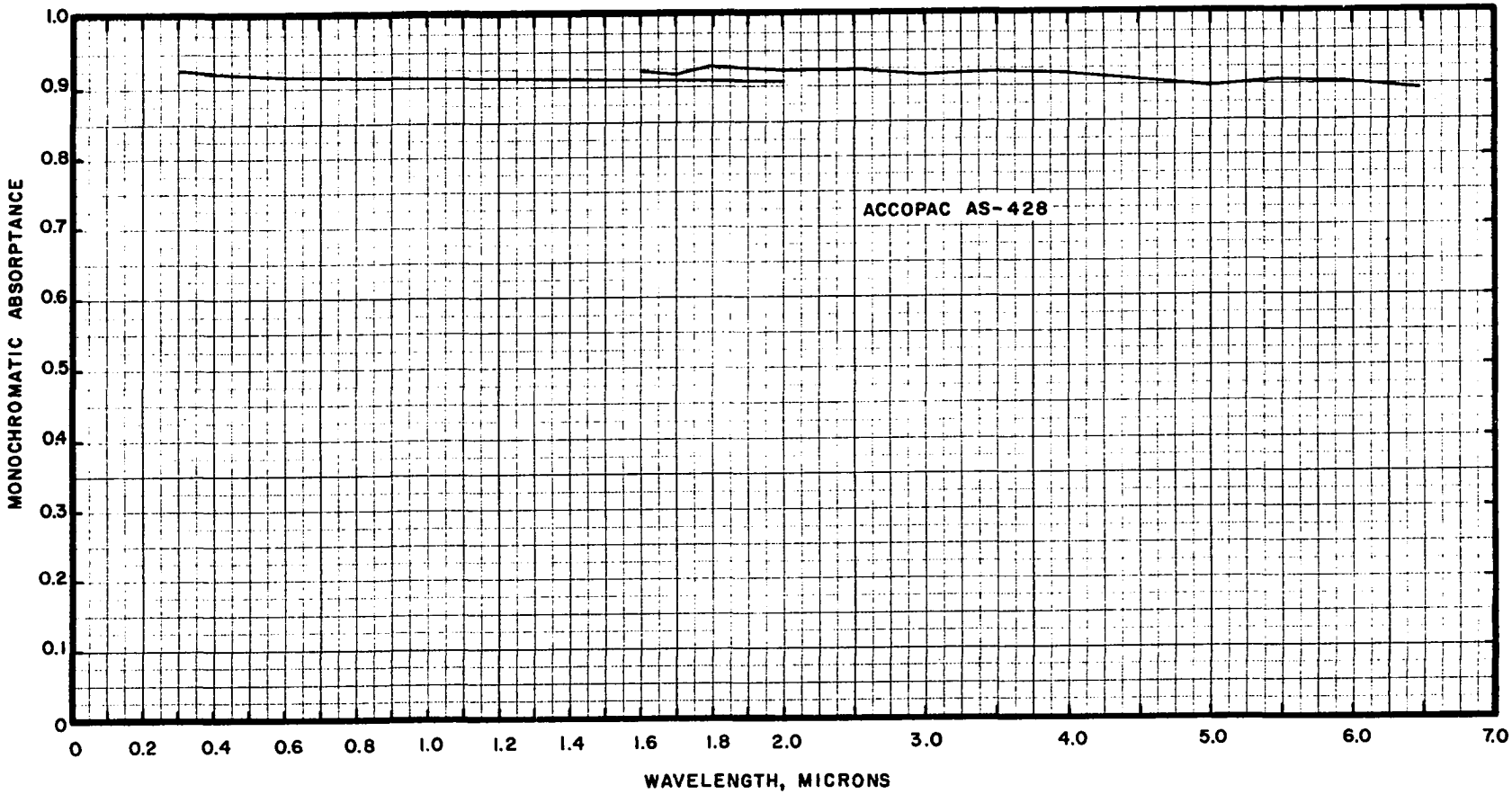

Figure D-13. Spectral Absorptance of Accopac AS-428.

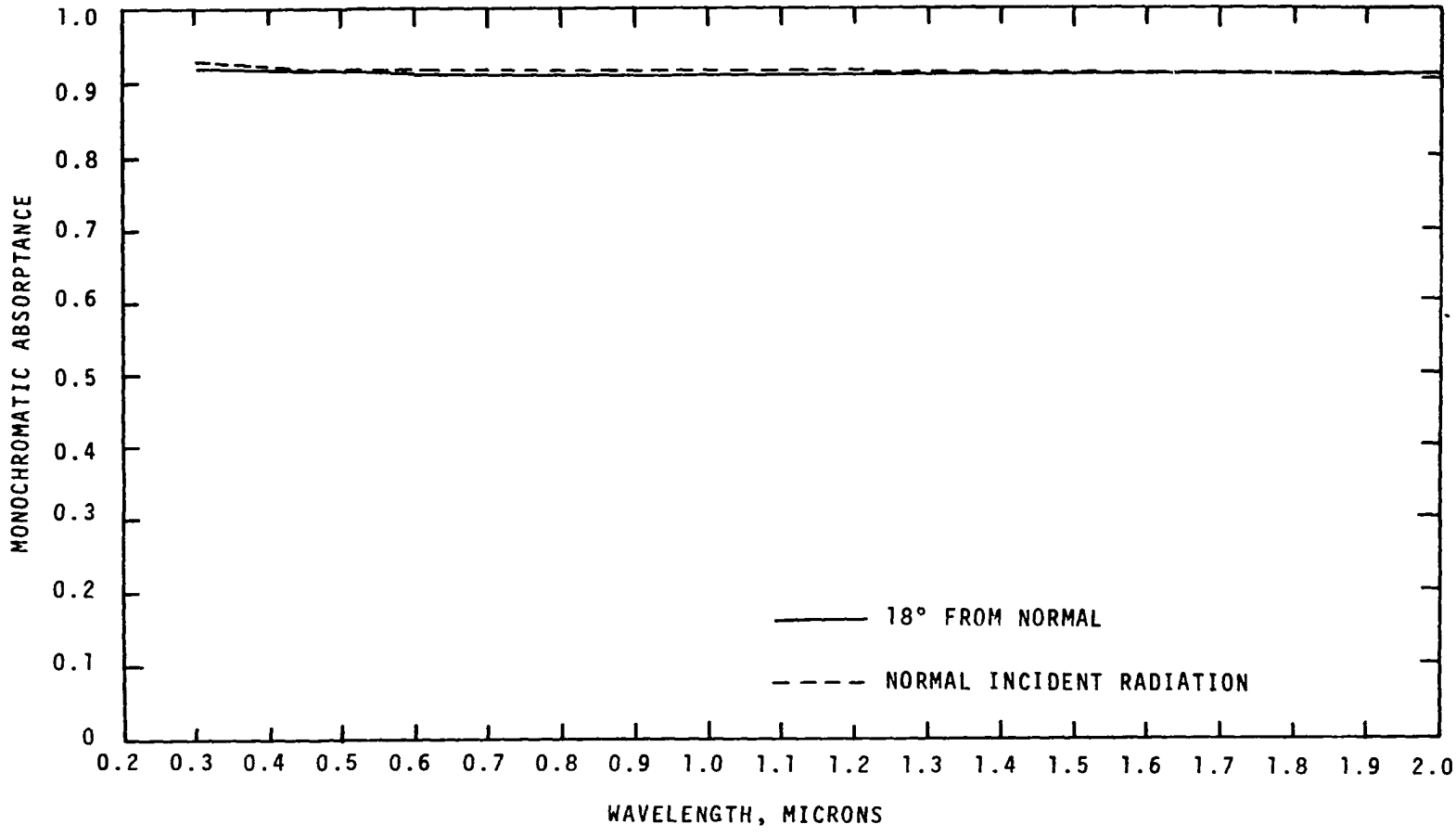

Figure D-14. Angular Variation of Absorptance of Accopac AS-428.

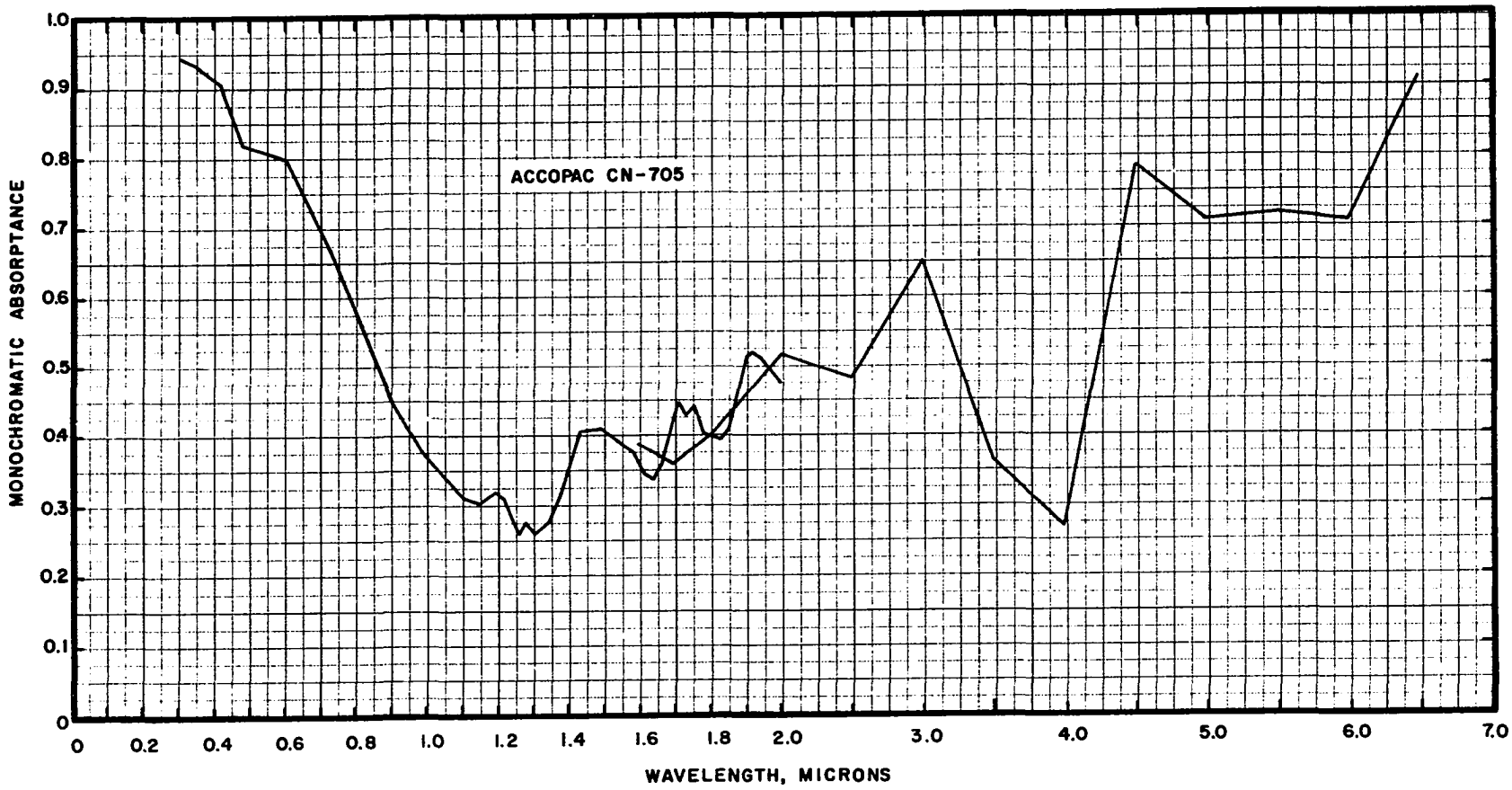

Figure D-15. Spectral Absorptance of Accopac CN-705.

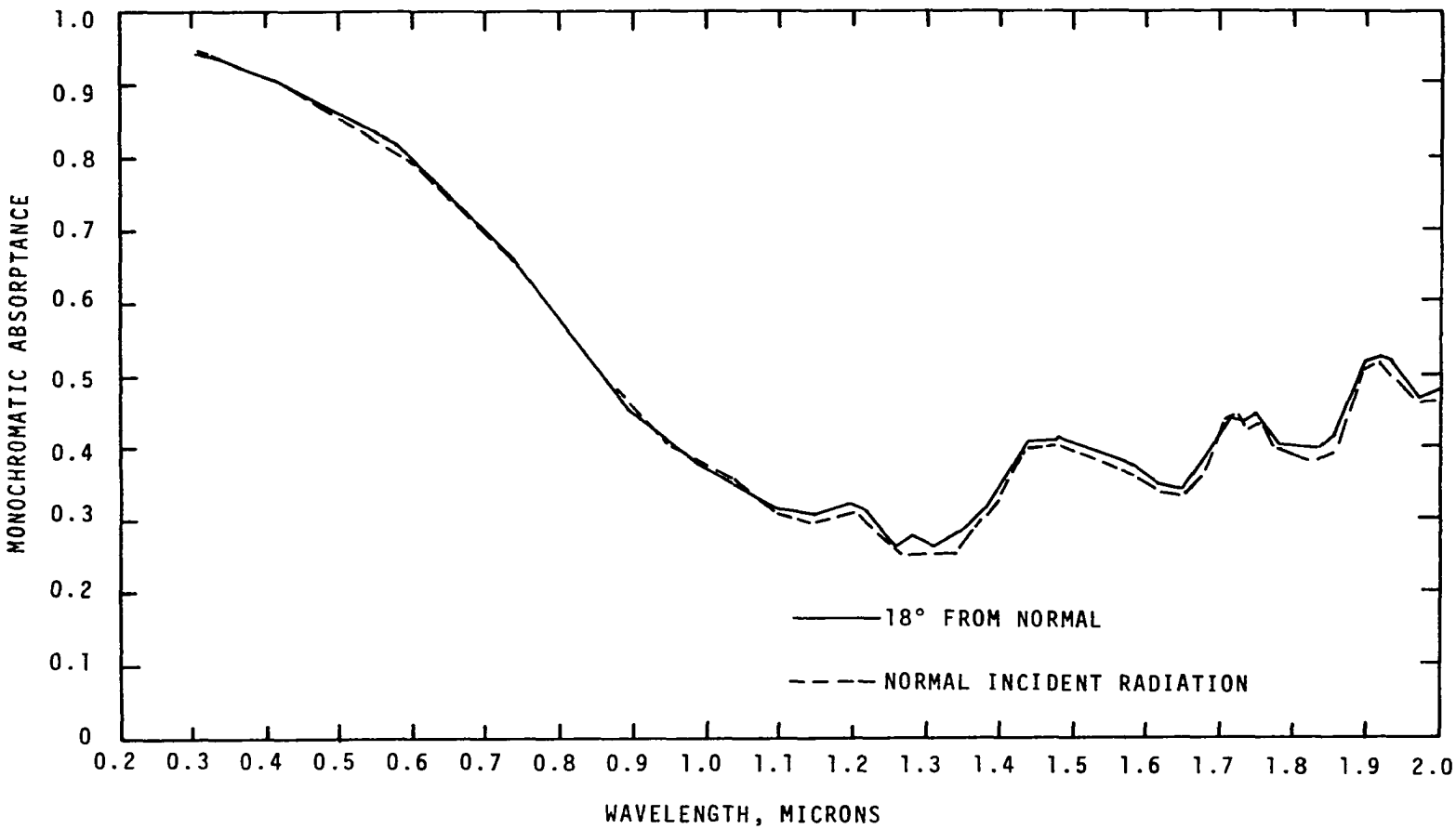

Figure D-16. Angular Variation of Absorptance of Accopac CN-705.

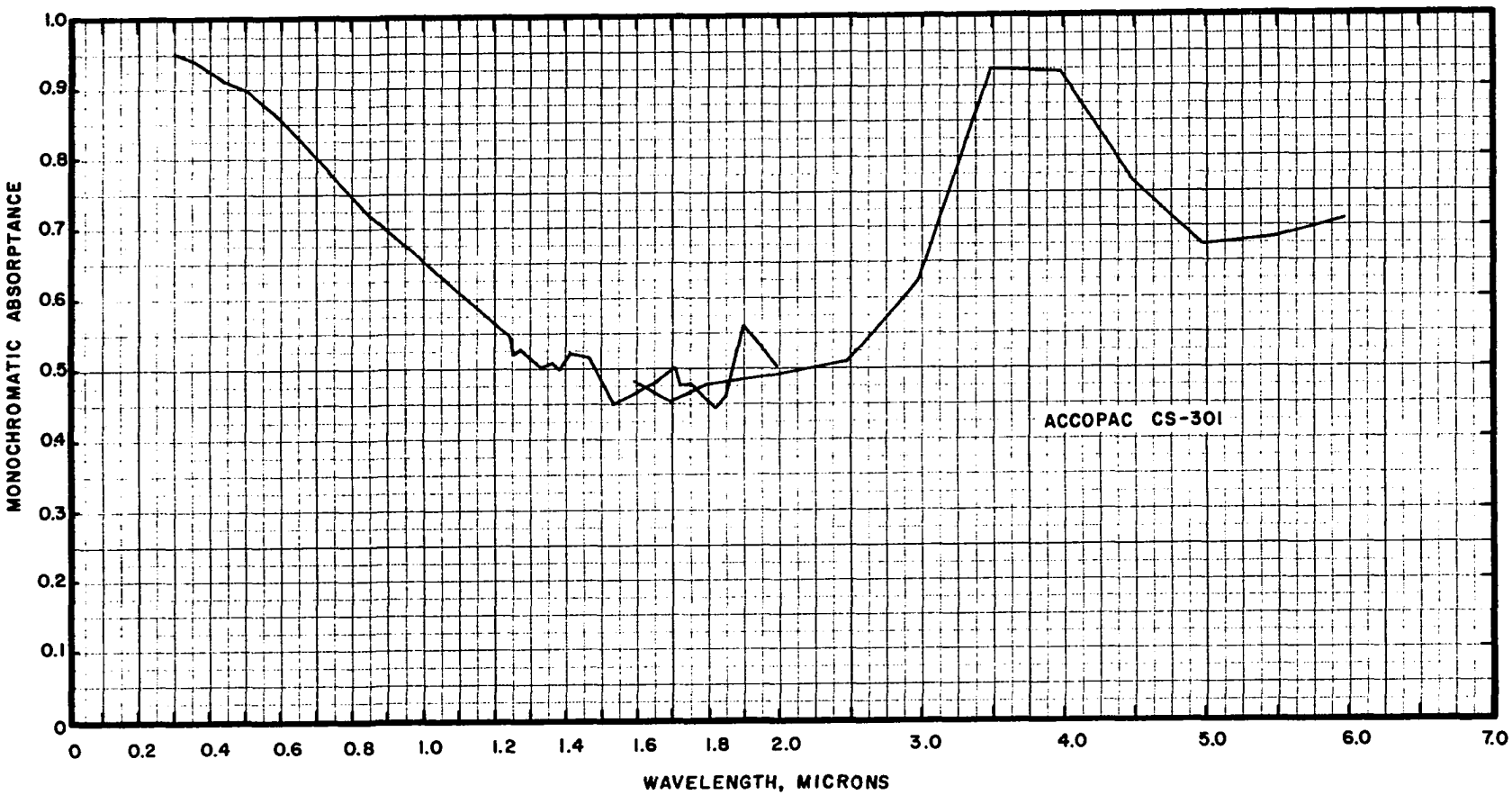

Figure D-17. Spectral Absorptance of Accopac CS-301.

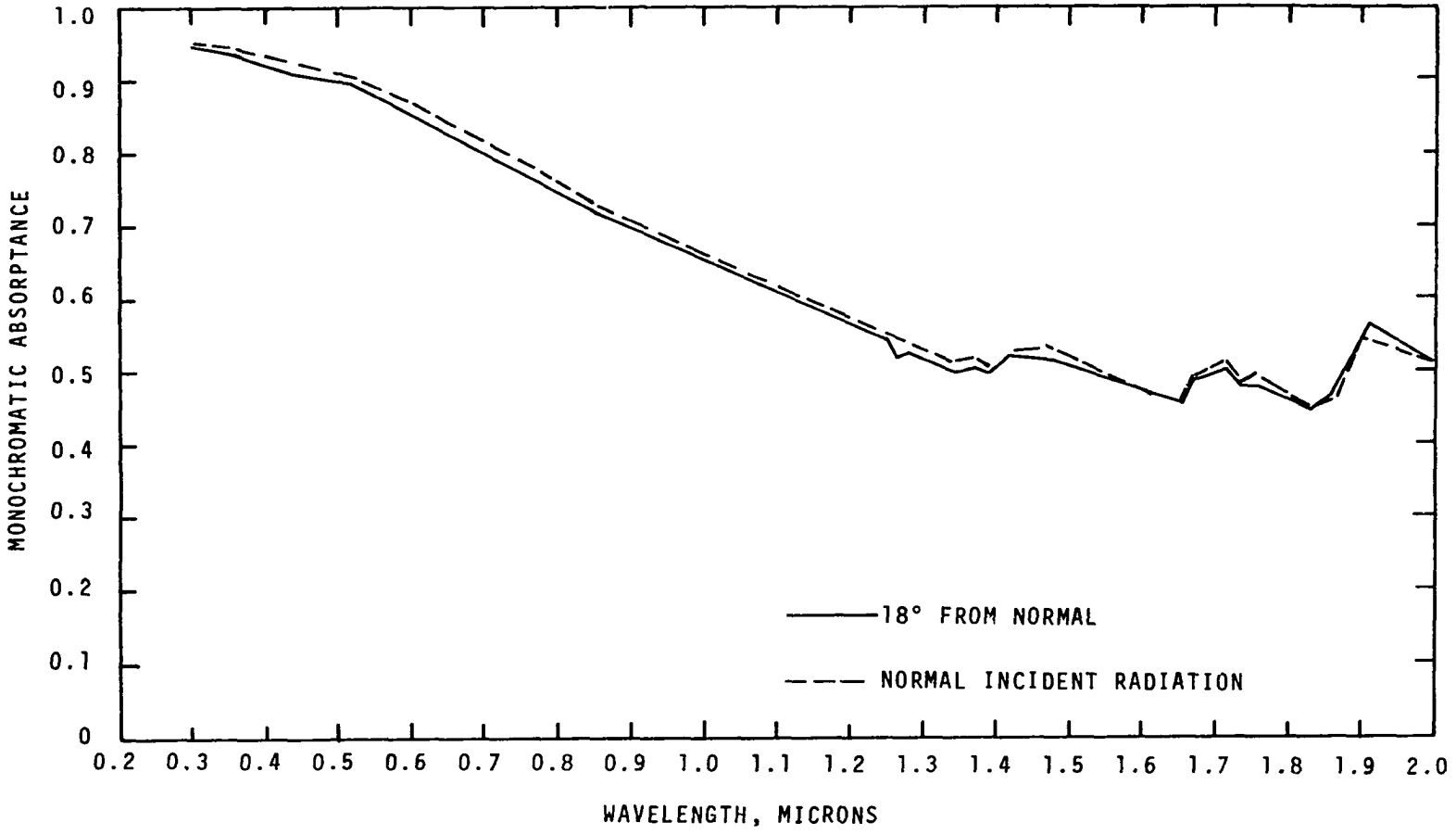

Figure D-18. Angular Variation of Absorptance of Accopac CS-301.

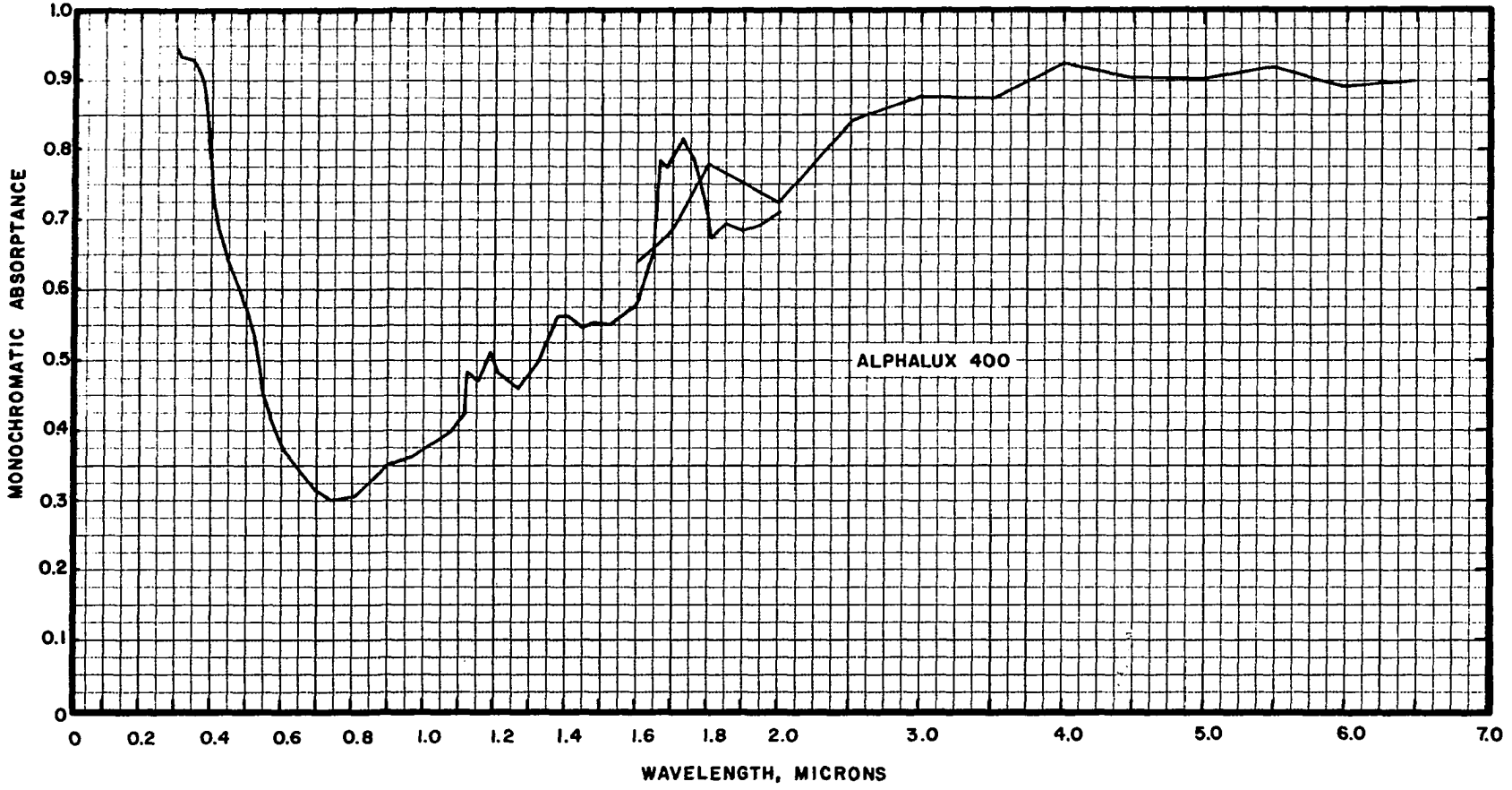

Figure D-19. Spectral Absorptance of Alphalux 400 (PPO).

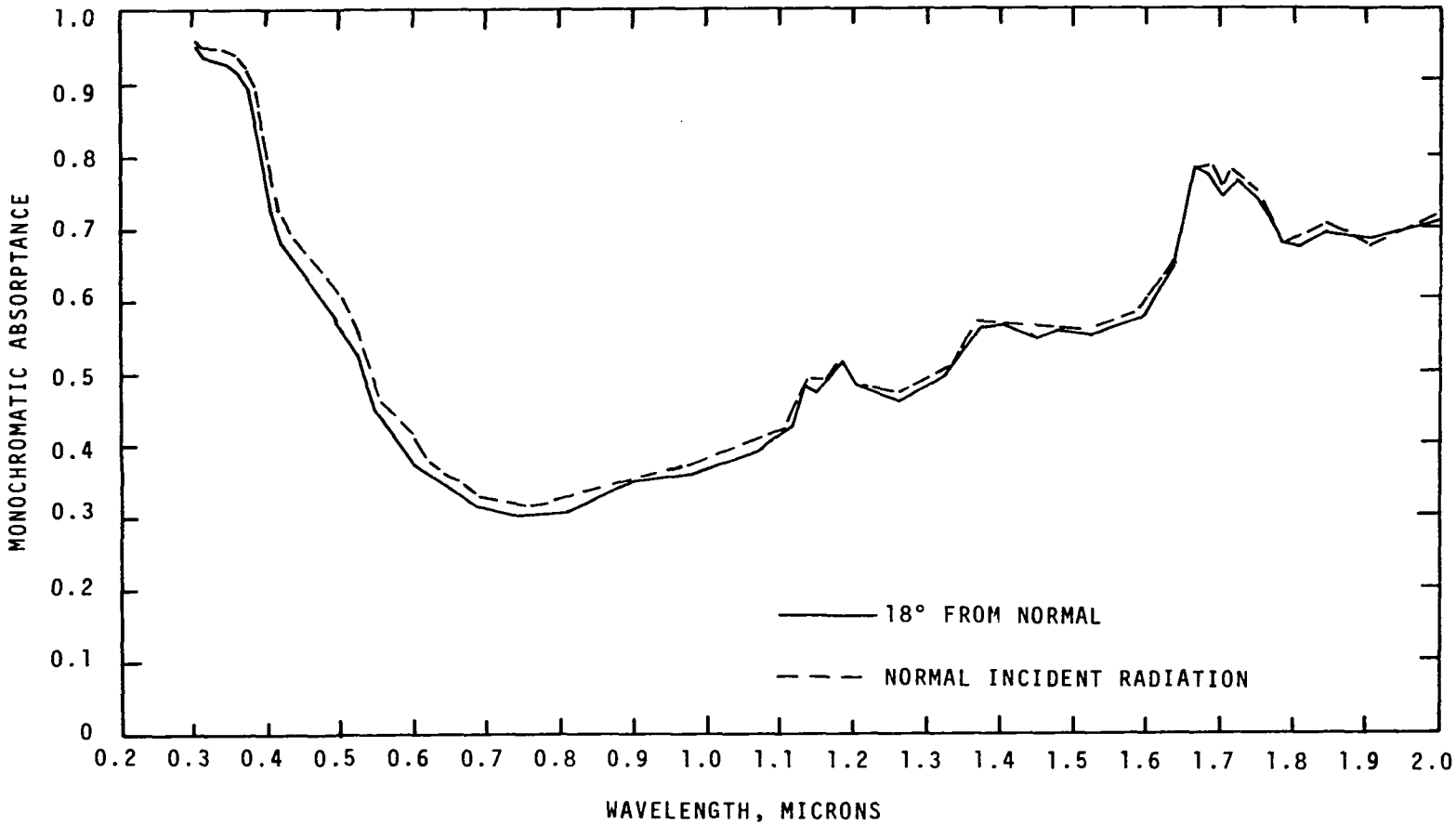

Figure D-20. Angular Variation of Absorptance of Alphalux 400.

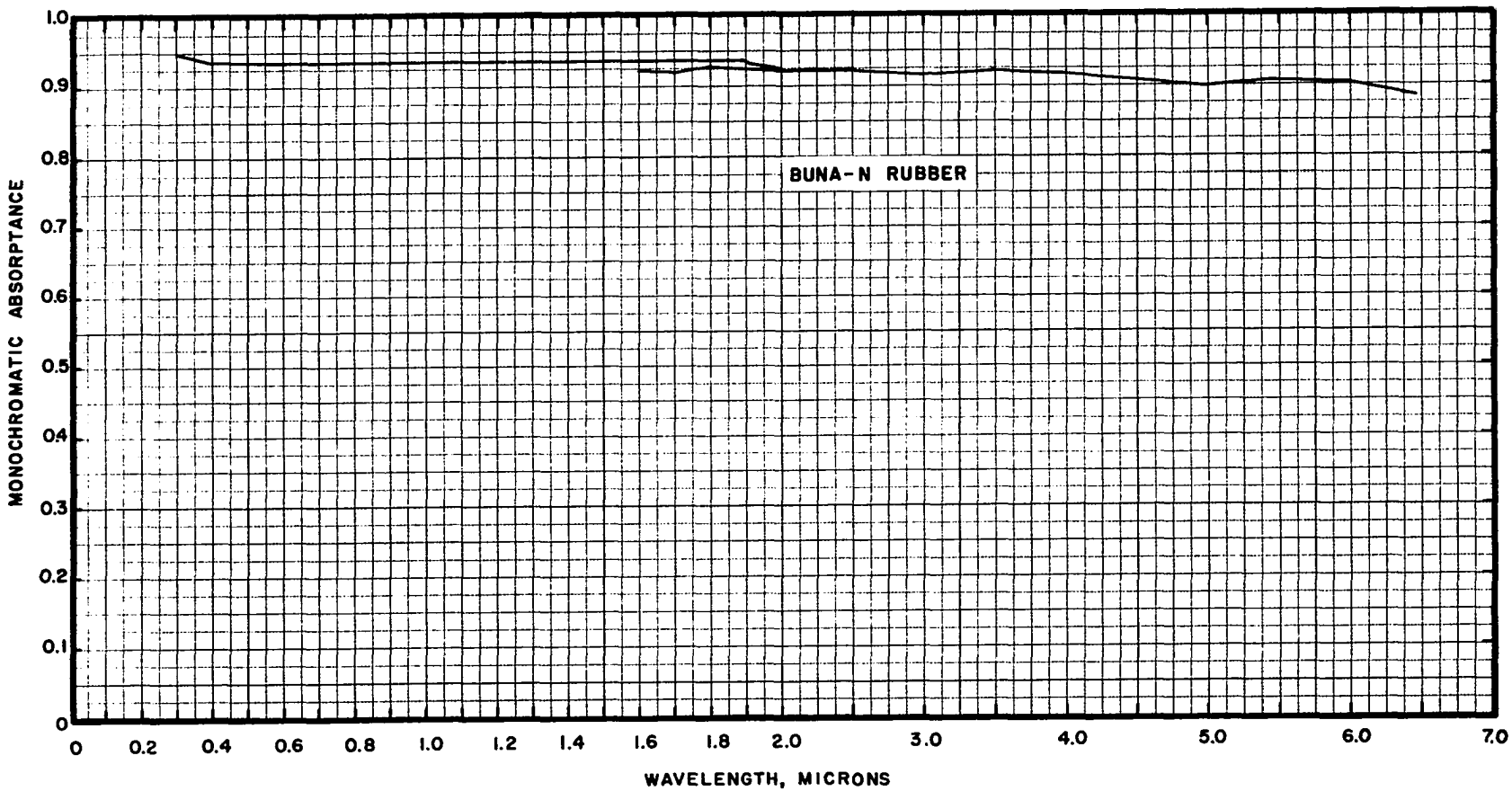

Figure D-21. Spectral Absorptance of Buna-N Rubber.

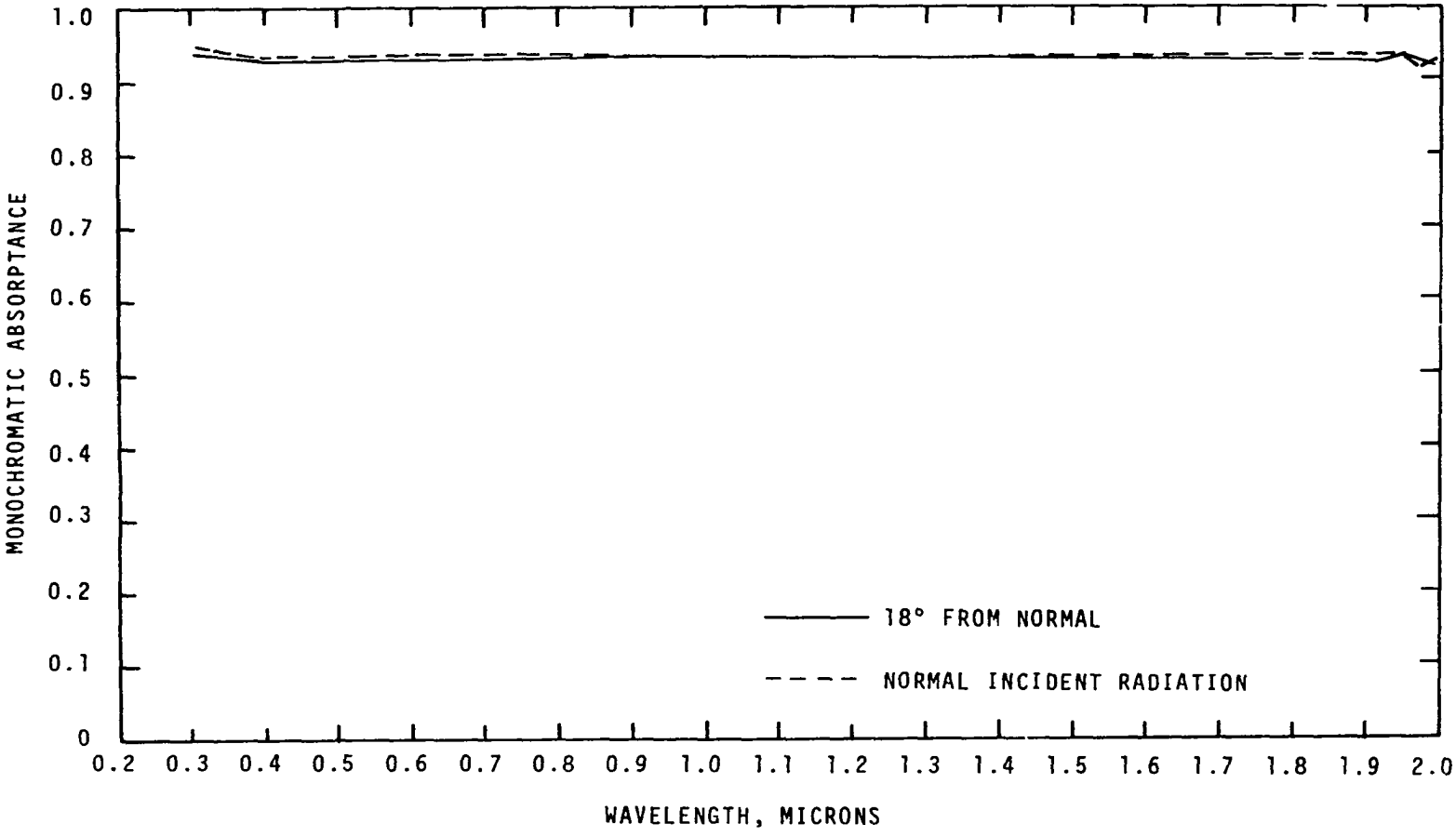

Figure D-22. Angular Variation of Absorptance of Buna-N Rubber.

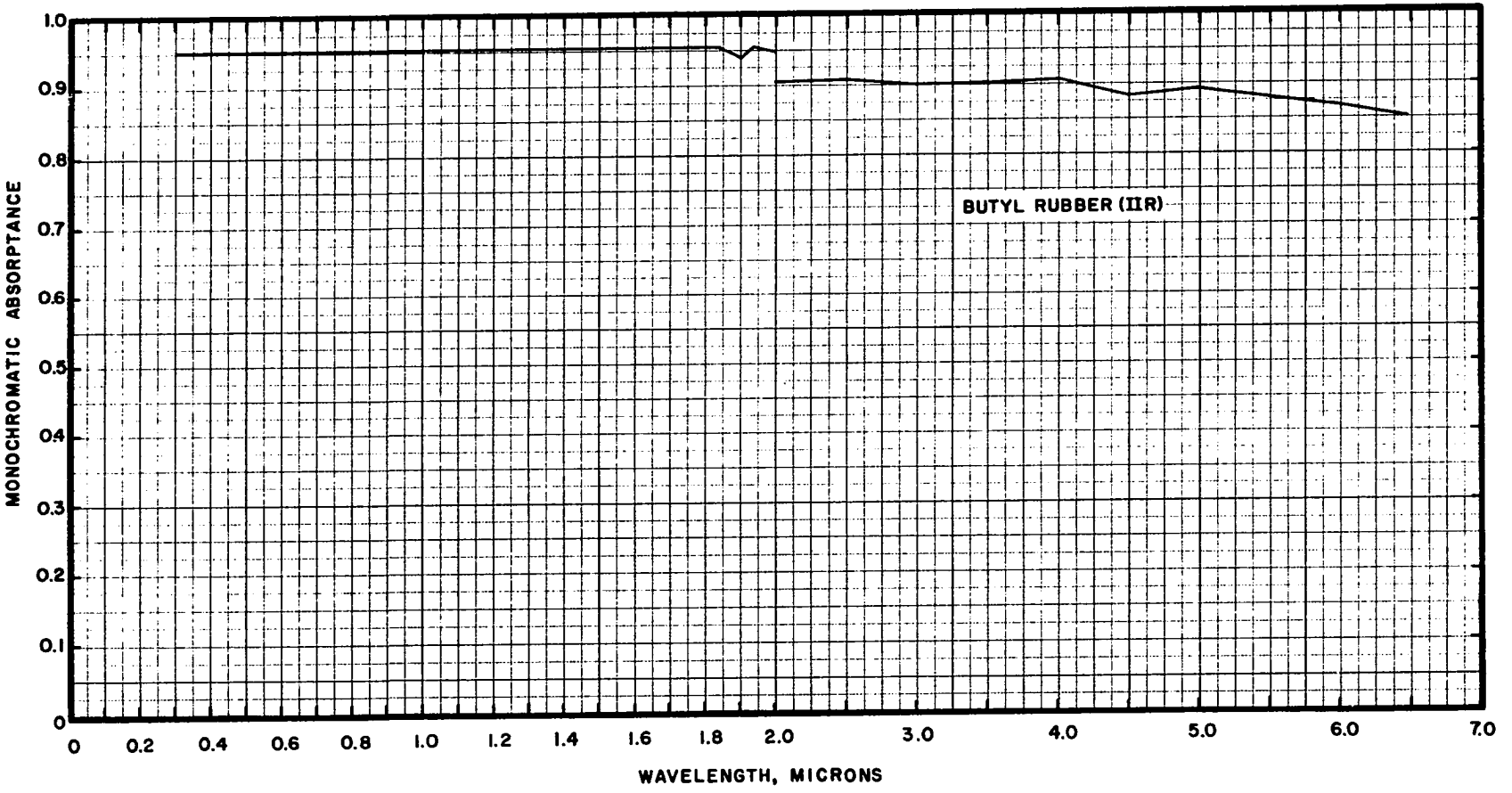

Figure D-23. Spectral Absorptance of Butyl Rubber IIR.

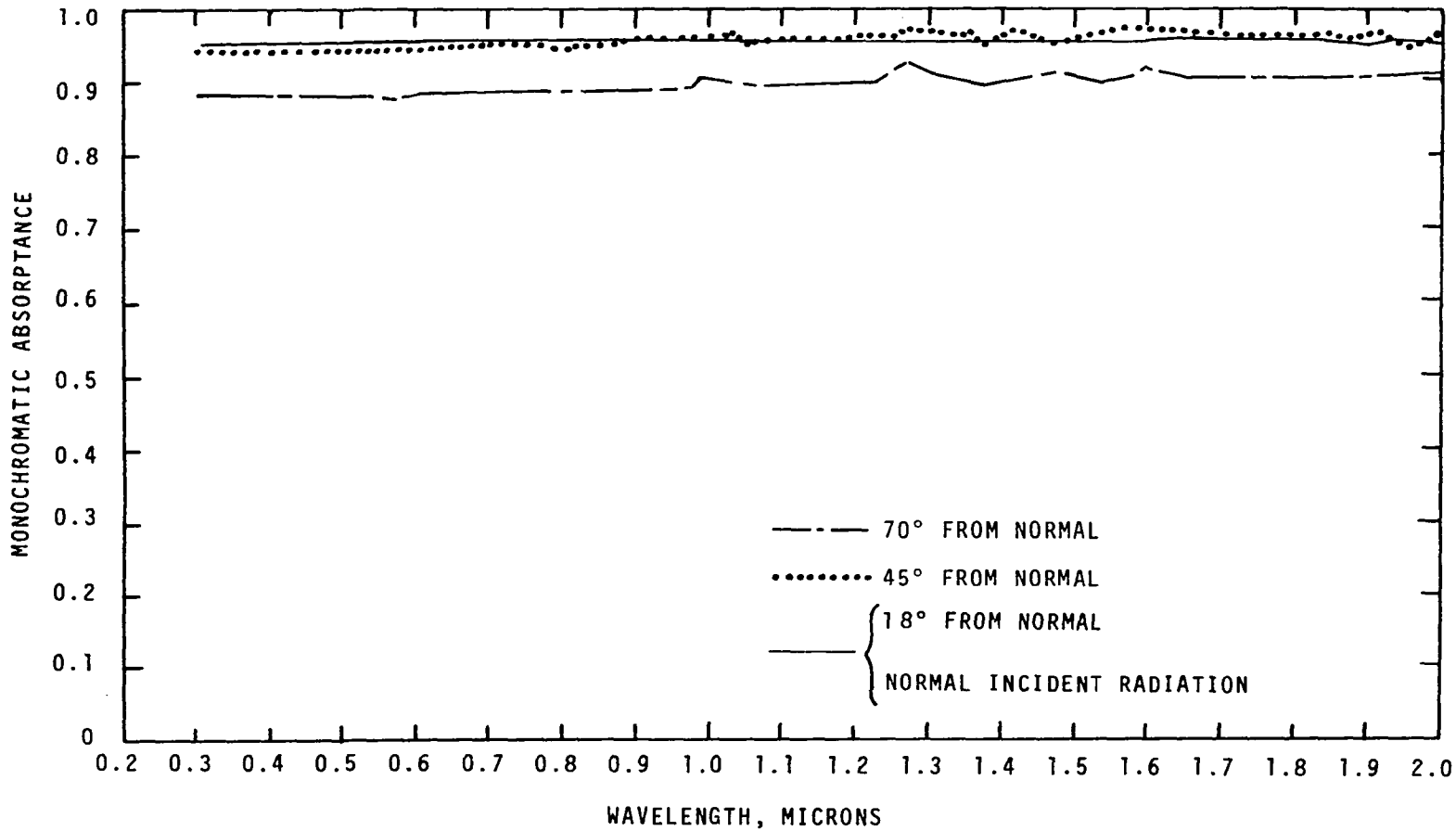

Figure D-24. Angular Variation of Absorptance of Butyl Rubber.

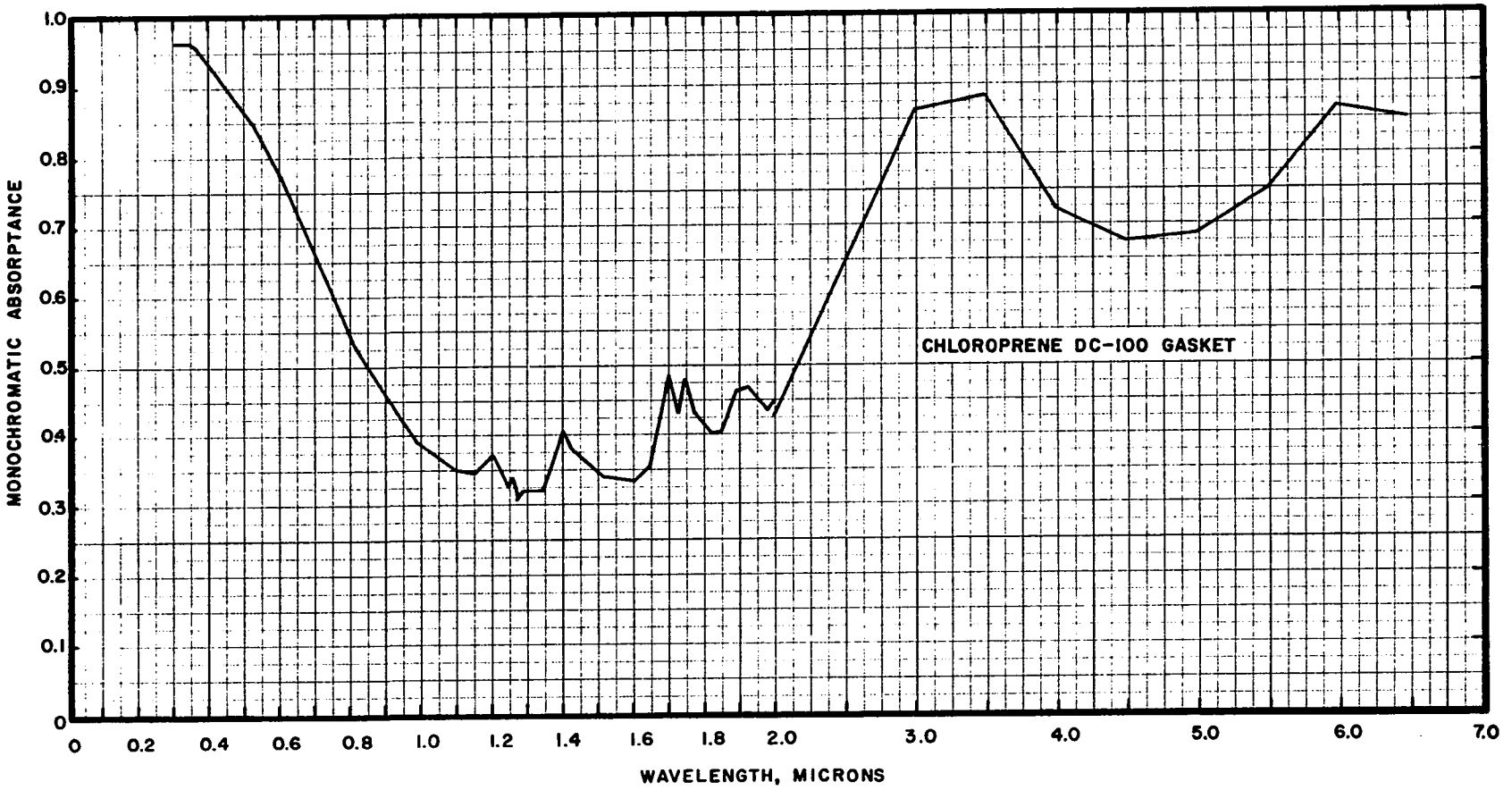

Figure D-25. Spectral Absorptance of Chloroprene DC-100 Gasket.

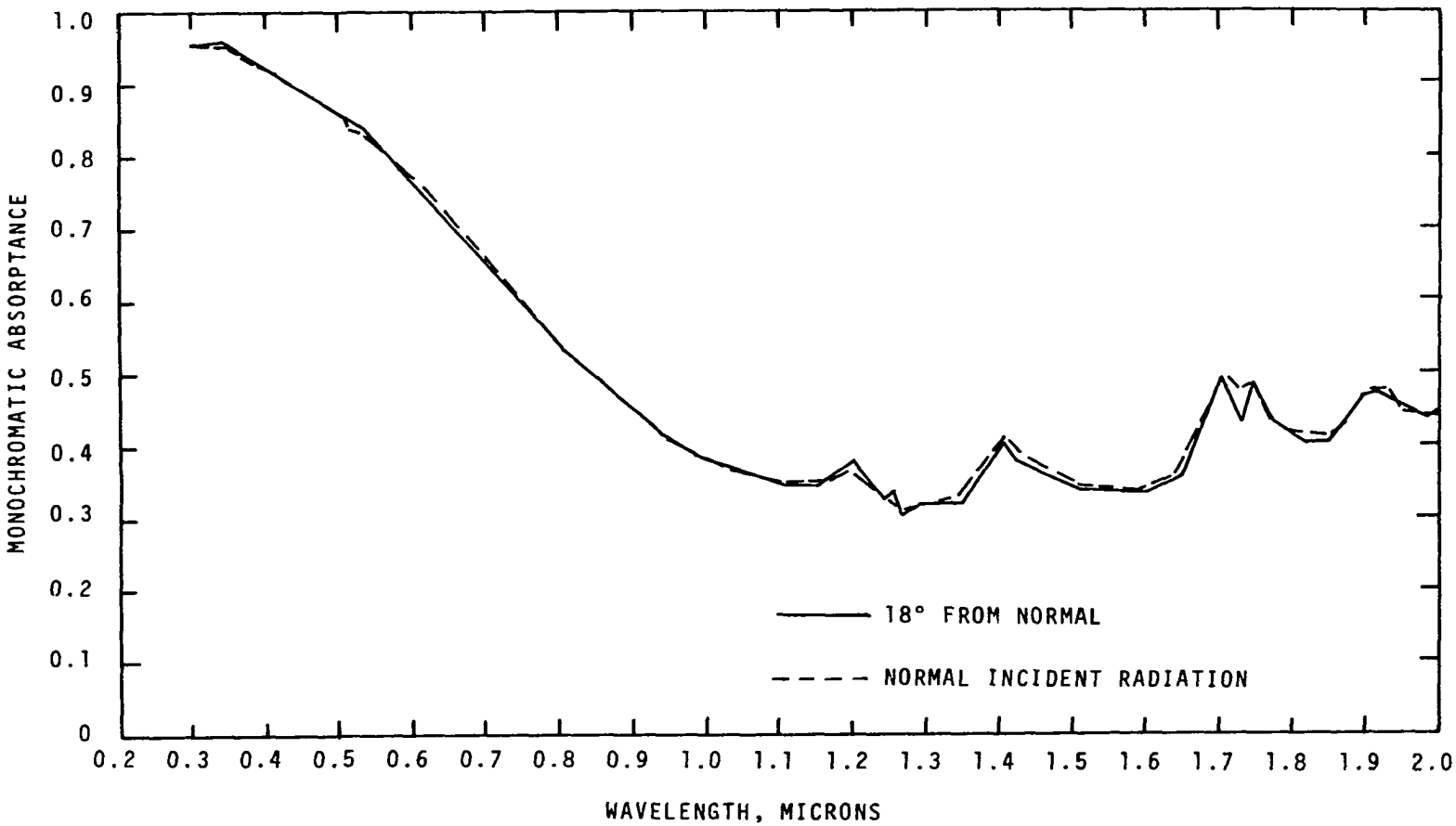

Figure D-26. Angular Variation of Absorptance of DC-100 Gasket.

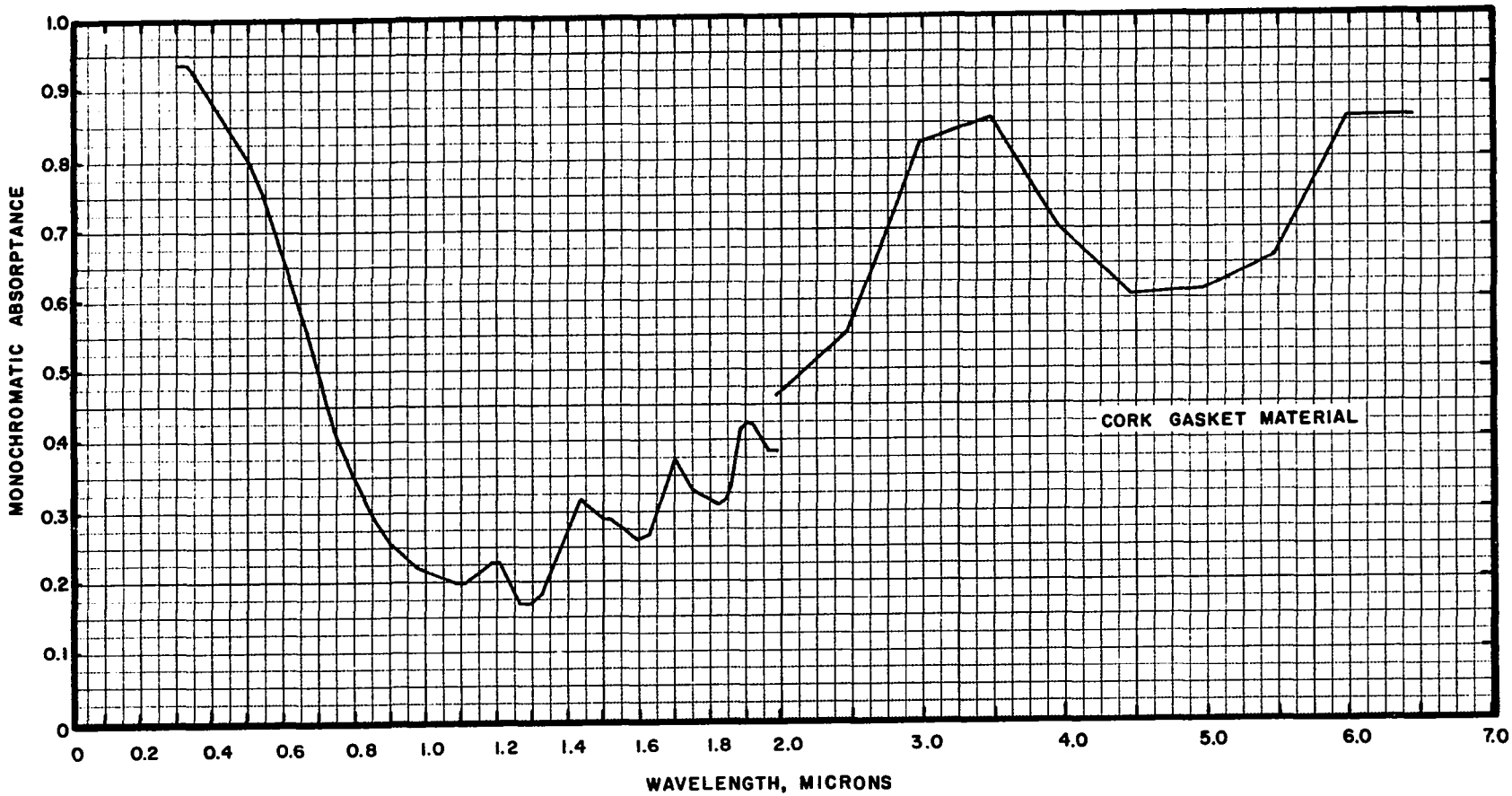

Figure D-27. Spectral Absorptance of Cork Gasket Material.

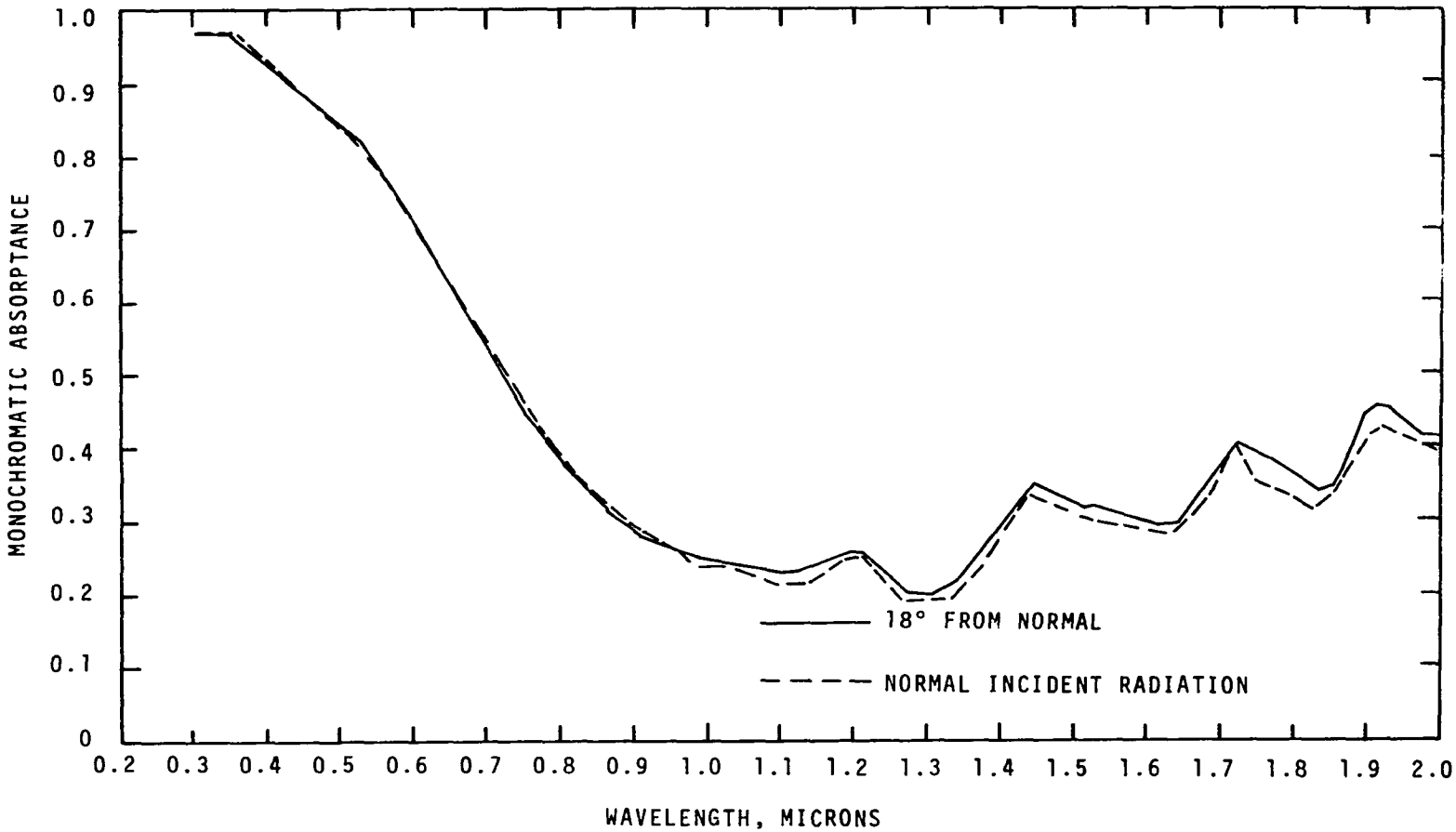

Figure D-28. Angular Variation of Absorptance of Cork Gasket.

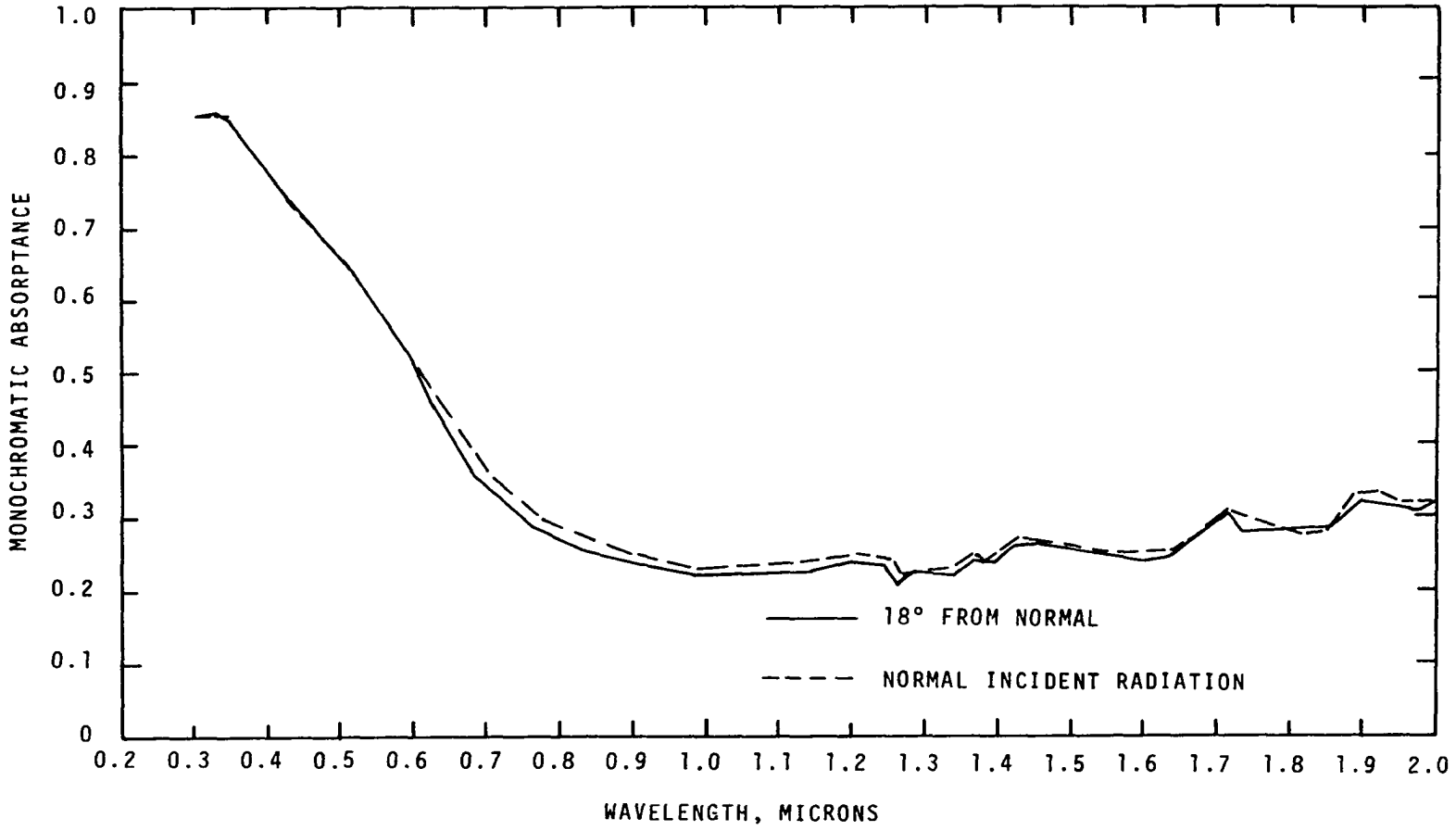

Figure D-29. Angular Variation of Absorptance of Bottle Cork.

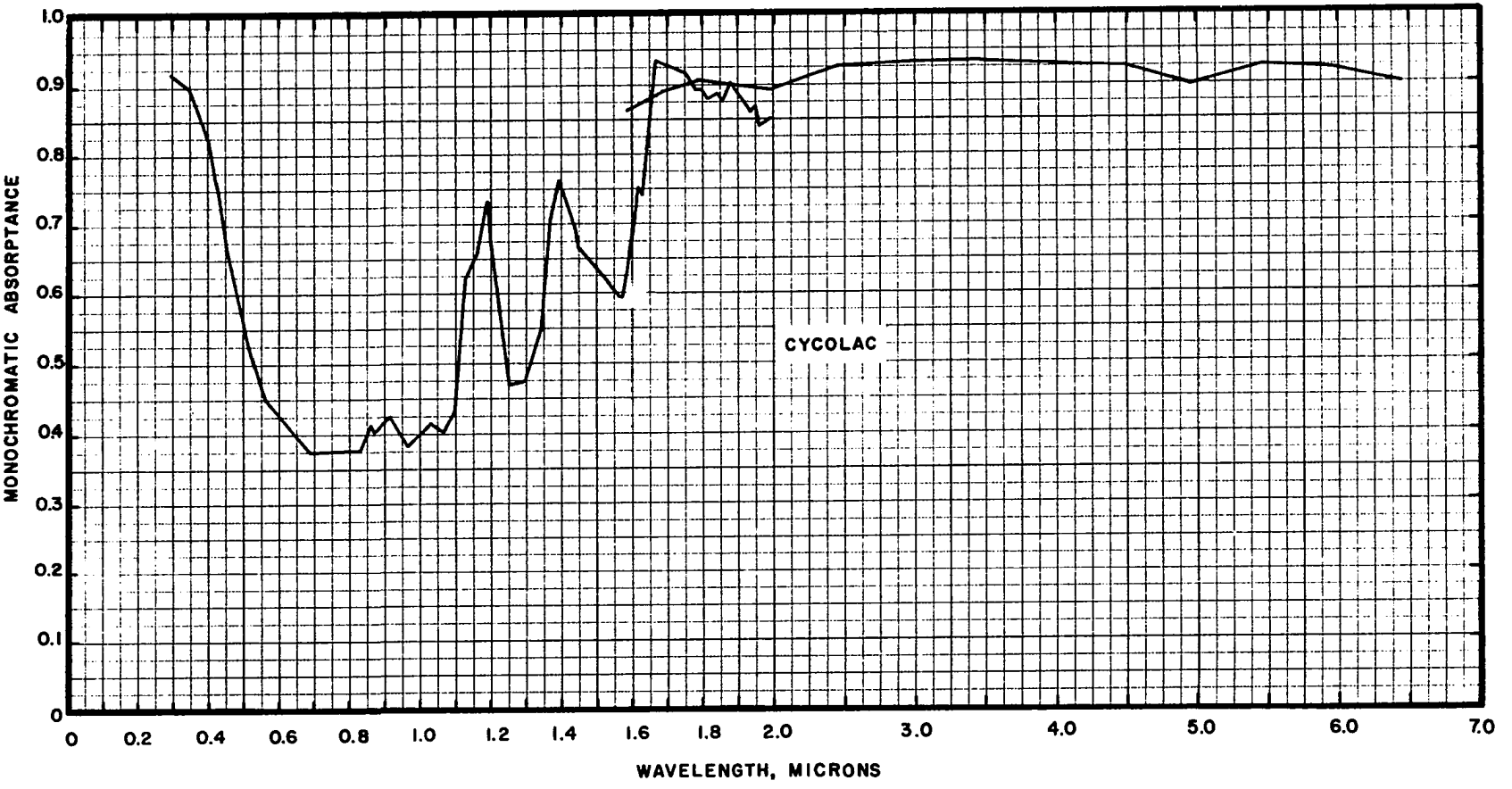

Figure D-30. Spectral Absorptance of Cycolac.

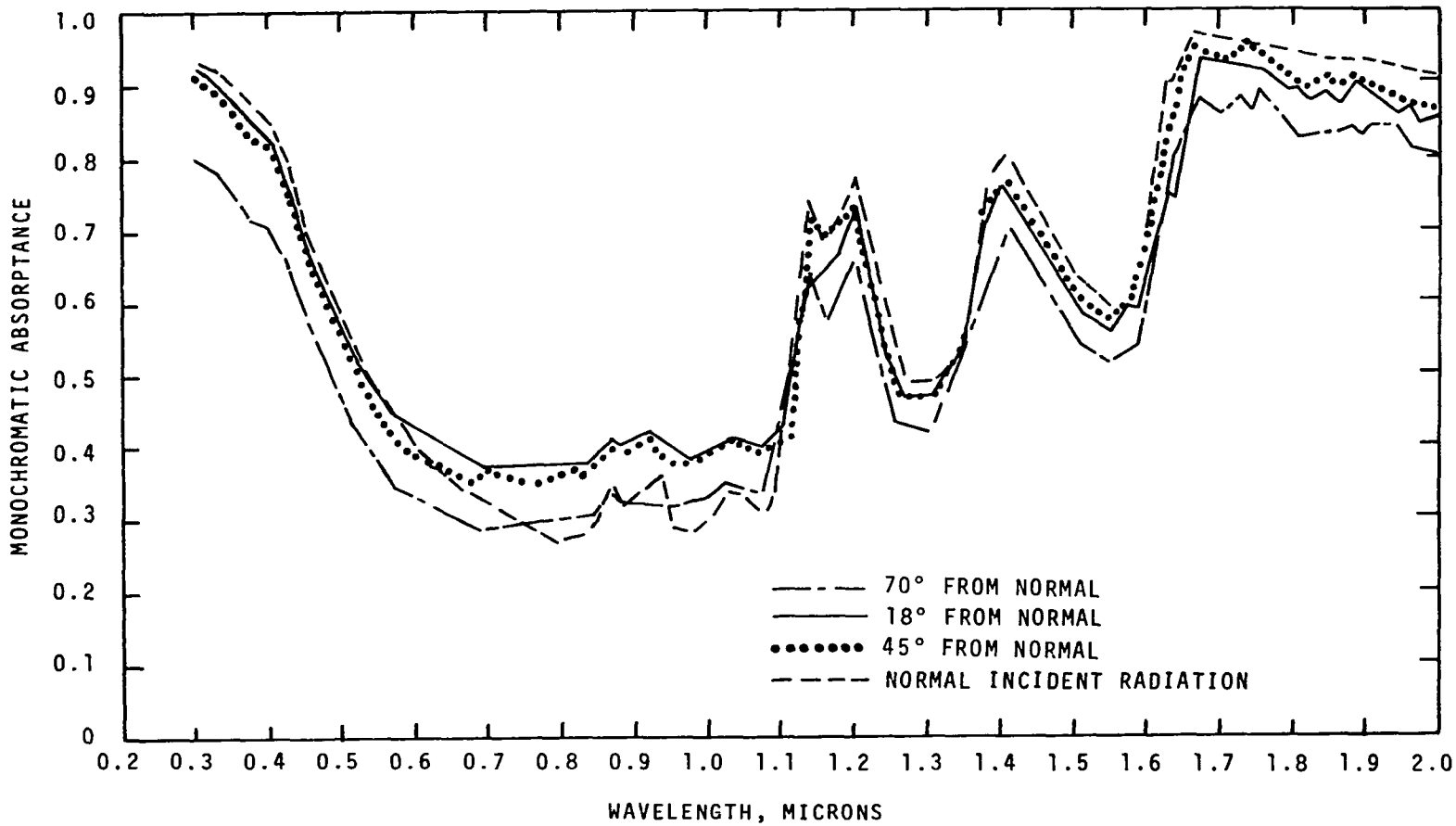

Figure D-31. Angular Variation of Absorptance of Cycolac.

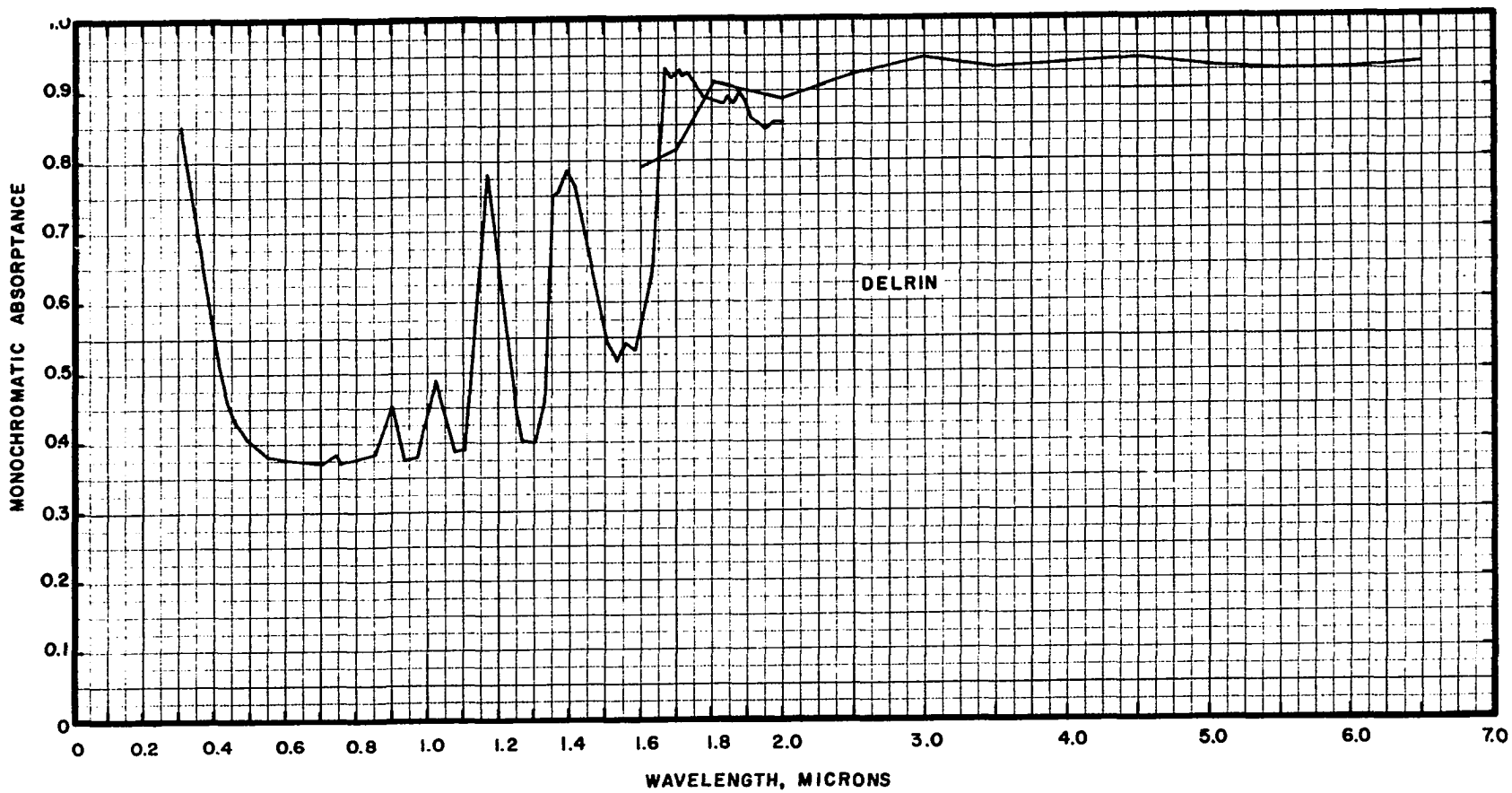

Figure D-32. Spectral Absorptance of Delrin.

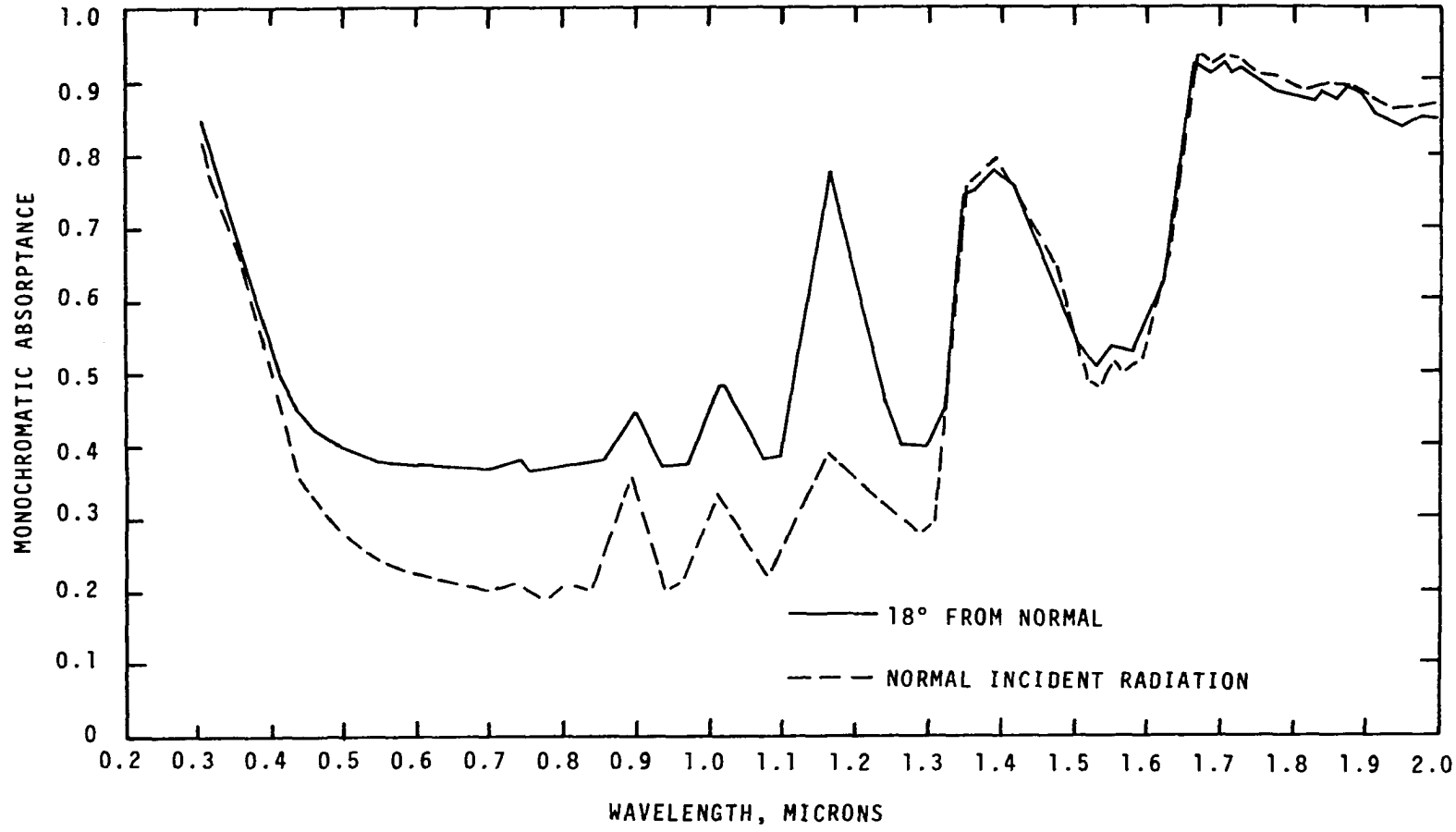

Figure D-33. Angular Variation of Absorptance of Delrin.

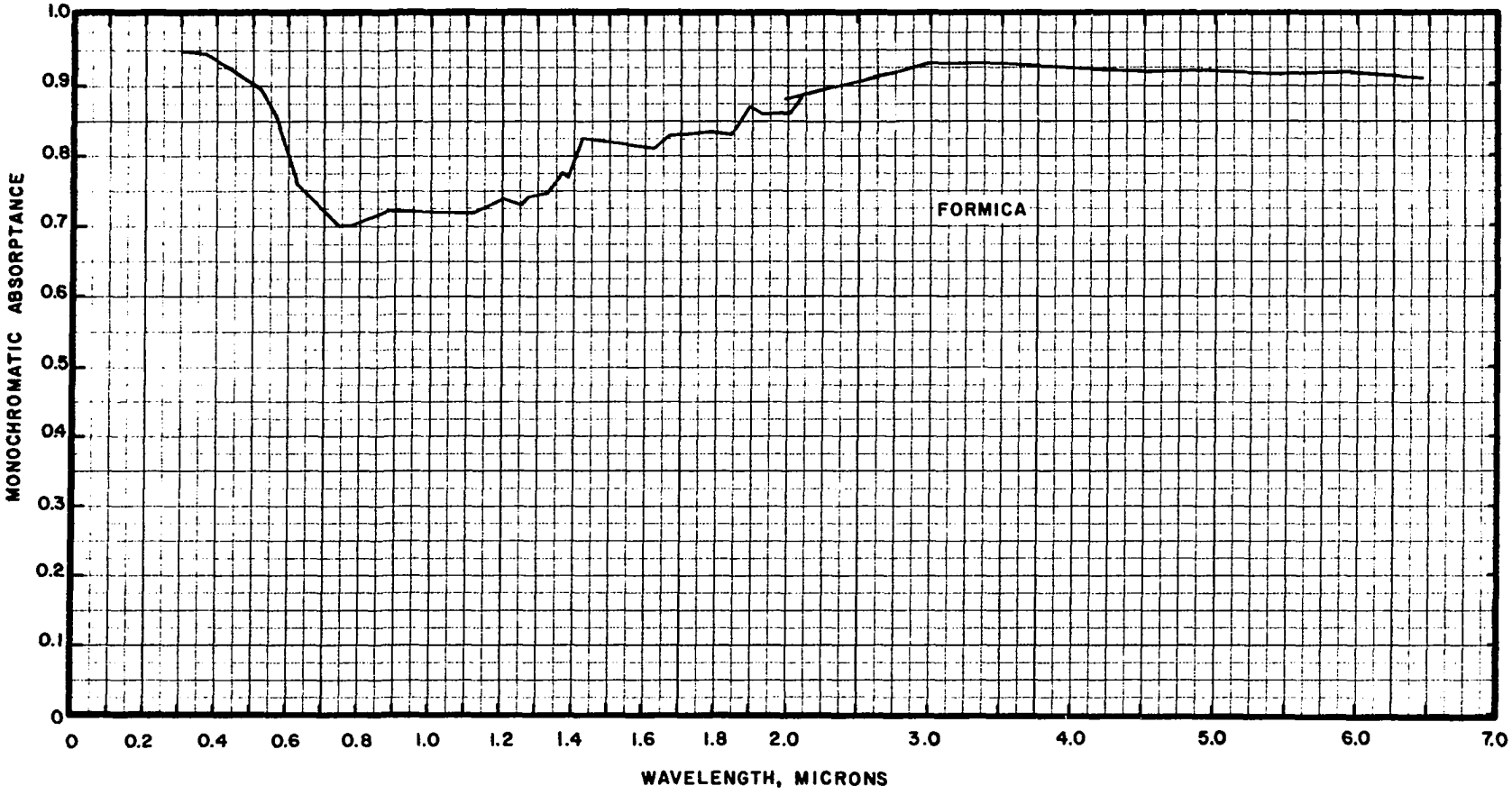

Figure D-34. Spectral Absorptance of Formica.

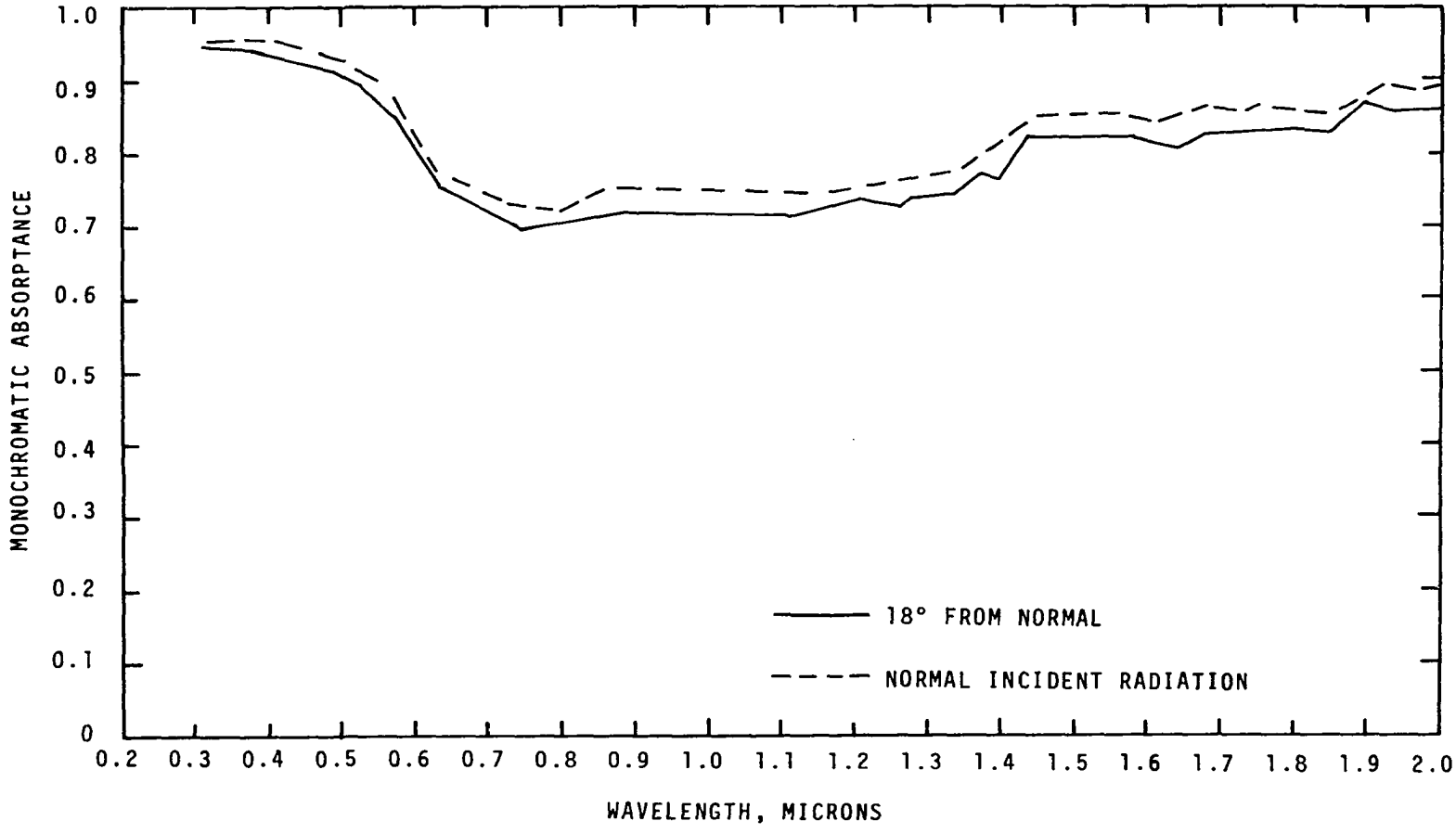

Figure D-35. Angular Variation of Absorptance of Formica.

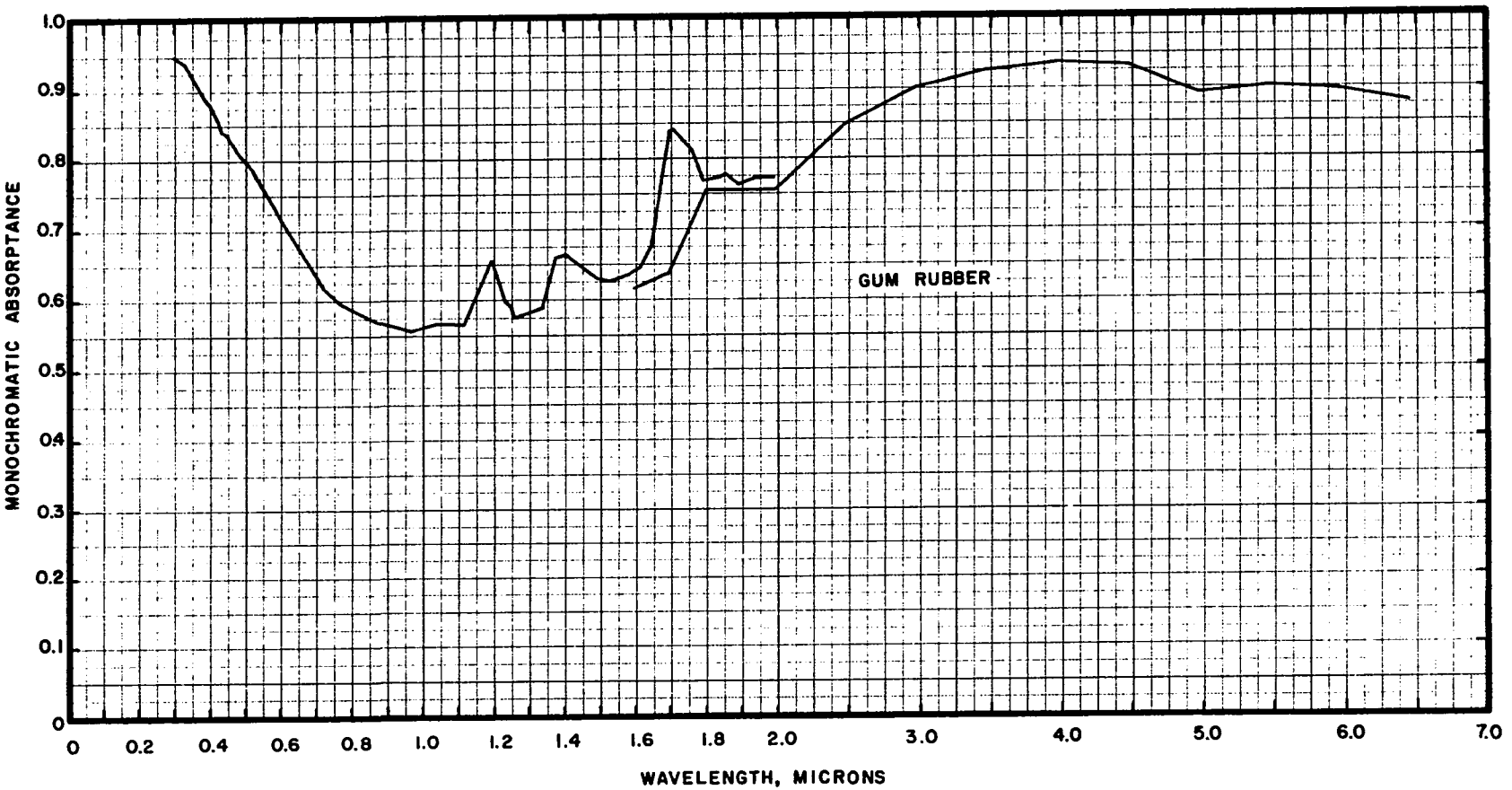

Figure D-36. Spectral Absorptance of Gum Rubber.

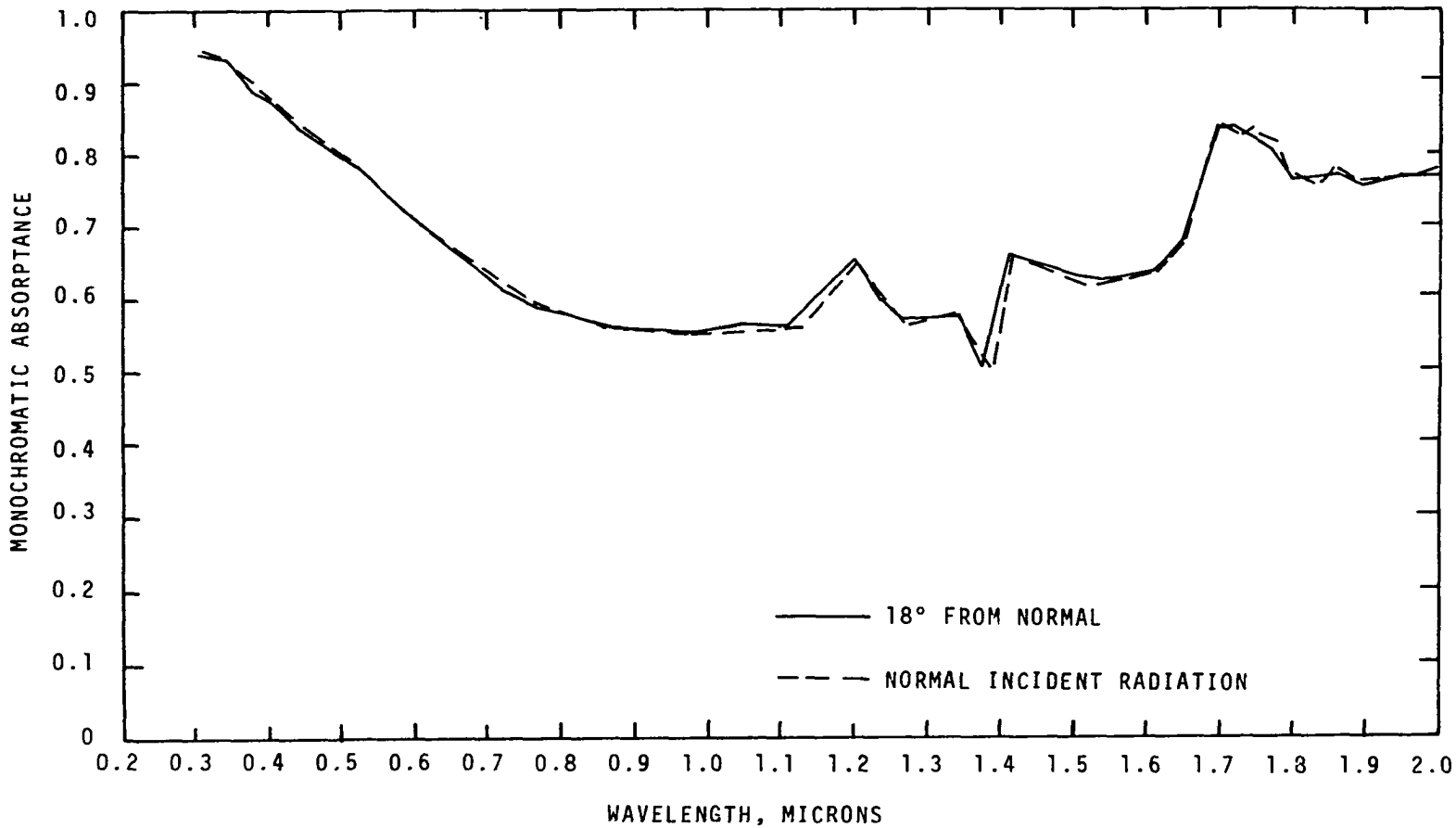

Figure D-37. Angular Variation of Absorptance of Gum Rubber.

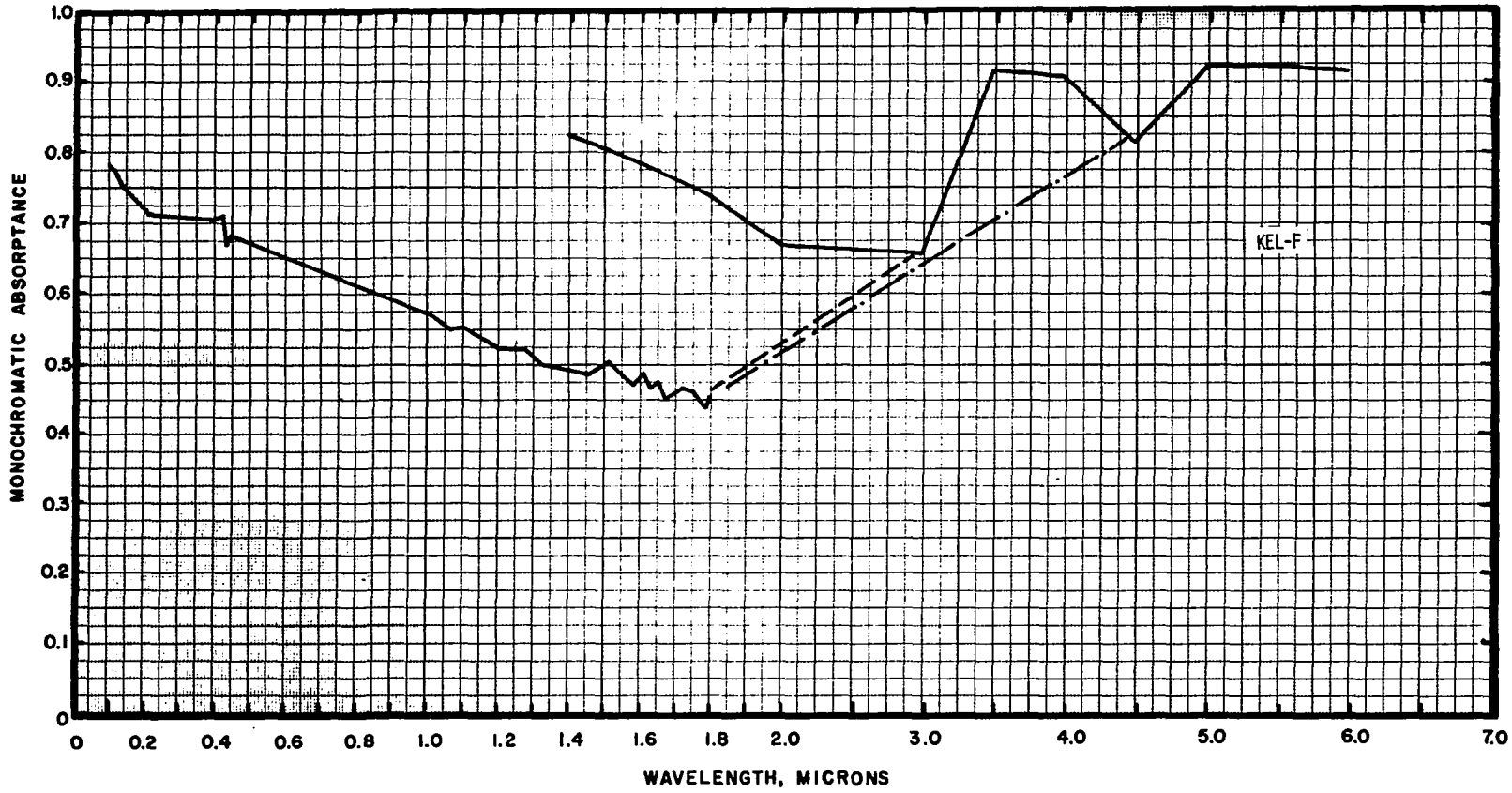

Figure D-38. Spectral Absorptance of Kel-F.

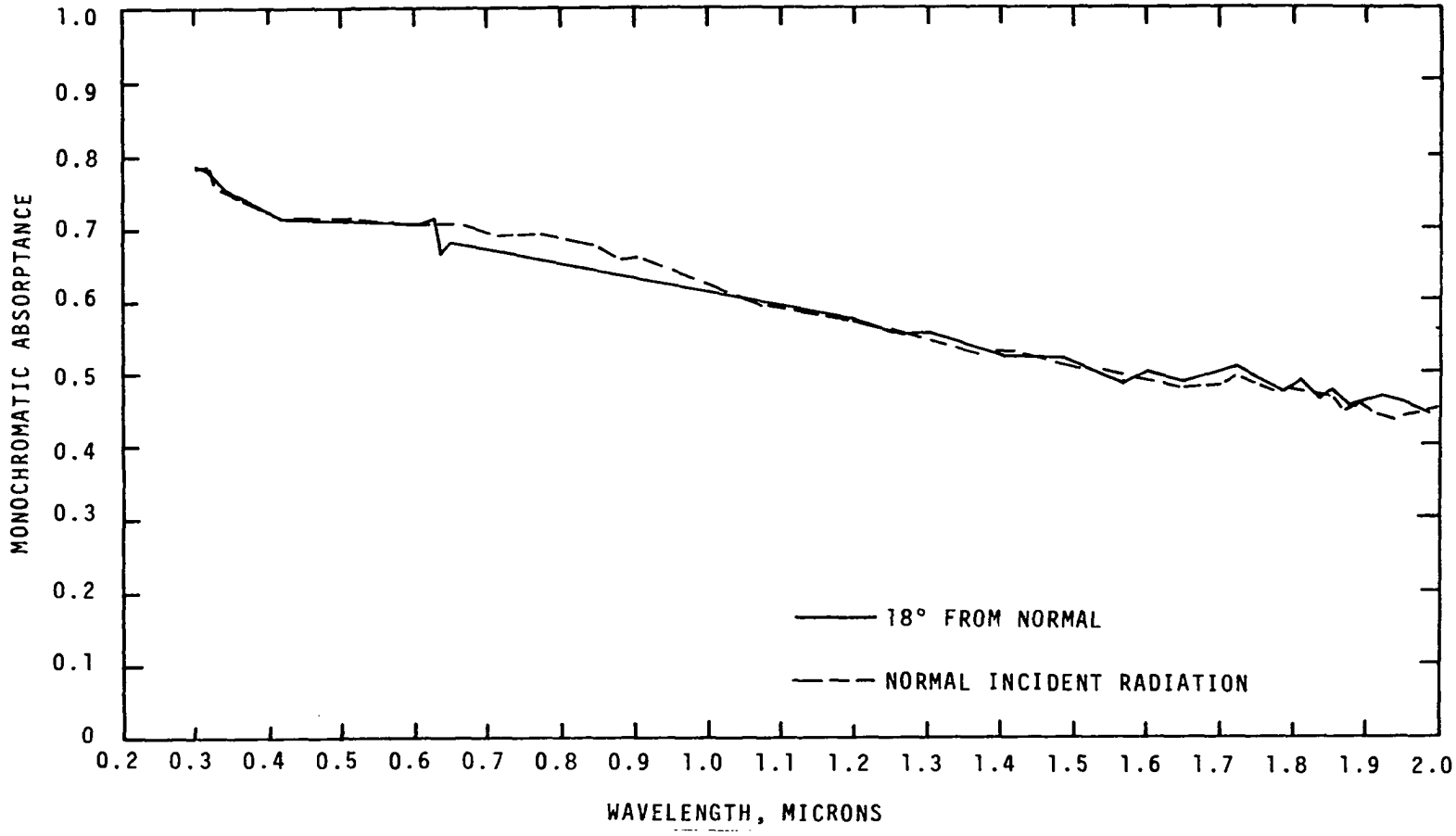

Figure D-39. Angular Variation of Absorptance of Kel-F.

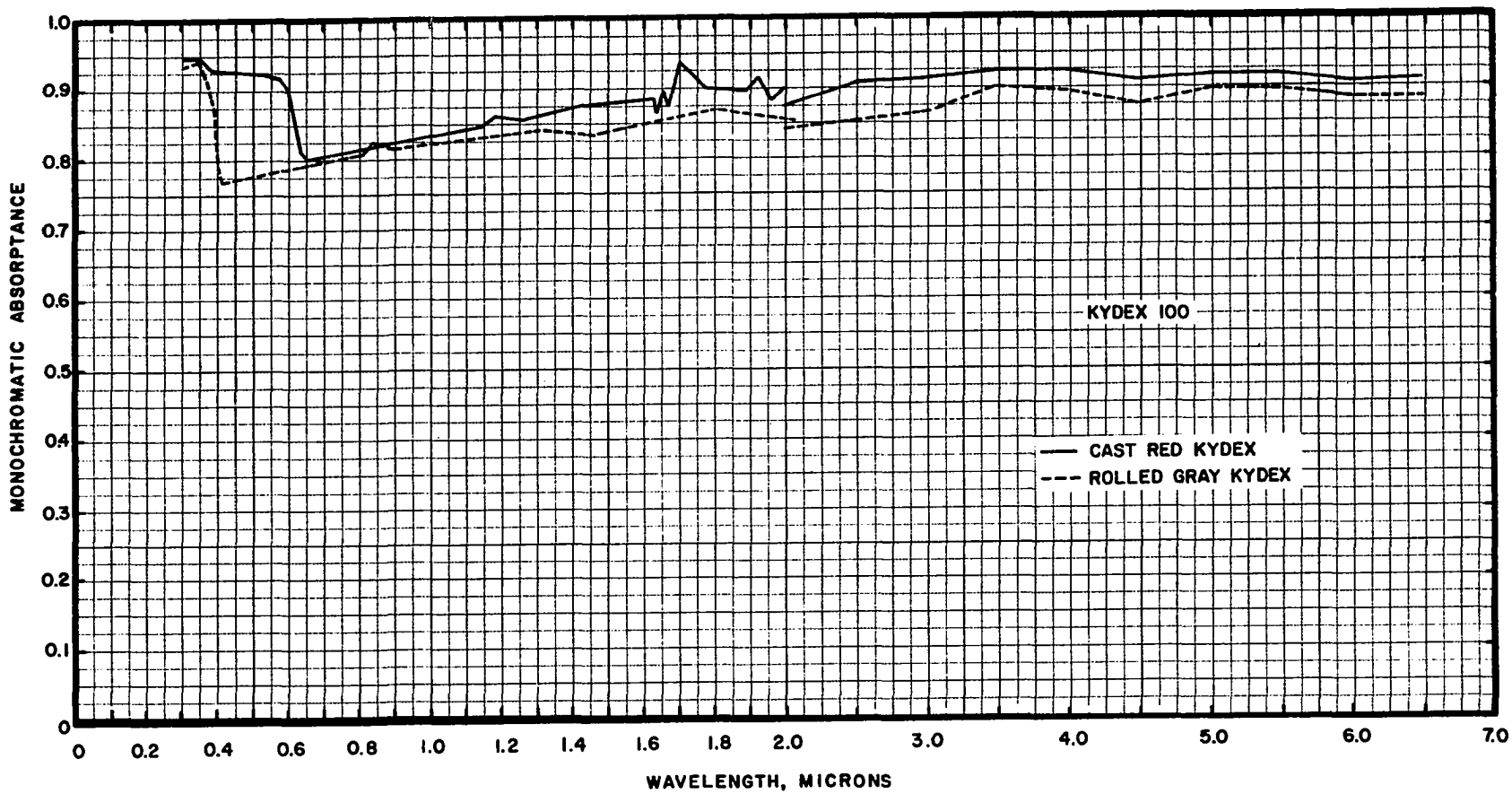

Figure D-40. Spectral Absorptance of Kydex 100.

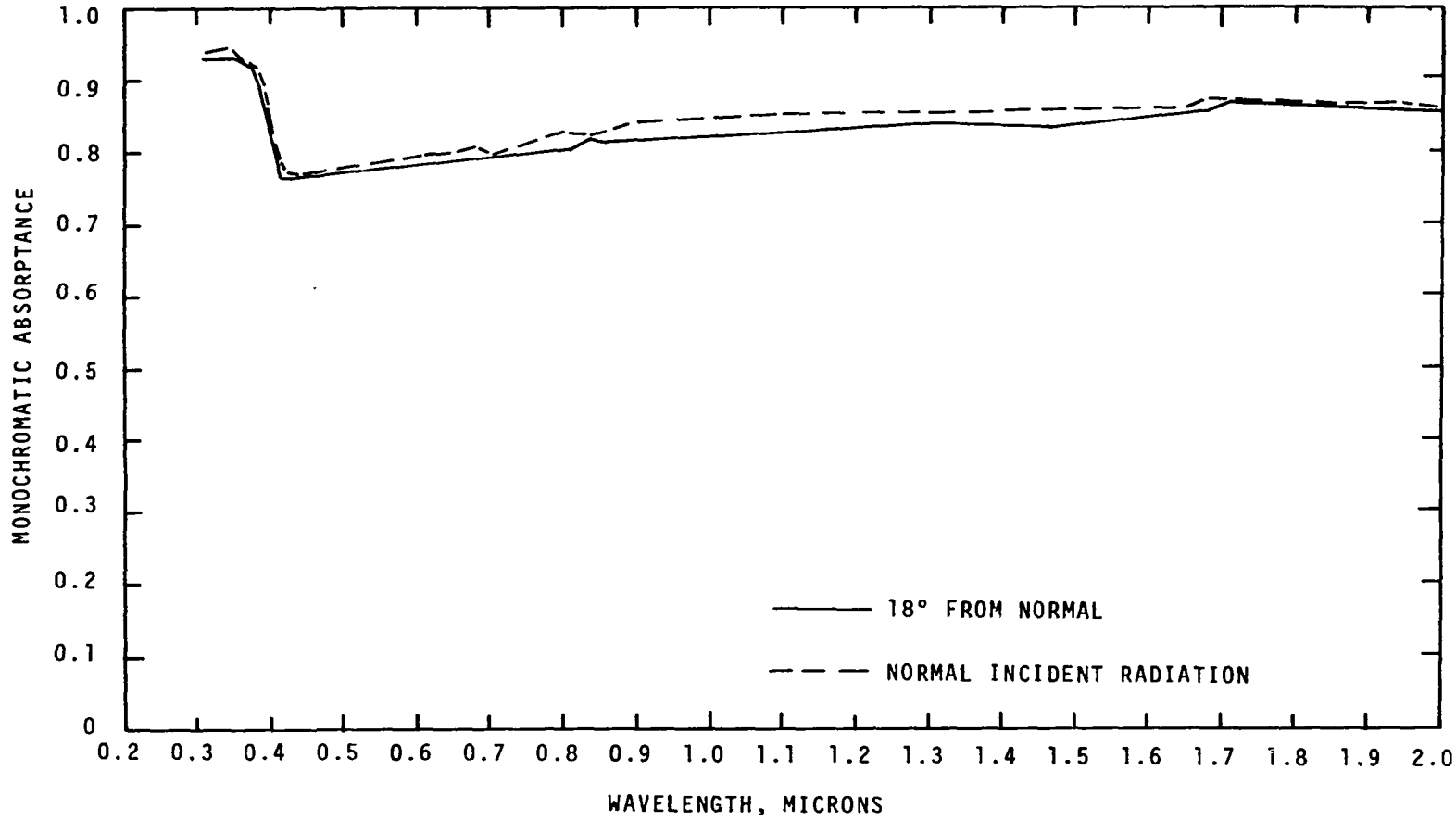

Figure D-41. Angular Variation of Absorptance of Gray Kydex 100.

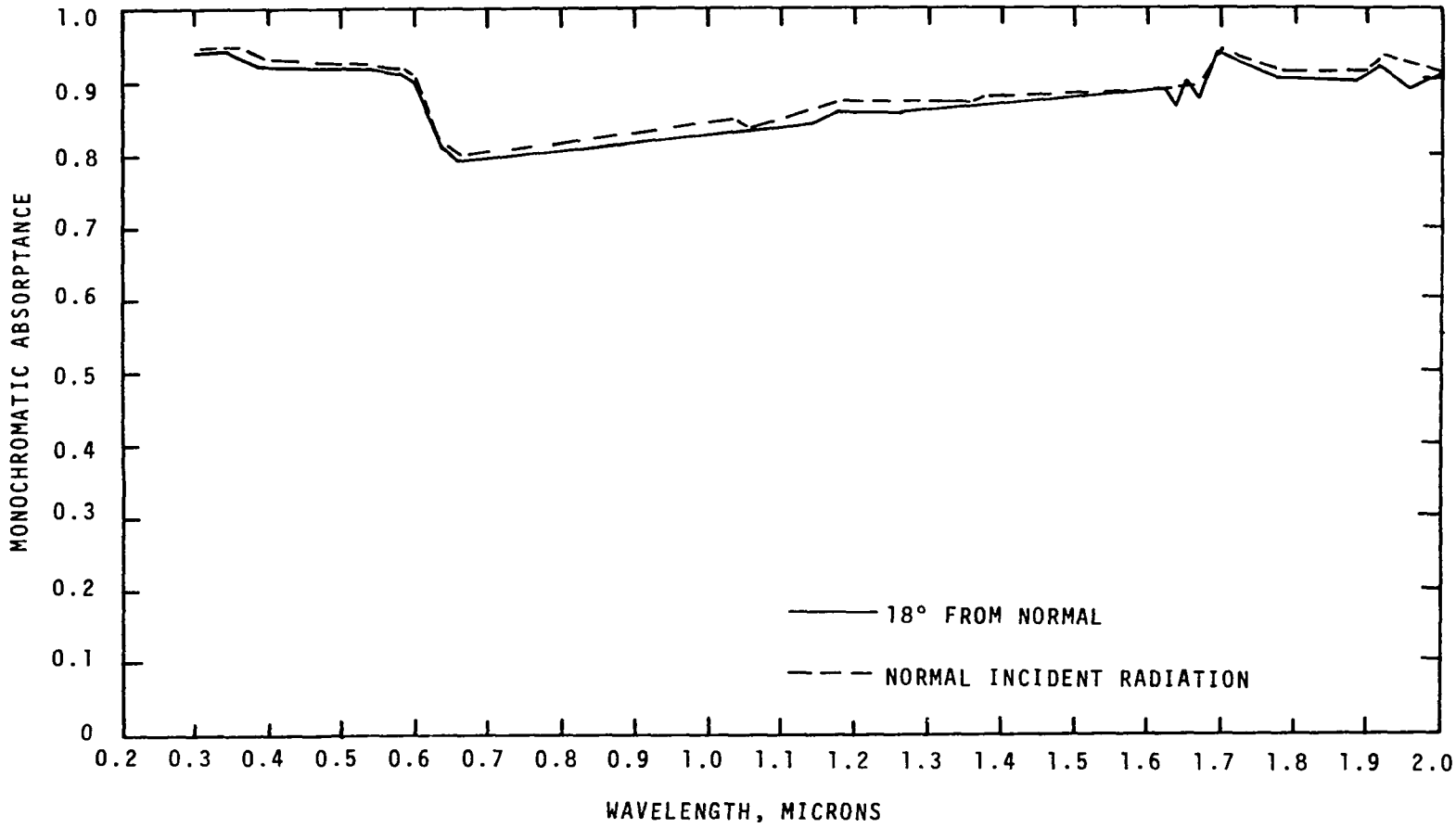

Figure D-42. Angular Variation of Absorptance of Red Kydex 100.

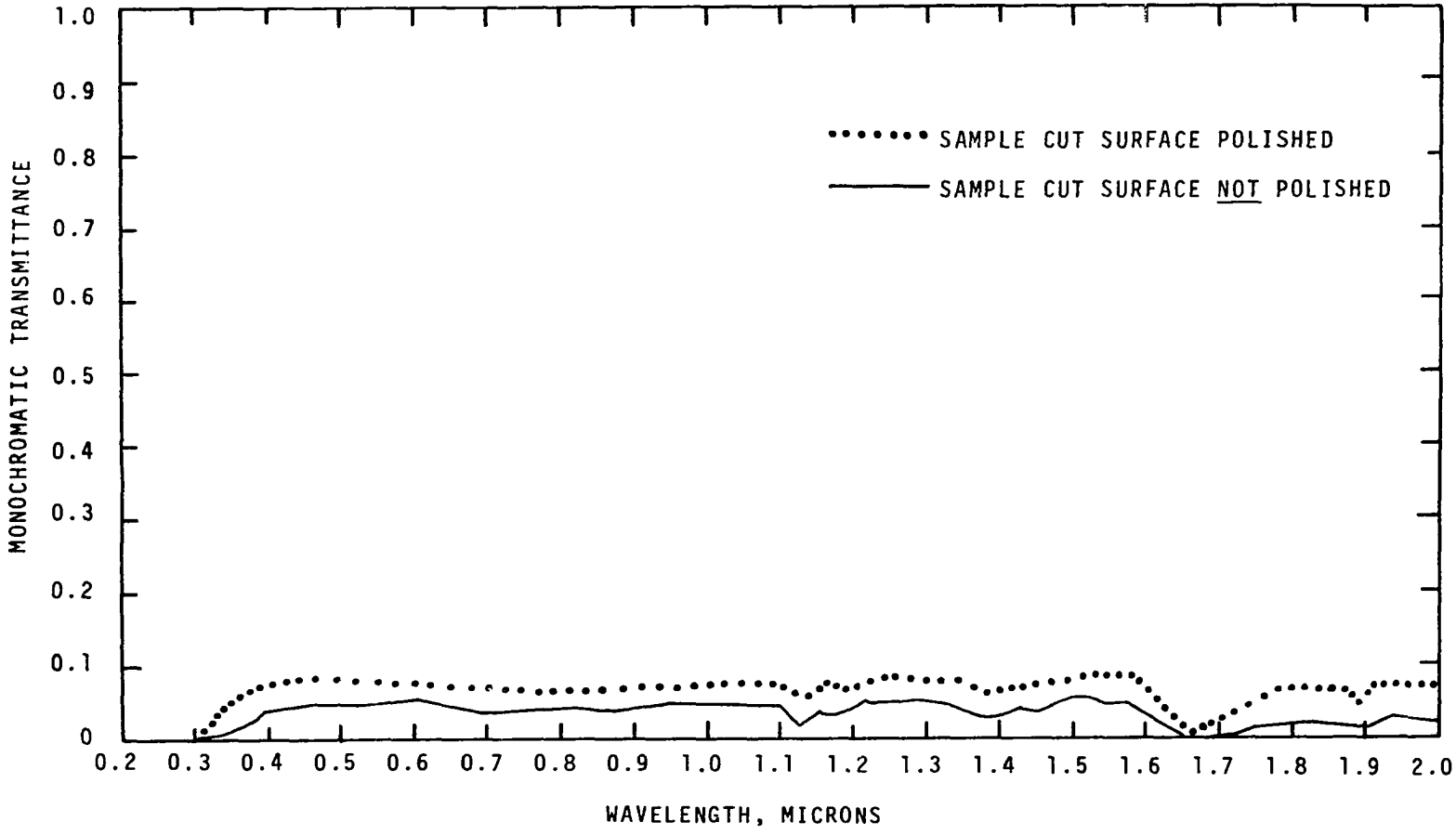

Figure D-43. Spectral Transmission of Lexan with Surface Variations.

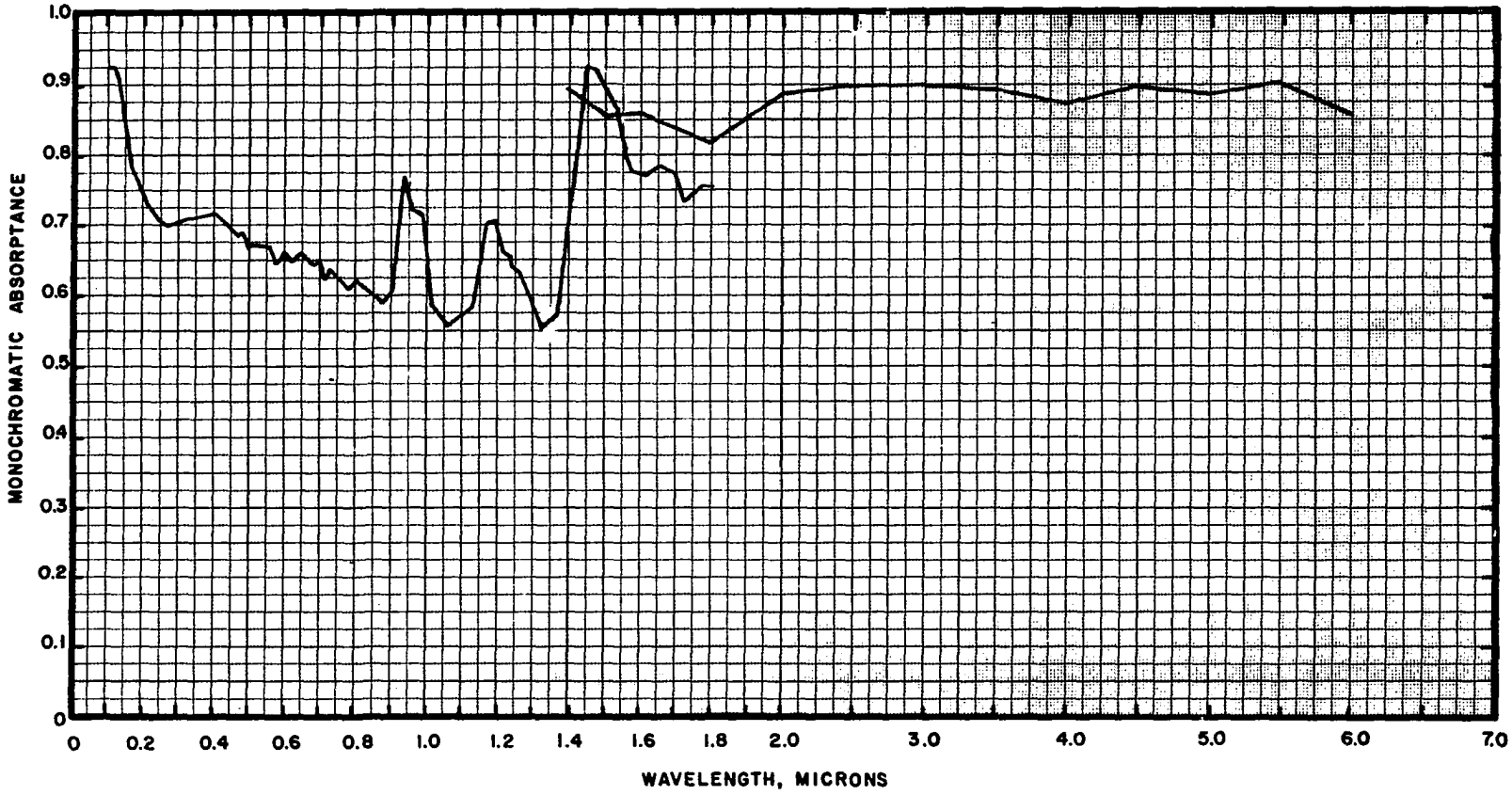
MONOCHROMATIC ABSORPTANCE
1.0
0.9
0.8
0.7
0.6
0.5
0.4
0.3
0.2
0.1
0
0
0.2
0.4
0.6
0.8
1.0
1.2
1.4
1.6
1.8
2.0
3.0
4.0
5.0
6.0
7.0
WAVELENGTH, MICRONS

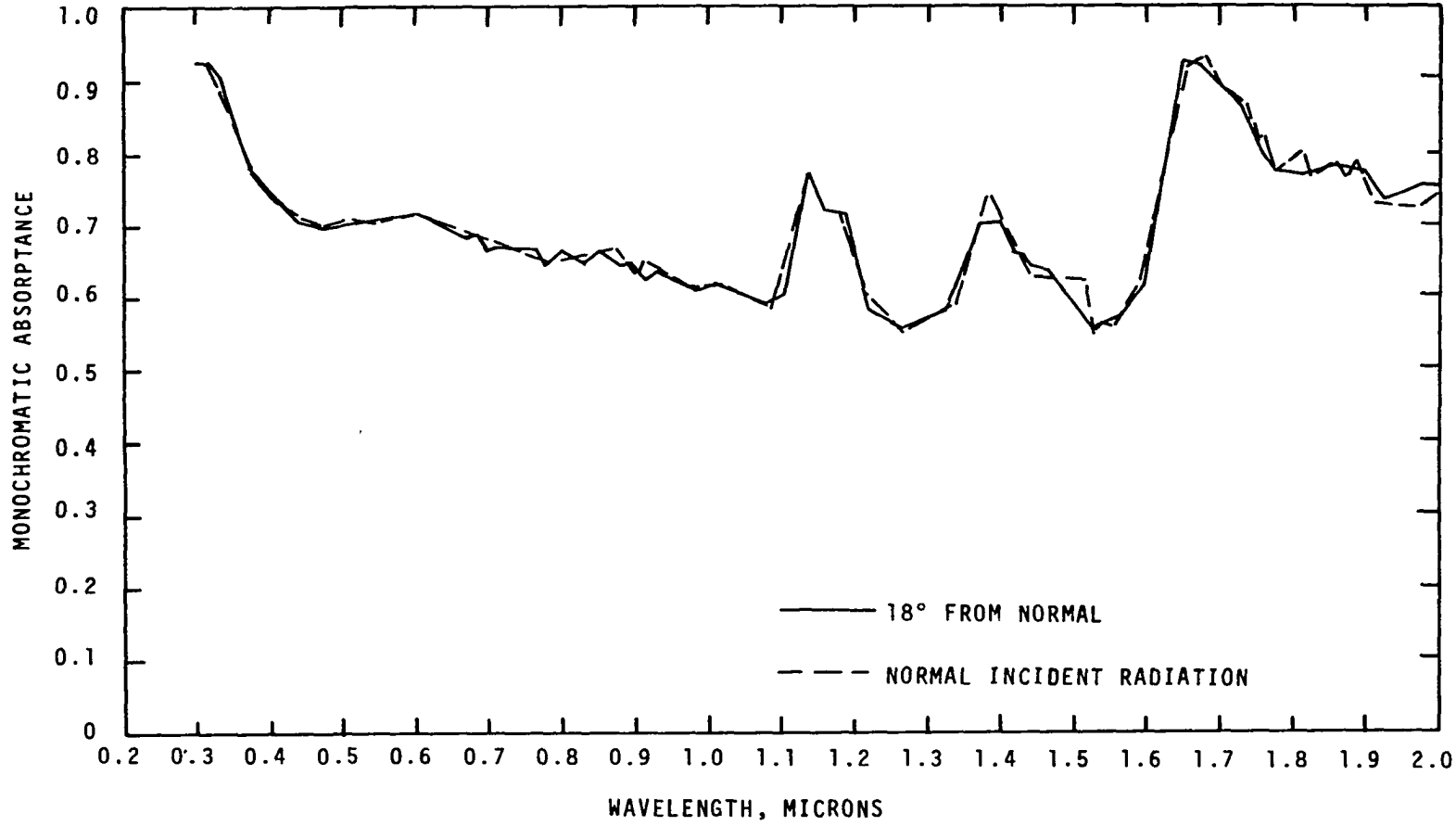

Figure D-45. Angular Variation of Absorptance of Lexan, Rough Surfaces.

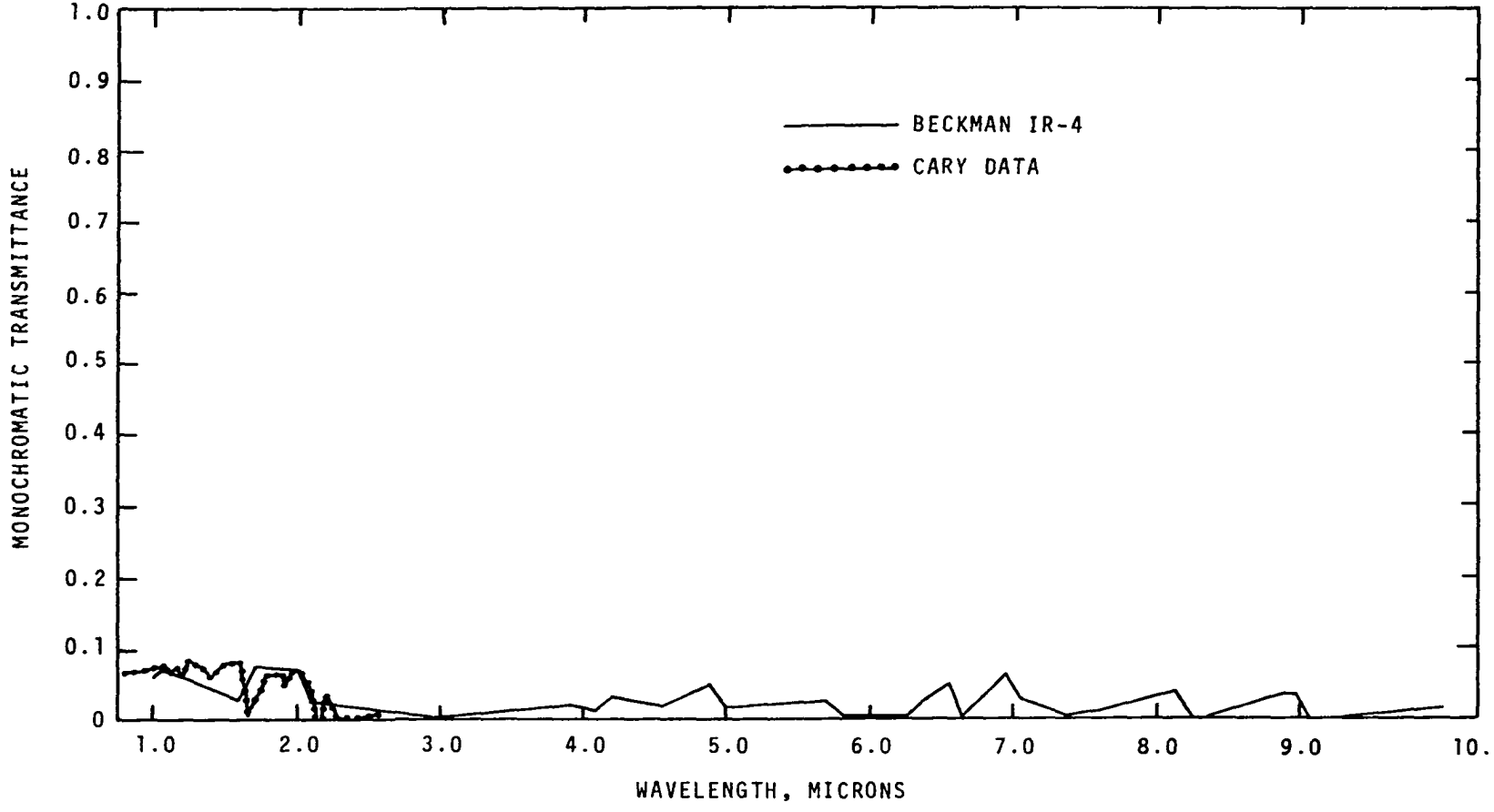

Figure D-46. Spectral Transmission of Lexan, Polished Surfaces.

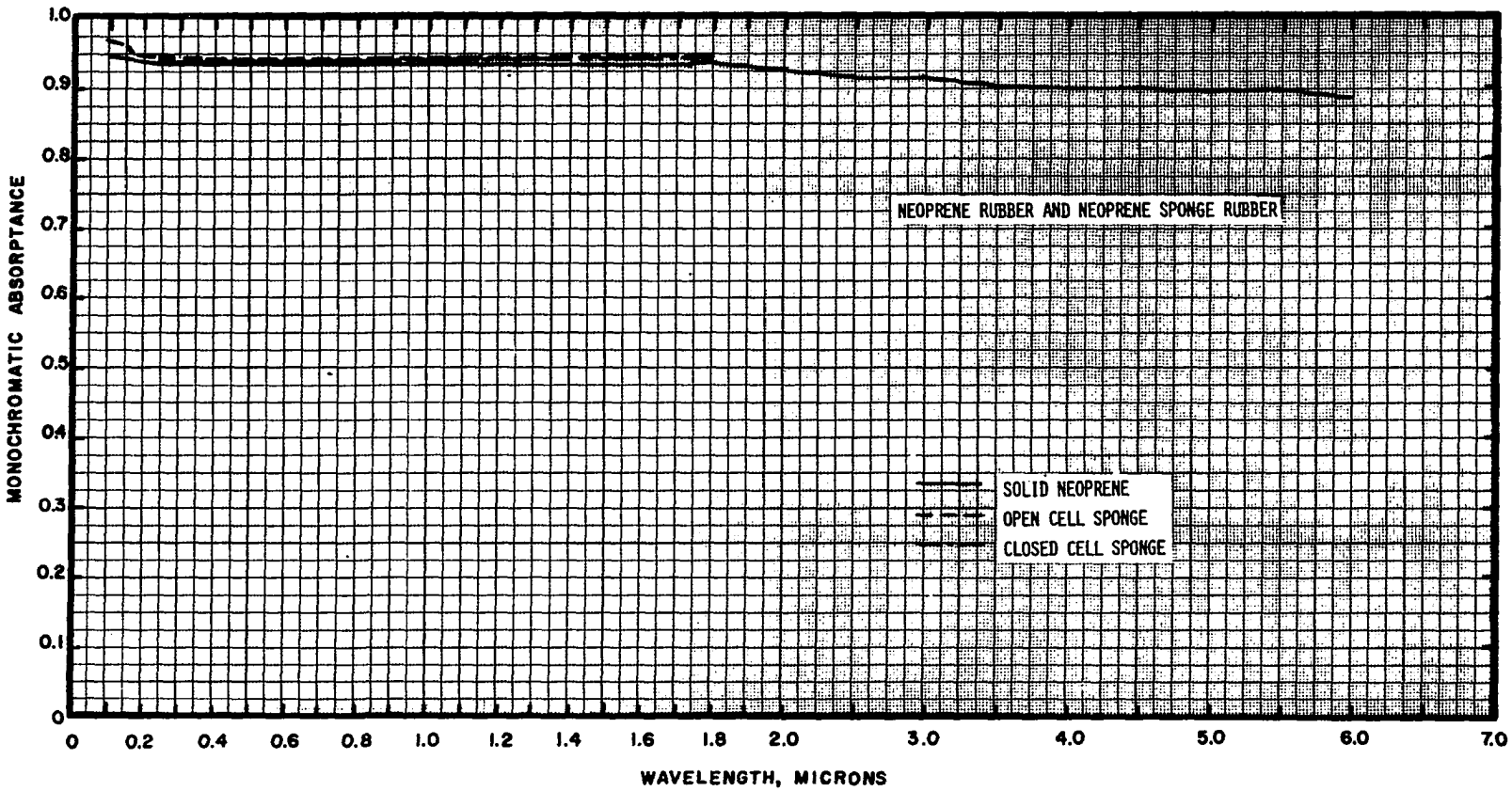

Figure D-47. Spectral Absorptance of Neoprene Rubber and Neoprene Sponge Rubbers.

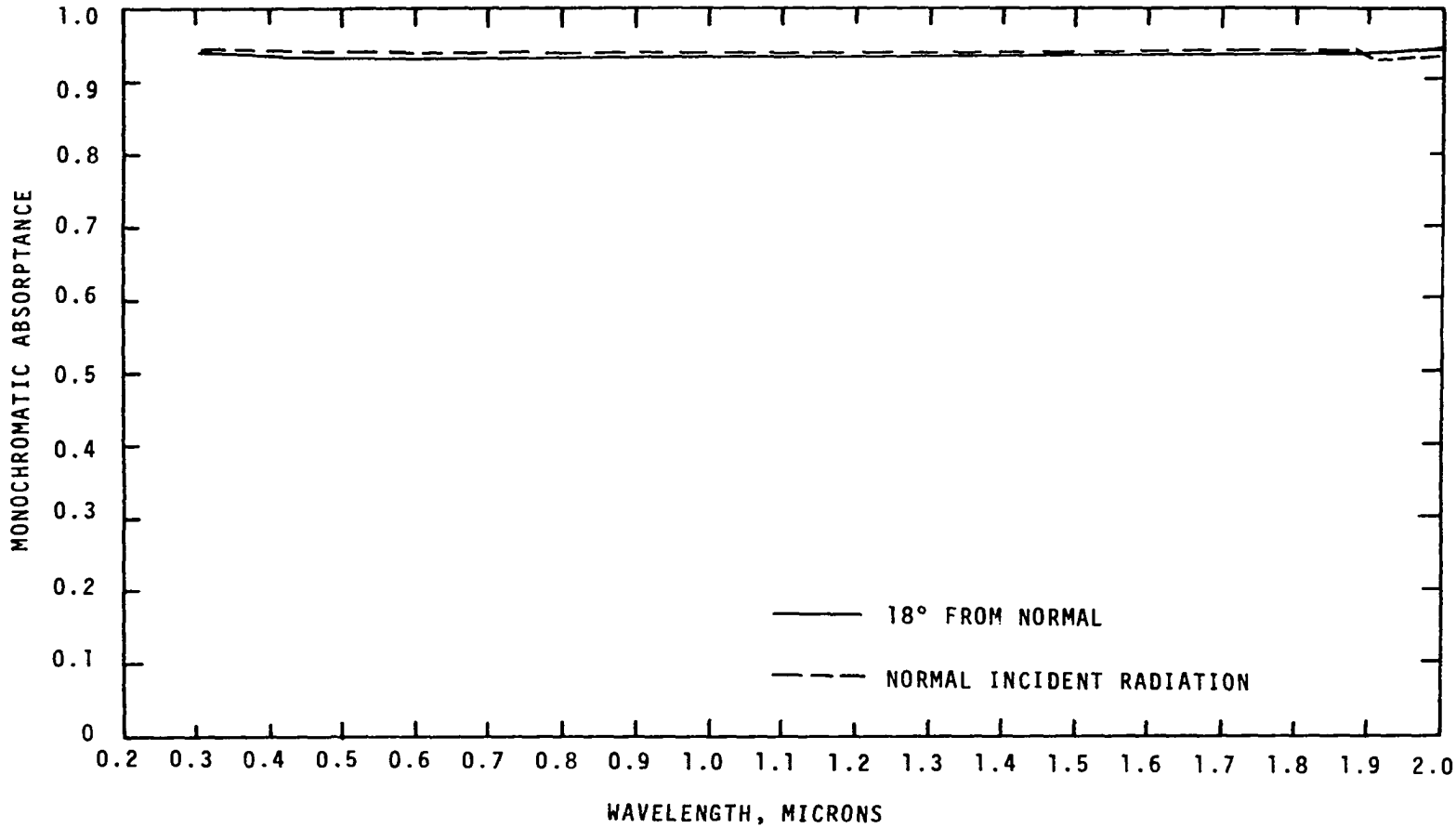

Figure D-48. Angular Variation of Absorptance for Neoprene Rubber.

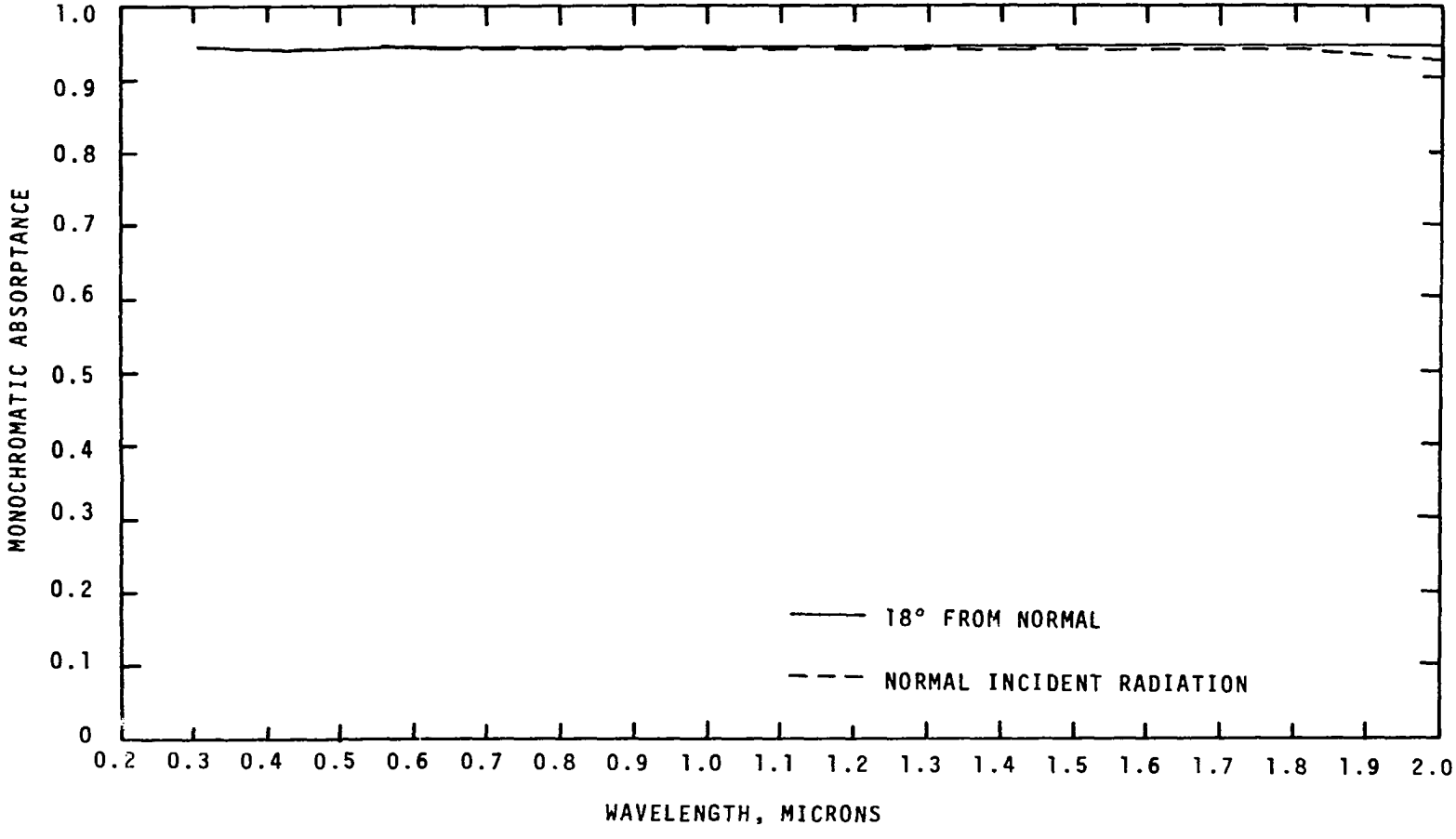

Figure D-49. Angular Variation of Absorptance for Neoprene Closed Cell Sponge Rubber.

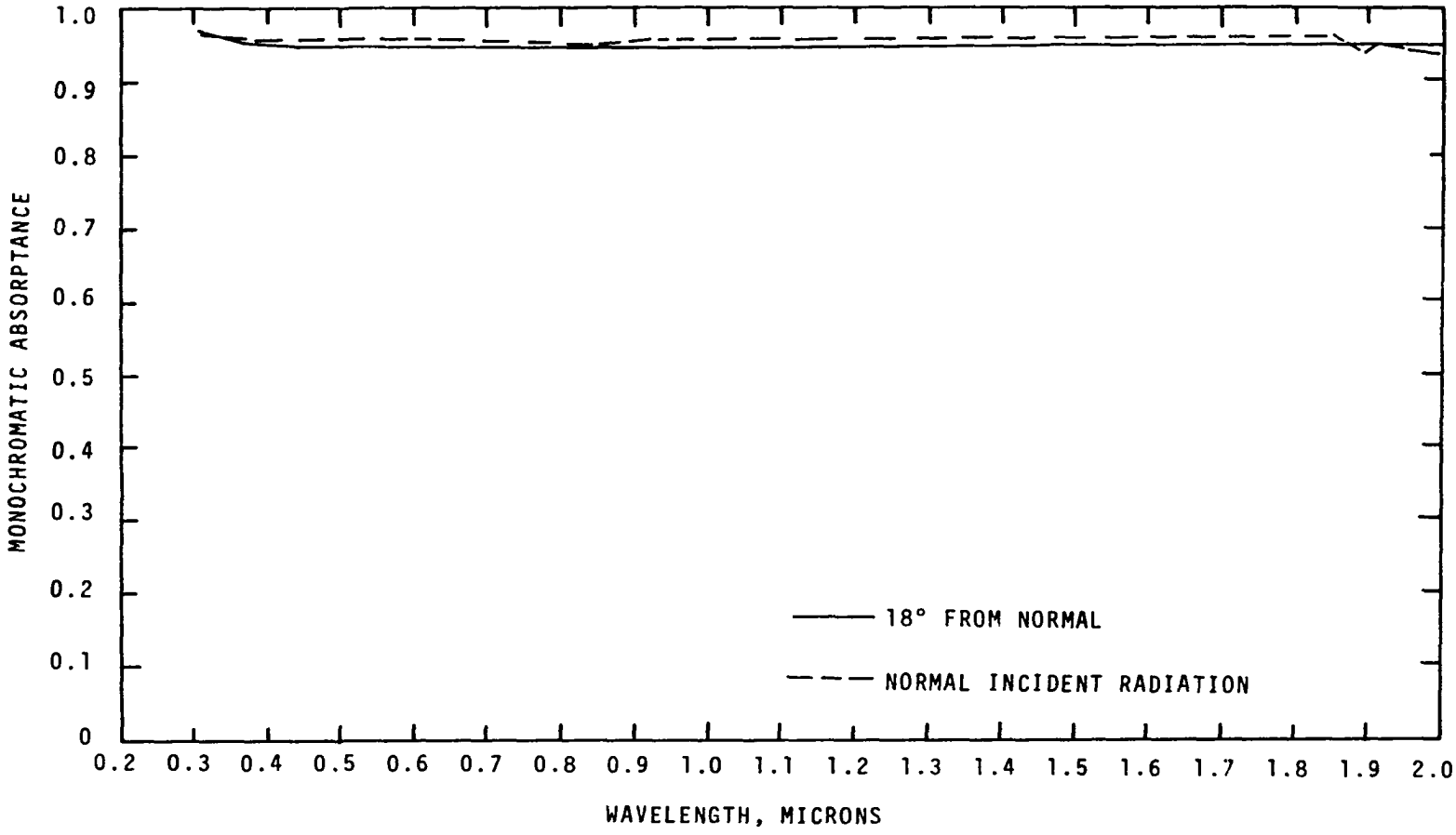

Figure D-50. Angular Variation of Absorptance for Neoprene Open Cell Sponge Rubber.

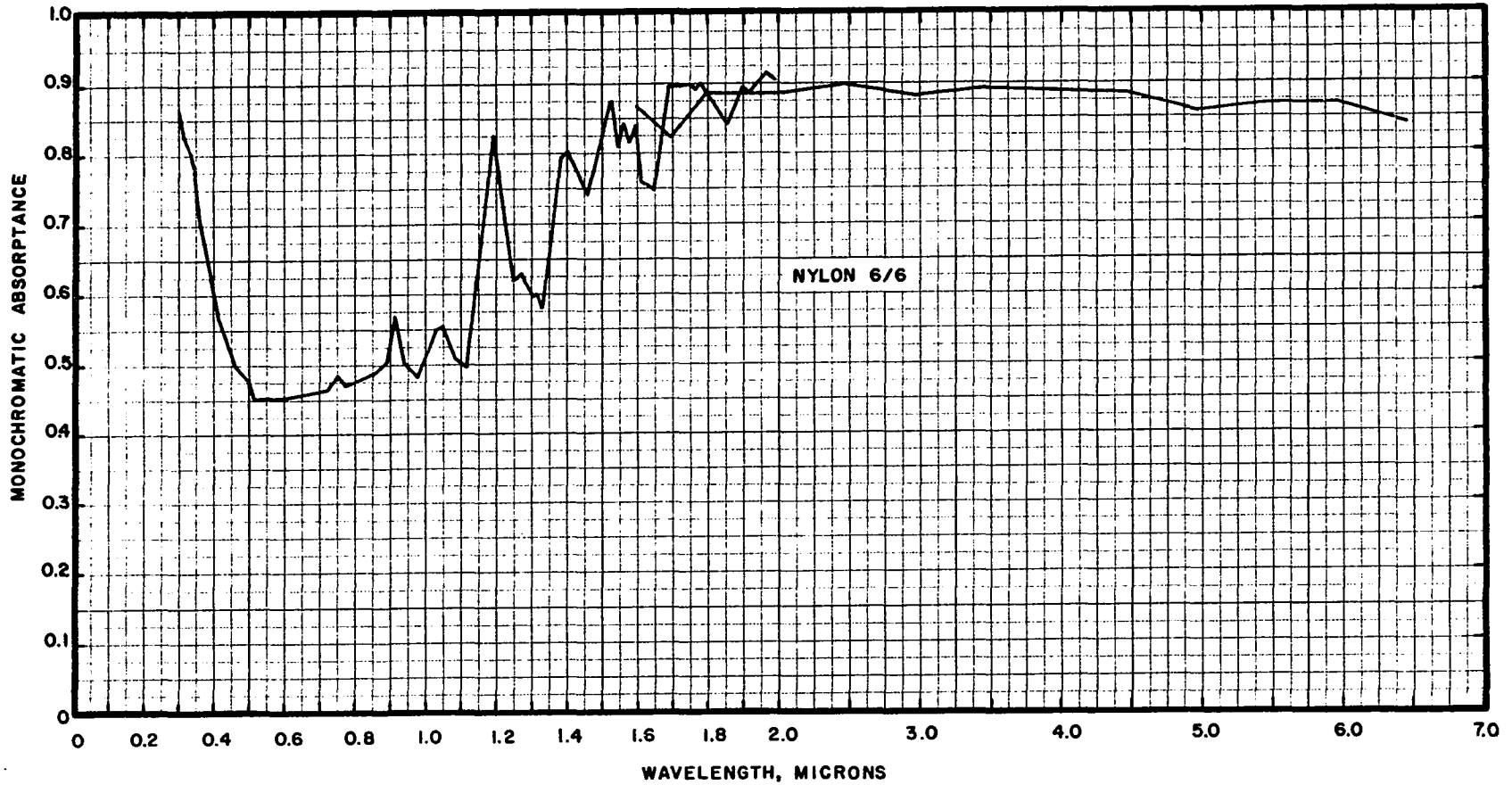

Figure D-51. Spectral Absorptance of Nylon 6/6.

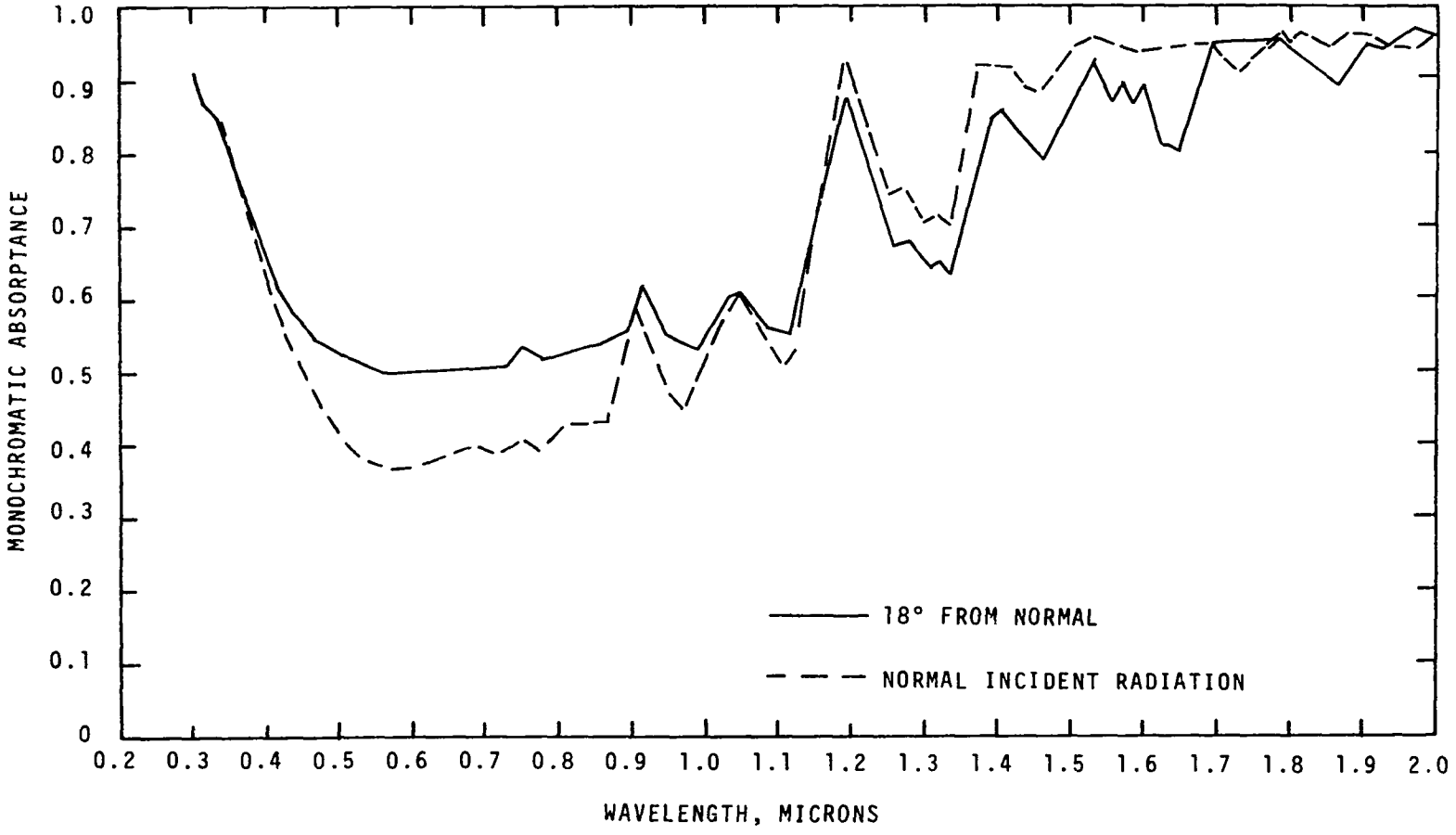

Figure D-52. Angular Variation of Absorptance of Nylon 6/6.

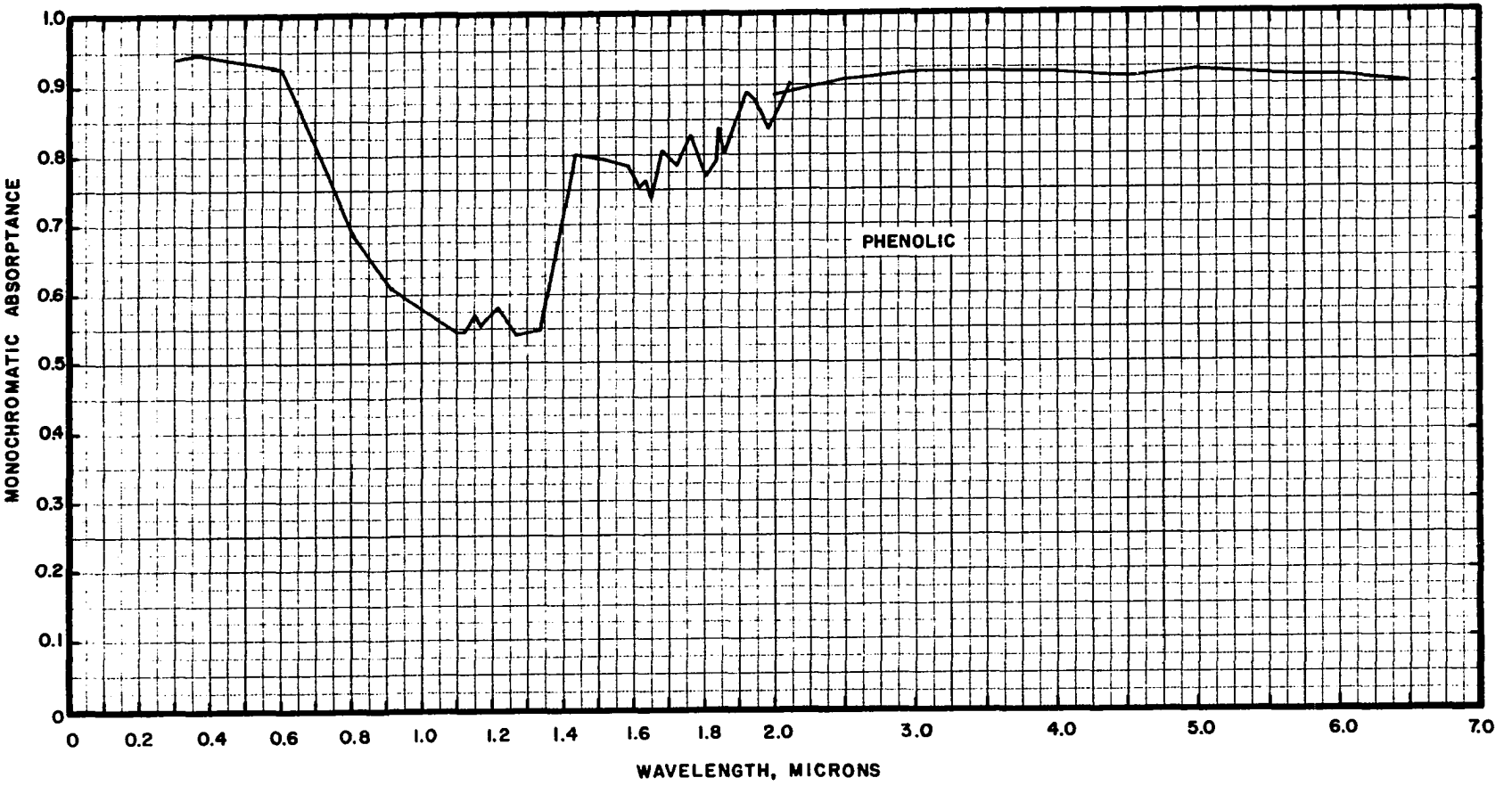

Figure D-53. Spectral Absorptance of Phenolic (Bakelite).

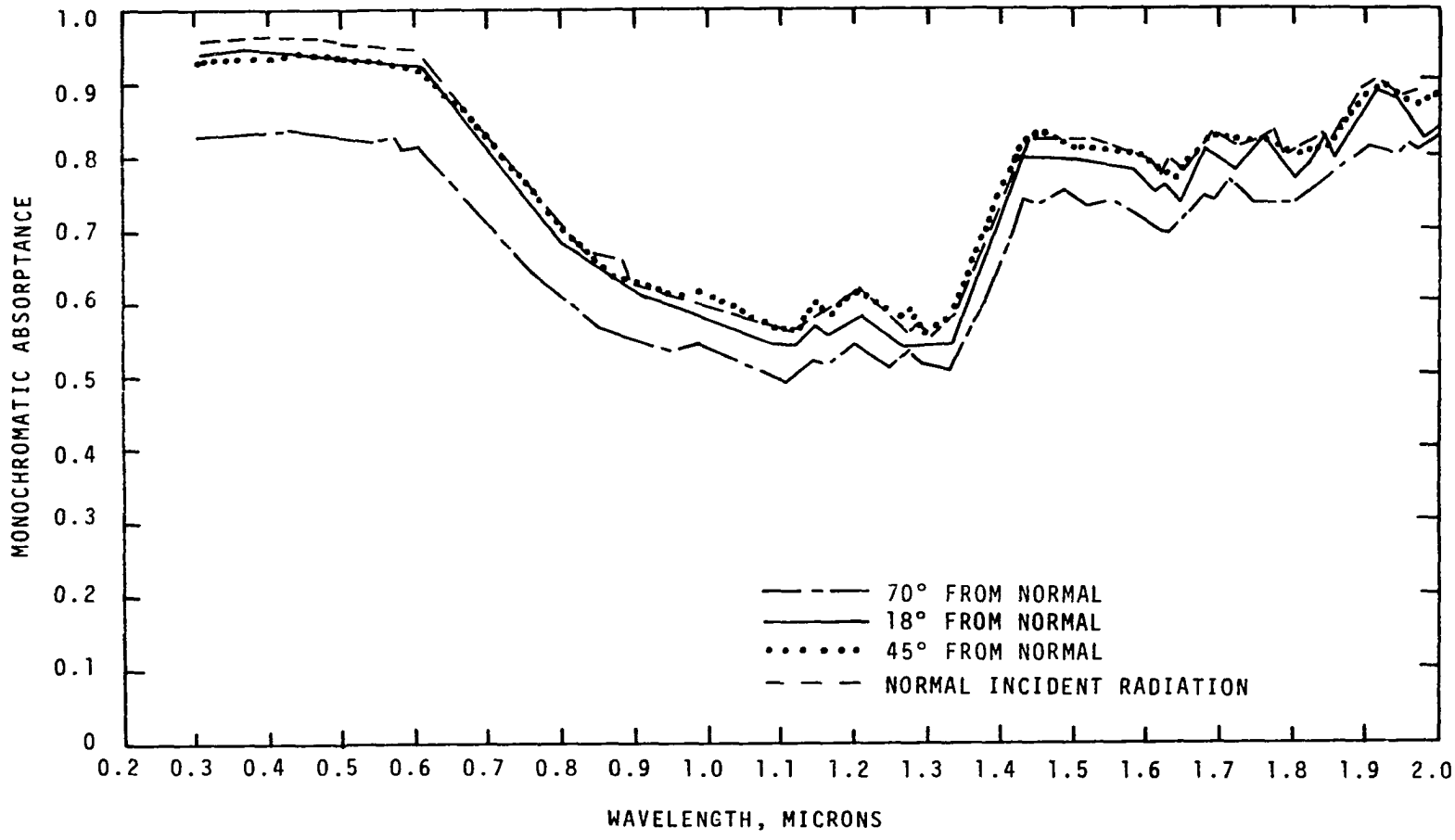

Figure D-54. Angular Variation of Phenolic.

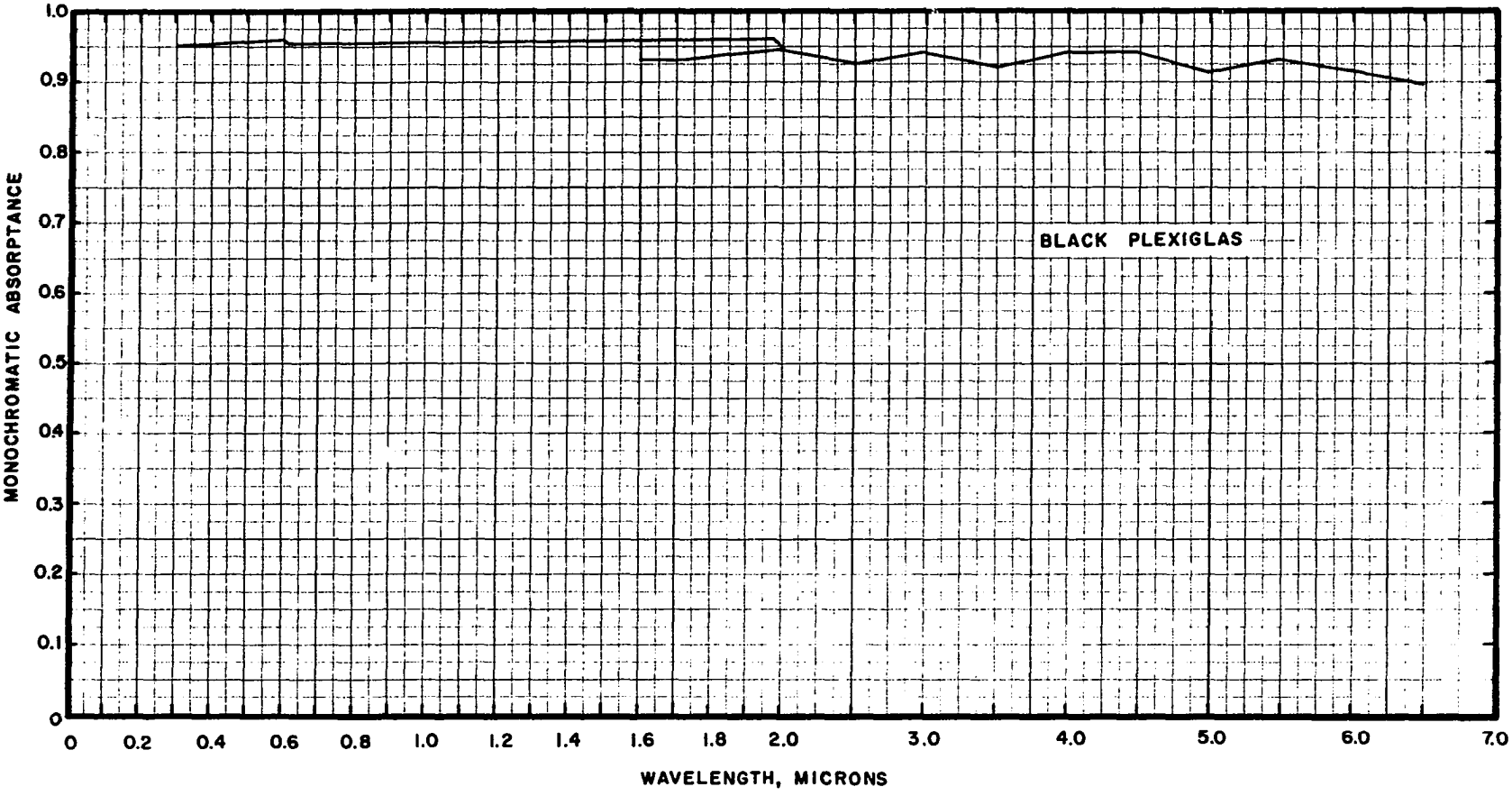

Figure D-55. Spectral Absorptance of Black Plexiglas.

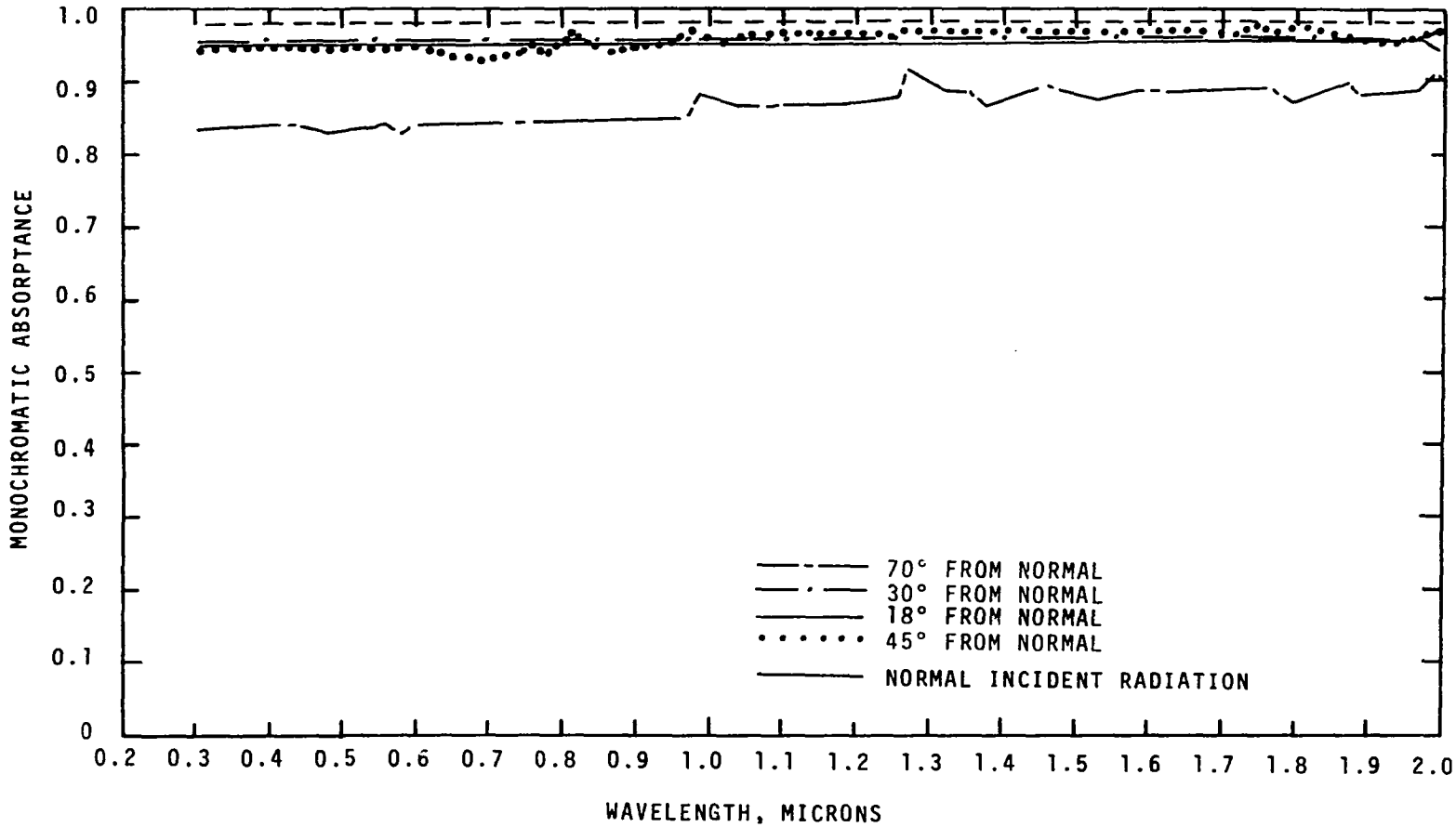

Figure D-56. Angular Variation of Absorptance for Black Plexiglas.

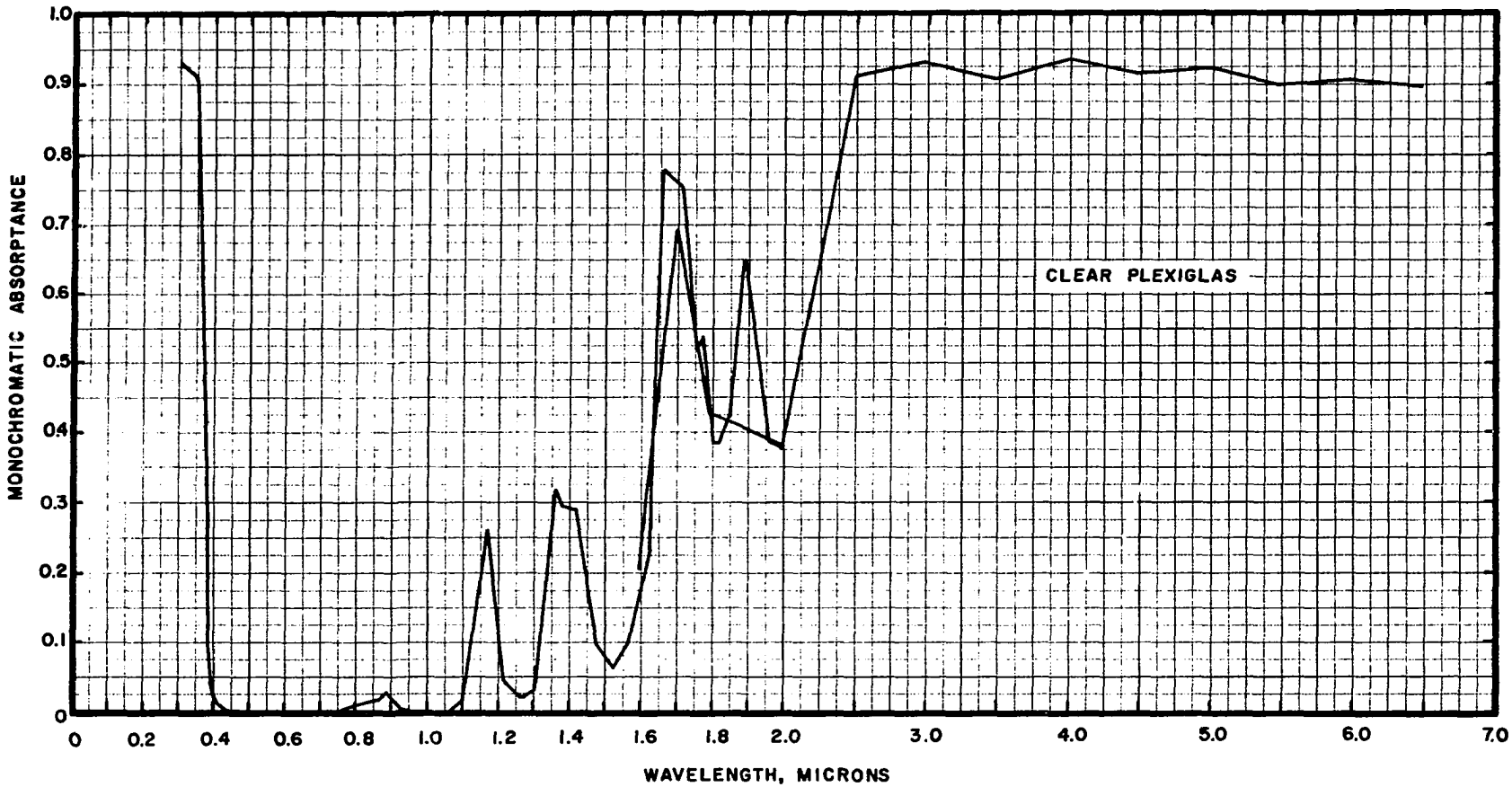

Figure D-57. Spectral Absorptance of Clear Plexiglas.

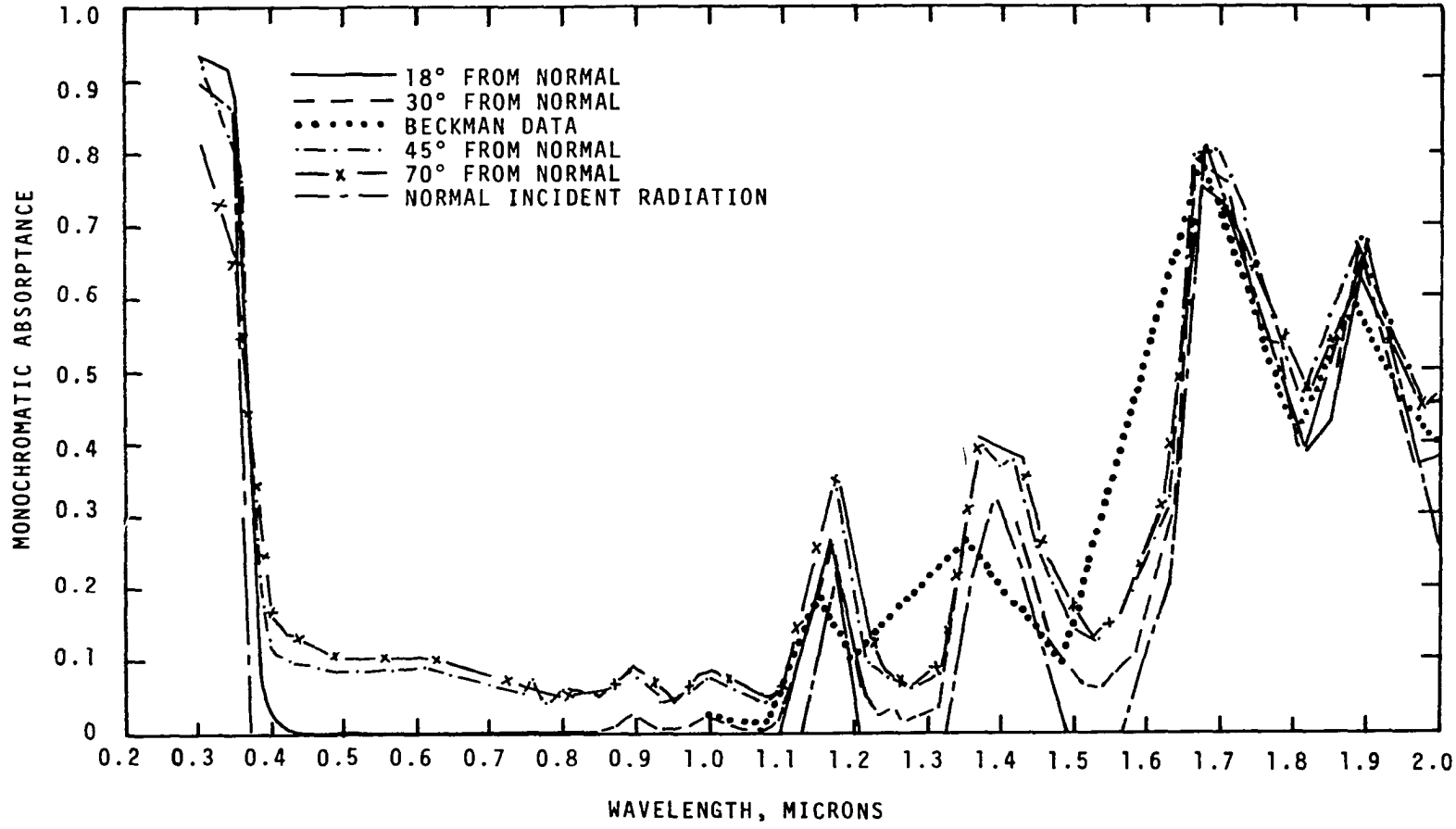

Figure D-58. Angular Variation of Absorptance for Clear Plexiglas.

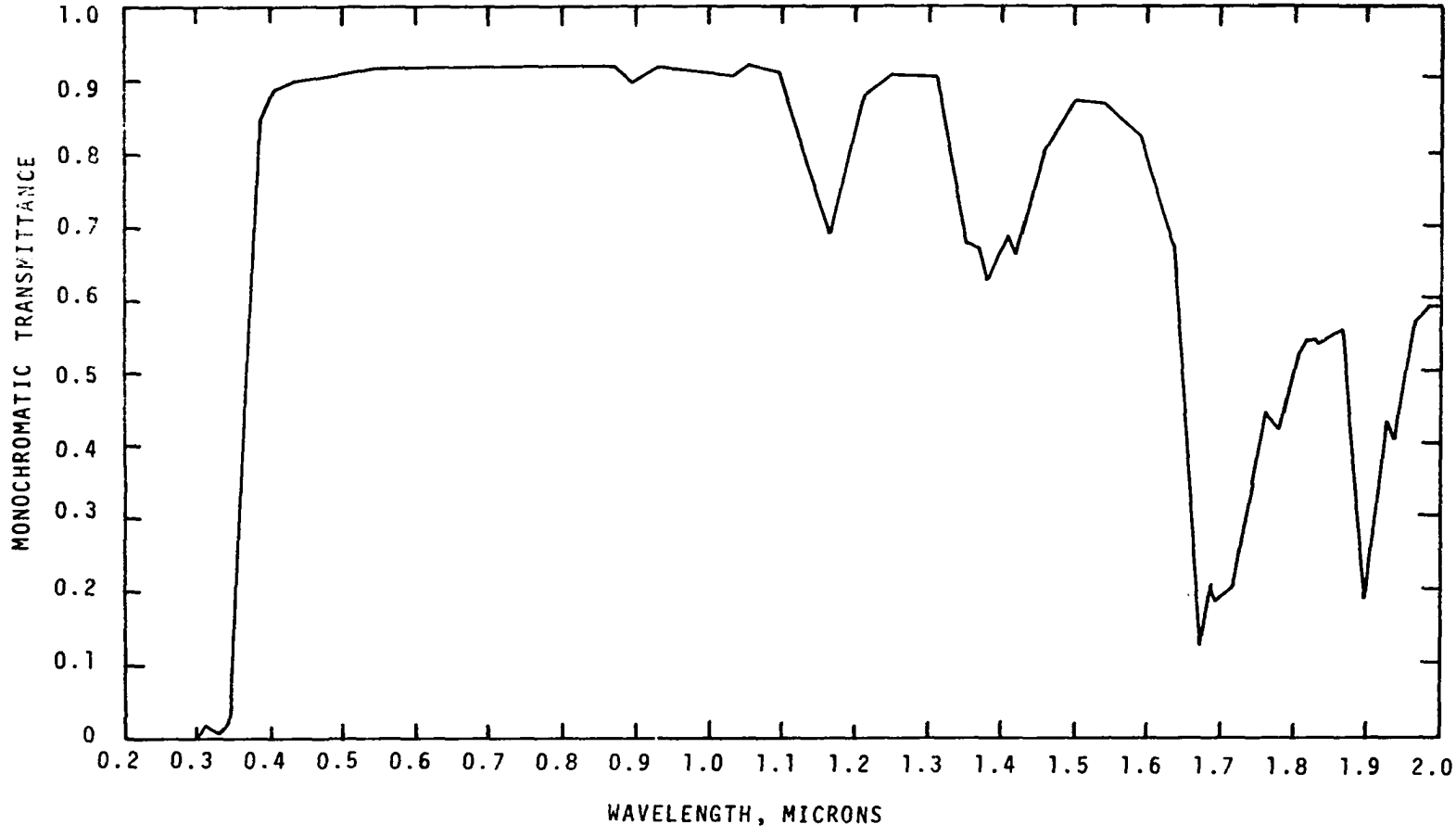

Figure D-59. Spectral Transmittance of Clear Plexiglas, 0.3 - 2.0 Microns.

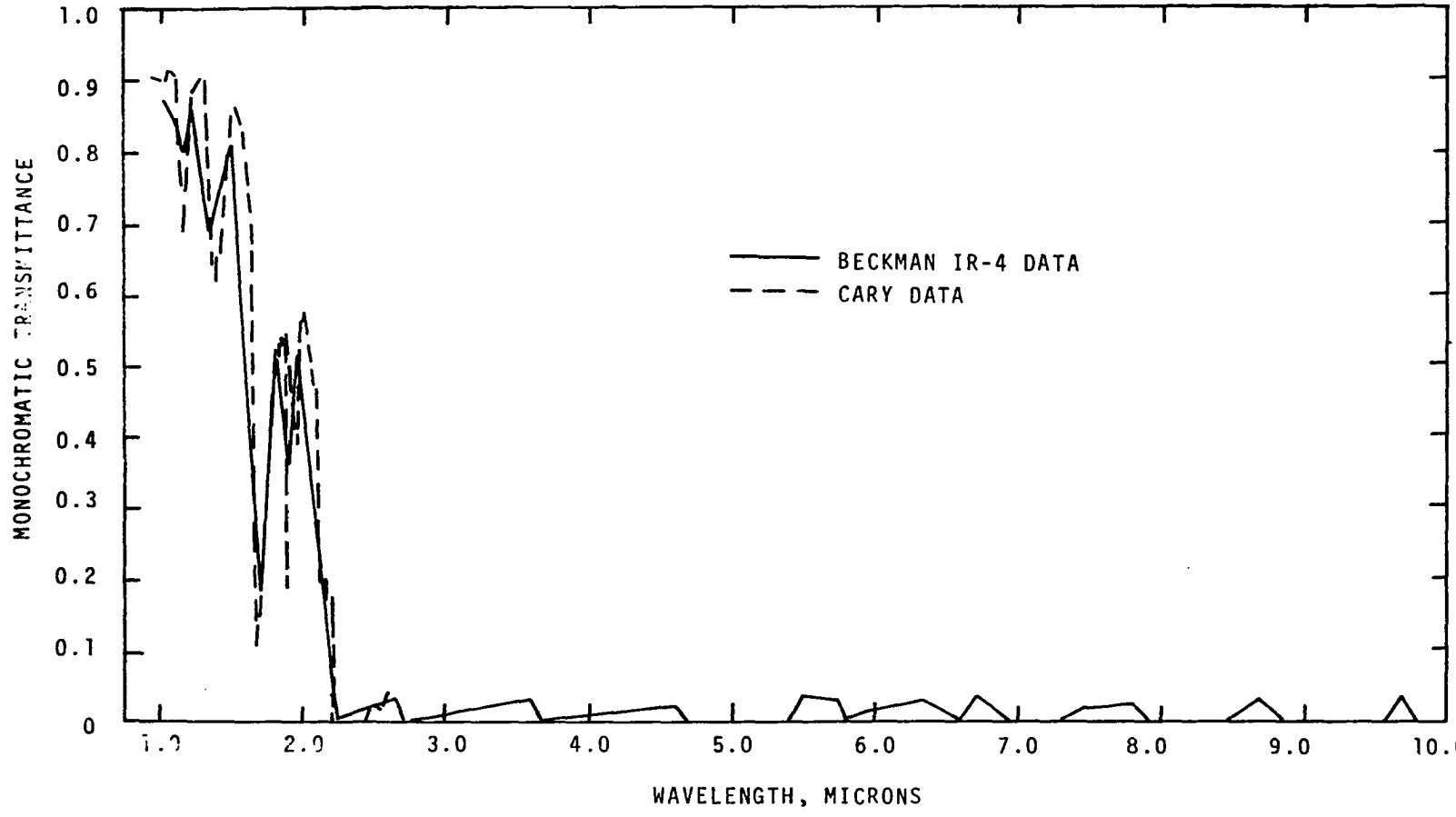

Figure D-60. Spectral Transmittance of Clear Plexiglas, 1.0 - 10.0 Microns.

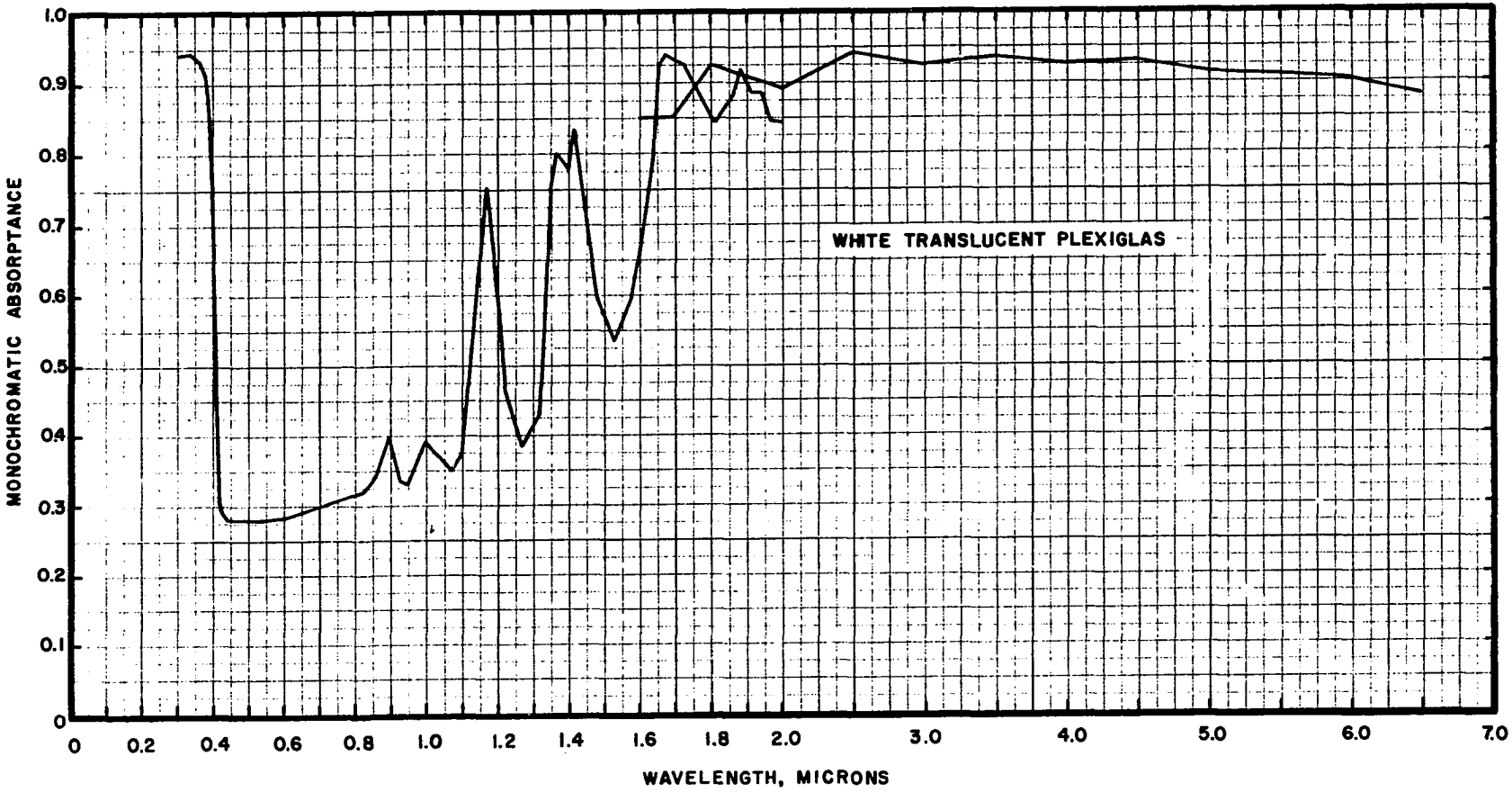

Figure D-61. Spectral Absorptance of White Translucent Plexiglas.

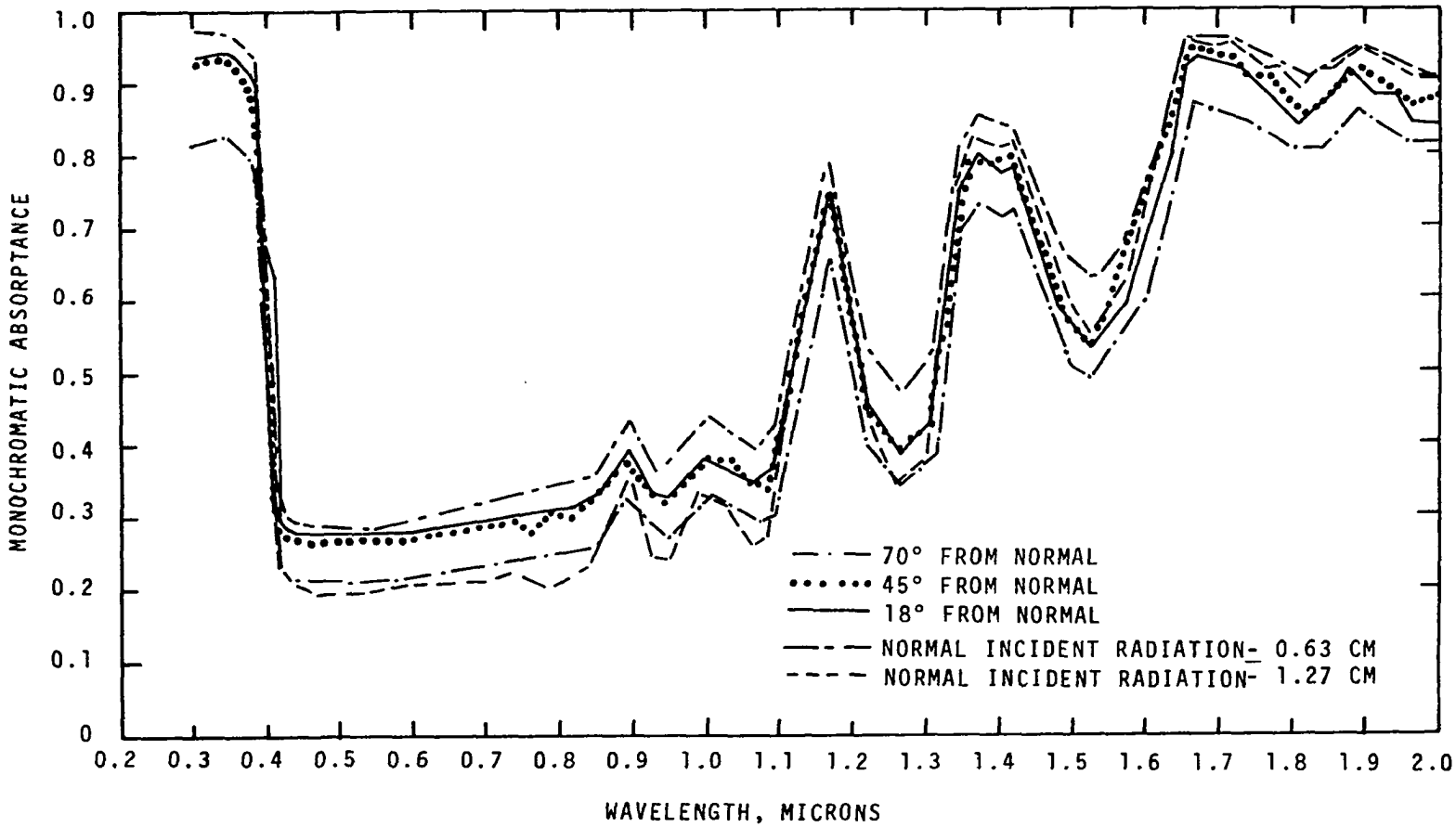

Figure D-62. Angular Variation of Absorptance for Plexiglas.

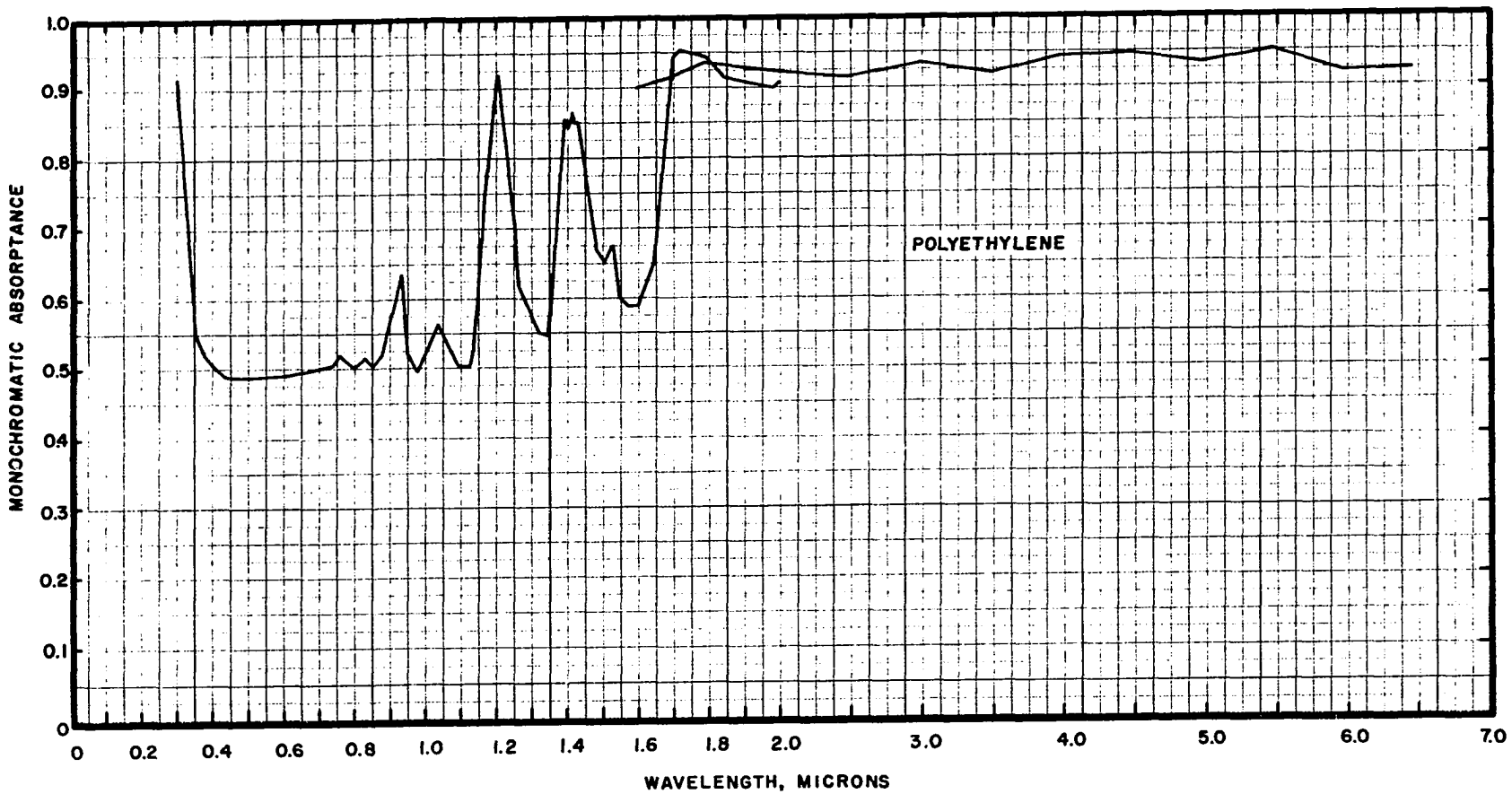

Figure D-63. Spectral Absorptance of Polyethylene.

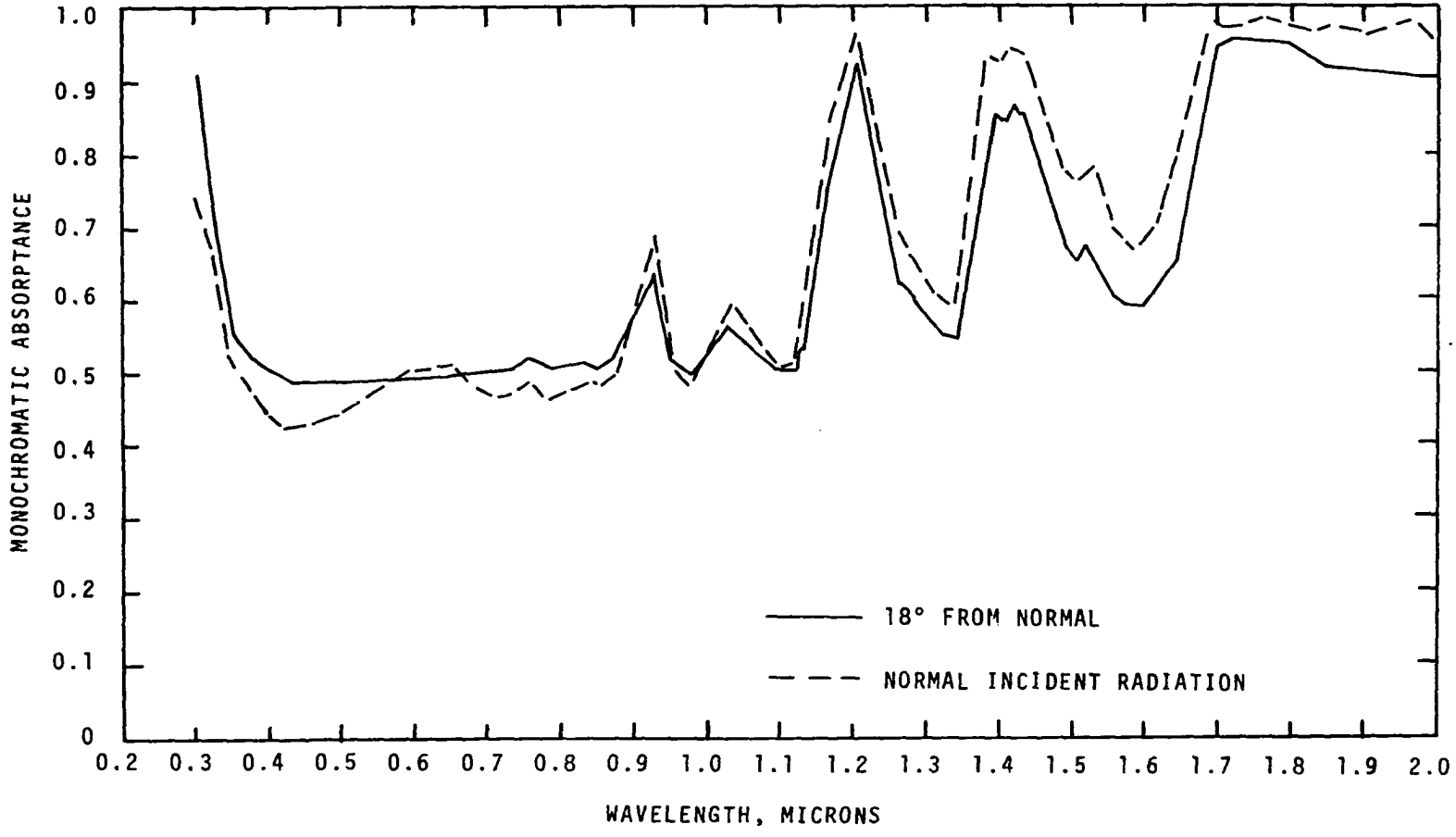

Figure D-64. Angular Variation of Absorptance for Polyethylene.

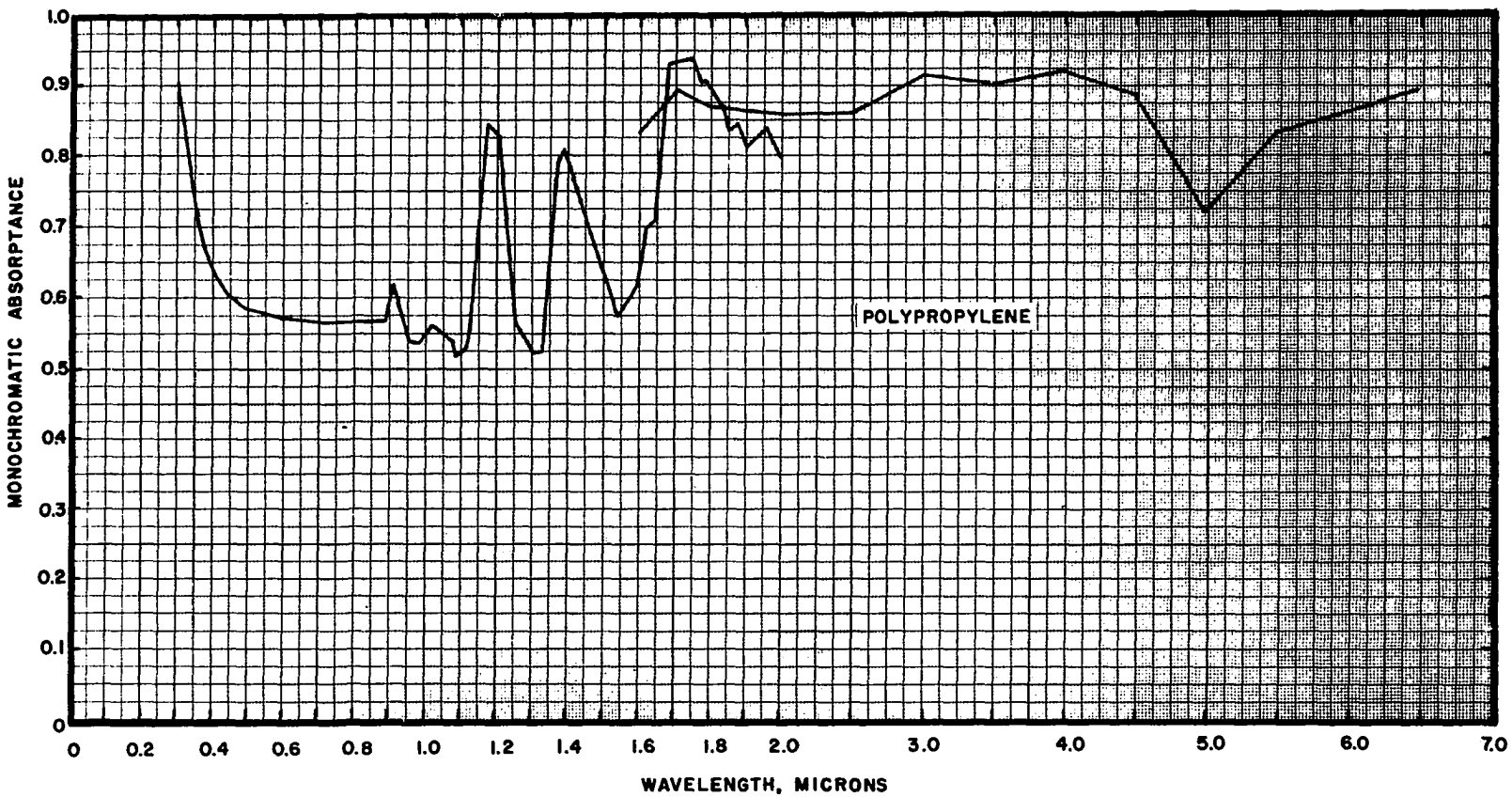

Figure D-65. Spectral Absorptance of Polypropylene.

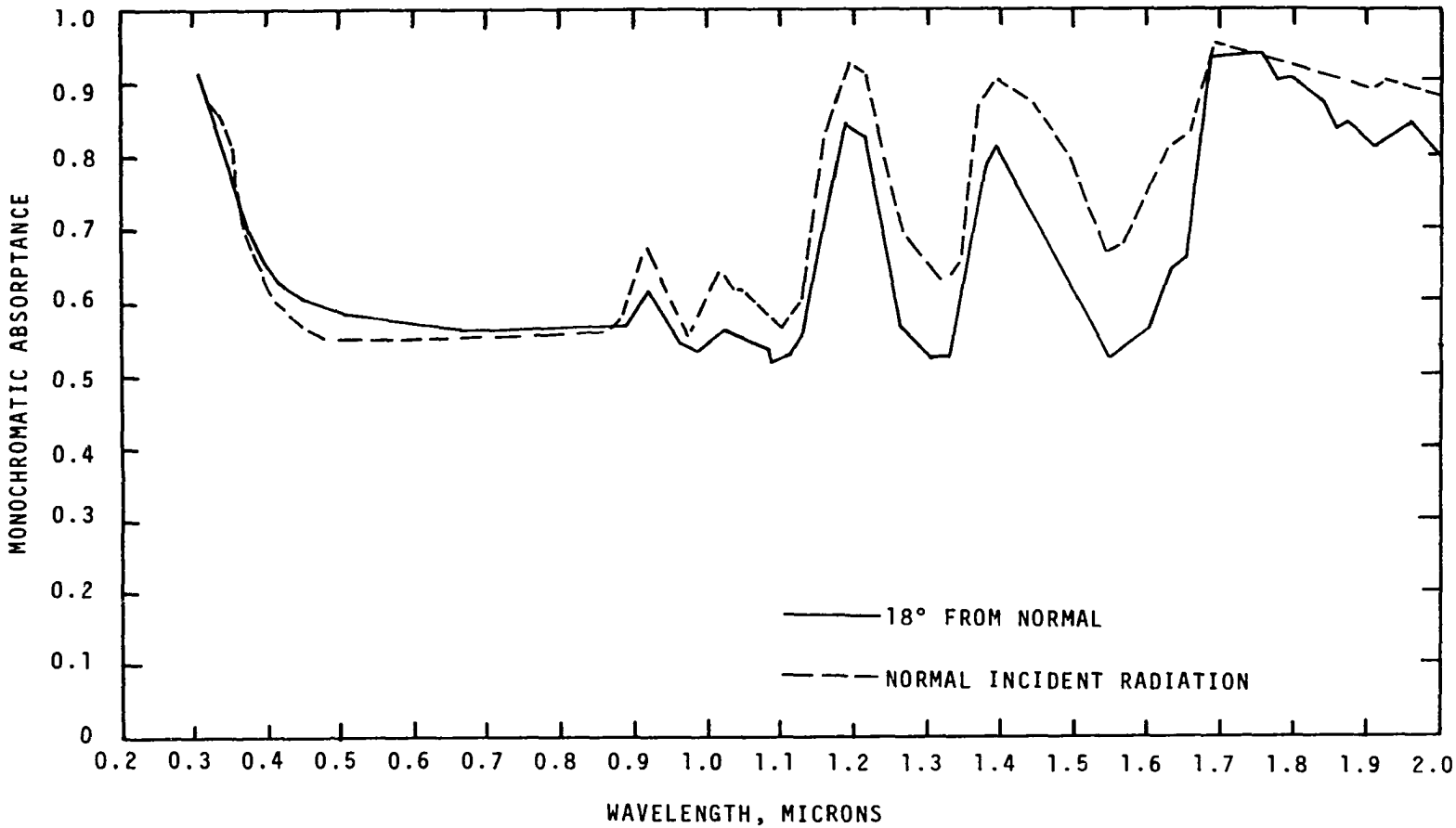

Figure D-66. Angular Variation of Absorptance for Polypropylene.

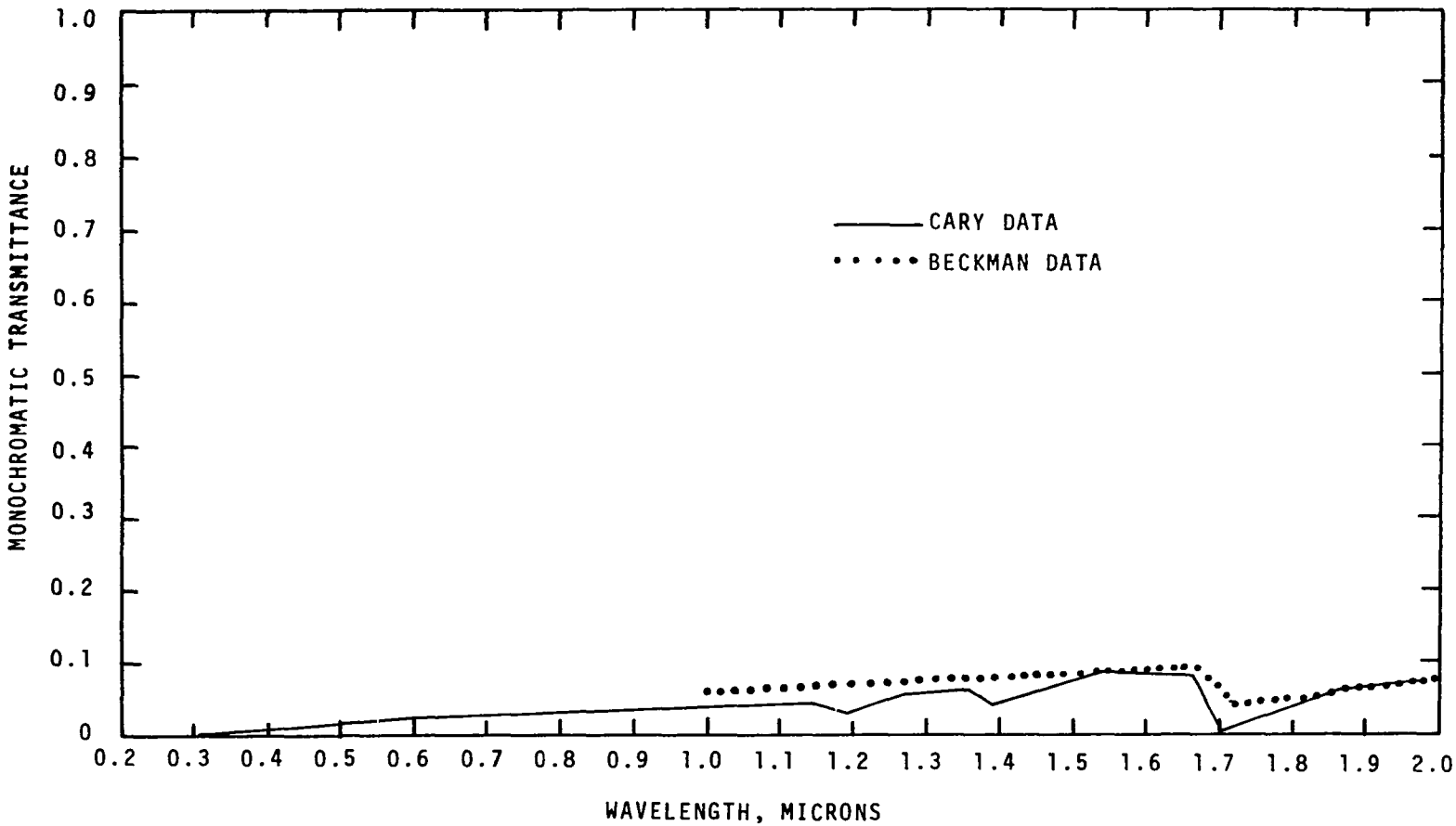

Figure D-67. Spectral Transmittance of Polypropylene, 0.3 - 2.0 Microns.

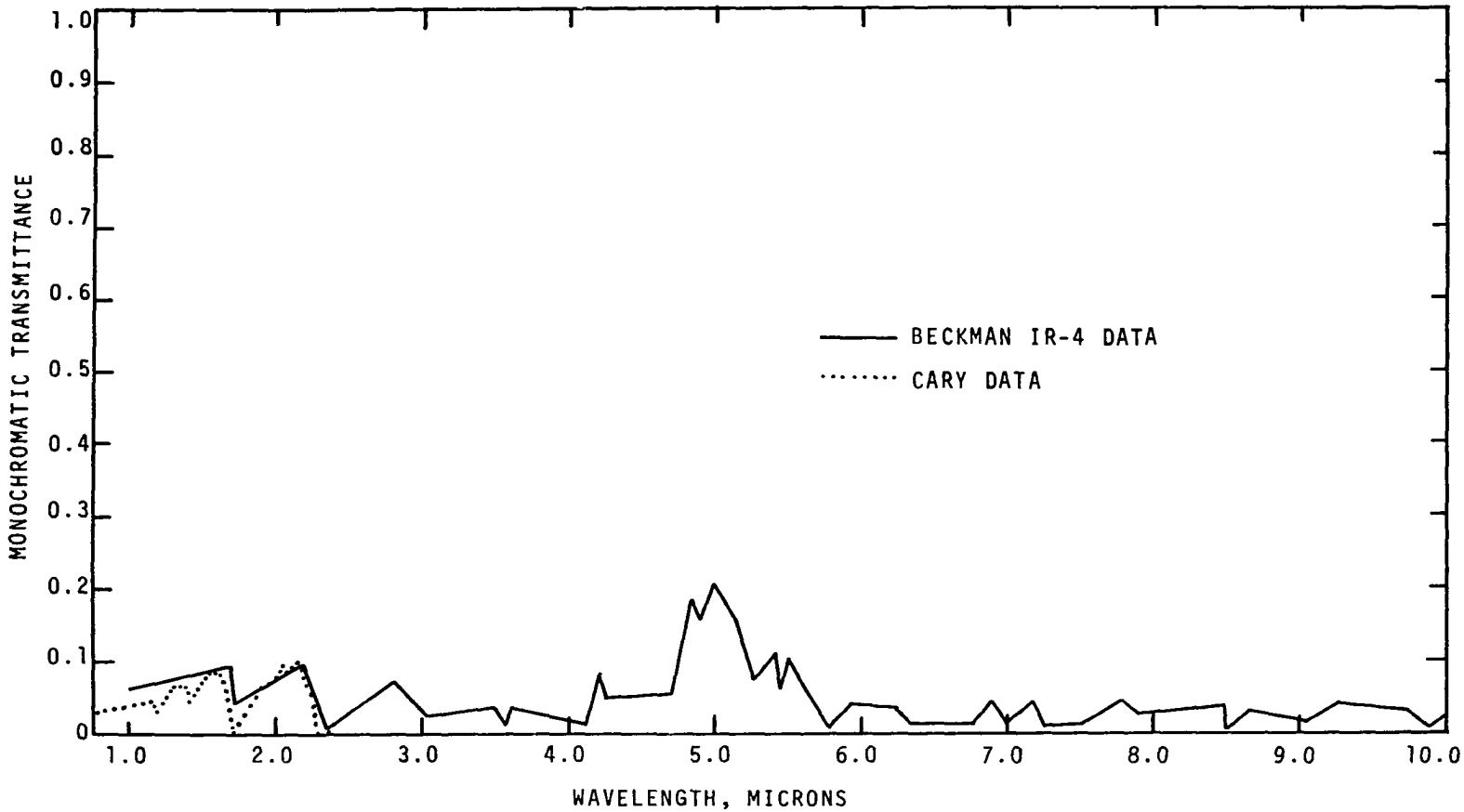

Figure D-68. Spectral Transmittance of Polypropylene, 1.0 - 10.0 Microns.

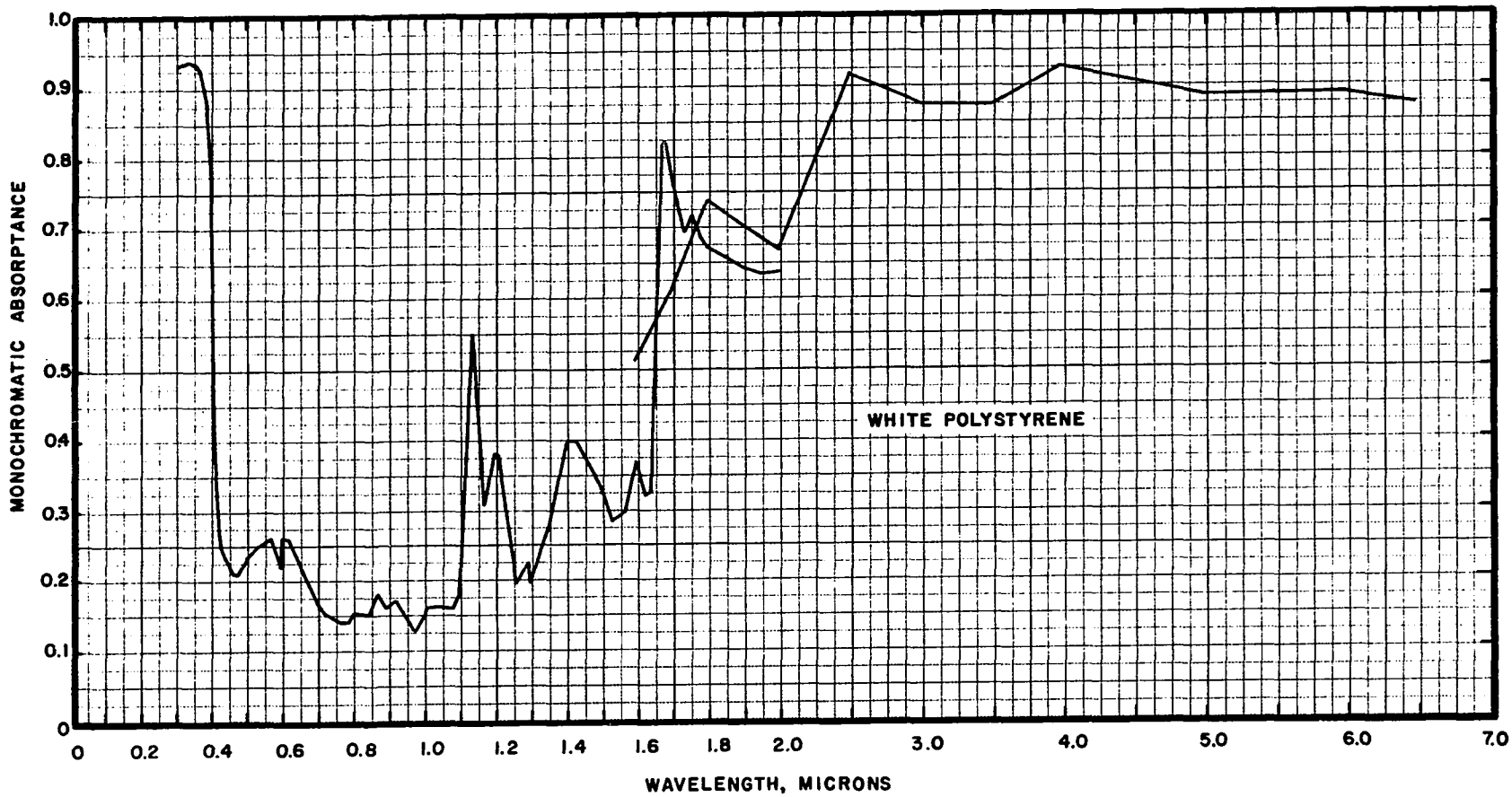

Figure D-69. Spectral Absorptance of White Polystyrene.

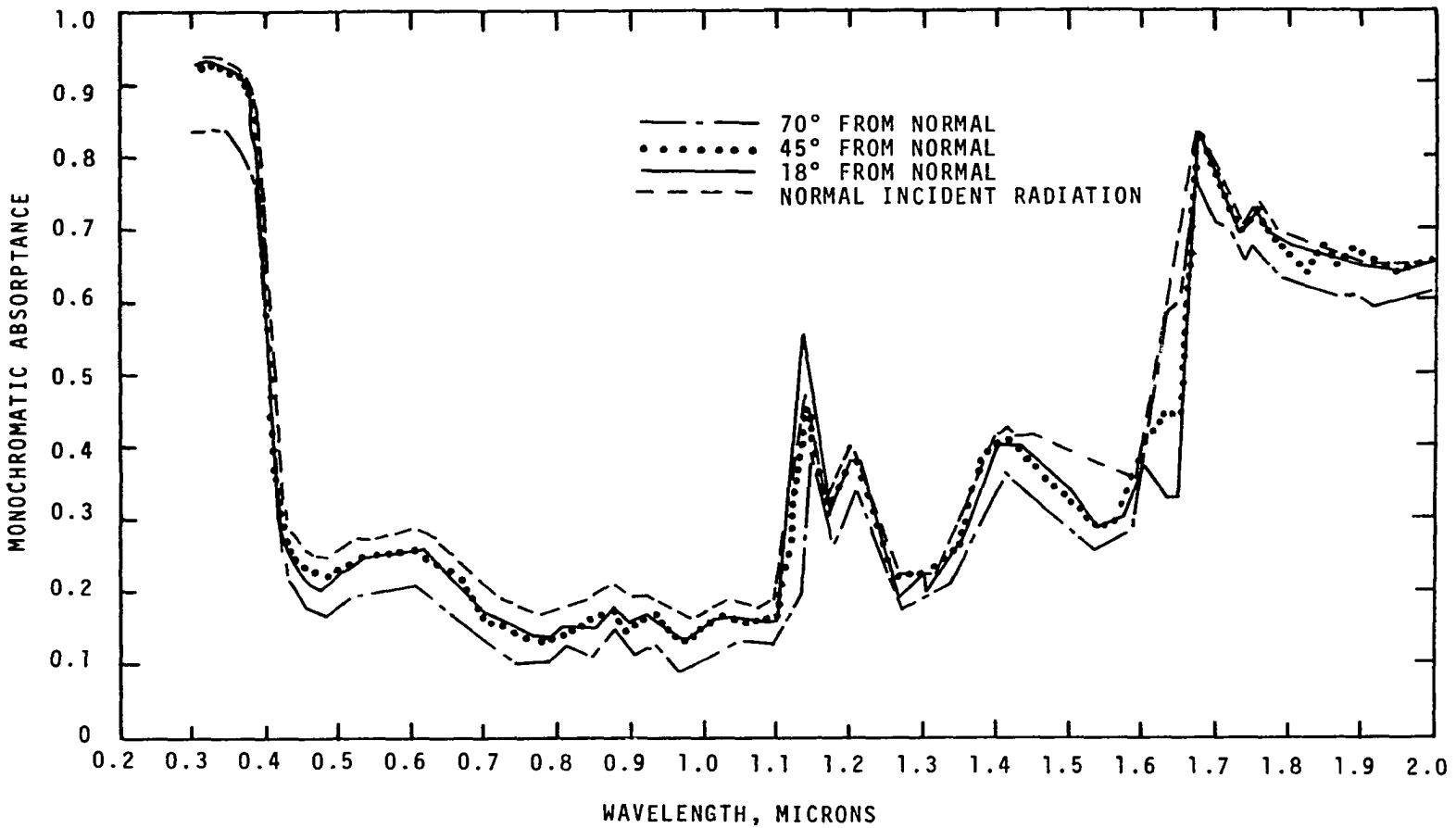

Figure D-70. Angular Variation of Absorptance for White Polystyrene, Sample I.

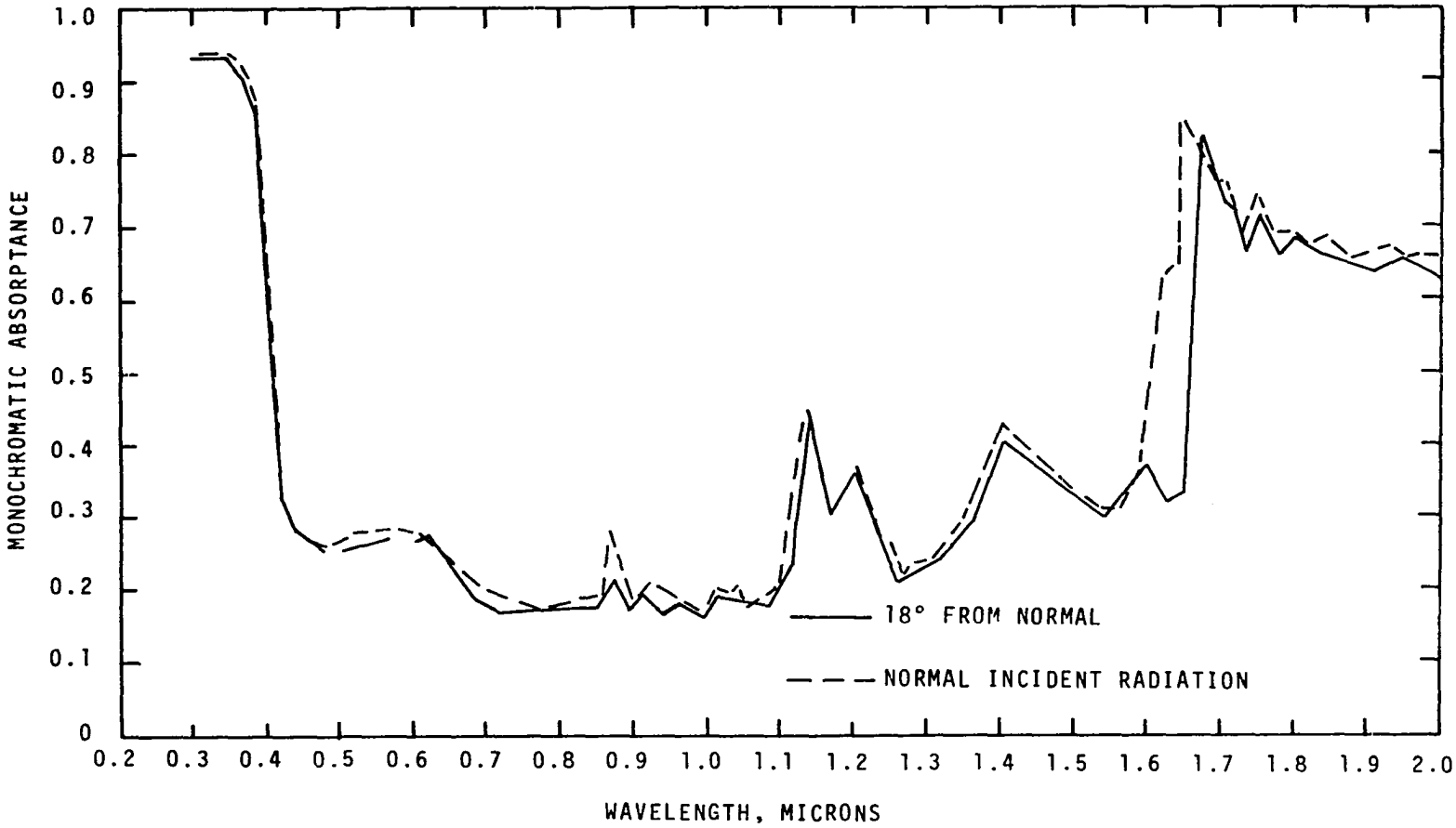

Figure D-71. Angular Variation of Absorptance for White Polystyrene, Sample II.

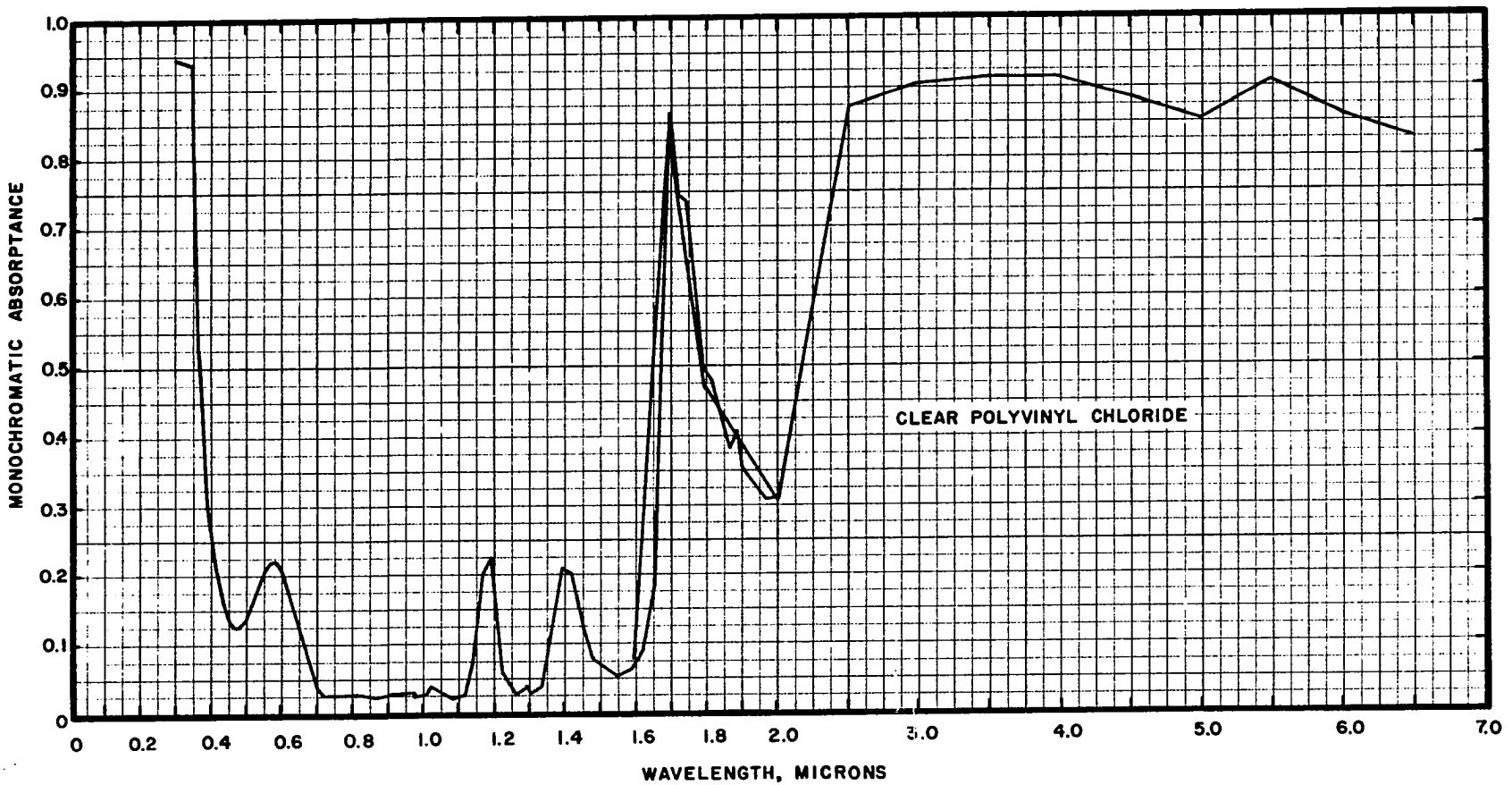

Figure D-72. Spectral Absorptance of Clear Poly(vinyl chloride).

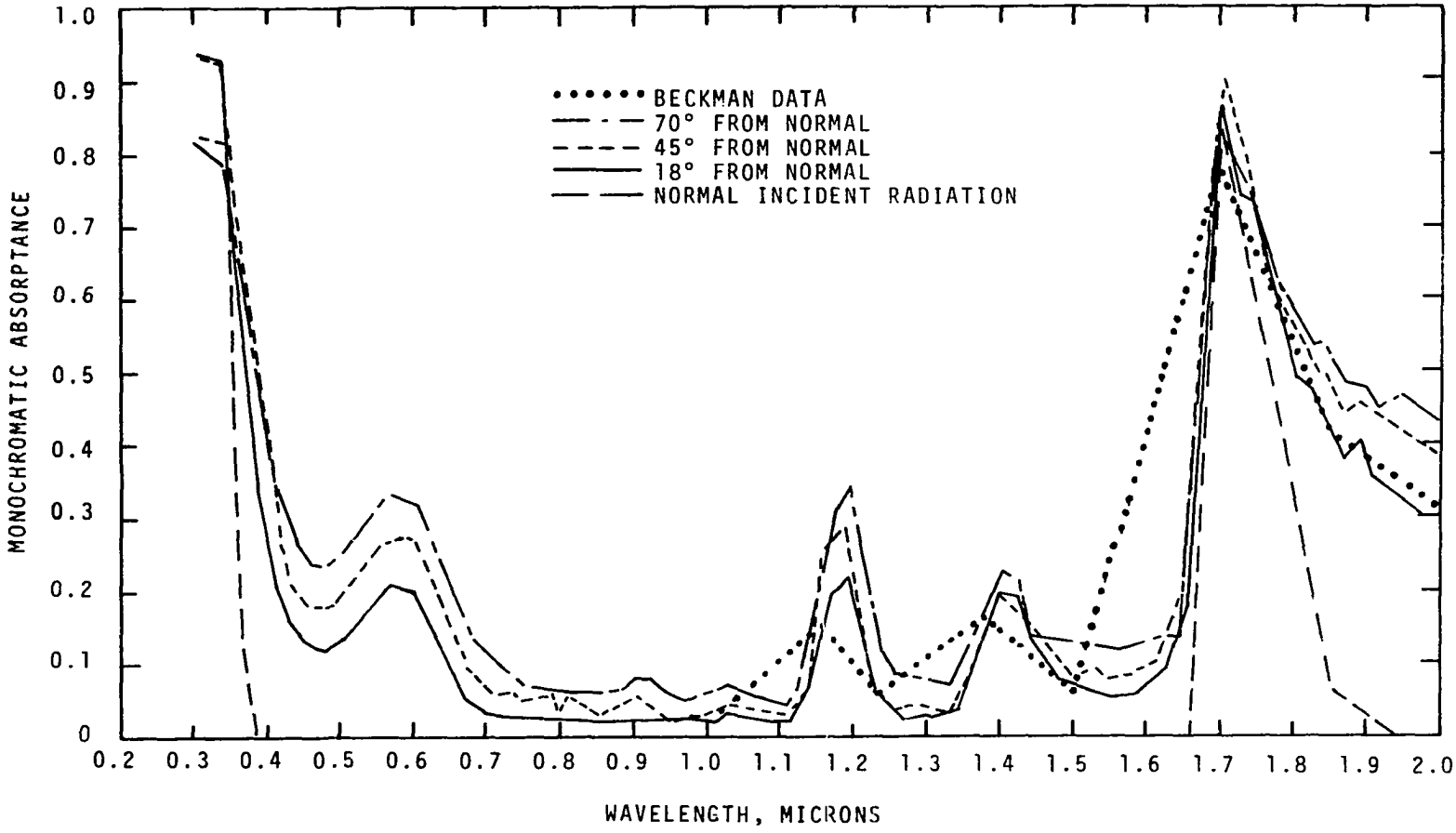

Figure D-73. Angular Variation of Absorptance of Clear Poly(vinyl chloride).

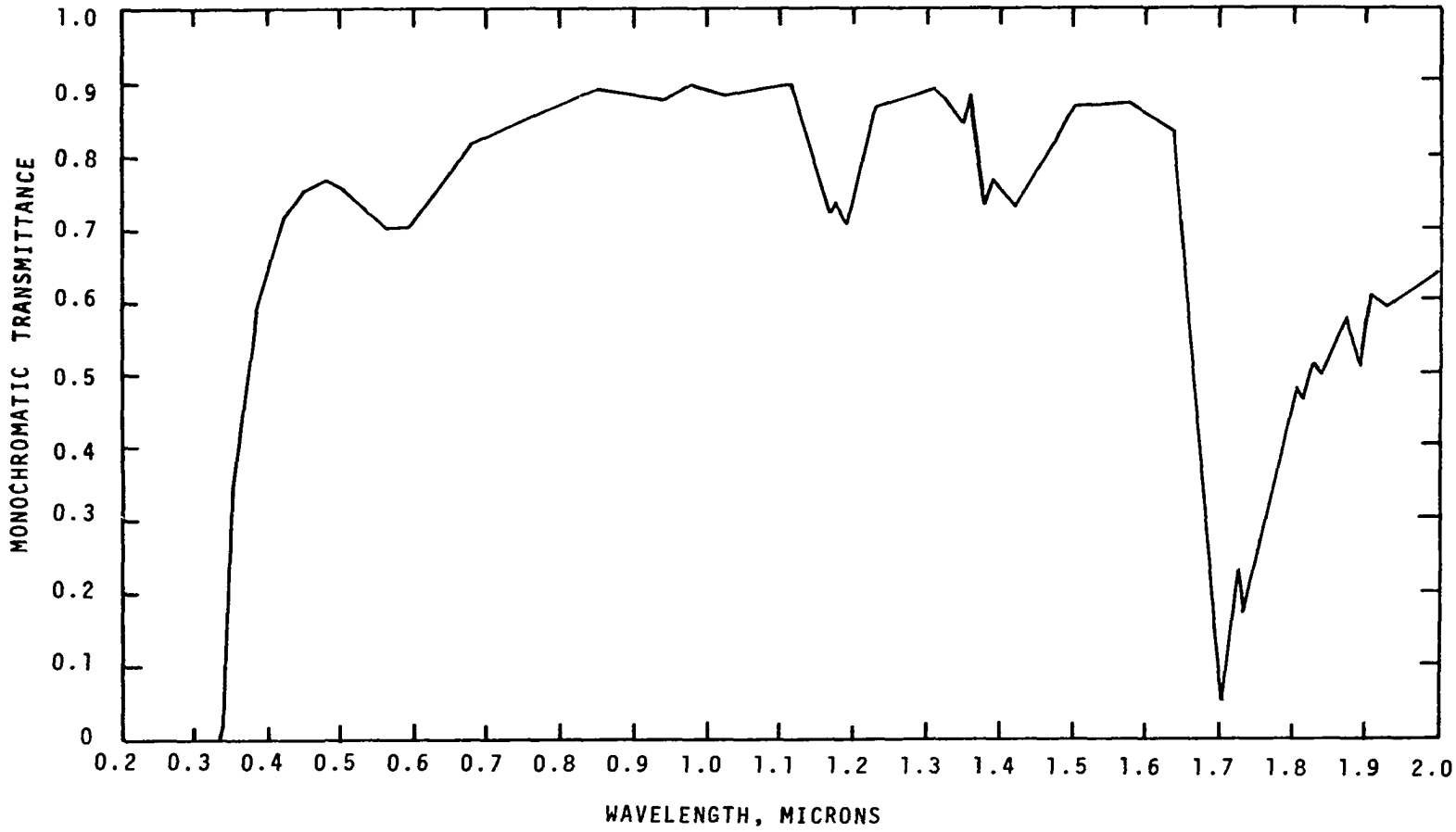

Figure D-74. Spectral Transmittance of Clear Poly(vinyl chloride), 1.0 - 10.0 Microns.

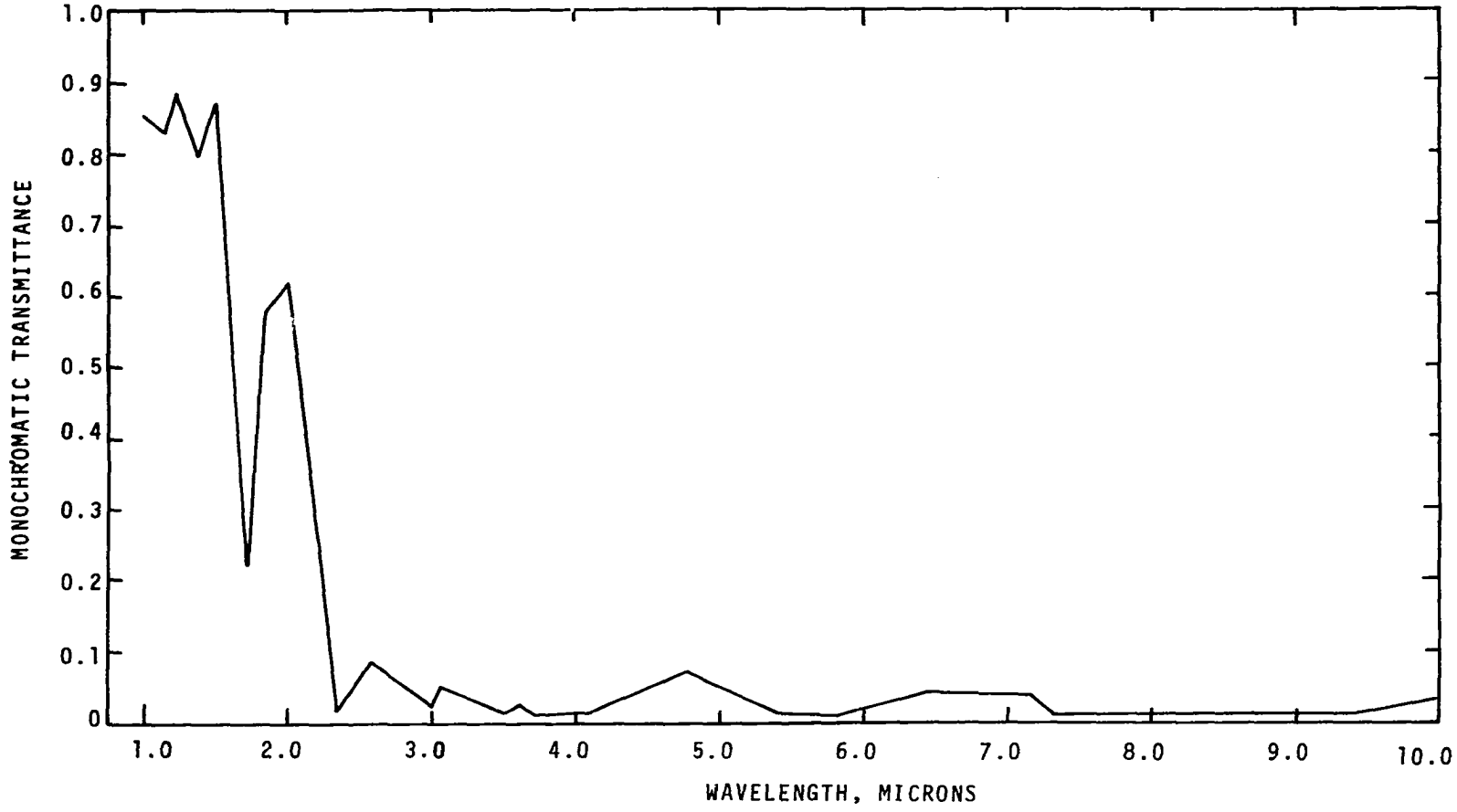

Figure D-75. Spectral Transmittance of Clear Poly(vinyl chloride), 1.0 - 10.0 Microns.

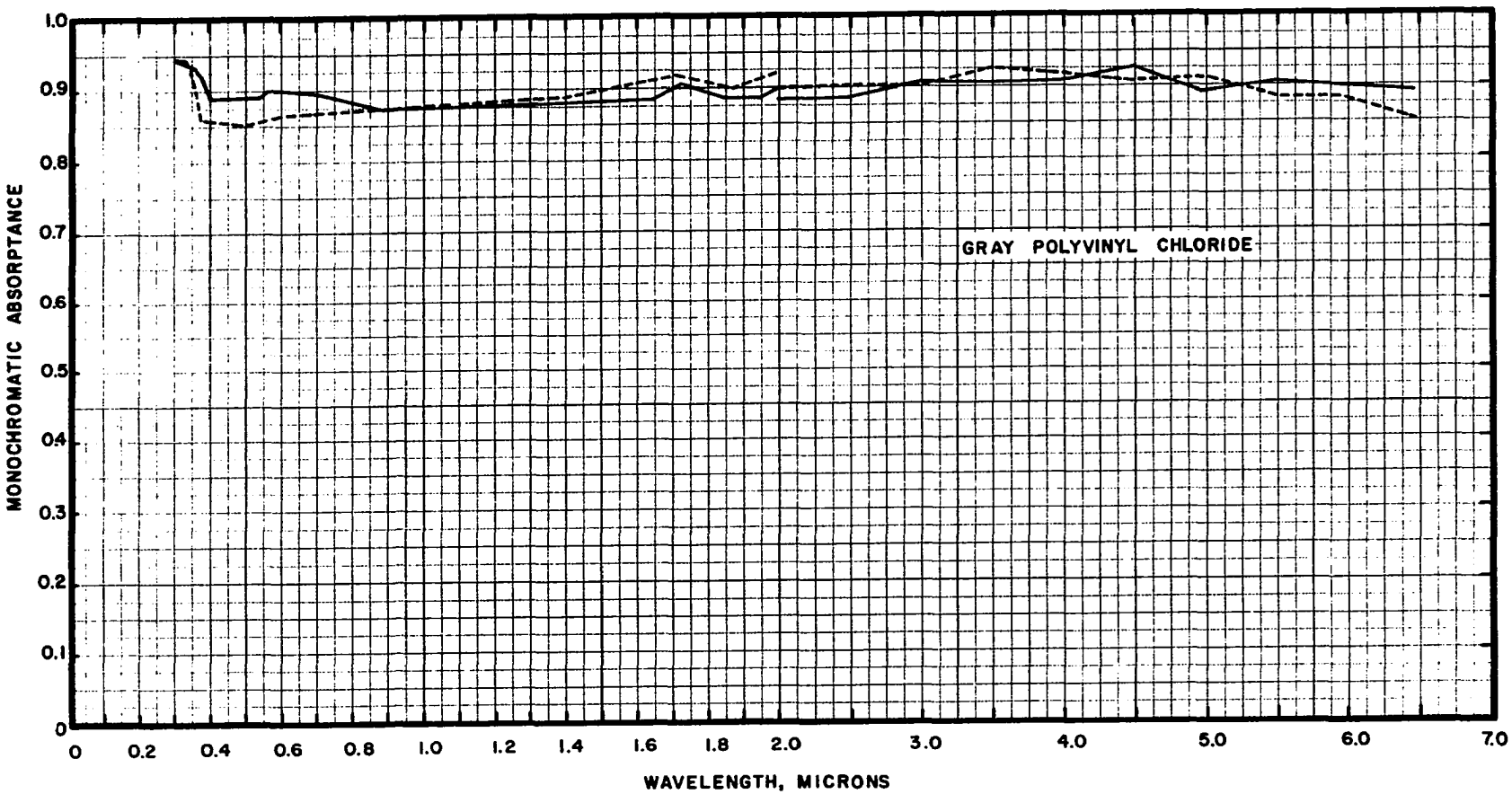

Figure D-76. Spectral Absorptance of Gray Poly(vinyl chloride).

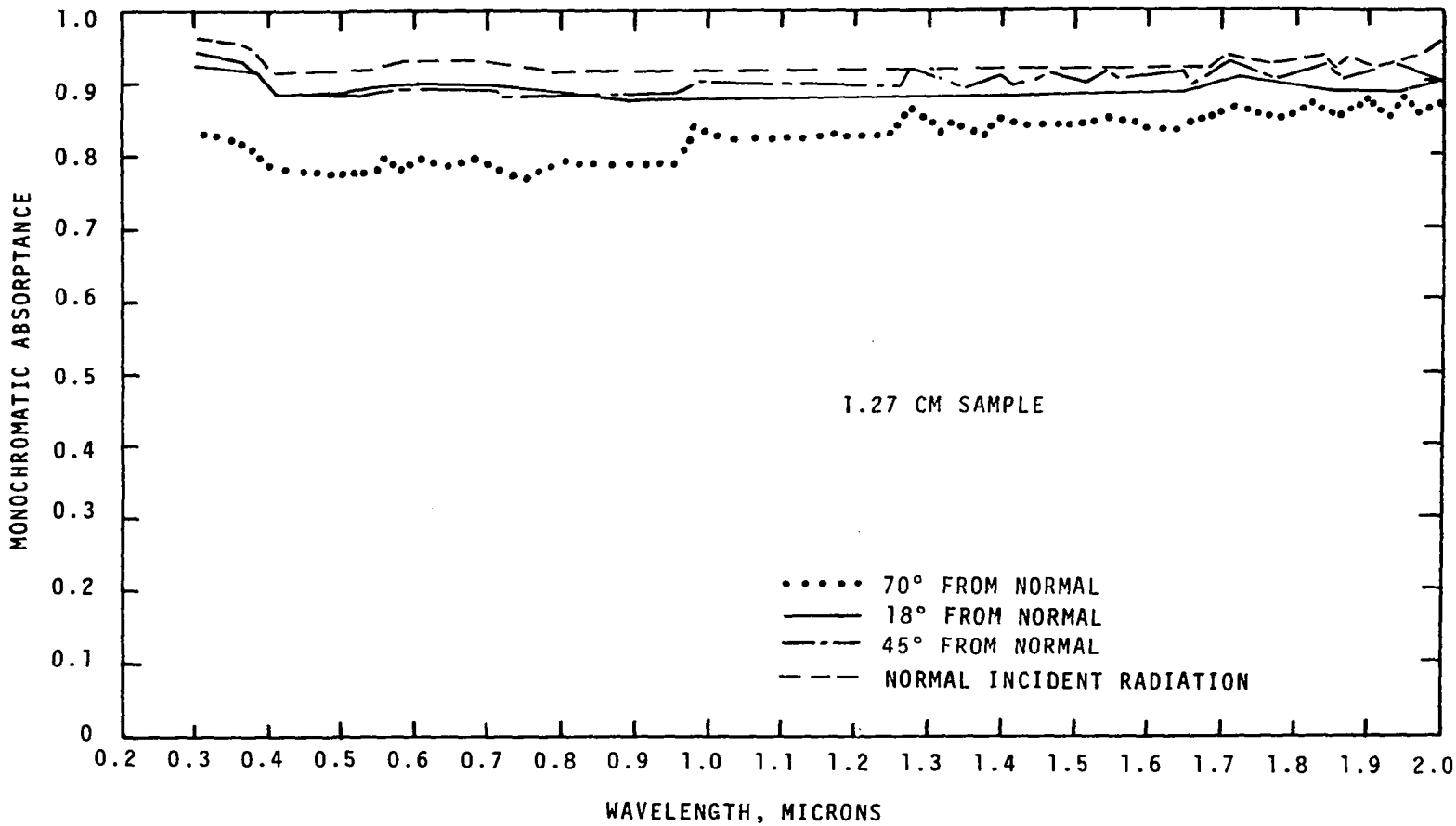

Figure D-77. Angular Variation of Absorptance of Gray Poly(vinyl chloride).

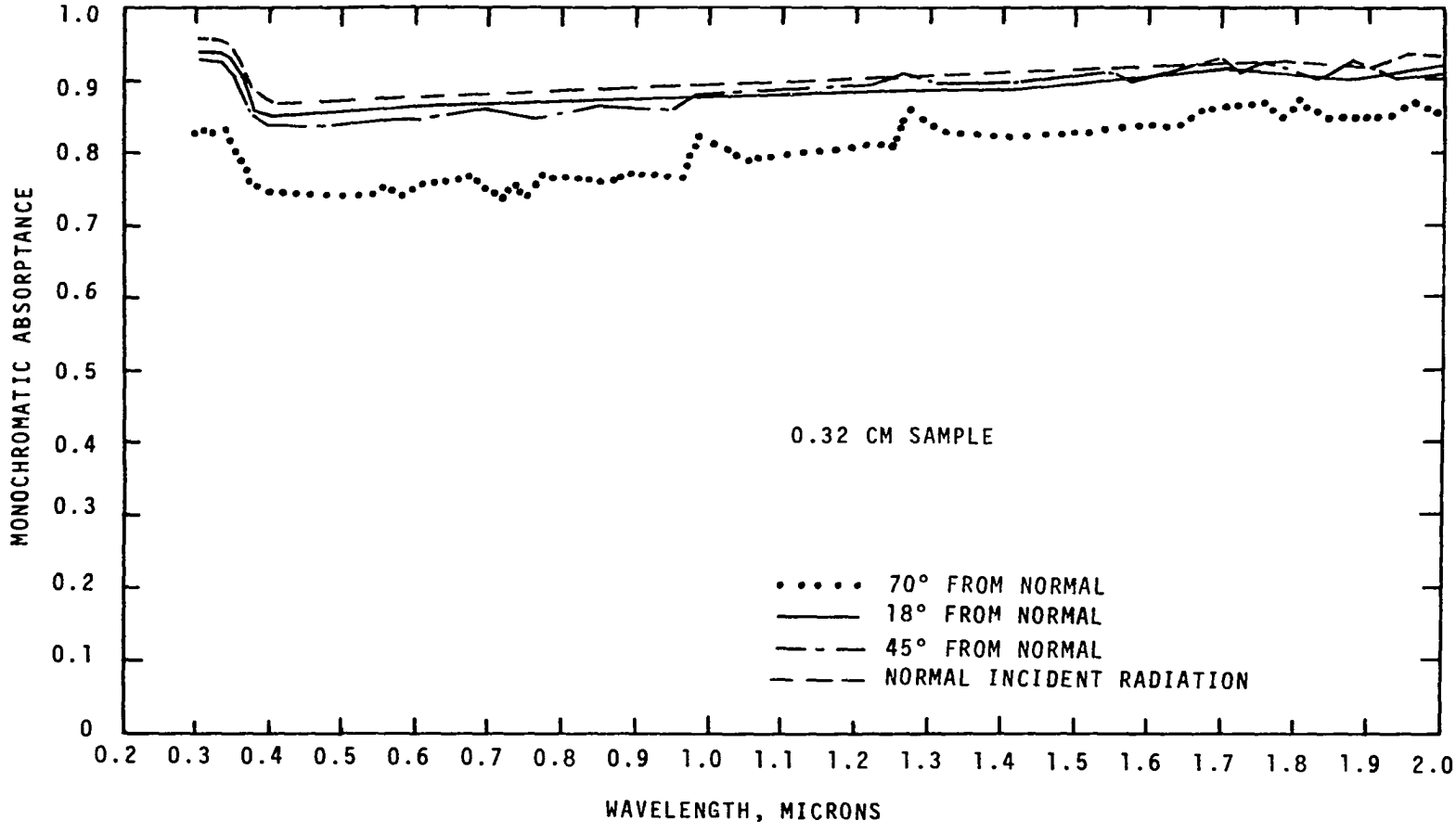

Figure D-78. Angular Variation of Absorptance of Gray Poly(vinyl chloride).

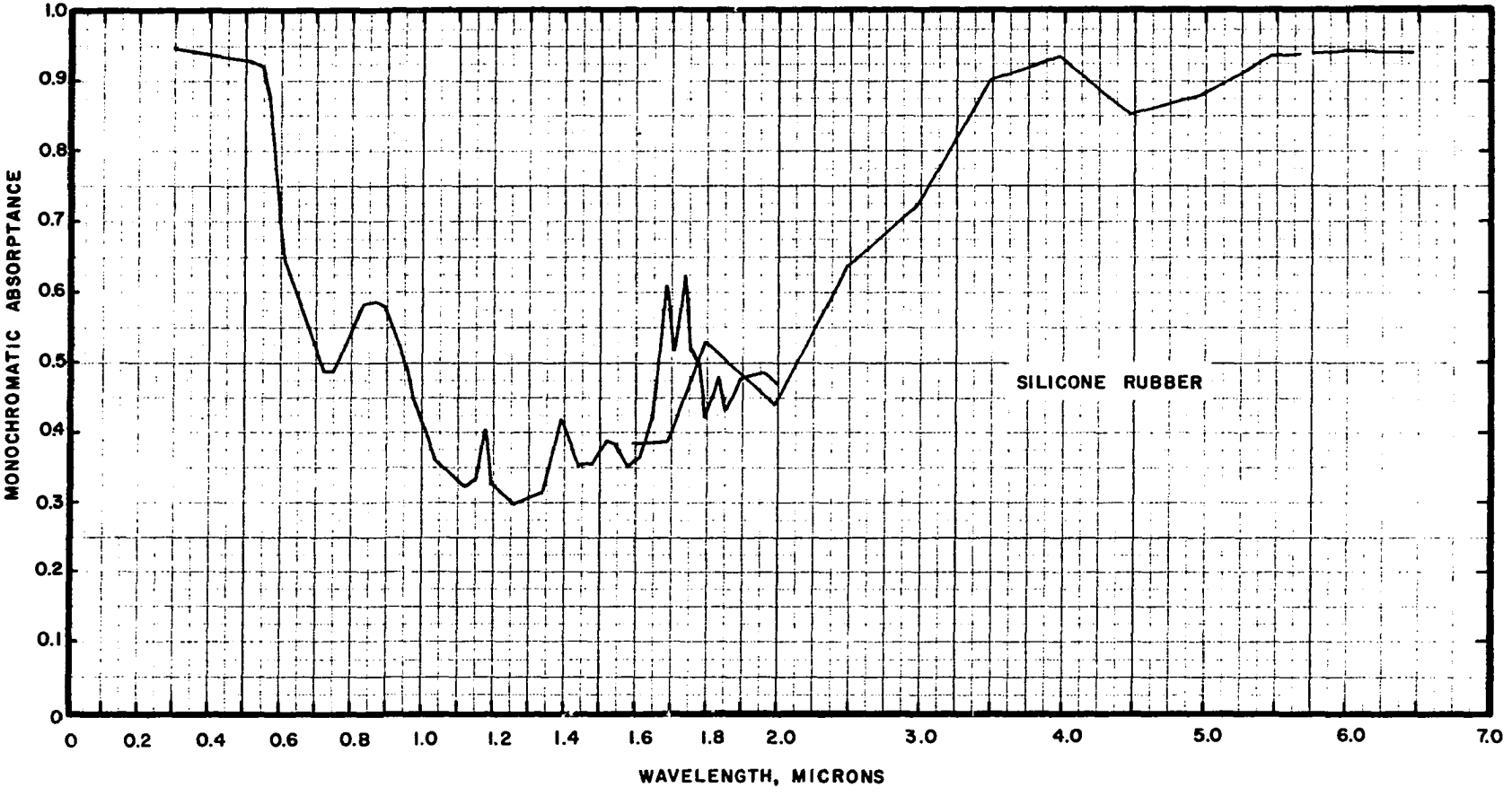

Figure D-79. Spectral Absorptance of Silicone Rubber.

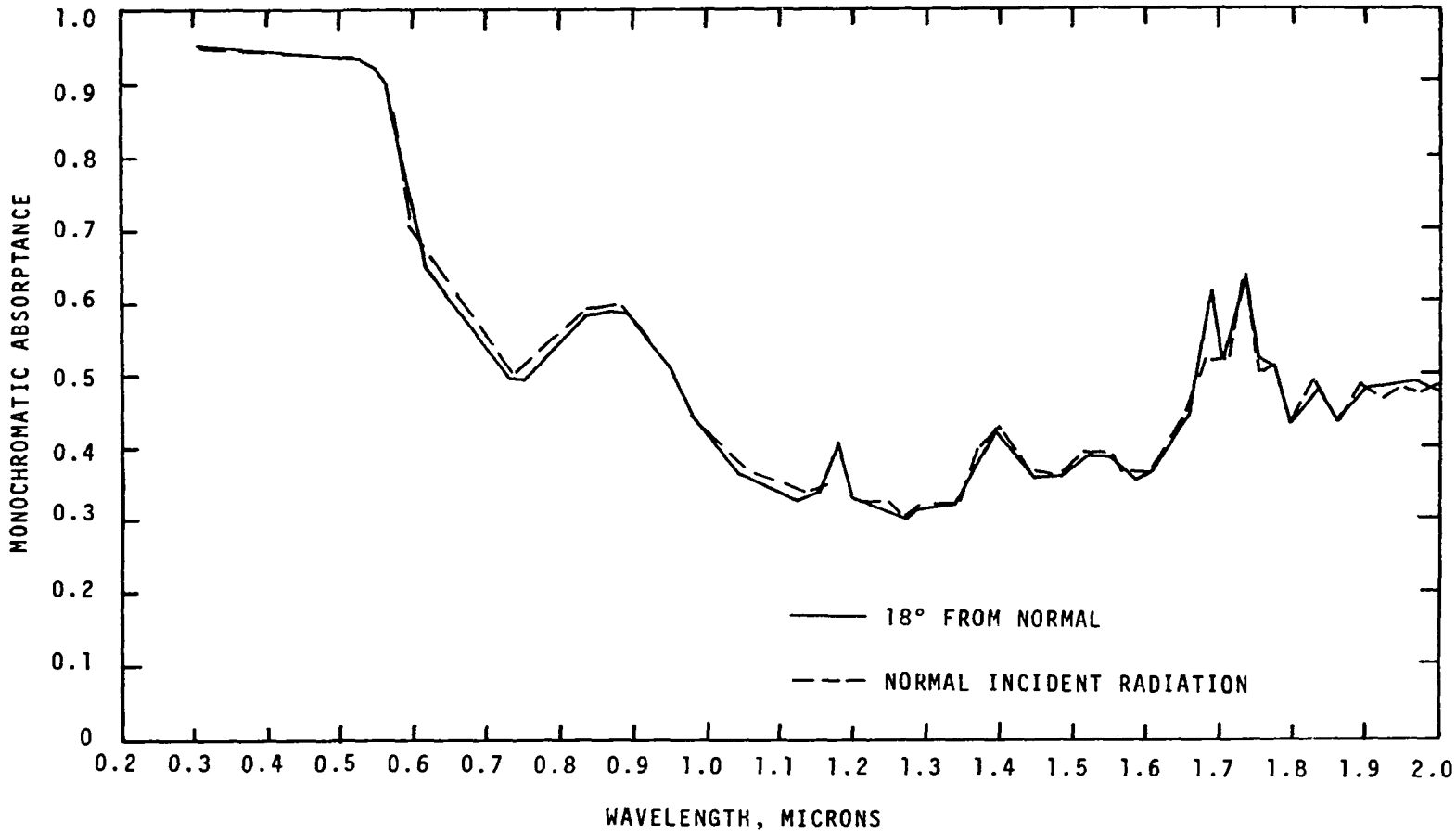

Figure D-80. Angular Variation of Absorptance of Silicone Rubber.

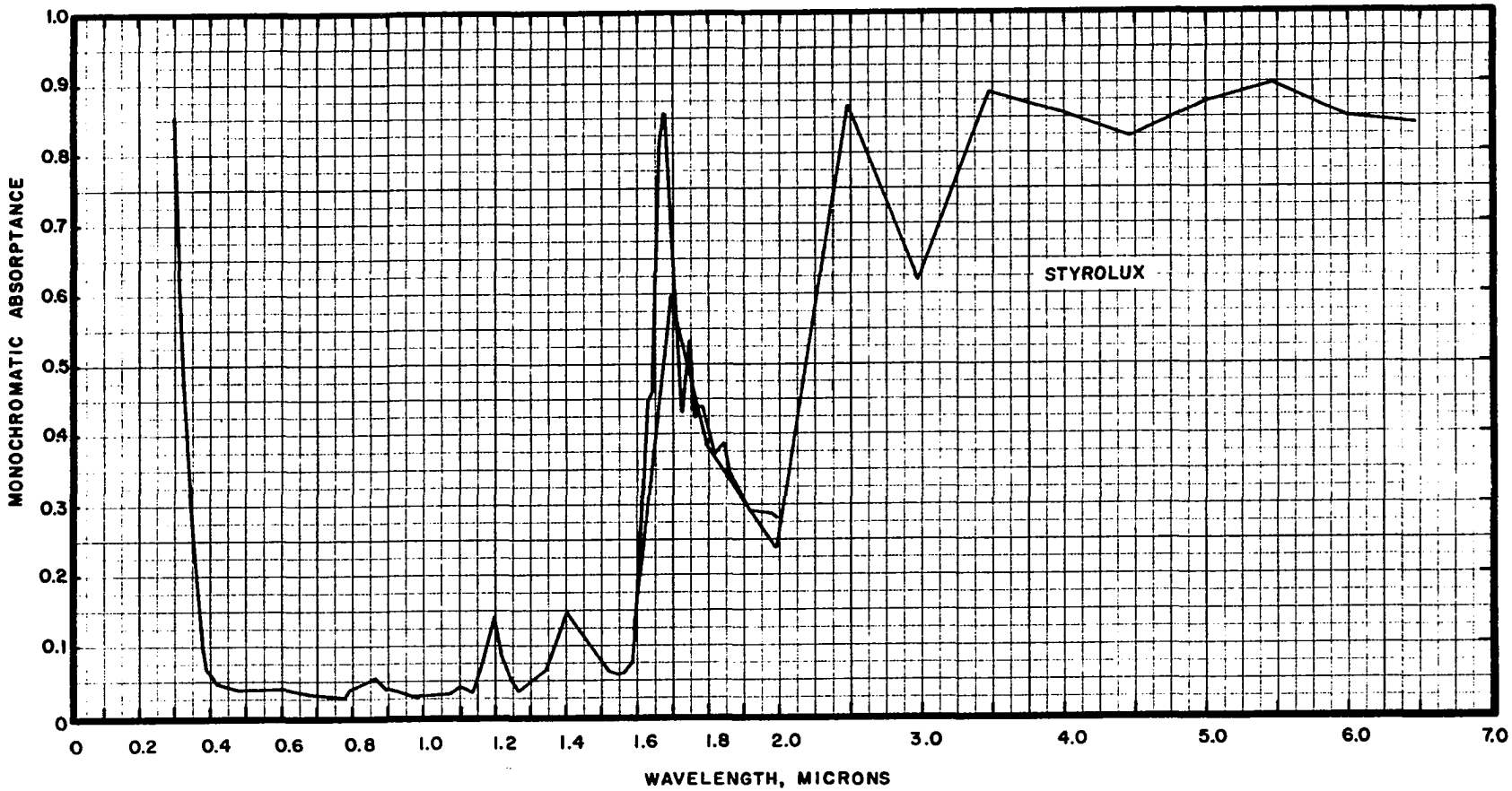

Figure D-81. Spectral Absorptance of Styrolux (Polystyrene).

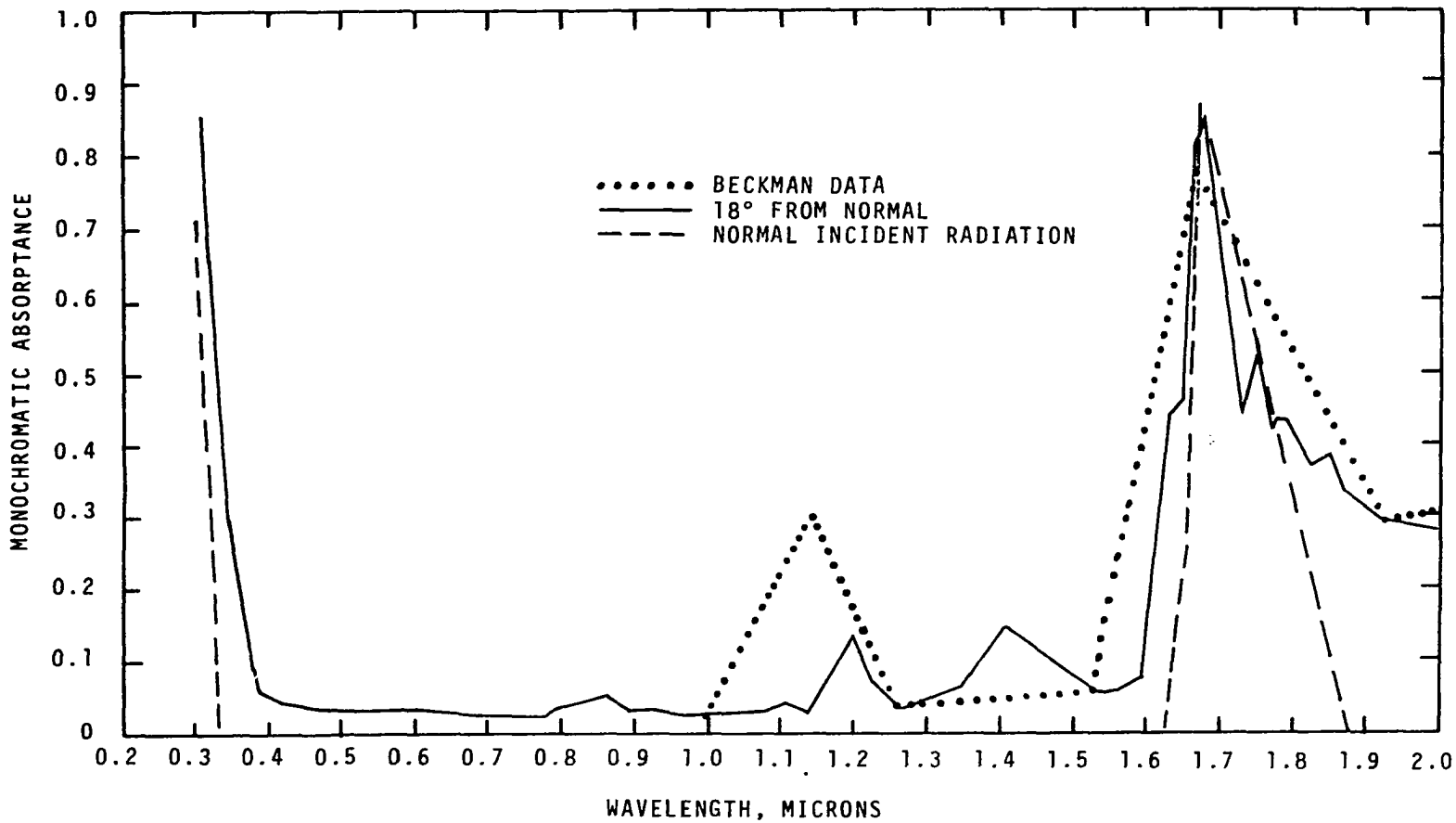

Figure D-82. Angular Variation of Absorptance of Styrolux.

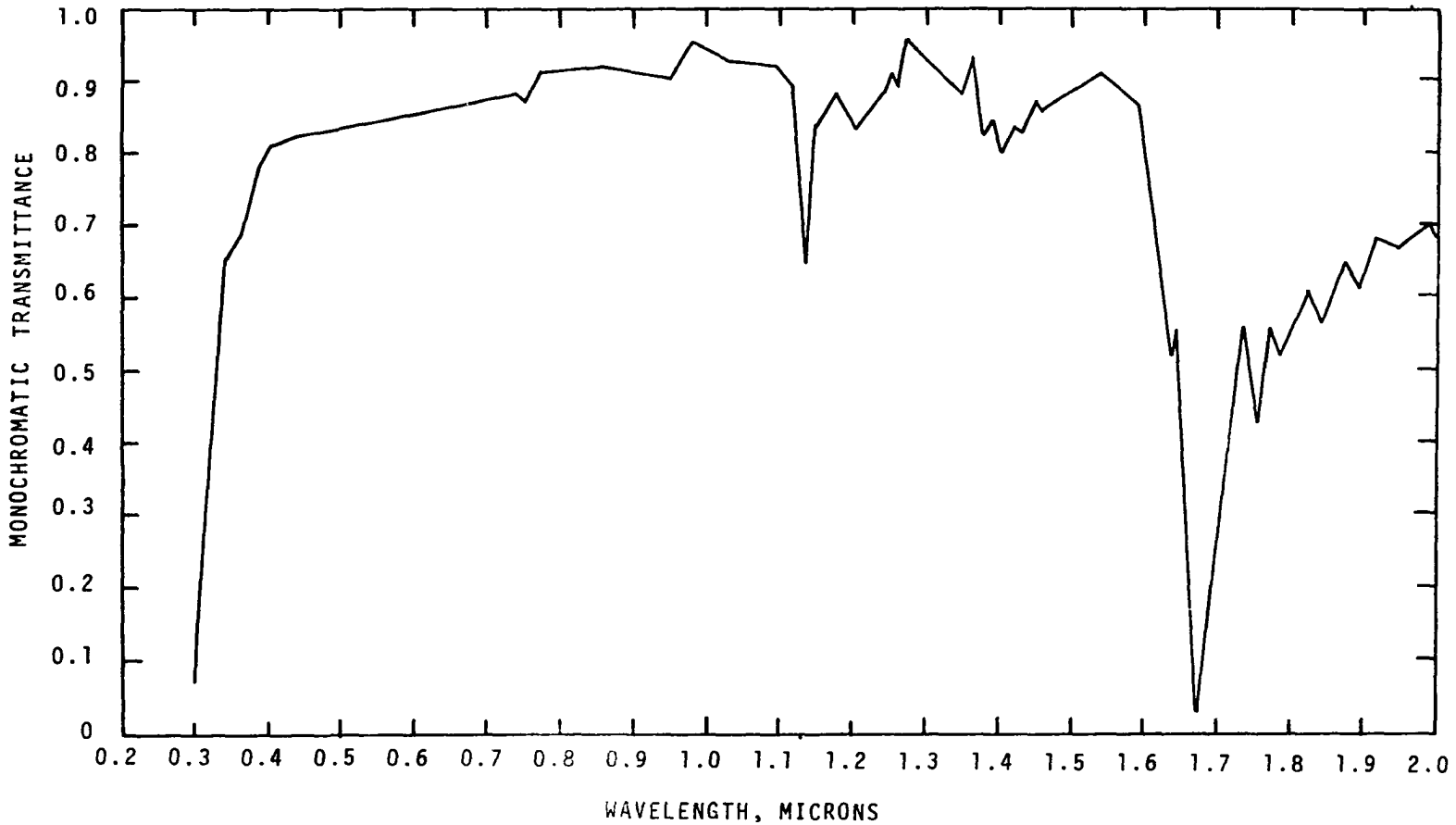

Figure D-83. Spectral Transmittance of Styrolux, 0.3 - 2.0 Microns.

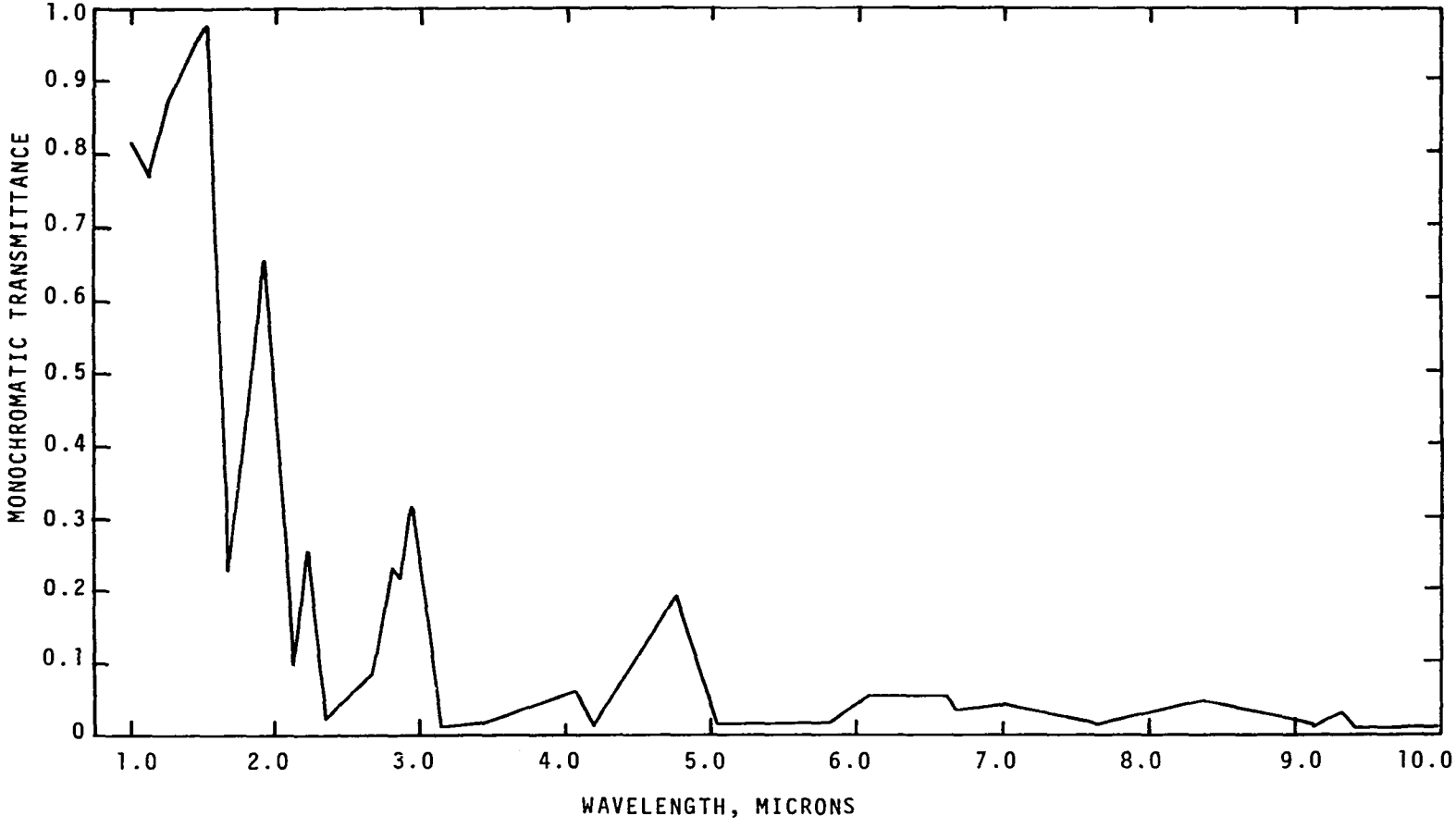

Figure D-84. Spectral Transmittance of Styrolux, 1.0 - 10.0 Microns.

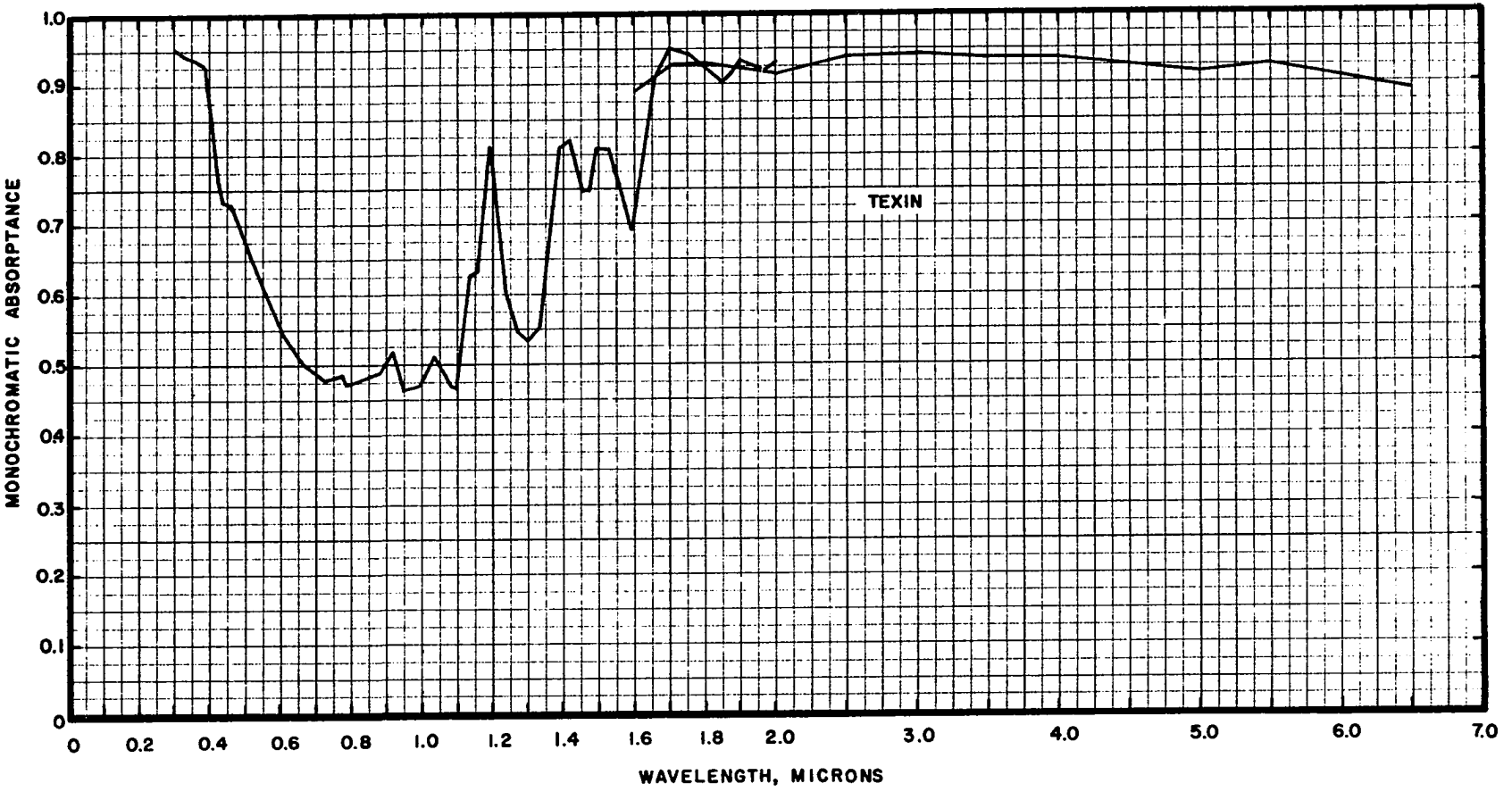

Figure D-85. Spectral Absorptance of Texin.

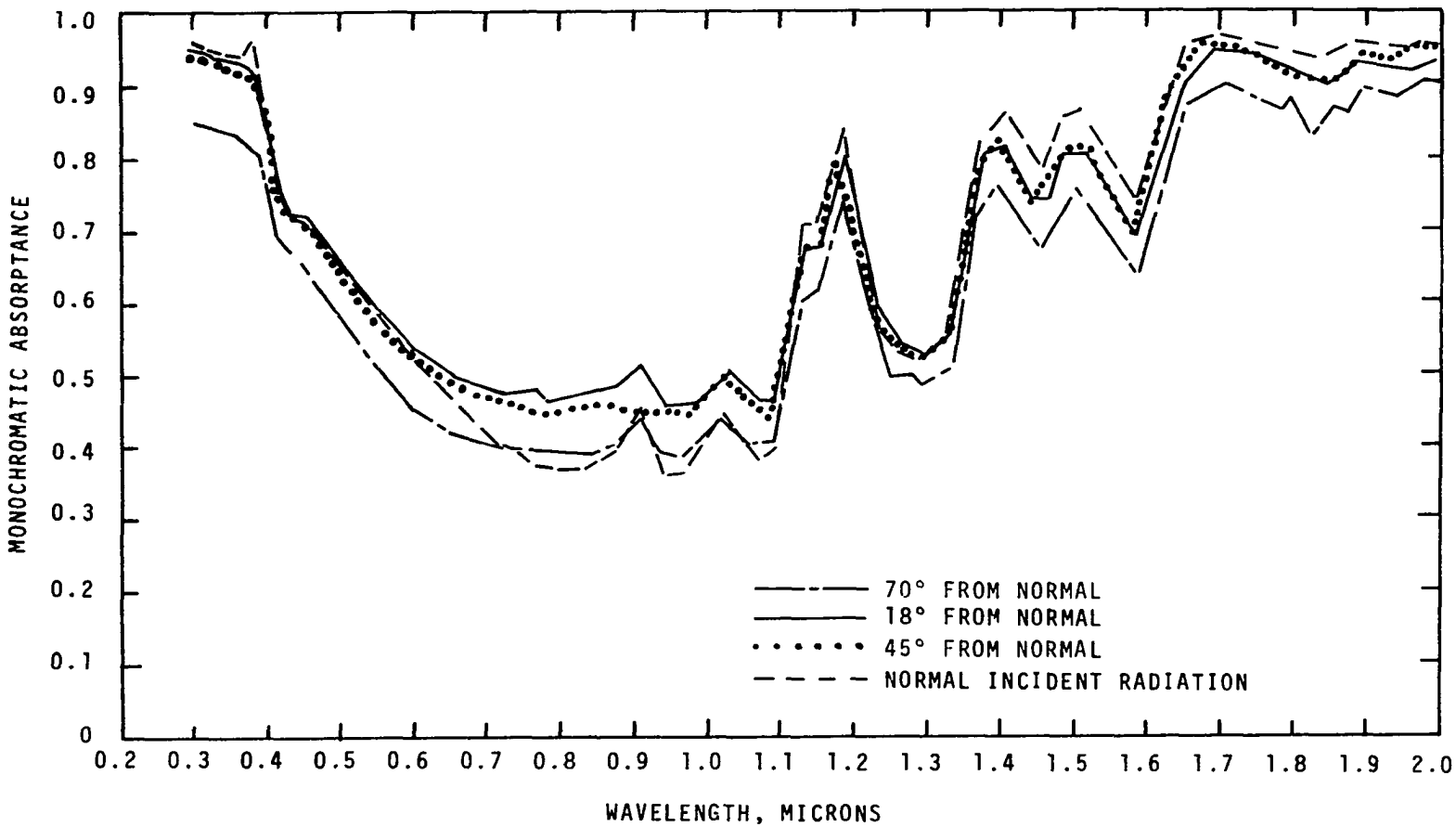

Figure D-86. Angular Variation of Absorptance of Texin.

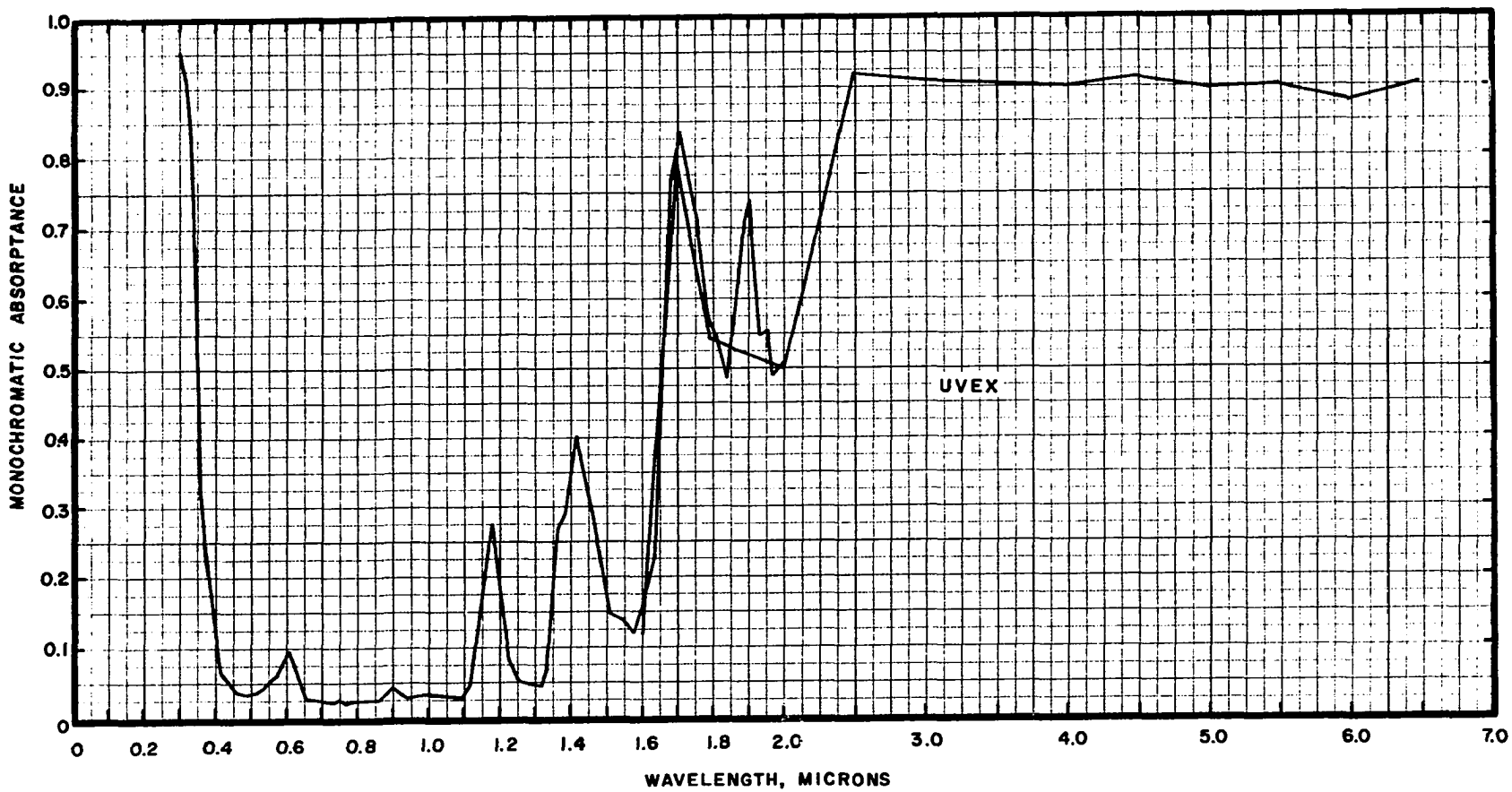

Figure D-87. Spectral Absorptance of Uvex (Cellulose Acetate Butyrate).

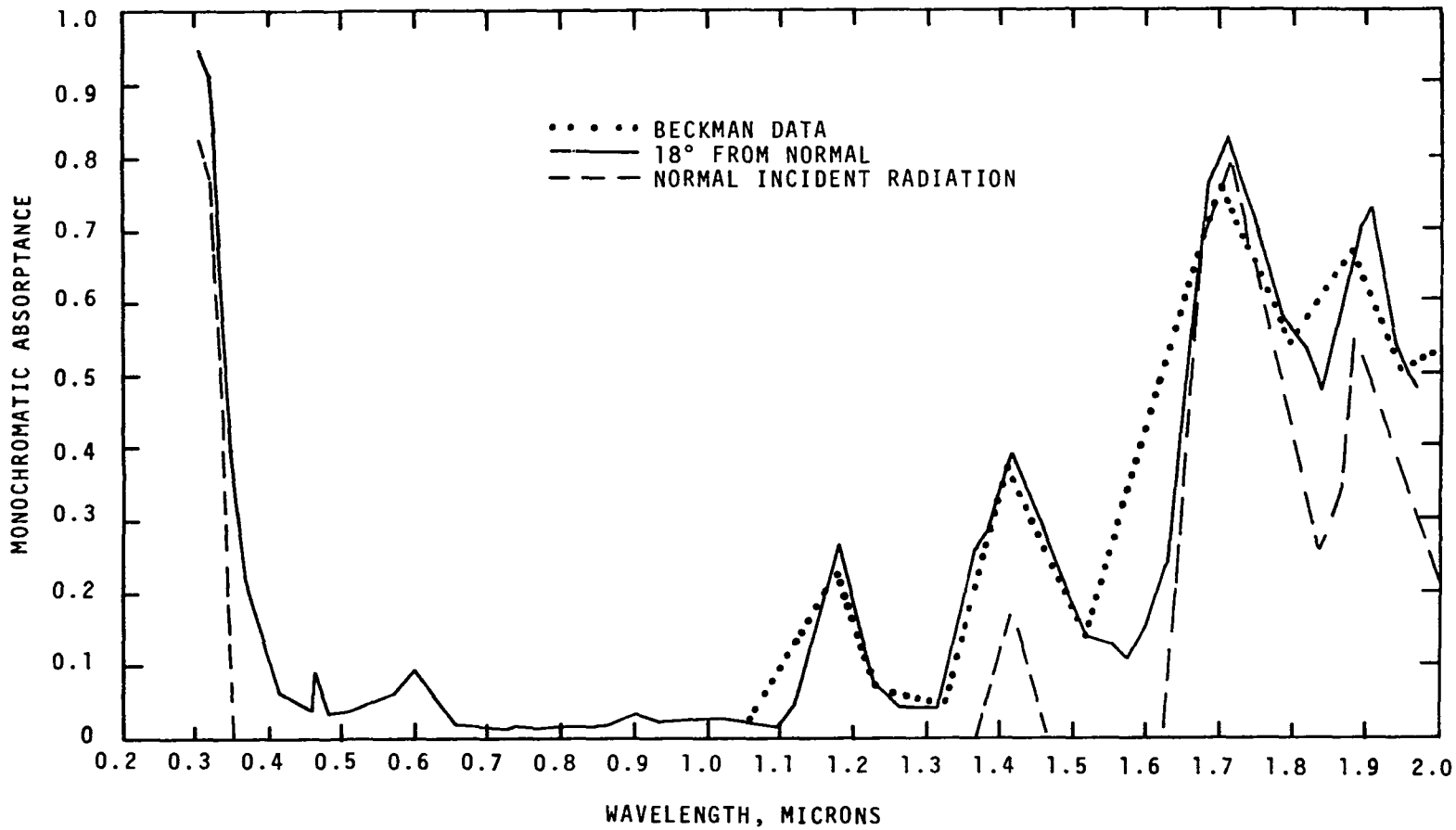

Figure D-88. Angular Variation of Absorptance of Uvex.

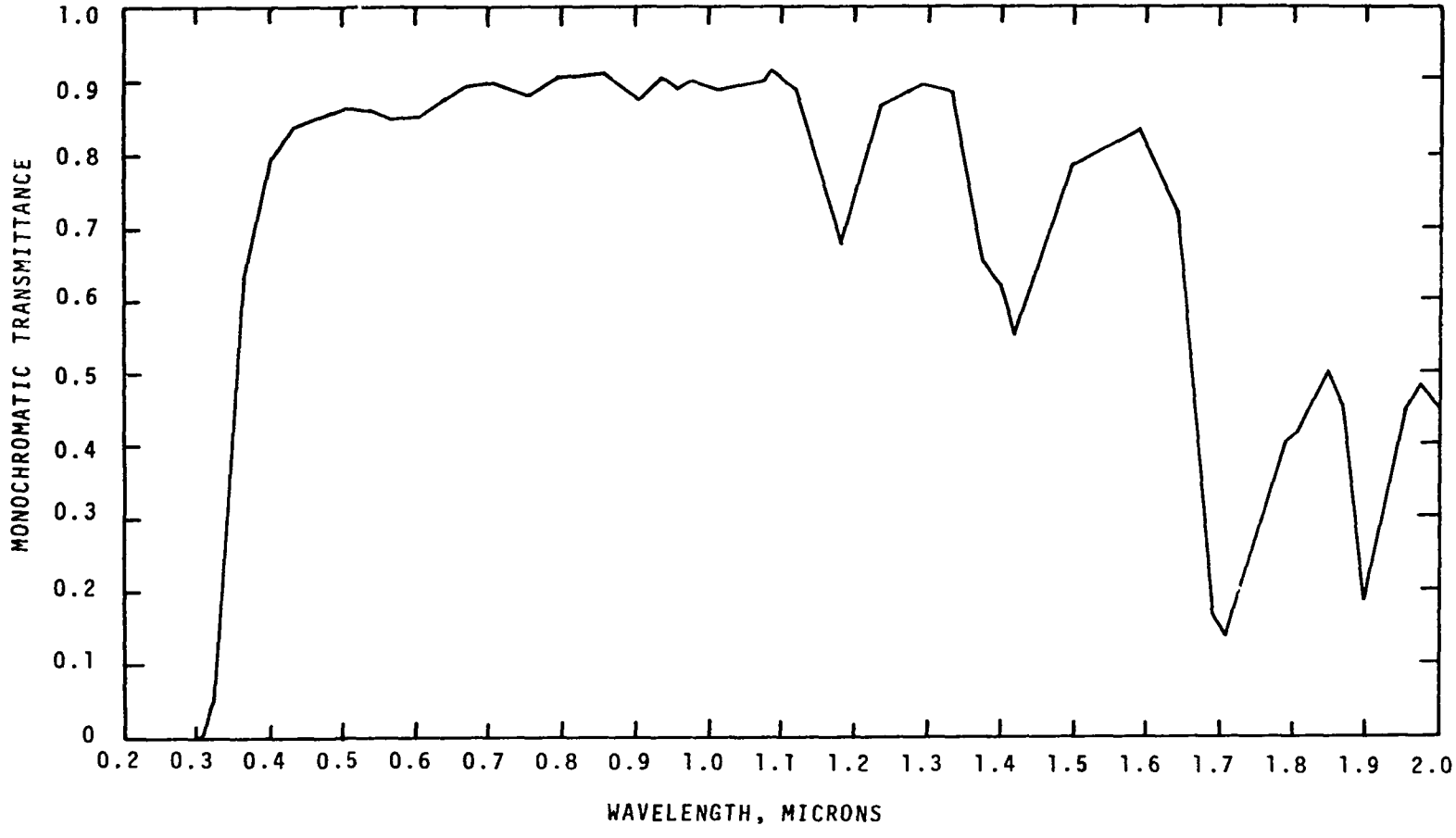

Figure D-89. Spectral Transmittance of Uvex, 0.3 - 2.0 Microns.

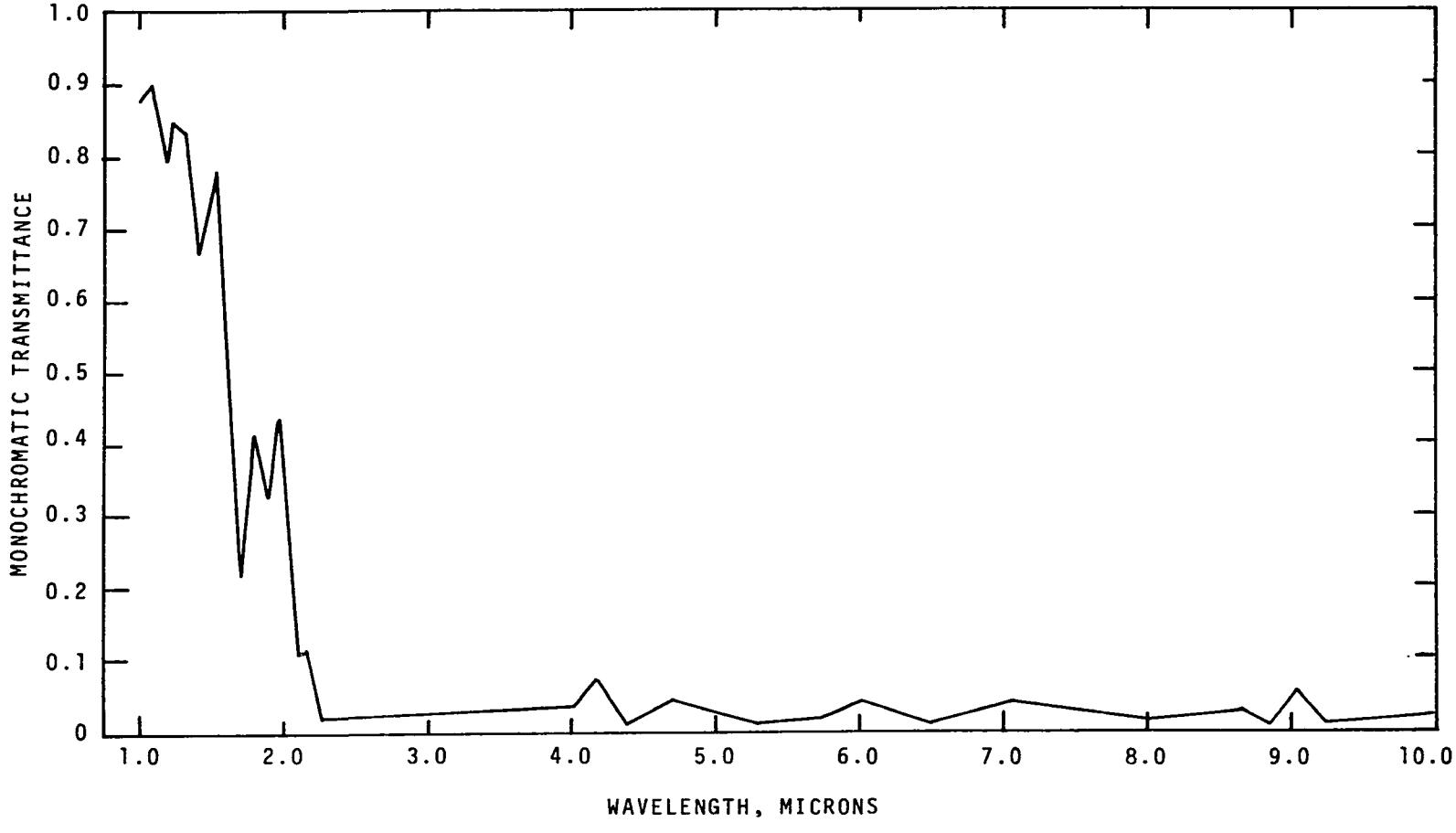

Figure D-90. Spectral Transmittance of Uvex, 1.0 - 10.0 Microns.

APPENDIX E

NOMENCLATURE

A	= area; area of sphere	cm^2
A_d	= area of detector	cm^2
A_o	= pre-exponential factor	cm/sec
B	= linear burning rate	cm/sec
B_o	= pre-exponential factor	cm/sec
C_g	= average heat capacity of decomposition gases	cal/gm-°C
C_p	= specific heat of solid	cal/gm-°C
C_s	= coefficient of directional reflectance characteristics	dimensionless
E_d	= depolymerization energy	cal/mol
E_ℓ	= random chain scission energy	cal/mol
ΣE	= total activation energy; $\Sigma E = E_d + E_\ell + \ldots$	
ΔE	= activation energy	cal/mol
E_s	= activation energy at surface	cal/mol
$F_1, F_2, \ldots$	= fraction of incident energy associated with extinction coefficients $\gamma_1, \gamma_2, \ldots$	dimensionless
H	= unreflected, or absorbed energy	cal/cm^2-sec
H_x	= net inward flux at depth x	cal/cm^2-sec

$H_s(\theta,\phi)$ = energy reflected from sample cal/cm^2-sec

ΔH_c^o = standard heat of combustion cal/gm

ΔH_f^o = standard heat of formation cal/gm

ΔH_f = latent heat of fusion cal/gm

ΔH_p^o = standard heat of polymerization cal/gm

ΔH_v = latent heat of vaporization cal/gm

H_o = incident irradiance cal/cm^2-sec

IG = ignition criteria unspecified

I_o = incident irradiance cal/cm^2-sec

$\frac{I_i}{\pi}$ = energy incident to a specimen from a hemispherical area cal/cm^2-sec

I_1 = intensity of incident beam cal/cm^2-sec

I_2 = intensity of reflected beam cal/cm^2-sec

$I_{\theta,\phi}$ = intensity of the individual rays from the total hemisphere cal/cm^2-sec

I_α = intensity of absorbed energy cal/cm^2-sec

J = radiant energy arriving at the detector cal/cm^2-sec

K = optical system constant

L = slab thickness cm

M = molecular weight gm

Q_B = heat at beginning of a time period, t_o cal

Q_c = convective heat cal

Q_E = heat at end of a time period, $t_o + \Delta t$ cal

Q_z = heat of pyrolysis, assumed to be of first order, per unit mass cm^2-sec/gm

R	= universal gas constant	cal/mol-°C
T	= absolute temperature	°K, °C
T_g	= gas film temperature	°K, °C
T_i	= ignition temperature	°K, °C
T_o	= ambient temperature; bulk temperature	°K, °C
T_s	= surface temperature	°K, °C
T_z	= pyrolysis temperature	°K, °C
$\bar{T}$	= source temperature	°K, °C
ΔT	= $(T_s - T_o)$; = $(T_i - T_o)$; = $(T_z - T_o)$	°C
Q	= volumetric heat of pyrolysis	cal/gm-cm^3
V_s	= energy detected from specimen	cal/cm^2-sec
V_{st}	= energy detected from standard	cal/cm^2-sec
V_w	= energy detected from walls	cal/cm^2-sec
a, b, c	= coefficients	dimensionless
f	= frequency factor	1/sec
h	= overall heat transfer coefficient	cal/cm^2-sec-°C
h_c	= convective heat transfer coefficient	cal/cm^2-sec-°C
k	= thermal conductivity	cal/cm^2-sec-°C/cm
$\dot{m}_d$	= mass rate of decomposition	gm/cm^2-sec
n	= limiting oxygen index; power	dimensionless
r	= reflectance	dimensionless
$r(\theta,\phi)$	= hemispherical-directional reflectance	dimensionless
r_λ	= monochromatic reflectance	dimensionless

r_m	= mirror reflectance	dimensionless
r_s	= surface or specimen reflectance	dimensionless
r_s'	= second reflectance from surface	dimensionless
r_w	= wall reflectance	dimensionless
r_{sm}	= measured specimen reflectance	dimensionless
s	= surface	dimensionless
t	= time	second
t_{I1}	= time at irradiance level I_1	second
x	= distance	cm
x_ℓ	= distance below irradiated surface	cm
α_λ	= monochromatic absorptance	dimensionless
α_{av}	= average absorptance based upon a particular heat source	dimensionless
Φ	= equation constant	dimensionless
γ_λ	= Lambert's law attenuation factor for wavelength λ	1/cm
$\gamma_1, \gamma_2, \ldots$	= extinction coefficients	1/cm
$\delta = \frac{k}{\rho C_p}$	= thermal diffusivity	cm^2/sec
ε	= emittance	dimensionless
ε_λ	= monochromatic emittance	dimensionless
ε_s	= surface emittance	cal/cm^2-sec
ε_t	= detector emittance	cal/cm^2-sec
λ	= wavelength	microns, μ
$\theta; \theta_1$	= cosine of the incident angle	dimensionless
θ_2	= cosine of the reflected angle	dimensionless
ϕ	= azimuth angle	degrees

ρ	= density	gm/cm^3
Σ	= summation	
$\rho = \frac{dT}{dt}$	= heating rate	°C/sec
τ_λ	= monochromatic transmittance	dimensionless
μ	= microns	
ω	= weight of material	gm
ω_f	= weight of melted polymer per unit volume	gm/cm^3
ω_v	= weight of vaporized polymer per unit volume	gm/cm^3
ω_z	= weight of decomposed polymer per unit volume	gm/cm^3
$\frac{\partial \omega}{\partial t}$	= rate of weight loss	gm/sec
ω_o	= initial weight of material	gm
σ	= Stephan-Boltzmann constant, 1.356×10^{-12}	$cal/cm^2\text{-sec-}°K$

APPENDIX F

INSTRUMENTATION DESIGN

Measurement of ignition temperature has been made by numerous investigators but the results indicate that there is wide discrepancy in the values found. In Chapter II, several of the methods used to measure ignition temperature have been discussed. In the analysis of the ignition phenomena, it was found that the ignition temperature is a parameter that is most necessary in any determination of the ignition characteristics of a material.

In the present research and study of plastics and rubbers, the design of the ignition cabinet (Chapter III) permits a modified method of obtaining the ignition temperature in conjunction with the ignition time and magnitude of the irradiance of the heat source. Figures F-1 and F-2 diagram the test apparatus while Figure F-3 details the thermocouple probe.

Operation of the probe is the following: When the heat shield is opened, the probe is moved to a central position in front of the specimen and the thermocouple, TC, is approximately 1/4" - 3/8" away from the specimen surface,

maintained by a spring force. At ignition, the solenoid is energized either manually or by use of the ignition detector circuit, and a wedge is forced between the probe tube and the cabinet wall, in turn, moving the probe face and the projecting TC onto the sample face. If the TC bead is small, i.e., less than 0.004" diameter, the surface temperature should be recorded in 0.1 seconds or less (if the recorder pen response is adequate). After test, the probe is reset to ready and a new sample inserted. It must be noted that extreme care must be exercised in the sample placement so that the probe TC bead projects no more than 0.002" into the sample face.

The details and operation of the proposed probe should find application to surface temperature measurement at low to medium irradiances (less than 2.0-2.5 cal/cm^2-sec). The measurement at high irradiance (greater than 2.7 cal/cm^2-sec) may be questionable due to overheating of the probe itself.

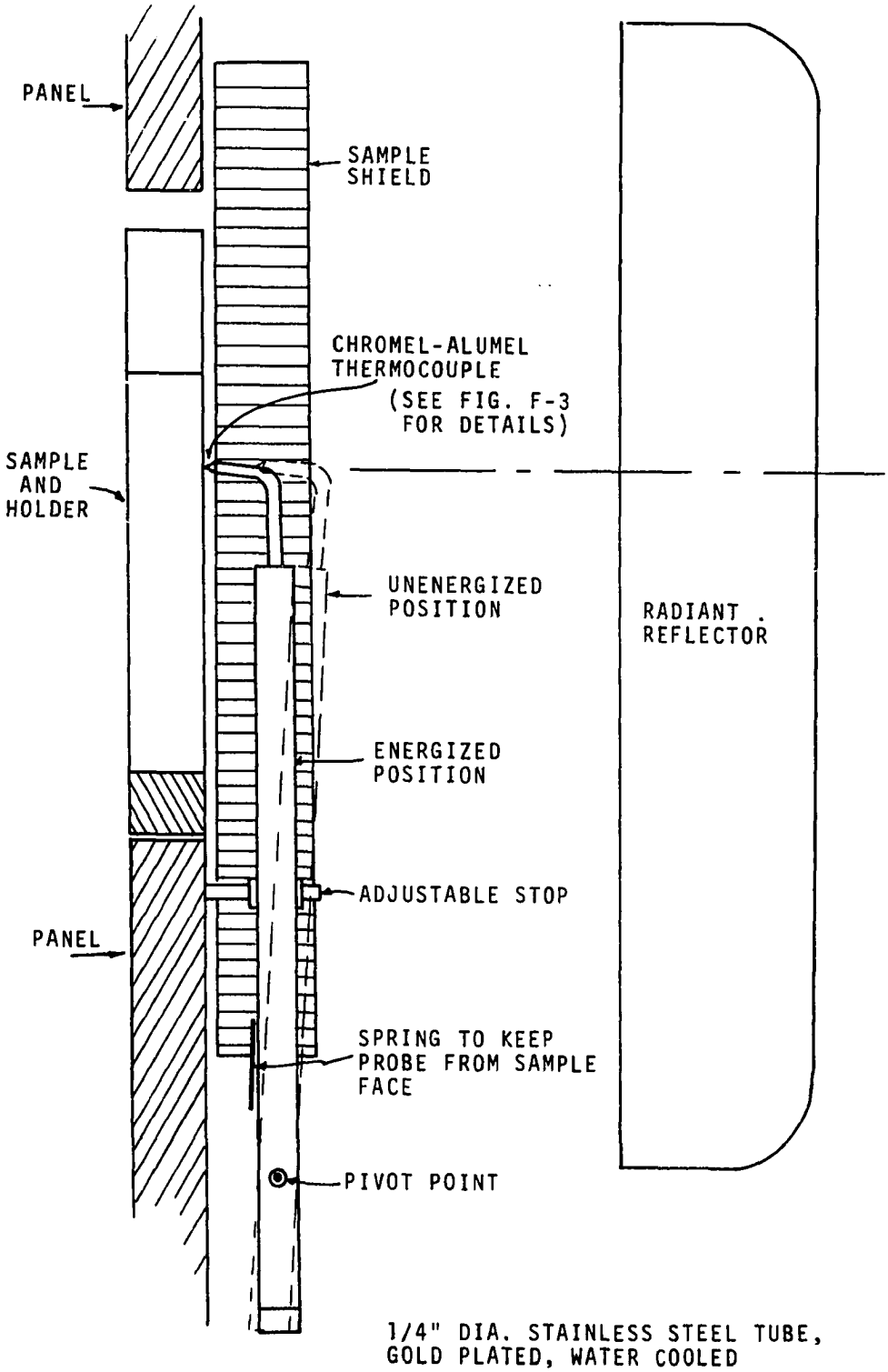

Figure F-1. Diagram of Surface Temperature Measuring System.

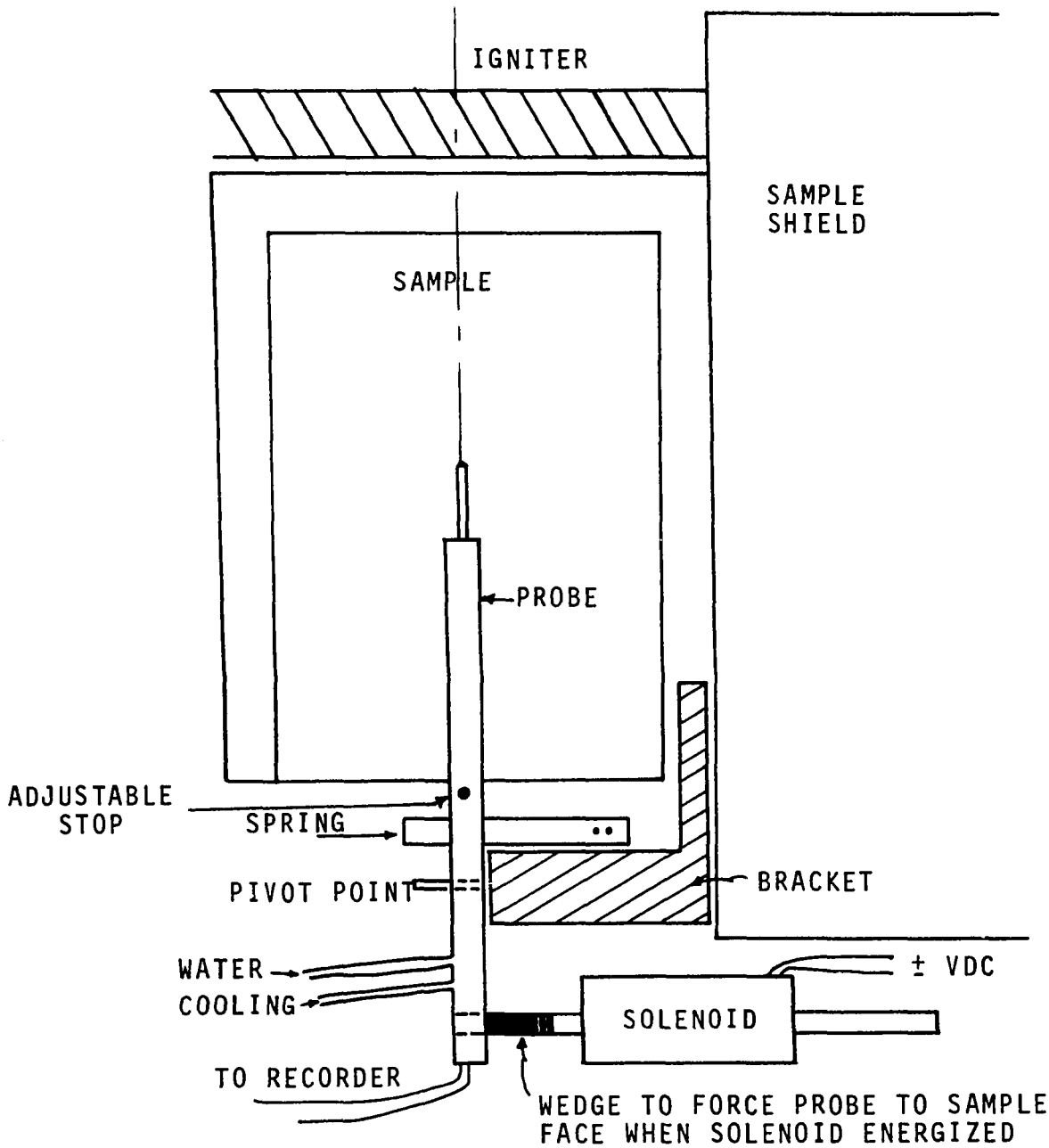

Figure F-2. Diagram of Temperature Measuring System Attachment.

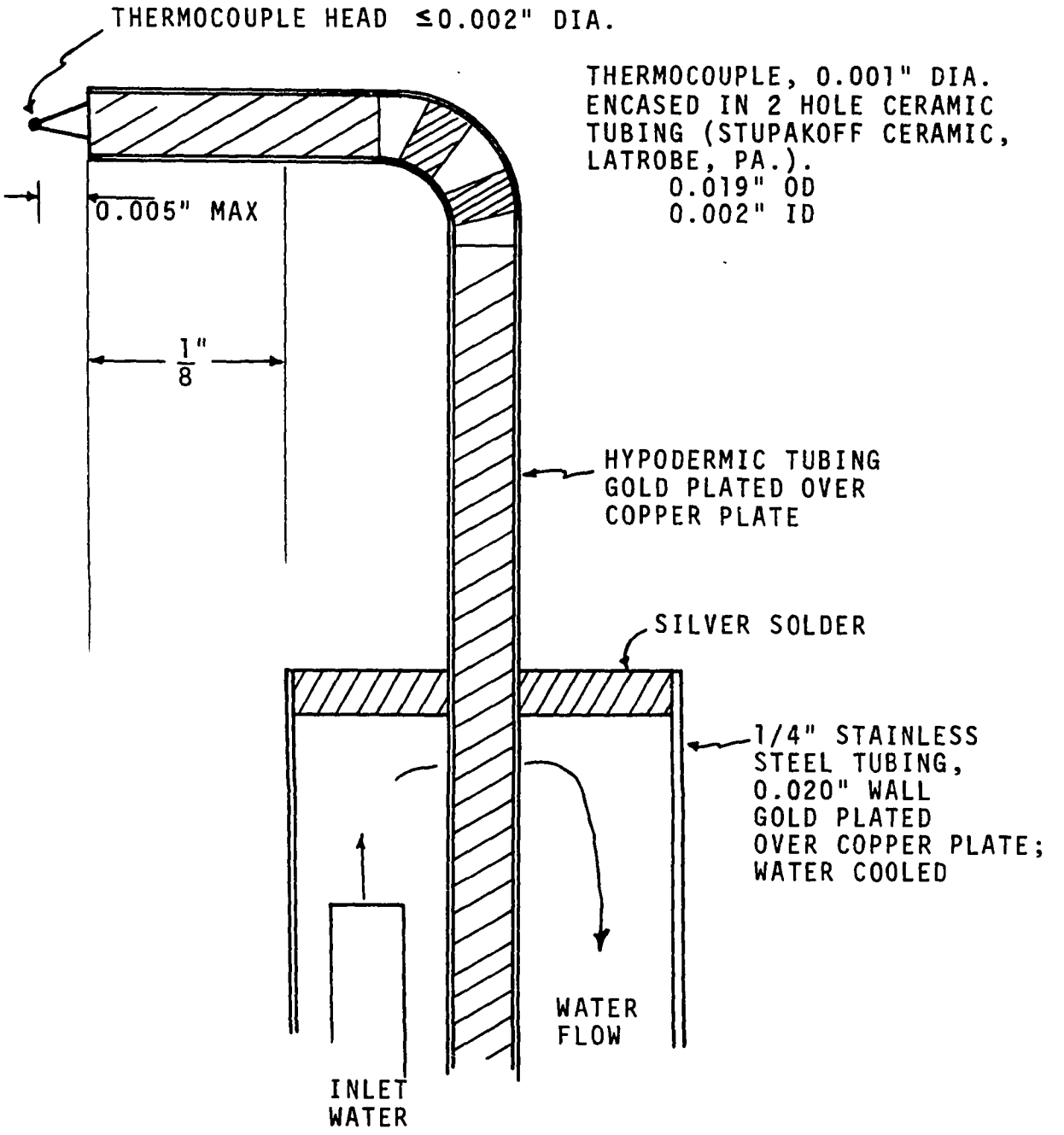

Figure F-3. Detail of Thermocouple Probe.

BIBLIOGRAPHY

1. Achammer, B. G.; Reinhart, F. W.; and Kline, G. M. "Mechanism of the Degradation of POlyamides." Journal of Research of the National Bureau of Standards, XLVI (May, 1951), pp. 391-421.

2. Achhammer, B. G.; Reinhart, F. W.; and Kline, G. M. "Mechanism of the Degradation of Polyamides." Journal of Applied Chemistry, I (July, 1951), pp. 301-320.

3. Adomeit, G. "Ignition of Gases at Hot Surfaces Under Non-Steady-State Conditions." Tenth International Symposium on Combustion. Pittsburgh: The Combustion Institute, 1965, pp. 237-243.

4. Anderson, W. H. "Comments on Gas Film Effects in the Linear Pyrolysis of Solids." A.I.A.A. Journal, II (February, 1964), pp. 404-406.

5. Arnold, L. K. Introduction to Plastics. Ames: The Iowa State University Press, 1968.

6. Ausobsky, S. "Danger Rating of Combustion Gases from Plastics." VFDE (Vereinigung zur Foerderung des Deutschen Brandschutzes) Zeitschrift, XVI (2, 1967), pp. 58-66.

7. Averson, A. E.; Barzykin, V. V.; and Merzhanov, A. G. "On Thermal Ignition Theory of Solid Materials." Translated by H. H. Bradley and H. N. Browne, Jr. NOTS TP 4202, U. S. Naval Ordnance Test Station, China Lake, Calif. (October, 1966).

8. Bamford, C. H.; Crank, J.; and Malan, D. H. "The Combustion of Wood. Part I." Proceedings of the Cambridge Philosophy Society, XLII (1946), pp. 166-182.

9. Barsh, M. K.; Anderson, W. H.; Bills, K. W.; Moe, G.; and Schultz, R. D. "Improved Instrument for the Measurement of Linear Pyrolysis Rate of Solids." Review of Scientific Instruments, XXIX (May, 1958), pp. 392-395.

10. Bevilacqua, E. M. "Degradation of Polyisoprene Networks by Oxygen." Journal of the American Chemical Society, LXXX (1958), pp. 5364-5367.

11. Birkebak, R. "Measurement Techniques in Thermal Radiation." Unpublished Ph.D. dissertation. University of Kentucky, Department of Mechanical Engineering.

12. Black, R. M.; List, C. F.; and Wells, R. J. "Thermal Stability of p-Phenylene Sulfide Polymers." Journal of Applied Chemistry, XVII (October, 1967), pp. 269-275.

13. Blackshear, P. L. "The Measurement of Physico-Chemically Controlled Ablation Rates." Technical Report #1, NBS Contract CST-677. Minneapolis, Minn.: University of Minnesota, July 15, 1962.

14. Bobear, W. J. "Silicone Rubber Reactions During High Temperature Testing." Rubber Age, XCVIII (September, 1966), pp. 73-79.

15. Boehringer, J. C., and Spindler, R. J. "Radiant Heating of Semi-Transparent Materials." Technical Report RAD-TR-61-8. AVCO Corporation, 1961.

16. Boettner, E. A.; Ball, G.; and Weiss, B. "Analysis of the Volatile Combustion Products of Vinyl Plastics." Journal of Applied Polymer Science, XIII (1969), pp. 337-391.

17. Bornengo, M. "A Few Aspects of the Thermal Degradation of Polymers." Materie Plastiche Elastomeri, XXXII (4, 1966), pp. 383-387.

18. Brown, C. R. "The Determination of the Ignition Temperatures of Solid Materials." Fuel, XIV (1935), pp. 14-18, 56-59, 80-85, 112-116, 149-152, 173-179.

19. Burge, S. J., and Tipper, C. F. H. "The Burning of Polythene." Chemistry and Industry, IX (March 4, 1967), pp. 362-363.

20. Carpenter, D. A. "Flammability Tests for Expanded Polystyrene." British Plastics, XXXVIII (May, 1965), pp. 284-288.

21. Carslaw, H. S., and Jaeger, J. C. Conduction of Heat in Solids. 2nd ed. Oxford: Clarendon Press, 1959.

22. Chaiken, R. F.; Anderson, W. H.; Barsh, M. K.; Mishuck, E.; Moe, G.; and Schultz, R. D. "Kinetics of the Surface Degradation of Polymethyl Methacrylate." Journal of Chemical Physics, XXXII (January, 1960), pp. 141-146.

23. Chatelin, B. "Manufacturing Process for Butachlor Polychloroprene Rubber." Officiel des Activities des Plastiques et du Caoutchouc, XVII (7, 1967), pp. 670-673.

24. Coleman, E. H. "Gaseous Combustion Products from Plastics." Plastics, XXIV (1959), pp. 416-418.

25. Delmonte, J., and Azam, M. A. "Ignition Points of Plastic Materials." Modern Plastics, XX (1943), pp. 88-124.

26. Dotreppe-Grisard, N. "Contributions to the Study of Compounds Obtained by Combustion of Plastics." Centre Belge d'Etude et de Documentation des Eaux, Bulletin Trimestriel de CEBEDEAU, XXI (294, 1967), pp. 247-248.

27. Dotreppe-Grisard, Mrs. "Combustion Products of Plastic Materials." Revue Belge des Matieres Plastiques, IX (2, 1968), pp. 79-81.

28. Doyle, C. D. "Estimating Thermal Stability of Experimental Polymers by Empirical Thermogravimetric Analysis." Analytical Chemistry, XXXIII (1, 1961), pp. 77-79.

29. Elias, H. G. "New Developments in Plastics Chemistry." Schweizer Archiv fuer Angewandte Wissenschaft und Technik, XXXIII (5, 1967), pp. 134-142.

30. Emmons, H. W. "Fire Research Abroad." Fire Technology, III (August, 1967), pp. 225-231.

31. Eshbach, O. W. Handbook of Engineering Fundamentals. 2nd ed. New York: John Wiley & Sons, Inc., 1963.

32. "Federal Test Method Standard 406." Method 2023, General Services Administration. Washington, D. C.: Government Printing Office, October, 1961.

33. Fenimore, C. P., and Martin, F. J. "Candle-Type Test for Flammability of Polymers." Modern Plastics, XLIII (11, 1966), pp. 141-192.

34. Fenimore, C. P., and Martin, F. J. "Polymer Flammability Measured Precisely." Product Engineering, XXXIX (May 6, 1968), pp. 89-90,

35. Feuer, S. S., and Torres, A. F. "Flame-Resistance Testing of Plastics." Chemical Engineering, LXIX (April 2, 1962), pp. 140-142.

36. Fisher, H. D., and Gerstein, M. Investigation of Material Combustibility and Fire Explosion Suppression in a Variety of Atmospheres. AD484005, CFSTI. Monrovia, California: Dynamic Science Corporation, 1966.

37. Friedman, H. L. "Kinetics and Gaseous Products of Thermal Decomposition of Polymers." Journal of Macromolecular Science, (Chemistry), AI(1), (1967), pp. 57-79.

38. Friedrich, M. "Plastics in Fire." Zeitschrift Forschung und Technik in Brandschutz, IV (1958), pp. 176-181.

39. Gale, J. A.; Stewart, R. W.; and Alfers, J. B. "Flame Resistance of Thermosetting Plastics." American Institute of Testing Material Bulletin, No. 131 (December, 1944), pp. 23-27.

40. Geddes, W. C. "Mechanism of PVC Degradation." Rubber Chemistry and Technology, XL (February, 1967), pp. 177-216.

41. Geddes, W. C. "The Thermal Decomposition of Polyvinylchloride. I. Kinetics of Dehydrochlorination." European Polymer Journal, III (2, 1967), pp. 267-281.

42. Gnessin, J. R., and Dummer, R. S. "Radiative Properties of Kapton." Report No. 40069-1, Contract 951971. Ryan Aeronautical Company, San Diego, California.

43. Golding, B. Polymers and Resins, Their Chemistry and Chemical Engineering. New York: D. van Nostrand, 1959.

44. Gray, P., and Harper, M. J. "The Thermal Theory of Induction Periods and Ignition Delays." Seventh International Symposium on Combustion. London: Butterworths, 1959, pp. 425-430.

45. Groggins, P. H. Unit Processes in Organic Synthesis. 5th ed. New York: McGraw-Hill, 1958.

46. Guillemonat, A. "Recent Progress in the Study of the Chemical Composition of Cork." Annales de la Faculte des Sciences, Marseille, XXX (1960), pp. 43-54.

47. Hauck, J. E. "Flame Retardant Plastics." Materials in Design Engineering, LX (6, 1964), pp. 83-90.

48. Havens, J. A. "Thermal Decomposition of Wood." Unpublished Ph.D. dissertation. University of Oklahoma, 1968.

49. Hicks, B. L. "Theory of Ignition Considered as a Thermal Reaction." Journal of Chemical Physics, XXII (March, 1954), pp. 414-429.

50. Hilado, C. J. "Flammability Tests for Cellular Plastics, Part I." Fire Technology, IV (February, 1968), pp. 32-45.

51. Hilado, C. J. "Flammability Tests for Cellular Plastics, Part II." Fire Technology, IV (May, 1968), pp. 142-149.

52. Hilado, C. J. "Analysis of Some Flammability Characteristics of Cellular Polymers." Industrial and Engineering Chemistry, Product Research and Development, VII (June, 1968), pp. 81-93.

53. Hilado, C. J. Flammability Handbook for Plastics. Stamford, Conn.: Technomic Publishing Co., 1969.

54. Hottel, H. C., and Williams, C. C. III. "Transient Heat Flow in Organic Materials Exposed to High Intensity Thermal Radiation." Industrial and Engineering Chemistry, XLVII (June, 1955), pp. 1136-1143.

55. Houwink, R., ed. Elastomers and Plastomers, Their Chemistry, Physics and Technology. Elsevier's Polymer Series, Vol. III. Delft, Holland: Elsevier Pub. Co., 1948.

56. "Intermittent Flame Test." The Hooker Chemical Company, September, 1955.

57. Jellinek, H. H. G. "Thermal Degradation of Polystyrene, Part I." Journal of Polymer Science, III (1948), pp. 850-865.

58. Jellinek, H. H. G. "Thermal Degradation of Polystyrene, Part II." Journal of Polymer Science, IV (1949), pp. 1-12.

59. Jellinek, H. H. G. "Thermal Degradation of Polystyrene and Polyethylene. Part III." Journal of Polymer Science, IV (1949), pp. 13-36.

60. Jessenig, W. R. "Classification of High Polymer Construction Materials on the Basis of Their Combustion Behavior." Praktische Chemie (Vienna), XIX (10, 1968), pp. 380-381.

61. Khoroshaya, E. S.; Korol'kova, K. D.; Galutvina, L. F.; Friedgeim, K. I.; Plotnikov, I. V.; Rishin, A. E.; and Kuznetsov, Yu. I. "Muffle Methods in Determination of Flame-Resistances of Polymers and Other Materials." Moscow, Vsesoiyznyi Nauchnoissledovatil'skii Institut Plenochnykj Materialov i Iskusstvennoi Kozhi NAUCHNOISSLEDOVATEI'SKIE TRUDY (Iskusstv) XVII (1966), pp. 187-191.

62. King, H. A. "Get More Out of YOur Thermal Tests for Plastics." Materials in Design Engineering, LXV (March, 1962), pp. 116-119.

63. Kingslake, R. Applied Optics and Optical Engineering. Vol 1. New York: Academic Press, 1965.

64. Kingslake, R. Applied Optics and Optical Engineering. Vol 4. New York: Academic Press, 1965.

65. Kingslake, R. Applied Optics and Optical Engineering. Vol 5. New York: Academic Press, 1965.

66. Klimke, P. M. "Evaluation of Test Results Obtained in Testing the Fire Behavior of Plastics on a Laboratory Scale." Plastverarbeiter, XVIII (6, 1967), pp. 389-398.

67. Kline, H. F. "A Study of Ignition Point Values of Nonmetallic Materials in Simulated Spacecraft Engironment." Society of Aerospace Materials and Process Engineering. National Symposium Exhibition, XI (1967) pp. 101-109.

68. Kline, L. M. "Burning, Arcing, Ignition, and Tracking of Plastics Used in Electrical Appliances." Underwriters' Laboratories Bulletin of Research, LV (February, 1964), p. 141.

69. Kniege, W., and Muller, E. "Silicone Rubber Technology." Industria della Gomma, X (12, 1966), pp. 40-44.

70. Koohyar, A. N. "Ignition of Wood by Flame Radiation." Unpublished Ph.D. dissertation. University of Oklahoma, 1967.

71. Krueger, O. A.; Lyle, K. C.; and Jackson, D. E. "Butler Chimney Test." Journal of Cellular Plastics, III (11, 1967), pp. 497-501.

72. Lang, N. A. Handbook of Chemistry. 10th ed. New York: McGraw-Hill, 1961.

73. Lapp, R. E. Matter. Life Science Library. New York: Time Incorporated, 1963.

74. Lawrence, E. K. "Analytical Study of Flame Initiation." Unpublished Ph.D. dissertation. Department of Chemical Engineering, Massachusetts Institute of Techology, 1950.

75. Lee, B. T., and Alveres, N. J. "The Effects of Irradiance on the Ignition and the Rate of Fire Spread Along Composite Cellulosic Materials." 1967 Spring Meeting, Western States Section, the Combustion Institute. La Jolla, California, April 1967.

76. Lever, A. E., and Phys, J. "The Properties and Testing of Plastic Materials. Part I." Plastics, XX (3, 1955), pp. 91-92.

77. Lipska, A. E. "The Pyrolysis of Cellulosic and Synthetic Materials in a Fire Environment." USNRDL-TR-1113. U. S. Naval Radiological Defense Laboratory, San Francisco, California, 14 December 1966.

78. Love, T. J. Radiative Heat Transfer. Columbus, Ohio: Merrill Publishing Co., 1968.

79. Madorsky, S. L. Thermal Degradation of Organic Polymers. New York: Interscience, 1964.

80. Madorsky, S. L., and Straus, S. "Stability of Thermoset Plastics at High Temperatures." Modern Plastics, XXXVIII (February, 1961), pp. 134-210.

81. Manley, T. R. "Thermal Investigation of Acrylic Polymers." Chemistry and Industry, 43 (October 22, 1966), p. 1797.

82. Mark, H. F. Giant Molecules. Life Science Library. New York: Time Incorporated, 1966.

83. Marks, G. C.; Benton, J. L.; and Thomas, C. M. "The Thermal Degradation of Poly(Vinyl Chloride) in a Nitrogen Atmosphere." Society of Chemical Industries, Monograph No. 26 (1967), pp. 204-235.

84. Materials Selector Issue, Materials in Design Engineering, CX (Mid-October, 1964), pp. 211-249.

85. McAlevy, R. F. III; Lee, S. Y.; and Smith, W. H. "The Linear Pyrolysis of Polymethylmethacrylate." WSCI 66-24. Paper presented at the Western State Section of the Combustion Institute, Denver, Colorado April 25-27, 1966.

86. McNeill, I. C. "Thermal Volatilization Analysis of High Polymers." European Polymer Journal, III (1967), pp. 409-421.

87. McPherson, A. T., and Klenain, A. Engineering Uses of Rubber. New York: Reinhold Publishing Co., 1956.

88. Mitchell, N. D. "New Light on Self-Ignition." National Fire Protection Association Quarterly, XLV (1951), pp. 165-172.

89. Miner, D. F., and Seastone, J. B. Handbook of Engineering Materials. 1st ed. New York: John Wiley & Sons Inc., 1955.

90. Modern Plastics Encyclopedia. XLIII, No. 1A. New York: McGraw-Hill, September, 1965.

91. Myncke, H., and Van Itterbeek, A. "Method for the Simultaneous Measurements of the Thermal Conductivity of Insulating Materials at Different Mean Temperatures." Bulletin de l'Institut International du Froid, Annexe (2, 1966), pp. 15-22.

92. Nachbar, W., and Williams, F. A. "On the Analysis of Linear Pyrolysis Experiments." Ninth International Symposium on Combustion. New York: Academic Press, 1963, pp. 345-357.

93. Nametz, R. C. "Self-Extinguishing Polyester Resins." Industrial and Engineering Chemistry, LIX (May, 1967), pp. 99-112.

94. Nametz, R. C. "Self-Extinguishing Polyester Resins." Industrial and Engineering Chemistry, LIX (August, 1967), p. 12.

95. National Fire Protection Association. "A Method of Measuring Smoke Density." Quarterly of the National Fire Protection Association, LVII (1964), pp. 276-287.

96. Naunton, W. J. S. The Applied Science of Rubber. London: Edward Arnold, 1961.

97. Neu, J. T., of General Dynamics Convair, San Diego, California. Private communication.

98. Oakes, W. G., and Richards R. B. "The Thermal Degradation of Ethylene Polymers." Journal of the Chemical Society (London) (1949), pp. 2929-2935.

99. Patten, G. A. "Ignition Temperatures of Plastics." Modern Plastics, XXXVIII (7, 1971), pp. 119-180.

100. Payne, A. R., and Scott, J. R. Engineering Design with Rubber. New York: Interscience Publishers, 1960.

101. Penn, W. S. Synthetic Rubber Technology. Vol. 1. London: Maclaren and Sons, 1960.

102. Perry, J. H. Chemical Engineers Handbook. 4th ed. New York: McGraw-Hill, 1963.

103. Pfenning, D. B. "Radiative Transfer from Laminar Flames." Unpublished Ph.D. dissertation. University of Oklahoma, 1970.

104. Reich, L. "Polymer Degradation by Differential Thermal Analysis Techniques." Macromolecular Reviews, Vol. 3. New York: Interscience Publishers, 1968, pp. 49-112.

105. Rein, R. G., of University Engineers, Norman, Oklahoma. Private communication.

106. Rogers, T. H., and Roennau, R. B. Engineering ABS Resin Processing." Chemical Engineering Progress, LXII (11, 1966), pp. 94-97.

107. Roth, W. A., and Schumacher, E. R. "II. Methods of Operation of Thermochemistry and Results Obtained in the Field of High-Polymeric Substances." Kautshuk, XVII (1942), pp. 137-142.

108. Roth, W. A.; Wirths, G.; and Berendt, H. "Heats of Combustion and Specific Heat of Buna-S Treated in Various Ways." Kautshuk, XVII (1941), pp. 31-33.

109. Rumberg, E. "Testing Resistance of Plastics to Heat and Burning." Gummi, Asbest, Kunststoffe, XV (1968), pp. 960-968.

110. Ryan, L. R.; Penzias, G. J.; and Tourin, R. H. "An Atlas of Infrared Spectra of Flames. Part I. Infrared Spectra of Hydrocarbon Flames in the 1-5 μ Region." Scientific Report No. 1, Contract AF19 (604)-6106. Air Force Cambridge Research Laboratories, Bedford, Massachusetts, July, 1961.

111. Sauber, W. J., and Patten, G. A. "Flammability Tests for Plastics." Plastics World, XVIII (December, 1960), pp. 40-43.

112. Schmidt, J. "Burning and Hi-Temperature Behavior of Plastics." Plaste und Kautschuk, XIII (2, 1966), pp. 83-86.

113. Schoenborn, E. M., and Weaver, D. S., Jr. "Ignition Temperatures of Rigid Plastics." ASTM Bulletin, No. 146 (1947), pp. 80-87.

114. Schultz, R. D., and Dekker, A. O. "The Absolute Thermal Decomposition Rates of Solids. Part I. The Hot-Plate Pyrolysis of Ammonium Chloride and the Hot-Wire Pyrolysis of Polymethylmethacrylate (Plexiglas IA)." Fifth International Symposium on Combustion. New York: Reinhold, 1955, pp. 260-267.

115. Setchkin, N. P. "Discussion of Paper on the Ignition Temperature of Rigid Plastics." ASTM Bulletin, No. 151 (1948), pp. 66-69.

116. Setchkin, N. P. "A Method and Apparatus for Determining the Ignition Characteristics of Plastics." Journal of Research, National Bureau of Standards, XLIII (1949), pp. 591-605.

117. Setchkin, N. P., and Ingberg, S. H. "Test Criterion for an Incombustible Material." American Society of Testing Materials, Proceedings, XLV (1945), pp. 866-875.

118. Shreve, R. N. Chemical Process Industries. 3rd ed. New York: McGraw-Hill, 1967.

119. Simms, D. L.; Law, M.; Hinkley, P. L.; and Pickard, R. W. "The Effect of Size of Irradiated Area on the Spontaneous Ignition of Materials. Part I. The Effect on Ignition Times." Fire Research Note No. 307, England Joint Fire Research Organization, 1957.

120. Smith, W. K. "Ignition of Materials by Radiant Heat." TN 40604-8. Naval Weapons Center, China Lake, California, 14 June 1968.

121. Smithsonian Miscellaneous Collection, 74, No. 1. "Solar Function at Sea Level." Smith. Inst. Astrophy. Obs. Ann. V (1932), p. 108.

122. Smoley, E. M. "Gasket Materials and Forms." Machine Design, XLI (14, 1969), pp. 67-73

123. Stepek, J.; Vymazal, Z.; and Dolezel, B. "Thermal Degradation of PVC." Modern Plastics, XL (June, 1963), pp. 146-205.

124. Stokes, H. N., and Weber, H. C. P. "Effects of Heat on Celluloid and Similar Materials." Technologic Papers of the Bureau of Standards, No. 98 (October 15, 1917).

125. Thomas, P. H., and Bowes, P. C. "Thermal Ignition in a Slab with One Face at a Constant High Temperature." Transactions of the Faraday Society, LVII (1961), pp. 2007-2017.

126. Thomas, P. H., and Bowes, P. C. "Some Aspects of the Self-Heating and Ignition of Solid Cellulosic Materials." British Journal of Applied Physics, XII (May, 1961), pp. 222-229.

127. Tsuchiya, Y., and Sumi, K. "Thermal Decomposition Products of Polyvinyl Chloride." Journal of Applied Chemistry, XVII (December, 1967), pp. 364-366.

128. Underwriters Laboratories, Inc. "Survey of Available Information on the Toxicity of the Combustion and Thermal Decomposition Products of Certain Building Materials Under Fire Conditions." Bulletin of Research, No. 53 (July, 1963).

129. Weast, R. C.; Selby, S. M.; and Hodgman, C. D. Handbook of Chemistry and Physics. 55th ed. Cleveland: Chemical Rubber, Co., 1964.

130. Weatherford, W. D., and Sheppard, D. M. "Basic Studies of the Mechanism of Ignition of Cellulosic Materials." Tenth International Symposium on Combustion. Pittsburgh: The Combustion Institute, 1965, pp. 897-910.

131. Welker, J. R., of the University of Oklahoma Research Institute, Norman, Oklahoma. Unpublished research data.

132. Wesson, H. R. "The Piloted Ignition of Wood by Radiant Heat." Unpublished Ph.D. dissertation. University of Oklahoma, 1970.

133. Westwater, J. W., and DeFries, M. G. "Discussion of Paper on Ignition Temperatures of Rigid Plastics." ASTM Bulletin, No. 148 (1947), pp. 86-87.

134. Williams, C. C. "Damage Initiation in Organic Materials Exposed to High-Intensity Thermal Radiation." Unpublished Sc.D. thesis. Chemical Engineering School, Massachusetts Institute of Technology, 1953.

135. Wolf, H., and Wierke, R. "Semitechnical Study of the Combustion Behavior of Plastics-Containing Building Structures." Plaste und Kautschuk, XVI (6, 1969), pp. 427-429.